Investigación del *splicing* del pre-ARNm en el mieloma múltiple: desde su función en la patogenia a su abordaje terapéutico

Elizabeta de los A. Rojas Ricardo

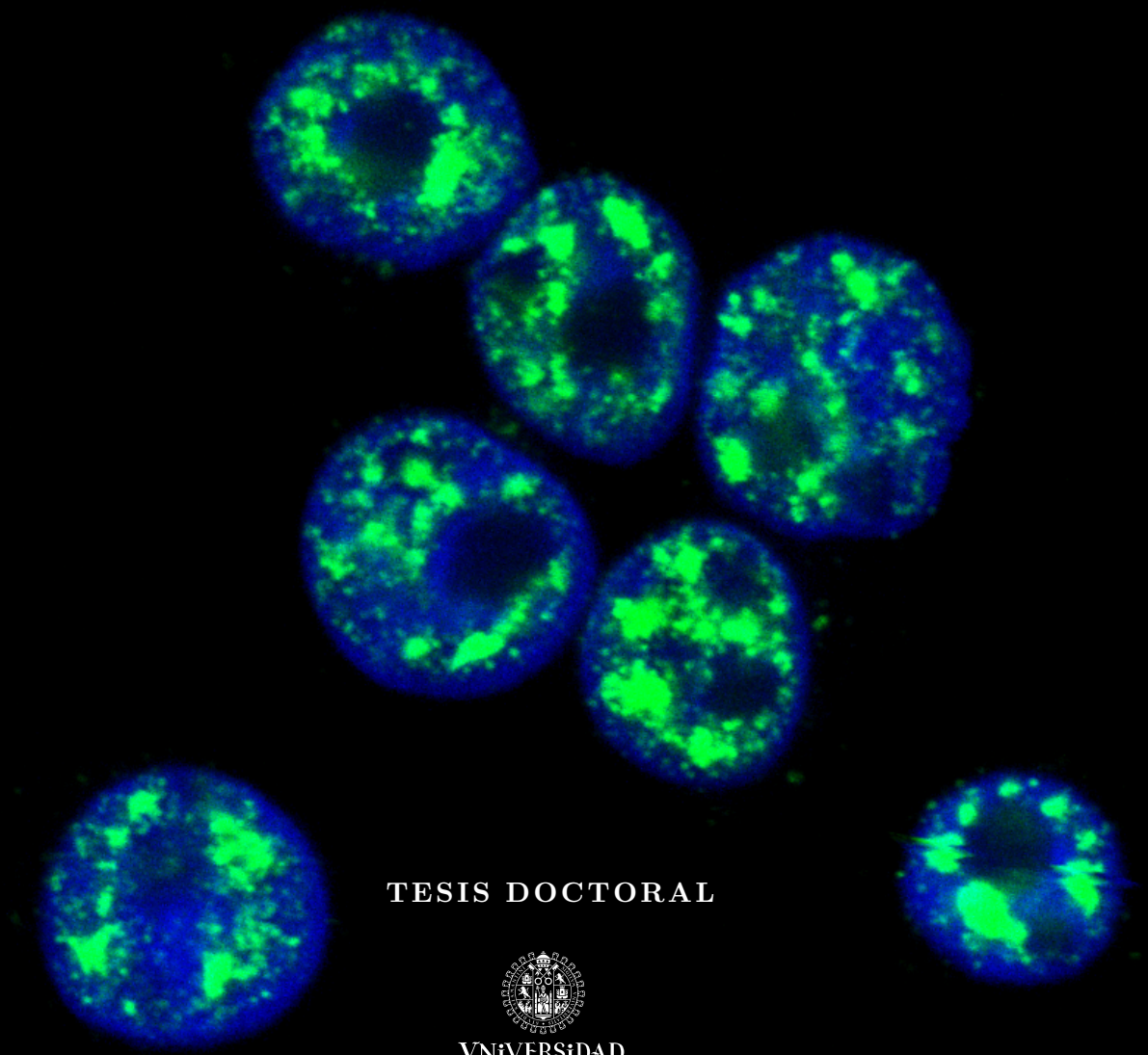

TESIS DOCTORAL

VNiVERSiDAD D SALAMANCA
CAMPUS DE EXCELENCIA INTERNACIONAL

Julio, 2022

Investigación del *splicing* del pre-ARNm en el mieloma múltiple: desde su función en la patogenia a su abordaje terapéutico

Elizabeta de los A. Rojas Ricardo

Directoras

Norma C. Gutiérrez

Irena Misiewicz-Krzeminska

Tutor

Marcos González Díaz

Tesis Doctoral

Universidad de Salamanca

Julio, 2022

D.ª Norma C. Gutiérrez, Doctora en Medicina y Cirugía, Profesora Asociada de Medicina de la Universidad de Salamanca y Médico Adjunto del Servicio de Hematología del Hospital Universitario de Salamanca, y

D.ª Irena Misiewicz-Krzeminska, Doctora en Farmacia por la Universidad Médica de Lodz, Investigadora del Instituto de Investigación Biomédica de Salamanca y del Instituto de Hematología y Transfusión de Varsovia,
como directoras,

y

D. Marcos González Díaz, Doctor en Medicina y Cirugía, Catedrático de la Universidad de Salamanca y Jefe del Servicio de Hematología del Hospital Universitario de Salamanca,
como tutor,

CERTIFICAN:

Que el trabajo realizado bajo nuestra dirección y tutoría por D.ª Elizabeta de los A. Rojas Ricardo, titulado "Investigación del *splicing* del pre-ARNm en el mieloma múltiple: desde su función en la patogenia a su abordaje terapéutico", reúne las condiciones de originalidad y calidad científica requeridas para optar al Grado de Doctor por la Universidad de Salamanca.

Y para que así conste a los efectos oportunos, firmamos el presente certificado a 24 de junio de 2022.

GUTIERREZ GUTIERREZ NORMA CARMEN - 09776609E
Firmado digitalmente por GUTIERREZ GUTIERREZ NORMA CARMEN - 09776609E
Nombre de reconocimiento (DN): c=ES, serialNumber=IDCES-09776609E, givenName=NORMA CARMEN, sn=GUTIERREZ GUTIERREZ, cn=GUTIERREZ GUTIERREZ NORMA CARMEN - 09776609E
Fecha: 2022.06.21 13:55:09 +02'00'

D.ª Norma C. Gutiérrez
Directora

MISIEWICZ-KRZEMINSKA IRENA - Y0616696B
Digitally signed by MISIEWICZ-KRZEMINSKA IRENA - Y0616696B
DN: c=ES, serialNumber=IDCES-Y0616696B, givenName=IRENA, sn=MISIEWICZ-KRZEMINSKA, cn=MISIEWICZ-KRZEMINSKA IRENA - Y0616696B
Date: 2022.06.21 18:33:29 +02'00'

D.ª Irena Misiewicz-Krzeminska
Directora

GONZALEZ DIAZ MARCOS - 06948715R
Firmado digitalmente por GONZALEZ DIAZ MARCOS - 06948715R
Fecha: 2022.06.21 16:01:03 +02'00'

D. Marcos González Díaz
Tutor

La realización de esta Tesis doctoral de D.ª Elizabeta de los A. Rojas Ricardo ha contado con las siguientes ayudas:

1. Beca predoctoral financiada por la Consejería de Educación de la Junta de Castilla y León y el Fondo Social Europeo (Resuelta en Orden EDU/574/2018, el 28 de mayo de 2018).
2. Proyectos de Acción Estratégica en Salud del Instituto de Salud Carlos III – Fondo de Investigación Sanitaria y FEDER (PI13/00111, PI16/01074 y PI19/00674).
3. Proyectos de la Gerencia Regional de Salud de Castilla y León (BIO/SA57/13, BIO/SA22/15, GRS 1344/A/16 y GRS 2058/A/19).

La presente tesis doctoral incluye tres trabajos originales publicados en revistas científicas indexadas en *Science Citation Reports*, según se detalla a continuación:

1. **Transcriptome analysis reveals significant differences between primary plasma cell leukemia and multiple myeloma even when sharing a similar genetic background**

   Elizabeta A. Rojas[1,3], Luis A. Corchete[1,3], María Victoria Mateos[1,2,3], Ramón García Sanz[1,2,3,5], Irena Misiewicz-Krzeminska[1,3,4]* y Norma C. Gutiérrez[1,2,3,5]*

   [1]Cancer Research Center-IBMCC (USAL-CSIC), Salamanca, Spain.
   [2]Hematology Department, University Hospital of Salamanca, Salamanca, Spain.
   [3]Institute of Biomedical Research of Salamanca (IBSAL), Salamanca, Spain.
   [4]National Medicines Institute, Warsaw, Poland.
   [5]Centro de Investigación Biomédica en Red de Cáncer (CIBERONC), CB16/12/00233, Salamanca, Spain.

   Blood Cancer J. 2019;9(12):90. Published 2019 Nov 20. DOI: 10.1038/s41408-019-0253-1

2. **Expression of p53 protein isoforms predicts survival in patients with multiple myeloma**

   Elizabeta A. Rojas[1,2], Luis A. Corchete[1,2], Cristina De Ramón[1], Patryk Krzeminski[1,2,3], Dalia Quwaider[1,2], Ramón García-Sanz[1,2,12,13], Joaquín Martínez-López[4,8,12,13], Albert Orio[l5,13], Laura Rosiño[l6,13], Joan Bladé[6,13], Juan José Lahuerta[7,13], Jesús F. San Migue[l9,12,13], Marcos González[1,2,12], María Victoria Mateos[1,2,12,13], Jean-Christophe Bourdon[10], Irena Misiewicz-Krzeminska[1,2,11]* y Norma C. Gutiérrez[1,2,12,13]*

   [1]Hematology Department, University Hospital of Salamanca, IBSAL, Salamanca, Spain.
   [2]Cancer Research Center-IBMCC (USAL-CSIC), Salamanca, Spain.
   [3]Department of Nanobiotechnology and Experimental Ecology, Institute of Biology, Warsaw University of Life Sciences, Warsaw, Poland.
   [4]Medicine Department, Complutense University, Madrid, Spain.
   [5]University Hospital Germans Trias i Pujol, Barcelona, Spain.
   [6]Hospital Clinic of Barcelona; Instituto de Investigaciones Biomédicas August Pi i Sunyer (IDIBAPS), Barcelona, Spain.
   [7]Hematology Department, University Hospital 12 de Octubre, Madrid, Spain.
   [8]Spanish National Cancer Research Center (CNIO), Madrid, Spain.
   [9]Clínica Universidad de Navarra, Centro de Investigaciones Médicas Aplicadas (CIMA); Instituto de Investigación Sanitaria de Navarra (IdiSNA), Pamplona, Spain.
   [10]School of Medicine, University of Dundee, Dundee DD1 9SY, United Kingdom.
   [11]Experimental Hematology Department, Institute of Hematology and Transfusion Medicine, Warsaw, Poland.
   [12]Centro de Investigación Biomédica en Red de Cáncer (CIBERONC), CB16/12/00233, Salamanca, Spain.
   [13]Grupo Español de Mieloma (GEM), Spain.

   Am J Hematol. 2022;97(6):700-710. DOI: 10.1002/ajh.26507

3. Amiloride, an old diuretic drug, is a potential therapeutic agent for multiple myeloma

Elizabeta A. Rojas[1,3], Luis Antonio Corchete[1,2,3], Laura San-Segundo[1,3], Juan F. Martínez-Blanch[5], Francisco M. Codoñer[5], Teresa Paíno[1,3], Noemí Puig[1,2,3], Ramón García-Sanz[1,2,3], María Victoria Mateos[1,2,3], Enrique M. Ocio[1,2,3], Irena Misiewicz-Krzeminska[1,3,4*] y Norma C. Gutiérrez[1,2,3*]

[1]Cancer Research Center-IBMCC (USAL-CSIC), Salamanca, Spain.
[2]Hematology Department, University Hospital of Salamanca, Spain.
[3]Institute of Biomedical Research of Salamanca (IBSAL), Salamanca, Spain.
[4]National Medicines Institute, Warsaw, Poland.
[5]Lifesequencing S.L., Valencia, Spain.

Clin Cancer Res. 2017;23(21):6602-6615. DOI: 10.1158/1078-0432.CCR-17-0678

A mi madre.

A Andrés.

A mi familia y al caribe mágico

"Observar sin pensar es tan peligroso como pensar sin observar".

— Santiago Ramón y Cajal

Agradecimientos

¡Ha llegado el día! Hoy finaliza una importante etapa de mi vida, y no puedo más que expresar mi más sincero agradecimiento a todos los que habéis hecho posible esta tesis doctoral.

Recuerdo con especial cariño mis primeros días en Salamanca y los primeros pipeteos y charlas en el laboratorio del Dr. Marcos González y Dr. Ramón García. Nunca olvidaré el especial cariño con el que todos me trataron. Fue todo un honor aprender de los mejores. Alicia, Montse, María Eugenia, Ana, Carmen, Miguel, ¡muchas gracias! Cuántos recuerdos...

Quiero agradecerle al Dr. Jesús San Miguel, que facilitó el comienzo de mi etapa predoctoral en el grupo de la Dra. Gutiérrez. Muchas gracias, Norma, por confiar en mí desde el primer momento y por todas sus enseñanzas durante estos años. Por compartir su tiempo, y su pasión por la ciencia (¡y la literatura!), y ayudarme a materializar este sueño que ha sido todo un desafío. Ha sido un placer compartir este tiempo de ciencia con usted, y poder preguntarle hasta la más mínima duda sobre medicina a deshoras. Debo decir que mi pasión por la ciencia y por la hematología ha crecido enormemente gracias a usted. Irena, tú fuiste la primera persona que creyó en mí, que me impulsó a querer formarme como científica. Gracias por tu paciencia, por guiarme siempre, por explicarme cada mínimo detalle, por enseñarme de esa rigurosidad tan importante en ciencia, y por tu cariño. No existen palabras para expresar mi más sincero agradecimiento a ambas. Ha sido un honor tenerlas como directoras de tesis y aprender también de vuestra calidad humana. ¡Muchas gracias a las dos!

Muchas gracias al team NCGG 😊: Luis, muchas gracias por tu infinita paciencia. Por enseñarme sobre el apasionante mundo de la estadística, por tu rigurosidad y tu transparencia científica. ¿Hoy sí sales en las fotos, verdad? May the force be with you, and with me too! Cris, gracias por tu cariño, tu amabilidad, tu entusiasmo y tu alegría. Qué buenos ratos pasamos con la RNA-Seq hasta las tantas, jejejejeje. Gracias a Patryk, Ignacio, Antonio, Aida, y Sandra (la granaína más maja que he conocido). Muchas gracias, Myriam, por tu comprensión y tu amabilidad. A Isabel, gracias por tu empatía y tu valiosa ayuda y disposición para todo lo que he necesitado, y por enseñarme de FISH. ¡¡¡Gracias miles, chicos!!!

Quiero agradecer también a todo el Servicio de Hematología del Hospital Universitario de Salamanca, a todo el personal de los laboratorios y muy especialmente a las chicas y chicos del laboratorio de Citogenética y Biología Molecular. A Teresa, Vanesa, Sandra, María, Alejandro, Cris, Isabel y Lucía, por todo el apoyo y la ayuda que me habéis brindado durante estos años. Me gustaría también agradecer a todos los integrantes del Grupo Español de Mieloma (GEM) por facilitar la inclusión de toda la valiosa información clínica en mi trabajo doctoral.

A mis amigas Dalia, Luzalba y Kamila. Muchas gracias por compartir tantas cosas, desde debates científicos hasta excursiones, bailes, cenas, clases de natación, cumpleaños. Por ser mi familia. Las quiero mucho, y las llevo dentro de mi corazón, siempre.

¡Muchas gracias a todo el laboratorio 12! Teresa, mil gracias por tenderme la mano siempre, por tu bondad y tu simpatía, y por acoger a las golondrinas 😊. A Merche y Juan Luis, ¡mejor dueto imposible! ¡Sois unos cracks! Lorena, gracias por tu paciencia y por enseñarme de MTTs y de WB. Gracias a Andrea, Pedro y Miguel por enseñarme a ver las cosas con más simplicidad, ¡sois fenomenales!

Gracias al Team Citogenética: Anita, Eva, María H. y María A., Mónica, Claudia, Miguel, Alberto, Sara, Irene y Ana. Sois lo máximo chicos! Todos llegaréis muy lejos porque sois fantásticos amigos y científicos. A Teresa, la gallega sideral, y al Dr. Jesús M. por compartir su visión del mundo y las charlas sobre política y cultura.

Gracias a todos los que me habéis regalado unas sonrisas por el CIC, me habéis alegrado muchos de mis días aquí. Y también a todos aquellos que han dedicado tiempo a explicarme dudas, y a contarnos la vida. O a comentarme que se encontraron un pajarito en su calle 😊.

Un agradecimiento especial para todo el personal de servicios del CIC, especialmente a Marga, a las "chicas del almacén", Sonia y Eugenia, y a Manolo de Secuenciación del Departamental, por facilitarme tanto las cosas, por los buenos ratos charlando de cosas triviales y pajaritos bonitos. Esos momentos son los que quedan por siempre en nuestros recuerdos y nuestro corazón. ¡Gracias a Carlos y Celso! Nunca olvido que cada vez que me ven me sacan una sonrisa.

A mi amigo del alma, José, gracias por todo. Gracias por apoyarme siempre, por los ánimos y la fuerza que me trasmites cada momento. A José Miguel, gracias por confiar en mí, por alegrarte de mis logros y por tu apoyo y consejos en todo momento. Tu visión del futuro es impresionante.

A mi familia cubana y a mi familia española. Sin ellos nada de esto hubiera sido posible. Pili, gracias por todo. Eres una de las personas más bondadosas que he conocido en mi vida. Gracias por hacerme sentir parte de la familia, por arroparme y estar a mi lado e inculcarme el amor por las cosas simples y a valorar tanto una buena amistad. A Piti, Pato y Miguel, porque la vida sería muy aburrida sin ellos. A Anita, Laura, Luis (no me olvido de los mochuelos), Nines, Argi, Isa y Chini. A Luni y Pepi ¡gracias!

A todo el equipazo de las DUNAS, porque me han hecho amar más y más a esas criaturas maravillosas que son las aves.

Mis tías del alma, Lely, Nancy, y mamá Chichela. A Isabel, Yaquelín y Leticia, que siempre me han apoyado. Estarán muy orgullosas y se alegrarán por mí a pesar de las distancias físicas. ¡Las quiero mucho! A mi padre, Rafael, que me enseñó que para lograr las cosas hay que trabajar duro.

Gracias eternas a mi madre, que siempre ha estado a mi lado y ha sido mi mayor apoyo y ejemplo a seguir. Tu bondad infinita y tu enorme corazón me llenan de orgullo. Gracias por enseñarme que no importa de dónde vengas. Con esfuerzo, sacrificio y mucho trabajo se pueden alcanzar los sueños. Pero sobre todo, gracias por sembrar en mí la semillita del amor por la Bioquímica. Tus relatos de la carrera de Medicina fueron la mayor y mejor motivación que tuve para elegir qué quería hacer en la vida. ¡Te quiero!

Me considero afortunada de haberte conocido, Andrés. Gracias por mantenerte incondicionalmente a mi lado en esta etapa de mi vida. Ajustando siempre tu tiempo al mío, acompañándome al laboratorio a deshoras para darle comida a las celulitas, por ser mi confidente y cuidar de mí. Por tener una paciencia iiiinfinita (casi como la gravedad de un agujero negro 😉), poniéndomelo todo más fácil. Por embarcarnos juntos en la gran aventura del mundo de las aves. Gracias por motivarme a ser mejor persona cada día, por ayudarme a vencer los miedos, por tu integridad y empatía, por retarme a aprender cosas nuevas. Hoooora de aventuras llegó...

Índice general

Glosario de abreviaturas

A

ACD	Anticuerpos monoclonales conjugados a drogas
ADN	Ácido desoxirribonucleico
ARN	Ácido ribonucleico
ARNm	ARN mensajero
AR-SA	Anemia refractaria con sideroblastos en anillo, del inglés *refractory anemia with ringed sideroblasts*
ASO	Oligonucleótidos antisentido

B

BiTEs	Reclutadores biespecíficos de células T, del inglés *Bispecific T cell Engager*
BP	Punto de ramificación, del inglés *branch point*
BR	Región básica

C

CAR-T	Células T con receptor de antígeno quimérico
CELMoDs	Moduladores de la ligasa cereblón E3
CM	Componente monoclonal
CNA	Anomalías en el número de copias, del inglés *copy number alteration*
CP	Células plasmáticas

D

DBD	Dominio de union al ADN, del inglés *DNA-binding domain*

E

ESE	Elementos reguladores exónicos estimuladores del *splicing*, del inglés *exonic splicing enhancers*
ESS	Elementos reguladores exónicos inhibidores del *splicing*, del inglés *exonic splicing silencers*

F

Fc	Región constante
FDA	Administración de Alimentos y Medicamentos
FISH	Hibridación *in situ* fluorescente

G

GMSI	Gammapatía monoclonal de significando incierto

H

hnRNPs	Ribonucleoproteínas heterogéneas nucleares, del inglés *heterogeneous nuclear ribonucleoproteins*

I

IMiDs	Agentes inmunomoduladores
IMWG	Grupo Internacional de Trabajo en Mieloma, del inglés *International Myeloma Working Group*
ISEs	Elementos reguladores intrónicos estimuladores del *splicing*, del inglés *intronic splicing enhancers*
ISSs	Elementos reguladores intrónicos inhibidores del *splicing*, del inglés *intronic splicing silencers*

L

LCBGD	Linfoma de células B grandes difuso
LCP	Leucemia de células plasmáticas
LCPp	Leucemia de células plasmáticas primaria
LCPs	Leucemia de células plasmáticas secundaria
LLC	Leucemia linfocítica crónica
LMA	Leucemia mieloide aguda
LMMC	Leucemia mielomonocítica crónica

M

MDEs	Eventos que definen al mieloma, del inglés *myeloma defining events*
MDRs	Regiones mínimamente delecionadas
miRNAs	MicroARNs
MM	Mieloma múltiple
MMQ	Mieloma múltiple asintomático, también denominado quiescente o *smoldering*
MO	Médula ósea

N

NGS	Secuenciación de nueva generación, del inglés *new generation sequencing*
NLS	Dominio de localización nuclear, del inglés *nuclear localization signal*
NMP	Neoplasia mieloproliferativa

O

OD	Dominio de oligomerización, del inglés *oligomerization domain*

P

PRD	Dominio rico en residuos de prolina, del inglés *proline-rich domain*
pre-ARNm	Precursor del ARN mensajero

S

SP	Sangre periférica
scFv	Anticuerpo monocatenario de cadena sencilla, del inglés *single-chain variable fragment*
snRNPs	Ribonucleoproteínas pequeñas nucleares, del inglés *small nuclear ribonucleoproteins*
SR	Arginina (R) y serina (S)
ss	Sitio de splicing, del inglés *splicing site*
SMDs	Síndromes mielodisplásicos
SMD-SA	Síndrome mielodisplásico con sideroblastos en anillo
SMA	Atrofia muscular espinal, del inglés *spinal muscular atrophy*

T

TAPH	Trasplante autólogo de progenitores hematopoyéticos
TAD	Dominio de transactivación, del inglés *transactivation domain*

W

WHO	Organización Mundial de la Salud, del inglés *World Health Organization*

Introducción

1. Generalidades de las gammapatías monoclonales

Las discrasias de células plasmáticas engloban un grupo de entidades neoplásicas caracterizadas por la expansión y acumulación descontrolada de células plasmáticas (CPs) clonales en la médula ósea (MO). Bajo esta definición se incluyen fundamentalmente la gammapatía monoclonal de significando incierto (GMSI), el mieloma múltiple asintomático también denominado quiescente o *smoldering* (MMQ), el mieloma múltiple (MM) y la leucemia de células plasmáticas (LCP). La seña de identidad de estas enfermedades es la producción por las CPs clonales de una inmunoglobulina (Ig) monoclonal, comúnmente denominada componente monoclonal (CM) o paraproteína, que puede ser detectada en suero y/u orina. Por este motivo, también se utiliza el término de gammapatías monoclonales para referirse a estos trastornos. No obstante, en algunos casos puede no detectarse el CM.

La GMSI se considera una entidad premaligna de CPs que cursa de forma asintomática. Alrededor del 50 % de las gammapatías monoclonales son GMSI[1]. Su prevalencia se incrementa con la edad hasta llegar a un 6.6 % en personas mayores de 80 años. El MMQ es también una entidad premaligna y asintomática, pero con un comportamiento clínico y biológico intermedio entre la GMSI y el MM[2]. Mientras que los pacientes con GMSI presentan un 1 % por año de riesgo de progresión a MM, aquellos con MMQ tienen un 10 % de riesgo anual dentro de los 5 años posteriores al diagnóstico[3]. Hay pacientes con MMQ que tienen un curso clínico similar al de la GMSI con una baja tasa de progresión; en cambio, otros progresan a MM en los 2 primeros años desde el diagnóstico[4].

El MM representa el 1 % de todos los tipos de cáncer y aproximadamente el 10 % de las neoplasias hematológicas, por lo que es el segundo cáncer hematológico más frecuente después del linfoma no Hodgkin. En el 2020 la Agencia Internacional de Investigación en Cáncer estimó una incidencia mundial de MM de 2.3 casos nuevos por cada 100 000 personas por año. Concretamente en España, se diagnosticaron 3 214 nuevos casos en el 2020, que representa una tasa de 6.9 por cada 100 000 individuos por año (https://gco.iarc.fr). Es una enfermedad que afecta mayoritariamente a personas de edad avanzada, con una mediana de edad al diagnóstico de 66-70 años, aunque el 37 % de los pacientes con MM son menores de 65 años[5].

Las manifestaciones clínicas más comunes que definen el MM sintomático derivan del daño de órganos producido por la expansión incontrolada de las CPs y por el exceso de inmunoglobulina clonal. Estas manifestaciones se agrupan bajo el acrónimo "CRAB": hiperCalcemia, insuficiencia Renal, Anemia, y/o lesiones óseas (*Bone lesions*). La actualización de los criterios diagnósticos del MM publicada en 2014 por el *International Myeloma Working Group* (IMWG)[6] incluyó dentro de los eventos que definen el MM (*myeloma defining events*) la presencia de uno de los tres biomarcadores de malignidad, independientemente de la presencia o no de signos CRAB (Tabla 1).

La leucemia de células plasmáticas (LCP) es una neoplasia poco frecuente y muy agresiva. Representa menos del 3 % de todas las neoplasias de CPs y su incidencia ha sido estimada

Tabla 1. Clasificación y criterios diagnósticos de las gammapatías monoclonales según el *International Myeloma Working Group* (IMWG)[6].

Gammapatía	**CM**	**% de CPs en MO**	**Eventos MDEs***
Gammapatía monoclonal de estado incierto	<30 g/L	<10 %	Ausentes
Mieloma múltiple quiescente	≥30 g/L (ó ≥500 mg/24 h en orina)	10-60 %	Ausentes
Mieloma múltiple	Presente, o ausente en el MM no secretor	≥10 % / plasmocitoma (confirmado por biopsia)	Presentes

***Eventos MDEs (*myeloma defining events*):**

Sintomatología CRAB (uno o más de los siguientes):

- Hipercalcemia: calcio sérico >0.25 mmol/L (>1 mg/dL) del límite alto de la normalidad o 2.75 mmol/L (>11 mg/dL).
- Insuficiencia renal: creatinina sérica >177 µmol/L (>2 mg/dL) o aclaramiento de creatinina <40 mL/min.
- Anemia: hemoglobina >2 g/dL por debajo del límite inferior de la normalidad, o hemoglobina <10 g/dL.
- Lesiones óseas: una o más lesiones osteolíticas (≥5 mm) detectadas en la serie ósea, por tomografía computarizada (TC) o tomografía por emisión de positrones (PET-TC).

o

Al menos uno de los biomarcadores de malignidad:

- ≥60 % de CPs en MO.
- Ratio de cadena ligera libre implicada/no implicada ≥100.
- Detección de >1 lesión focal con diámetro mínimo de 5 mm, detectada mediante resonancia magnética nuclear de cuerpo entero o de columna vertebral.

en 0.04 casos por 100 000 personas por año[7]. La LCP puede ser primaria (LCPp) cuando se origina *de novo*, sin evidencia previa de MM, o secundaria (LCPs) cuando se produce una progresión leucémica en el contexto de un MM en recaída o refractario. La LCPp representa entre el 60-70 % de los casos de LCP y tienen una mediana de edad de 55 años[8,9]. En cambio, la mediana de edad de los pacientes con LCPs es de 65 años[9–11]. El número de casos de LCPs se ha incrementado en los últimos años debido al aumento de la supervivencia de los pacientes con MM que experimentan múltiples recaídas a lo largo del curso de la enfermedad. El pronóstico de las LCP, tanto primarias como secundarias, es infausto, si bien las LCPs se caracterizan por un curso clínico peor y supervivencia más corta.

El diagnóstico de LCPp ha requerido la presencia en sangre periférica de más de un 20 % de CPs y un número absoluto de CPs superior a 2 x 109 CP/L[12]. Sin embargo, varios estudios han demostrado que los pacientes con un número menor de CPs circulantes tienen un pronóstico igualmente desfavorable[13–15]. Por ello, el IMWG ha publicado recientemente que la LCPp se define por la presencia de un 5 % o más de CPs en sangre periférica[16]. La sintomatología asociada a la LCP incluye anemia, trombocitopenia, y un compromiso extramedular extenso por infiltración de CPs en órganos como el hígado, el bazo, los ganglios linfáticos, o incluso el sistema nervioso central. A diferencia del MM, las lesiones osteolíticas son excepcionales en la LCPp[10,17–21].

2. Alteraciones genómicas del mieloma múltiple

Desde el punto de vista genético, el MM es una neoplasia muy heterogénea y compleja. En el MM no existe una alteración genética específica que lo defina. Se han descrito eventos genéticos primarios que comprenden los genes involucrados en la génesis de la enfermedad, y eventos genéticos secundarios responsables de la progresión, pues confieren una ventaja en la supervivencia y la proliferación celular (Figura 1).

Los primeros estudios realizados con citogenética convencional y posteriormente, con hibridación *in situ* fluorescente (FISH) han revelado la mayoría de las anomalías cromosómicas más recurrentes del MM. Recientemente, las tecnologías genómicas más avanzadas basadas en *microarrays* y en la secuenciación de nueva generación (NGS) han contribuido a completar el conjunto de alteraciones genómicas, que se pueden clasificar en translocaciones, anomalías en el número de copias (CNA) y mutaciones somáticas puntuales.

2.1. Traslocaciones cromosómicas

Las traslocaciones del gen *IGH*, localizado en la banda cromosómica 14q32, están presentes en casi el 60 % de los pacientes con MM. Como resultado de la traslocación recíproca, el *enhancer* o potenciador del gen *IGH* provoca un aumento en la expresión del gen que participa en la traslocación[22]. Las traslocaciones de *IGH* más frecuentes en el MM son la t(11;14)(q13;q32),

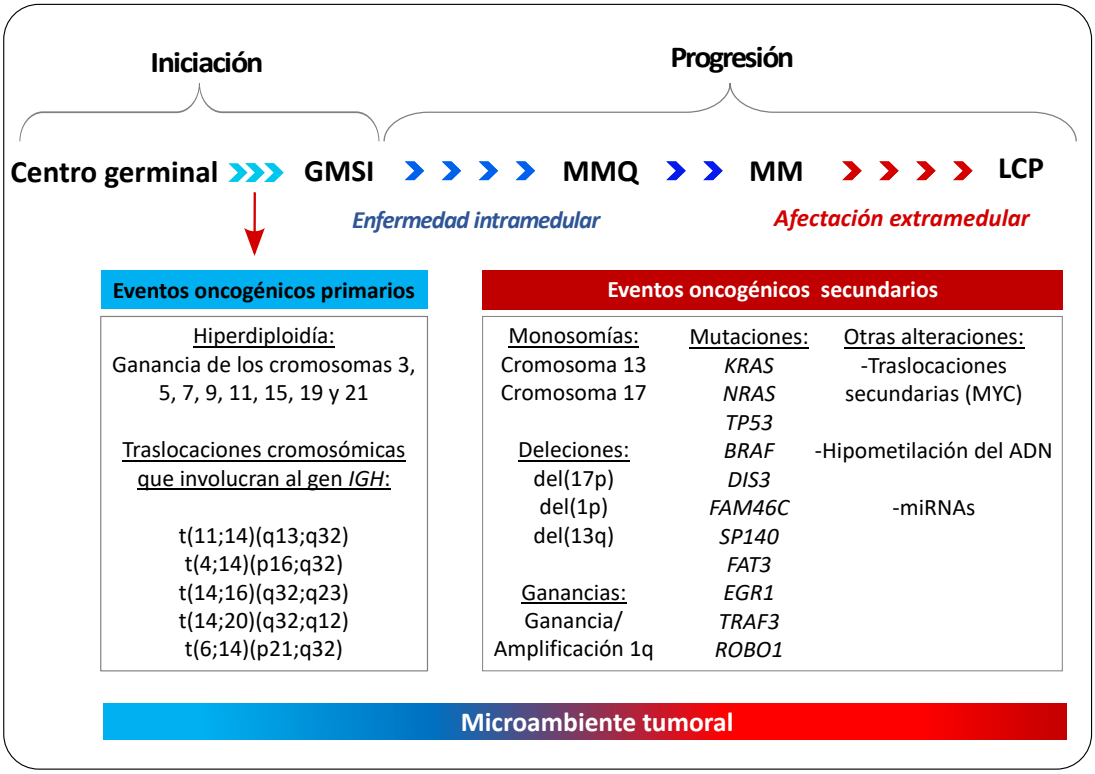

Figura 1. Eventos genéticos implicados en la iniciación y progresión del MM, desde la GMSI hasta la LCP.

que involucra al gen de la ciclina D1 (*CCND1*), generalmente inactiva en las células B maduras; la t(4;14)(p16;q32), que implica al gen que codifica para la metiltransferasa *NSD2* (anteriormente conocido como *MMSET*) y al que codifica para el receptor tirosina cinasa *FGFR3*; y la t(14;16)(q32;q23) que implica al factor de transcripción MAF. Las t(14;20)(q32;q12) y t(6;14)(p21;q32) que afectan a los genes *MAFB* y *CCND3*, respectivamente, son muy infrecuentes.

Las traslocaciones que involucran al oncogén *MYC*, provocando su sobreexpresión, son consideradas eventos secundarios y se observan en aproximadamente el 15 % de los pacientes con MM de nuevo diagnóstico[23]. Generalmente el oncogén se trasloca con los genes de las inmunoglobulinas, aunque alrededor del 40 % de los reordenamientos de *MYC* afectan a otros genes[23].

2.2. Anomalías en el número de copias

Las CPs del MM ganan y pierden cromosomas completos o regiones cromosómicas que hacen que casi todos los MM sean aneuploides. Según el estado de ploidía, el MM se suele clasificar en hiperdiploide y no hiperdiploide. La hiperdiploidía, que se observa en alrededor del 50 % de los casos, se caracteriza por trisomías de los cromosomas impares 3, 5, 7, 9, 11, 15, 19 y 21[24,25]. El grupo de pacientes con MM no hiperdiploide abarca casos hipodiploides de hasta 44/45

cromosomas, pseudodiploides desde 44/45 hasta 46/47 cromosomas, y casos casi tetraploides (más de 74). Los cromosomas más frecuentemente perdidos en el MM son el 13, el 14, el 16, y el 22[25].

Por lo general los pacientes con traslocaciones de *IGH*, desde el punto de vista de la ploidía, suelen ser no hiperdiploides, aunque en un porcentaje de casos menor del 10 % convergen ambas alteraciones, las trisomías y las traslocaciones.

El cromosoma 1 es el más afectado por ganancias y pérdidas. Aproximadamente, en el 50 % de los casos de MM de nuevo diagnóstico se observan ganancias (3 copias) o amplificaciones (más de 3 copias) del brazo largo del cromosoma 1[26,27]. Este porcentaje se ve incrementado hasta un 68 % en los pacientes con MM en recaída o en progresión[27]. La ganancia de 1q trae consigo la sobreexpresión de genes como *CKS1B* (banda 1q21), relacionado con la resistencia al tratamiento dado que favorece la proliferación y la supervivencia celular[28,29], y de otros genes implicados en la patogenia del MM como *MUC1*, *MCL1*, *PSMD4* y *PDZK1*[30–33]. La deleción del brazo corto 1p se observa en más del 30 % de los pacientes con MM[34–36]. Las regiones mínimamente delecionadas en 1p incluyen 1p12, 1p21, 1p22.1 y 1p32.3, donde están localizados los genes *FAM46C*, *CDC14A*, *MTF2* y *CDKN2C*, respectivamente[35,37].

La monosomía del cromosoma 13 o deleción intersticial de 13q está presente en el 45–50 % de los pacientes en el momento del diagnóstico[38–40]. La deleción del brazo corto del cromosoma 17 (del(17p)), donde se ubica el supresor tumoral *TP53*, se observa sólo en el 10 % de los pacientes con MM en el momento del diagnóstico, si bien su incidencia aumenta en las recaídas y estadios avanzados de la enfermedad[10,26,41].

Tanto las traslocaciones del gen *IGH* como las trisomías se observan ya en las etapas premalignas del MM, como son la GMSI y el MMQ[42]. Por este motivo, se les considera eventos genéticos primarios.

2.3. Mutaciones somáticas puntuales

La utilización de estrategias de NGS, tanto la secuenciación del genoma y del exoma completos, en miles de pacientes ha confirmado la heterogeneidad de la célula tumoral del MM también a nivel mutacional. En efecto, en el MM no existe una mutación puntual única y específica, sino que se han identificado varios genes recurrentemente mutados. Varios estudios de NGS han coincidido en los genes que están mutados en más del 5 % de los pacientes con MM: *KRAS* y *NRAS* (20-25 %), *TP53* (8-15 %), *DIS3* (∼11 %), *FAM46C* (∼10 %), *BRAF* (6-15 %), *TRAF3* (3-6 %), *ROBO1* (2-5 %), *EGR1* (4-6 %), *SP140* (5-7 %) y *FAT3* (4-7 %)[43–46]. Otros genes recurrentemente mutados en MM son *PRDM1* (5 %)[46] y *IRF4* (3.2 %)[47], que están implicados en la diferenciación del linaje B. A pesar de la poca frecuencia de mutaciones en el gen *TP53* en los MM de nuevo diagnóstico, más de la mitad de los pacientes con del(17p) tienen el otro alelo mutado, provocando la inactivación bialélica de este importante gen supresor tumoral[48].

Aunque el papel patogénico de las mutaciones de *RAS* y *TP53* ha sido muy estudiado, el efecto de las mutaciones que afectan a los demás genes aún es bastante desconocido. Nuestro grupo ha descrito recientemente que la inactivación de *FAM46C* promueve la migración celular en el MM[49].

En consecuencia, las vías de señalización que habitualmente presentan mutaciones en el MM son la vía de las *MAPK* en el 45 % de los casos, la vía *NF-κB* en el 15 %, la vía del metabolismo del ARN en el 15 %, la vía de diferenciación de la CP en el 3-10 %, y las vías de reparación del ADN en el 10 % de los casos[50].

3. Alteraciones en el transcriptoma del mieloma múltiple

La expresión génica del MM es también muy heterogénea. Sin embargo, la mayoría de los estudios coinciden en que existen diferentes subgrupos con un perfil de expresión génica específica, que se asocia con un comportamiento clínico característico. La expresión diferencial de los genes codificantes para las ciclinas D: *CCND1* (ciclina D1), *CCND2* (ciclina D2), y *CCND3* (ciclina D3), está incrementada en la práctica totalidad de los pacientes con MM y también en la GMSI, independientemente de las alteraciones citogenéticas presentes. Esta desregulación está considerada de hecho un evento común y temprano en la patogenia del MM[51]. No obstante, esta característica contrasta con el bajo índice proliferativo de las CPs clonales en la mayoría de los MM.

Los primeros estudios utilizando *microarrays* proporcionaron la primera visión global del transcriptoma de la CP tumoral y permitieron elaborar una clasificación molecular integrada por varios subgrupos de MM con un comportamiento clínico único asociado a su firma genéticačiteref:pmidZhan2006. Esta clasificación se ha reproducido con mínimos cambios en varios estudios posteriores. Fundamentalmente, la componen siete subgrupos moleculares: PR, LB, HY, MS, MF, CD-1 y CD-2[52]. Los subgrupos MF, MS CD-1 y CD-2 se caracterizan por la sobreexpresión de los genes *MAF*/*MAFB*, *MMSET*, *CCND1*/*CCND3* y *CCND2*, respectivamente. El grupo HY de hiperdiploidía se caracteriza por la sobreexpresión de los genes localizados en los cromosomas impares con trisomías en el MM como el *TNFSF10*, *FRZB* y *DKK1*. Los casos de MM incluidos en el grupo LB (*low bone disease*) se caracterizan por presentar una baja incidencia de lesiones óseas y elevada expresión de varios genes que incluyen la endotelina 1, el receptor de quimiocinas *CCR2*, el gen pro-apoptótico *BIK*, y el receptor de interleucina 6 (*IL6LR*); y bajos niveles de los genes *FRZB* y *DKK1*, involucrados en el desarrollo de lesiones osteolíticas. El grupo PR de proliferación se caracteriza por tener una alta tasa de proliferación y elevados niveles de expresión de genes de ciclo y proliferación celular como *CCNB2*, *CCNB1*, *MCM2*, *BUB1* y *CDC2*[52].

El incremento de los niveles de la ciclina D1 y D3 es consecuencia directa de la t(11;14) y la t(6;14), respectivamente. La polisomía del cromosoma 11, que se observa con frecuencia en

el MM, también puede aumentar los niveles de expresión de la ciclina D1[52–54]. En cambio, los mecanismos desencadenantes de la desregulación de la expresión de la ciclina D2 son aún en parte desconocidos. Se ha descrito que los factores de transcripción *MAF* y *MAFB* involucrados en la traslocación t(14;16) y t(14:20), respectivamente, inducen la expresión de la ciclina D2. Nuestro grupo ha descrito que la sobreexpresión de la isoforma corta de la ciclina D2, que presenta una región 3' UTR más corta debido a un sitio de poliadenilación alternativo, es uno de los mecanismos postranscripcionales responsables de la sobreexpresión de la ciclina D2 en el MM[55].

Por otra parte, muchos de los cambios observados en la expresión génica del MM, no están precedidos por alteraciones en el ADN genómico. Se sabe que los procesos de regulación postranscripcional son los responsables de buena parte de la desregulación de la expresión génica. Los microRNAs (miRNAs) han sido, sin duda, uno de los mecanismos de regulación postranscripcional más ampliamente estudiado. En el MM se ha demostrado su implicación en el desarrollo normal de la CP y en la patogenia del MM[56,57]. Además se ha observado que la desregulación de la expresión de los miRNAs está asociada con alteraciones cromosómicas específicas[58].

4. Alteraciones genómicas en la leucemia de células plasmáticas primaria

Las alteraciones cromosómicas que se observan en las LCPp son en general las mismas que se han descrito en el MM, aunque la frecuencia con la que aparecen algunas de ellas en las LCPp es significativamente diferente[59]. Más del 50 % de las LCPp presentan un cariotipo no hiperdiploide con una alta frecuencia de pérdidas cromosómicas[60,61]. La monosomía o deleción del cromosoma 13 es la alteración citogenética más frecuente en la LCPp (se observa en aproximadamente el 85 % de los casos)[10,62,63]. Igualmente, la ganancia/amplificación de 1q está presente en una proporción mayor de LCPp que de MM. Las ganancias de 1q se observan hasta en un 70 % de los casos de las LCPp[62–65]. La del(17p) llega a detectarse en aproximadamente un 50 % de las LCPp[10,62]. En cuanto a las traslocaciones que involucran al gen *IGH* uno de los resultados más consistente es que la t(11;14) es significativamente más frecuente en la LCPp que en el MM. Esta traslocación se observa en entre un 45 y un 70 % de las LCPp[10,61,62,66]. Por el contrario, en la mayoría de los estudios se ha descrito que la t(4;14) es menos frecuente en la LCPp que en el MM[64,67,68]. Las traslocaciones que involucran a *MYC* aparecen hasta en un 33 % de los casos de LCPp[10,69].

Los genes afectados por mutaciones puntuales coinciden en su mayoría con los descritos en el MM. Los más frecuentemente mutados en las LCPp son *K/NRAS* (20-50 %)[10,70] y *TP53* (25 %)[64,71,72]. También se han reportado mutaciones en más del 5 % de los casos en los genes *IRF4* , *FAM46C*, *DIS3* y *PRMD1*[64,71,73].

A nivel transcripcional, bien utilizando *microarrays* o bien mediante secuenciación del ARN (RNA-Seq), se han demostrado diferencias en el perfil de expresión génico de las LCPp

respecto del MM. Se ha observado una expresión elevada de genes involucrados en la regulación del ciclo celular y algunas dianas del oncogén *MYC*, y baja expresión de genes implicados en la vía de señalización de p53, de hipoxia y de la ruta biológica de *NF-κB*[71].

5. Repercusión de las alteraciones genómicas en el pronóstico de los pacientes

Determinadas alteraciones genéticas se han consolidado a lo largo del tiempo como uno de los factores con mayor influencia en el pronóstico del MM. Sin embargo, hoy por hoy su repercusión en las decisiones terapéuticas es escasa. Por otro lado, existe una buena proporción de pacientes con MM cuya supervivencia es impredecible utilizando estos biomarcadores. Incluso a veces se puede dar la circunstancia de que en un mismo paciente coexistan marcadores genéticos con un impacto en el pronóstico de signo opuesto.

En la actualidad la técnica más usada por su rapidez y nivel de estandarización para detectar estas alteraciones genéticas es la FISH. No obstante, en los últimos años la NGS utilizando paneles a medida se está implantando cada vez en más en los laboratorios.

Las traslocaciones t(4;14) y la t(14;16) se incluyen en la mayoría de las clasificaciones pronósticas como marcadores genéticos de mal pronóstico[74](Tabla 2). No obstante, la introducción de los inhibidores del proteasoma en los esquemas terapéuticos ha mejorado la supervivencia de los pacientes con t(4;14), y el doble trasplante podría superar el mal pronóstico de la t(14;16)[75]. En cambio, la t(11;14) no tiene una repercusión negativa en la supervivencia de los pacientes con MM[76]. Aunque no existe unanimidad en cuanto al valor pronóstico de las alteraciones del oncogén *MYC*, los últimos estudios demuestran supervivencias más cortas en los pacientes con reordenamientos de *MYC*, particularmente cuando implican a los genes de las inmunoglobulinas[23,50].

Respecto a las CNA, la deleción de 17p, que ocasiona la pérdida de *TP53*, es probablemente uno de los marcadores genéticos asociados a peor pronóstico[76–79]. Las alteraciones del cromosoma 1 también se han asociado con menor supervivencia, especialmente las pérdidas de 1p[80]. En el caso de las alteraciones de 1q, es la amplificación, definida como la presencia de más de tres copias, la que peor pronóstico acarrea[81,82]. Por el contrario, los cariotipos hiperdiploides que presentan trisomías como únicas alteraciones se asocian consistentemente con las supervivencias más prolongadas[76,83](Tabla 2).

Resulta curioso que todas estas alteraciones tienen un impacto significativo tanto en la supervivencia libre de progresión (SLP) como en la supervivencia global (SG), sin apenas tener repercusión en la respuesta al tratamiento.

Desde el punto de vista pronóstico la coexistencia de más de una alteración de alto riesgo supone un acortamiento significativo de la supervivencia respecto a la presencia de una de estas alteraciones de manera aislada. Así, los pacientes con una traslocación de *IGH* de mal pronóstico,

Tabla 2. Principales alteraciones genómicas en el MM y su valor pronóstico. Modificada de Manier *et al.* y Morgan *et al.*[24,50].

Alteración genética y genes implicados		Frecuencia en el MM	Valor pronóstico
Traslocaciones	**Traslocaciones del gen *IGH***	40-50 %	
	- t(11;14)(q13;q32): *CCND1*	15-20 %	Neutral
	- t(4;14) (p16;q32): *FGFR3/NSD2*	15 %	Adverso
	- t(14;16)(q32;q23): *MAF*	≤5 %	Adverso
	- t(6;14)(p21;q32): *CCND3*	1-4 %	Neutral
	- t(14;20)(q32;q12): *MAFB*	<2 %	Adverso
	Traslocaciones de *MYC*	15 %	Adverso
Anomalías en el número de copias	**Ganancias**		
	- Trisomía de 3, 5, 7, 9, 11, 15, 19 ó 21	50 %	Neutral
	- 1q: *MCL1*, *CKS1B*, *ANP32E*, *BCL9*	50 %	Adverso
	- 8q: *MYC*	15 %	Neutral
	- 11q: *CCND1*	15 %	Neutral
	Pérdidas		
	- Monosomía 13: *RB1*, *DIS3*	45 %	Neutral
	- 1p: *CDKN2C*, *MTF2*, *FAM46C*	20 %	Adverso
	- 17p: *TP53*	10 %	Adverso
Mutaciones	- Vía *MAPK*: *KRAS*, *NRAS*, *BRAF*	45 %	Neutral
	- Vía *NF-κB*: *CYLD*, *TRAF3*, *LBT*, *NIK*	15 %	Neutral
	- Metabolismo del RNA: *DIS3*, *FAM46C*	15 %	Neutral
	- Vía de reparación del ADN: *TP53*, *ATM*, *ATR*	10 %	Adverso
	- Diferenciación de células plasmáticas: *IRF4*, *PRDM1*	3-10 %	Favorable

una deleción de 17p y una ganancia de 1q tienen una mediana de supervivencia global en torno a nueve meses[84]. Igualmente, la inactivación bialélica de *TP53* por la presencia simultánea de mutación de un alelo y deleción del otro se asocia con un pronóstico infausto.

Mientras la t(11;14) no influye negativamente en el pronóstico del MM, un estudio reciente, que analiza casi un centenar de casos con LCPp, muestra que la presencia de esta traslocación en la LCPp se asocia con una supervivencia significativamente más larga[65]. Por otra parte, la t(4;14), las traslocaciones que involucran a *MYC*, la del(1p), así como las mutaciones de *TP53*, se han asociado a un peor pronóstico de las LCPp[10,62,69,71].

6. Microambiente medular

El MM es una de las neoplasias donde el papel en la oncogénesis del microambiente de la MO que rodea a las células plasmáticas está más demostrado. Se ha sugerido que el microambiente medular contribuye de manera significativa en la progresión maligna del MM, desde sus estadios asintomáticos, como la GMSI y el MMQ, hasta sus formas más agresivas como la LCP, que presenta una mayor capacidad de diseminación extramedular; así como en los procesos de resistencia a los medicamentos.

El microambiente de la MO está compuesto por dos compartimentos: a) compartimento celular que incluye células hematopoyéticas (linfocitos B, linfocitos T, células NK, células mieloides, y osteoclastos) y no hematopoyéticas (células estromales mesenquimales, fibroblastos, osteoblastos y células endoteliales); b) compartimento no celular que abarca la matriz extracelular y el medio líquido compuesto por citocinas y factores de crecimiento que son producidos por las diferentes poblaciones celulares dentro del microambiente de la MO.

Las células estromales mesenquimales de la MO son células precursoras de una variedad amplia de tipos celulares presentes en la MO, como los adipocitos, osteoblastos y fibroblastos. La interacción bidireccional entre estas células y las CPs tumorales promueve el desarrollo de la enfermedad activando diferentes vías de señalización en las CPs, que inducen la proliferación y migración celular, así como el aumento de la expresión de proteínas que contribuyen a evadir las señales de muerte celular por apoptosis y la resistencia a fármacos[85].

7. Tratamiento del mieloma múltiple

Antes del año 2000 la mediana de supervivencia global de los pacientes con MM rondaba los 30 meses[86], pero en los últimos 20 años el tratamiento del MM ha evolucionado notablemente, pasando desde la quimioterapia convencional a estrategias terapéuticas más dirigidas basadas en los mecanismos oncogénicos de la célula mielomatosa y en dianas concretas. Estos avances han prolongado significativamente la supervivencia de los pacientes con MM y mejorado su calidad de vida[87,88].

El tratamiento del MM de nuevo diagnóstico está definido en gran medida por la edad y por el estado general del paciente, ya que en los enfermos menores de 65 ó 70 años después del tratamiento de inducción a la remisión se lleva a cabo una consolidación y/o profundización de la respuesta mediante el trasplante autólogo de progenitores hematopoyéticos (TAPH) con un acondicionamiento basado en agentes alquilantes[86,89–93].

Los fármacos disponibles y los que están aún en fase de ensayo clínico se pueden agrupar en diferentes clases: corticosteroides, quimioterapia, inhibidores del proteasoma, agentes inmunomoduladores, fármacos con mecanismos de acción específicos, y la inmunoterapia. La posibilidad tan amplia de combinaciones que se pueden utilizar constituye todo un reto para los hematólogos, pero una gran esperanza para aquellos pacientes que desarrollan resistencias[94–97]. Las diferentes combinaciones de fármacos que constituyen los esquemas estándar en la actualidad han logrado que la mediana de SG en el MM sea actualmente de unos 6 años, y de hasta 10 años si el paciente es candidato a TAPH.

7.1. Corticosteroides y quimioterapia convencional

La dexametasona y el agente alquilante melfalán siguen siendo los fármacos más utilizados en el tratamiento del MM. La dexametasona forma parte de la mayoría de las combinaciones utilizadas en la actualidad y el melfalán fue el primer fármaco quimioterápico en demostrar actividad antimieloma desde los años 60[94,98–100], y en la actualidad forma parte del régimen de acondicionamiento para el TAPH. La quimioterapia convencional también abarca otros fármacos como la vincristina, la ciclofosfamida y la bendamustina[101–103].

7.2. Inhibidores del proteasoma

Los inhibidores del proteasoma como el bortezomib, el carfilzomib y el ixazomib, forman parte ya de los estándares de tratamiento para el MM y han conseguido prolongar la supervivencia de los pacientes. Estos tres compuestos son inhibidores de la subunidad catalítica β-5 del proteasoma, aunque el bortezomib y el ixazomib, ambos inhibidores reversibles, pueden también unirse a las subunidades β-1 y β-2 con una menor afinidad y a elevadas concentraciones[104,105]. El carfilzomib por su parte tiene una mayor afinidad que el bortezomib por la subunidad β-5 y su unión al proteasoma es irreversible[106].

En general, la inhibición del proteasoma da lugar a la acumulación de proteínas no plegadas en el retículo endoplasmático (RE), produciendo lo que se conoce como estrés del RE que conduce a la activación de señales antiproliferativas, desencadenándose una parada del ciclo y activación de la vía de muerte celular por apoptosis[107]. También se ha reportado que los inhibidores del proteasoma bloquean la activación de la vía *NF-κB*, estimulan la infraexpresión de moléculas de adhesión celular e inhiben los mecanismos de reparación del ADN así como la angiogénesis[108,109].

7.3. Fármacos inmunomoduladores

Los fármacos inmunomoduladores (IMiDs) utilizados en la actualidad son la lenalidomida y la pomalidomida. Su mecanismo de acción es pleiotrópico y engloba un efecto antitumoral directo, un efecto inmunomodulador y un efecto antiangiogénico. La actividad antitumoral de los IMiDs se ejerce a través de la inducción de muerte celular por apoptosis, y la inhibición de las interacciones entre las células mielomatosas y las células del microambiente que son vitales para la supervivencia y proliferación celular. El efecto inmunomodulador de los IMiDs está definido por la producción de interleucina 2 (*IL2*) e interferón gamma (*IFN*γ) por parte de las células efectoras del sistema inmune, lo que resulta en una potenciación de la proliferación de las células NKs (*natural killer*) y la citotoxicidad de las células T[110,111]. Finalmente, el efecto antiangiogénico que promueven los IMiDs se ha asociado con la disminución del factor de crecimiento del endotelio vascular (*VEGF*) y de la interleucina 6 (*IL6*)[112]. En el 2010, se descubrió que la proteína cereblón (*CRBN*) es la diana directa de los IMiDs[113,114]. El cereblón es uno de los cuatro componentes del complejo de ligasa culina-RING E3 que media la ubiquitinación y la degradación de las proteínas por el proteasoma. Cuando los IMiDs se unen al cereblón se altera la especificidad de los sustratos del complejo ligasa culina-RING E3, que lleva a la degradación de dos factores de transcripción vitales para la CP, Ikaros (*IKZF1*) y Aiolos (*IKZF3*), así como a la disminución en los niveles de sus respectivas dianas, Irf4 y c-Myc[115].

Los llamados moduladores de la ligasa cereblón E3 (CELMoDs), funcionalmente diferentes a los IMiDs pero basados en sus características, son también inmunomoduladores del complejo de ligasa E3 como los IMiDs[115]. Dentro de los CELMoDs que están actualmente en ensayos clínicos están la iberdomida (IBER/CC-220) (NCT02773030)[116], la avadomida (CC-122) (NCT01421524)[117] y el CC-92480 (NCT03374085)[118119].

7.4. Inhibidores de dianas específicas

Entre los fármacos con dianas específicas está el selinexor, un inhibidor de la exportina 1 (*XPO1*) que fue aprobado en el 2019 para el tratamiento de los pacientes con MM en recaída en combinación con el bortezomib y la dexametasona[120,121]. También encontramos el panobinostat, un inhibidor de deacetilasas de histonas aprobado también para el tratamiento de pacientes con MM refractario o en recaída en combinación con bortezomib y dexametasona. Sin embargo, preocupa especialmente su seguridad y tolerancia, debido a los efectos secundarios que produce, como trombocitopenia, y toxicidad gastrointestinal[122,123].

El venetoclax es un inhibidor de la proteína Bcl-2, aprobado por la Administración de Alimentos y Medicamentos (FDA) en Estados Unidos en 2016, para el tratamiento de los pacientes con leucemia linfocítica crónica (LLC) refractarios con deleción de 17p[124]. Este fármaco se une a Bcl-2 inhibiendo su actividad como proteína antiapoptótica con lo cual su efecto es mayormente la inducción de apoptosis[125]. Es particularmente más eficaz en aquellos casos de

MM con t(11;14) que suelen tener altos niveles de Bcl-2 comparado con los niveles de Bcl-XL y Mcl-1, otras 2 proteínas antiapoptóticas[126].

7.5. Inmunoterapia

Anticuerpos monoclonales

El uso de los anticuerpos monoclonales en el MM ha revolucionado el tratamiento de los pacientes[127–130]. Destacan los que se dirigen de manera específica frente a antígenos presentes en la superficie de las CP tumorales, como el daratumumab[131,132], el isatuximab/SAR-650984[133], y el felzartamab[134] que son anticuerpos anti-CD38; y el elotuzumab, que es un anticuerpo dirigido a la molécula SLAMF7/CD319[135–137].

Un avance más en la tecnología de los anticuerpos monoclonales con mayor interés y crecimiento en los últimos años es el desarrollo de los anticuerpos monoclonales conjugados a drogas, en los que se aprovecha la especificidad del anticuerpo para liberar drogas citotóxicas potentes en las células tumorales. Entre estos, el belantamab mafodotina compuesto por un anticuerpo frente al antígeno BCMA (*B cell maturation antigen*) conjugado con el inhibidor *microtubular monometil auristatina F* (MMAF) es el primero aprobado para el tratamiento del MM. El BCMA, también denominado TNFRSF17 y CD269, se expresa exclusivamente en las células con linaje B particularmente en la región interfolicular del centro germinal, en los plasmablastos y las CPs diferenciadas[138–140]. Dado que el BCMA está amplia y altamente expresado en las CPs tumorales del MM[141,142], constituye el antígeno ideal como diana para la inmunoterapia en el MM. En desarrollo se encuentran otros anticuerpos conjugados a droga dirigidos a CD56 (lorvotuzumab mertansina)[143] y CD74 (milatuzumab-doxorrubicina y STRO-001)[144,145].

Otra estrategia de inmunoterapia consiste en inhibir los llamados *checkpoints* o puntos de control inmunológicos para potenciar la vigilancia inmunológica del paciente frente a las células tumorales. Las CPs tumorales contrariamente a las CPs normales expresan PD-L1[146] y las células T de los pacientes con MM expresan niveles aumentados de su receptor, PD-1[147]. Así la interacción PD-1/PD-L1 promueve la inhibición del linfocito T. Anticuerpos anti-PD-1, como el pembrolizumab y el nivolumab, se han evaluado en monoterapia y en diferentes combinaciones en el MM en recaída o refractario[148–150].

Anticuerpos biespecíficos

El uso de anticuerpos biespecíficos es una de las nuevas estrategias de inmunoterapia con más desarrollo en estos momentos. Estos compuestos tienen dos dominios de unión, uno de ellos se une a un antígeno de superficie en las células tumorales y el otro lo hace a las células efectoras del sistema inmune como el CD3 en los linfocitos T, o el CD16 en las células NK[151]. Los anticuerpos biespecíficos se clasifican como de tipo IgG cuando tienen la región constante (Fc), y

de tipo no IgG, cuando no tienen una región Fc. Dentro de los de tipo no IgG, se encuentran los BiTEs (*Bispecific T cell Engager*) que son un tipo de *single-chain variable fragment* (scFv) en tándem, en el que los fragmentos scFv están diseñados para unirse a un antígeno de superficie en las células tumorales y a su vez al CD3 en las células T, redirigiéndolas contras las células tumorales[152]. El primer BiTE probado en el MM fue el BI 836909, dirigido a la activación de células T mediante la unión al CD3 y al antígeno BCMA. Los primeros estudios con el BI 836909 mostraron su efecto antimieloma selectivo en las células mielomatosas BCMA-positivas, *in vitro* e *in vivo*, mientras que las células BCMA-negativas no fueron afectadas[153]. AMG 701 es otro BiTE anti-BCMA con una vida media más larga[154], y CC-93269 es otro anticuerpo biespecífico que se une de forma bivalente al BCMA y monovalente al CD3[155].

Existen otros BiTE, con dianas distintas al BCMA, como son el cevostamab que es un anti-FcRH5/CD3; y el talquetamab/JNJ-64407564 que está dirigido al receptor GPRC5D (*orphan G protein–coupled receptor class C group 5 member D*), que se expresa en la superficie de las CPs en el MM y el MMQ[156,157].

7.6. Terapia de células T con receptor antigénico quimérico

En la actualidad la terapia de células T con receptor antigénico quimérico o también llamadas terapias de células CAR-T es un hito en el tratamiento del cáncer. Los linfocitos T se recolectan de la sangre del paciente, se modifican mediante ingeniería genética para que expresen anticuerpos monoclonales contra antígenos específicos de un tumor[95] en su superficie, y se vuelven a administrar al paciente después de una quimioterapia de linfodepleción.

Para el tratamiento del MM existen en la actualidad varios CAR-T dirigidos contra diferentes dianas que se han evaluado en diferentes estudios clínicos. Concretamente existen más de 40 ensayos clínicos que han evaluado o están evaluando terapias CAR-T en el MM. El antígeno BCMA es la diana más utilizada[95]. El idecaptagene vicleucel (Ide-cel/Abecma/bb2121), fue la primera terapia de células CAR-T dirigida contra el BCMA, que fue aprobada por la FDA en el 2021 para pacientes con MM en recaída o refractarios. El JNJ-4528 (JNJ-68284528/ciltacabtagene autoleucel/cilta-cel) es otro CAR-T con dos dominios de unión al BCMA[158,159].

Además de las terapias con CAR-T dirigidas contra el BCMA se están evaluado varias estrategias que difieren en el antígeno diana, utilizando otros como CD38, CD138, CD19 y SLAMF7. También se ha probado la combinación de antígenos o la incorporación de moléculas co-estimuladoras como por ejemplo 4.1BB y CD28, para obtener un CAR-T con una especificad múltiple[160].

7.7. Reposicionamiento de fármacos

El cáncer es la sexta causa de muerte en el mundo y la segunda en Europa, por detrás de las enfermedades cardiovasculares, según el informe de la Organización Mundial de la Salud

(WHO) de 2019. Si bien los avances tecnológicos han permitido el desarrollo de nuevas drogas que aumentan la supervivencia de los pacientes oncológicos, también se han generado nuevos mecanismos de resistencia a estos fármacos[161]. Por otro lado, el desarrollo de nuevos fármacos es un proceso largo y costoso. Algunos estudios han llegado a reportar un coste de 2 billones de dólares en promedio y de 13-15 años de desarrollo[162,163]. Así, el llevar a la práctica clínica estas nuevas formulaciones suele llevar mucho más tiempo del esperado y a un coste muy alto.

El proceso de desarrollo de nuevos fármacos tiene varias etapas. Una fase de descubrimiento o diseño de la droga, una posterior de experimentación, tanto *in vitro* como *in vivo*, para evaluar la eficacia antitumoral del fármaco y la seguridad, y dependiendo de los resultados experimentales se valora la realización del ensayo clínico que consta principalmente de 3 fases, hasta la posterior solicitud de aprobación y registro del fármaco, aunque en realidad son pocos los nuevos agentes terapéuticos que son capaces de pasar a fases clínicas de la investigación.

El reposicionamiento de medicamentos en oncología consiste en el uso de fármacos originalmente formulados para otras indicaciones que han mostrado una potencial actividad antitumoral. Esta estrategia de *new uses for old drugs*, no es nueva, sino que ha ido ganando seguidores, tanto investigadores como médicos, en los últimos años, sobre todo por las ventajas que presenta frente al desarrollo de nuevas drogas. El perfil farmacocinético, farmacodinámico y de toxicidad ya han sido establecidos previamente en sus estudios originales preclínicos y clínicos. Además, se conocen las dosis que se utilizan usualmente en humanos y se sabe si tienen efectos secundarios asociados, con lo que en los ensayos clínicos estas drogas podrían progresar rápidamente a una fase II o III, reduciéndose significativamente el coste y ganando en tiempo. Incluso, en la actualidad existen múltiples herramientas y bases de datos con información sobre los fármacos existentes, las interacciones entre ellos y la relación entre la droga y la enfermedad, así como sobre las vías de señalización y proteínas celulares que podrían ser potenciales dianas de fármacos existentes[164]. El proyecto internacional de colaboración ReDo (*Repurposing Drugs in Oncology*) es uno de estos recursos que puede ayudar en el proceso de reposicionamiento de fármacos (www.redo-project.org)[165], o el también conocido repositorio online *Drug Repurposing Hub* (www.broadinstitute.org/repurposing) que reúne información sobre más de 3 000 drogas que han sido testadas en ensayos clínicos[166].

La talidomida es el ejemplo clásico de reposicionamiento de drogas. Se utilizó en los años 50 para el tratamiento de las náuseas en las mujeres embarazadas, pero años después fue totalmente proscrita por sus graves efectos teratógenos. Sin embargo, en el 2006 fue aprobada por la FDA para el tratamiento en monoterapia del MM refractario[167]. La talidomida podía inducir una elevada tasa de respuestas duraderas en algunos pacientes con MM, incluyendo los refractarios después de altas dosis de quimioterapia[167]. Posteriormente, se demostró su eficacia en pacientes jóvenes con MM de nuevo diagnóstico combinada con la dexametasona como tratamiento de inducción previo al TAPH[168]. También la combinación de la talidomida con melfalán y prednisona fue superior al estándar de melfalán más prednisona en pacientes mayores de nuevo diagnóstico sin tratamiento previo[169,170].

El antiviral nelfinavir, un inhibidor de proteasas del virus de inmunodeficiencia humana, tiene también actividad antimieloma y es capaz de superar la resistencia al bortezomib[171]. De hecho, el ensayo clínico NCT01555281 en curso, está evaluando la combinación de nelfinavir con lenalidomida/dexametasona en pacientes con MM refractarios a terapia previa con lenalidomida. Otros fármacos utilizados para diferentes indicaciones que también presentan actividad antimieloma son el antiinflamatorio celecoxib, el inmunosupresor leflunomida, el ácido valproico, la fluvastatina y el tofacitinib[172–175].

8. Procesamiento o *splicing* del pre-ARNm

Los ARN mensajeros (ARNm) son el resultado del proceso celular conocido como transcripción, donde la información contenida en el ADN genómico es transcrita a moléculas de pre-ARNm, que serán procesadas, traducidas y expresadas en forma de proteínas para llevar a cabo su función celular[176]. El procesamiento o *splicing* constitutivo del pre-ARNm (denominado a partir de ahora como *splicing* del pre-ARNm) consiste en la escisión de las zonas no codificantes de la molécula de pre-ARNm, los intrones, y la consecutiva unión de las regiones codificantes, los exones, generándose los ARNs mensajeros maduros. El *splicing* del pre-ARNm es un proceso altamente regulado que es esencial para la expresión de más del 95 % de los genes humanos[177,178].

8.1. Maquinaria del *Spliceosoma*

El *splicing* del pre-ARNm se lleva a cabo por el *spliceosoma*, que es una de las maquinarias celulares más complejas. En términos generales, este macrocomplejo está compuesto por 5 ribonucleoproteínas pequeñas nucleares (snRNPs) U1, U2, U4, U5 y U6 que integran el núcleo catalítico, y alrededor de 200 proteínas que incluyen entre otras, a cinasas, fosfatasas y helicasas (Figura 2).

Todas ellas interactúan dinámicamente entre sí y con las 5 snRNPs, conformando cada uno de los complejos que participan en el ensamblaje del *spliceosoma* sobre la hebra del pre-ARNm para llevar a cabo su *splicing*[180–182].

El ensamblaje del *spliceosoma* es estrictamente dependiente de la presencia de secuencias consenso ubicadas en los intrones y en sus límites con el exón: 1) el sitio de *splicing* 5' (5'ss), con secuencia GURAGU, y 2) el sitio de *splicing* 3' (3'ss), que está conformado por 3 secuencias distintas localizadas en los 40 primeros nucleótidos previos a la unión exón-intrón, y que incluye la secuencia YNURAY llamada *branch point* (BP), un tracto de polipirimidinas YYY (4-24 nt), y el dinucleótido AG, en el extremo 3' del intrón[183–186]. La escisión del intrón ocurre a través de dos reacciones consecutivas de transesterificación, que implican la ruptura y formación de enlaces fosfodiéster (Figura 3).

El ensamblaje del *spliceosoma* comienza con el reconocimiento y unión al 5'ss de la snRNP

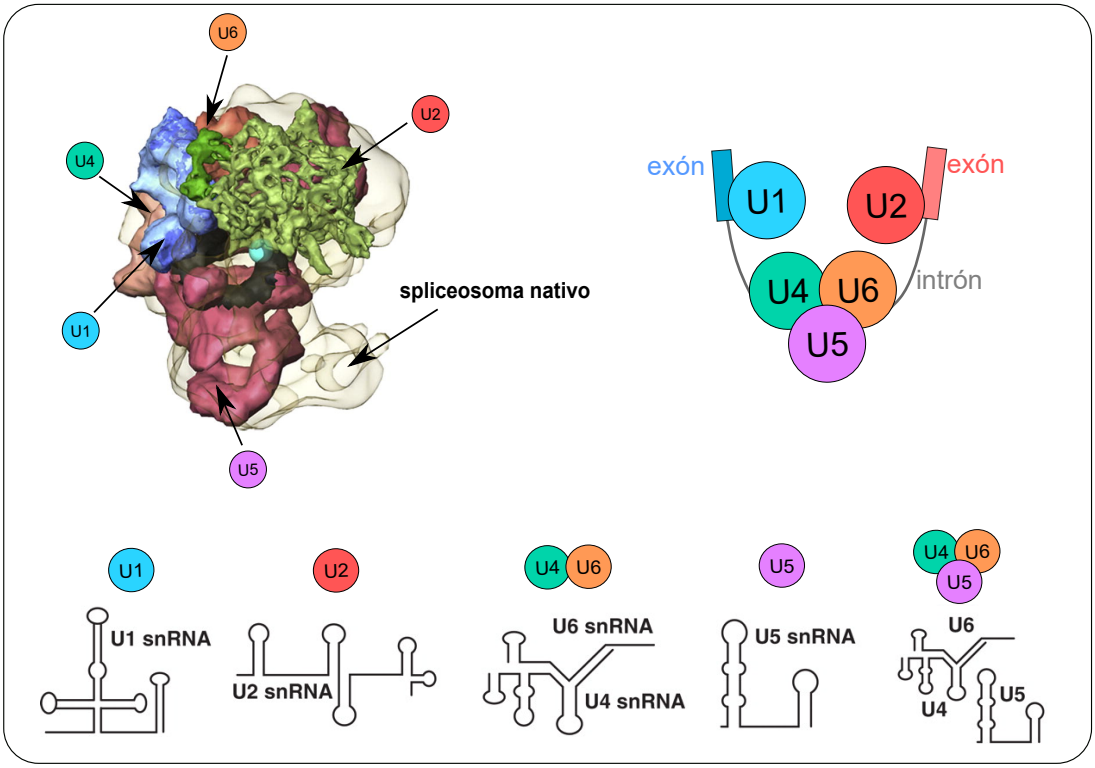

Figura 2. Estructura tridimensional y esquemática del *spliceosoma*. Se muestra la estructura secundaria de cada una de las 5 snRNPs. Modificada de Frankenstein *et al.*[179]

U1, la unión del factor de *splicing* 1 (SF1, también denominado proteína de unión al BP) al BP, y de las proteínas U2AF1 y U2AF2 al dinucleótido AG del 3'ss y al tracto de polipirimidina YYY, respectivamente, formando el complejo E o *spliceosoma* temprano. El siguiente paso conlleva la unión estable, dependiente de ATP, de la snRNP U2 alrededor de la secuencia YNURAY desplazando a la proteína SF1, y formándose el complejo A o pre-*spliceosoma*. La proteína SF3B1 es un componente esencial de U2 que reconoce el BP y la hélice de U2-pre-ARNm, facilitando la aproximación de la adenosina del BP al 5'ss, para que se produzca el primer paso de la

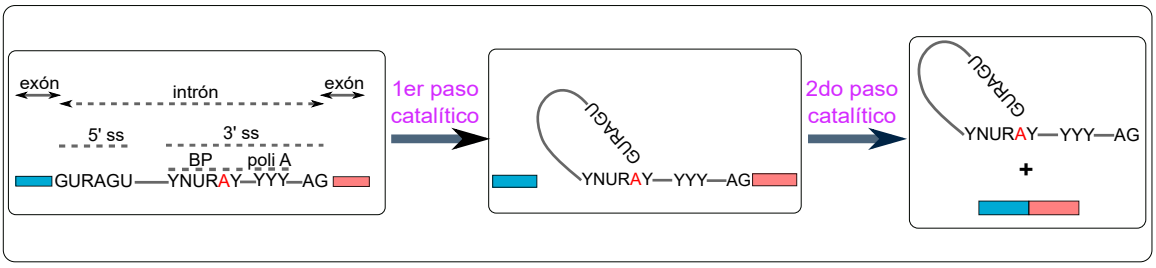

Figura 3. *Splicing* del pre-ARNm. El proceso químico de eliminación del intrón ocurre a través de dos sucesivas reacciones de transesterificación, que implican la ruptura y formación de enlaces fosfodiéster. El primer paso o reacción catalítica genera dos elementos intermedios: el exón 5' y una estructura en forma de lazo que contiene un inusual enlace 2'–5' fosfodiéster que involucra el nucleótido 5' del intrón y el residuo de adenosina interno (A). En la segunda reacción catalítica los dos exones se unen y el intrón es liberado en forma de lazo. Modificada de Bonnal y Valcárcel *et al.*[187] Y es una pirimidina, N es cualquier nucleótido, A es la adenosina involucrada en el segundo paso catalítico, y R es una purina.

reacción de *splicing*[188,189]. En este punto, la triada U4–U6–U5 se une formando el complejo B o pre-catalítico e induciendo importantes cambios conformacionales e interacción de proteínas participantes, que habilitan la formación del núcleo catalítico del *spliceosoma*, pasando por las conformaciones catalíticamente activas del complejo B activado (primer paso catalítico) y complejo C y C activado (segundo paso catalítico), para finalmente completar la reacción de *splicing*[190,191] (Figura 4). Es importante señalar que cada uno de los complejos que se forman en el ensamblaje del *spliceosoma* o ciclo del *splicing* tiene una composición única, y la conversión de los complejos es llevada a cabo por varias ATPasas/helicasas dependientes de ARN que son altamente conservadas. Además, estos complejos pueden adoptar distintas conformaciones que pueden variar su composición.

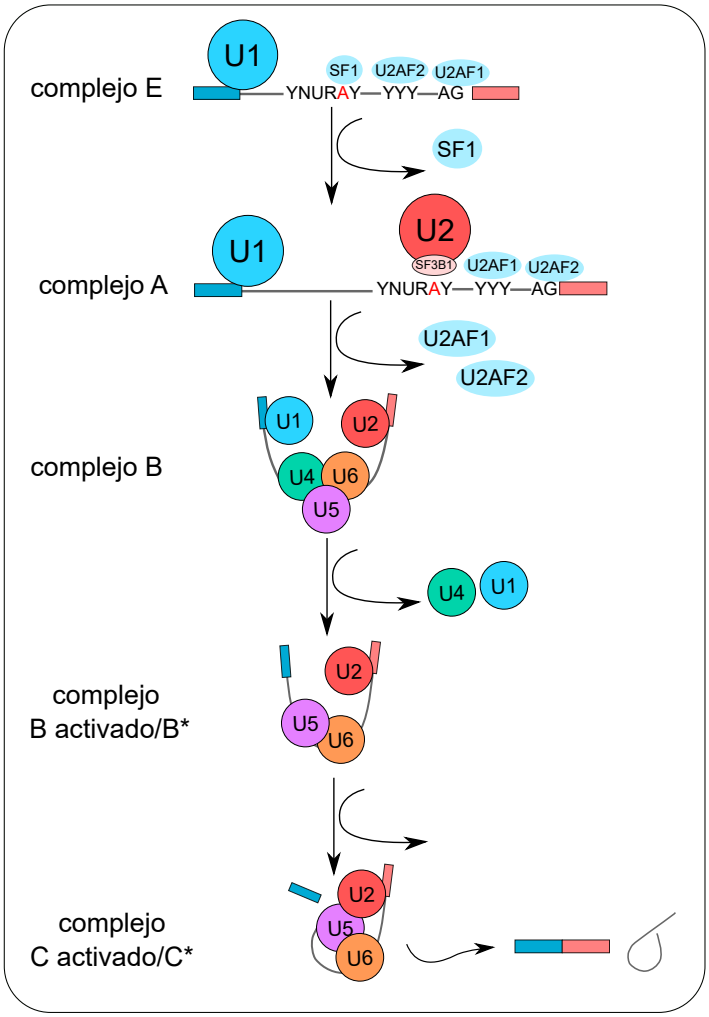

Figura 4. Ensamblaje del *spliceosoma*. El 5'ss, BP y 3'ss son reconocidos por U1, SF1 y U2AF (U2AF1 y U2AF2), respectivamente, formando el complejo E. SF1 es desplazada por la snRNP U2, constituyendo el complejo A o pre-*spliceosoma*, que seguidamente se asocia con la triada de snRNPs U4/U6-U5 para formar el complejo B o pre-catalítico. De esta forma el complejo B constituye el primer complejo que incluye las 5 snRNPs del *spliceosoma* acopladas al pre-ARNm. Existen adicionalmente al menos 6 complejos del *spliceosoma* distintos que se suceden seguidamente: complejo B activado (*spliceosoma* activado), complejo B* (*spliceosoma* catalíticamente activado), complejo C (primer paso catalítico), complejo C* (segundo paso catalítico), complejo P (complejo post-*splicing* y el complejo ILS (*spliceosoma* unido al lazo del intrón) que culmina con la liberación del intrón en forma de lazo.

9. *Splicing* alternativo

No fue hasta años después del descubrimiento del *splicing* constitutivo del pre-ARNm en 1977 por Phillip Allen Sharp[192] y Richard John Roberts[193], lo que les valió el Premio Nobel de Fisiología y Medicina en 1993, cuando se descubrió que el *splicing* no sigue un patrón invariable, sino que a partir de un gen se pueden obtener diferentes ARNm y en consecuencia producirse más de una proteína funcional. De manera que mientras que el *splicing* constitutivo del pre-ARNm es un proceso de eliminación de los intrones y unión de la mayoría de los exones que tiene un gen, el *splicing* alternativo desvía o altera esa preferencia por generar una secuencia única, y se salta determinados exones, dejándoles fuera de la secuencia del ARNm, resultando en otra variante o transcrito distinto al constitutivo. Este proceso, definido bajo el término de *splicing* alternativo, es uno de los responsables de la alta complejidad y heterogeneidad a nivel de transcriptoma y proteoma celular. De hecho, el proceso de *splicing* alternativo puede llegar a tener un importante efecto en la función de los genes, dado que los diferentes transcritos o isoformas generadas pueden estar implicadas en procesos biológicos distintos, o incluso llegar a tener funciones totalmente opuestas aunque provengan del mismo gen. Con lo cual queda en evidencia su relevancia en el mantenimiento de la homeostasis y la diferenciación celular[177,178]. Según el último informe (2021) de la anotación de referencia GENCODE 39 (GRCh38.p13), que recoge la identificación y descripción de los genes del genoma humano y de ratón, existen 61 533 genes anotados y 244 939 transcritos, también llamados isoformas y variantes del ARNm (www.gencodegenes.org). Así, por cada gen humano hay un promedio de 3-4 transcritos anotados, y de hasta 7 por cada gen codificante a proteína.

Los patrones de *splicing* alternativo son diversos, aunque alguno es más frecuente que otros. El evento de exclusión de exón es el más frecuente en mamíferos, pero también pueden ocurrir otros como los sitios de *splicing* 3' y 5' alternativos, el uso de promotores o sitios de poliadenilación alternativos, y retención de zonas intrónicas (Figura 5). También pueden darse simultáneamente varios de estos eventos con lo cual las posibilidades de tener un vasto repertorio de isoformas son bastante amplias.

10. Regulación del *splicing* del pre-ARNm

El *splicing* del pre-ARNm es un proceso muy regulado. Además de las secuencias consenso ubicadas en los intrones que son esenciales para el ensamblaje del *spliceosoma*, como se describió en el apartado anterior, existen elementos reguladores adicionales en *cis* y en *trans* que regulan la unión de otros factores del *splicing* (Figura 6). Los elementos reguladores en *cis* son secuencias que incluyen los sitios ESEs y ESSs (*exonic splicing enhancers* y *exonic splicing silencers*), y los sitios ISEs y ISSs (*intronic splicing enhancers* e *intronic splicing silencers*). Los 4 tipos de secuencias pueden estar localizados en cualquier lugar dentro de la secuencia del pre-ARNm. Los elementos reguladores en *trans* son factores proteicos de unión al ARN que incluye dos grandes

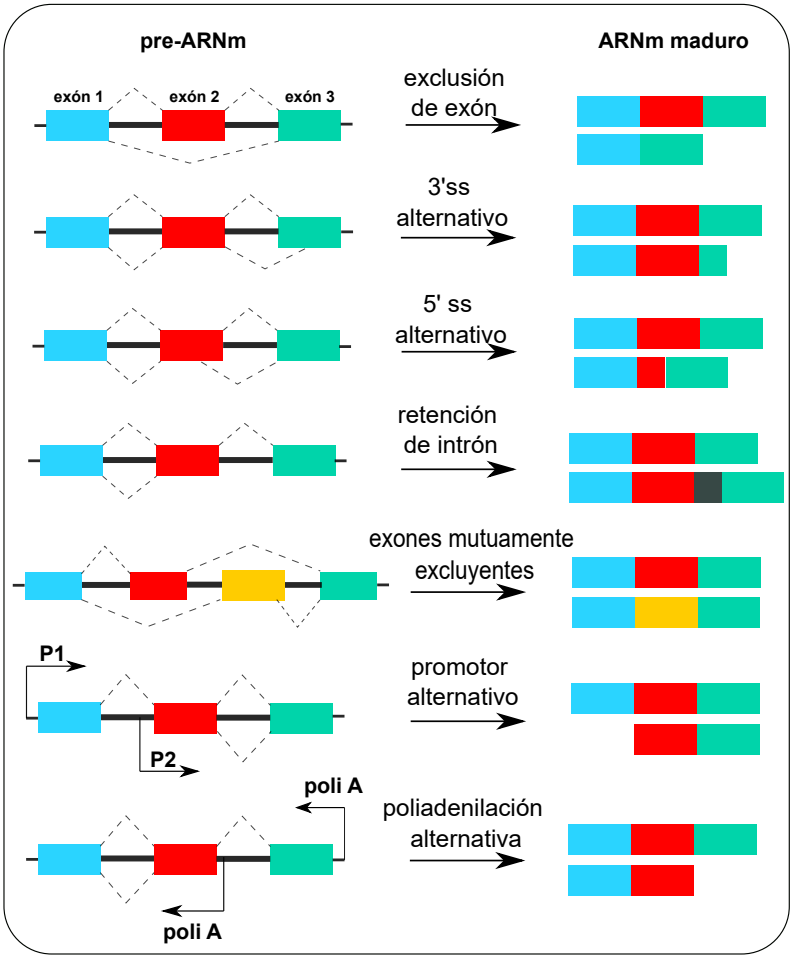

Figura 5. Eventos de *splicing* alternativo más comunes.

familias: la familia de proteínas SR, cuyo nombre hace referencia a los dominios carboxi-terminal ricos en residuos de serina y arginina, y que generalmente se unen a los sitios ESEs y promueven el *splicing* (estimuladores del *splicing*); y la familia de las proteínas hnRNPs (*heterogeneous nuclear ribonucleoproteins*), que reconocen los sitios ESSs e ISSs e inhiben el *splicing* (inhibidores del *splicing*)[194]. De manera que los elementos reguladores exónicos e intrónicos pueden estimular o inhibir el reconocimiento del 5'ss por la snRNP U1 o el 3'ss por las proteínas SF1, U2AF1, U2AF2 o la snRNP U2, afectando la elección del sitio de *splicing* y por lo tanto las decisiones del *splicing* alternativo.

Las proteínas SR son proteínas de unión al ARN caracterizadas por la presencia de un dominio C-terminal rico en residuos de arginina (R) y serina (S) (dominio SR), que actúa facilitando la interacción proteína-proteína y favoreciendo el ensamblaje del *spliceosoma*[195,196], y uno o dos motivos con capacidad de reconocimiento y unión al ARN (dominio RRM) en el dominio N-terminal. Ambos dominios están unidos mediante un espaciador rico en residuos de glicina y arginina (Figura 7). El dominio SR también actúa como una señal de localización nuclear, afectando la localización celular de las proteínas SR[197]. Las proteínas SR están evolutivamente

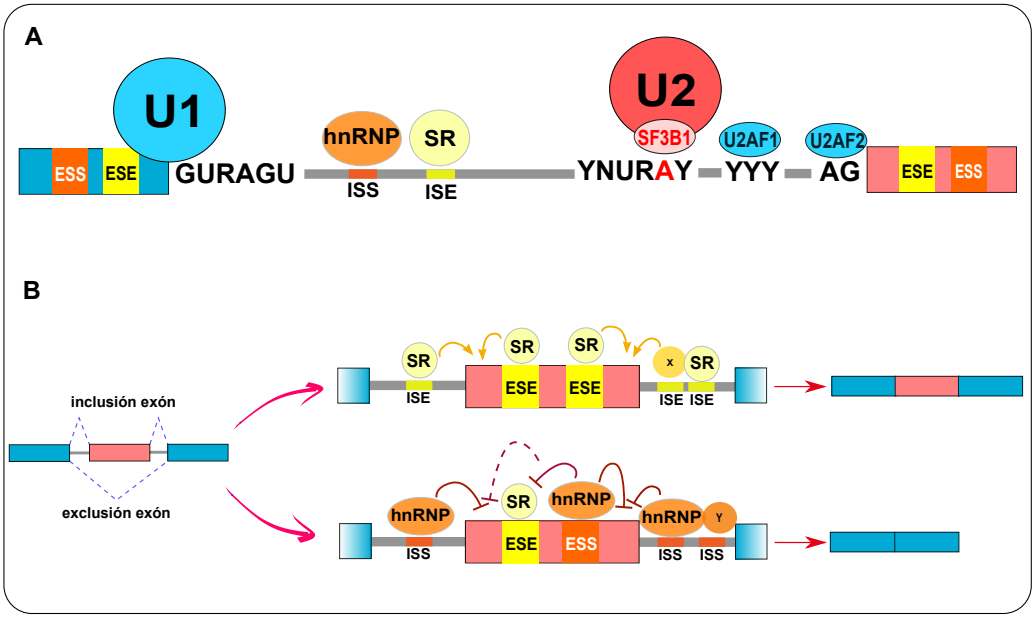

Figura 6. Mecanismos de regulación del *splicing*. (A) Las proteínas SR y las hnRNPs se unen a los elementos exónicos (ESE, ESS) o intrónicos (ISE, ISS) reguladores, promoviendo o inhibiendo el reconocimiento del sitio 5'ss por la ribonucleoproteína U1, o del sitio 3'ss por las proteínas SF1, U2AF2, U2AF1 o U2. (B) Ejemplo de cómo se regula la inclusión o exclusión de un exón a través de estos mecanismos de regulación. La unión de las proteínas hnRNPs a los elementos reguladores inhibe el reconocimiento de los sitios 5'ss y 3'ss del exón alternativo, resultando en la exclusión del exón alternativo de la secuencia del ARNm.

conservadas, la longitud del dominio SR y la adición de otros dominios definen a los 12 distintos miembros de la familia, desde el *SRSF1* hasta el *SRSF12*[198–200]. Esta familia no sólo participa en el *splicing* constitutivo del ARNm y el *splicing* alternativo sino también en otras funciones post-*splicing* como la exportación nuclear de los ARNm, y la traducción del ARNm a proteína. Así, la mayoría de las proteínas SR se localizan exclusivamente en el núcleo celular, mientras que otras pueden moverse y localizarse también en el citoplasma[201–203].

La fosforilación es uno de los principales mecanismos de regulación mejor estudiados de esta familia de proteínas, aunque también pueden ocurrir otros eventos postraduccionales como la metilación y la acetilación[204]. Los residuos de serina del dominio SR pueden ser fosforilados y de esta forma regular la localización celular de la proteína SR y su interacción con las proteínas del *spliceosoma*. Entre las cinasas que fosforilan a las proteínas SR se encuentra la familia *SRPK* (*SR protein kinase*)[205,206], la familia Clk/Sty[207] y la topoisomerasa I[208].

Las ribonucleoproteínas heterogéneas nucleares (hnRNPs) forman parte de una extensa familia de proteínas de unión al ARN, que participan en diferentes procesos del metabolismo de los ácidos nucleicos como la estabilización del ARNm, la regulación transcripcional y traduccional, y el *splicing* alternativo, donde específicamente actúan con función opuesta a la de las proteínas SR. La estructura general de las hnRNPs consiste en múltiples dominios de unión al ARN conectados por regiones enlazadoras de longitud variable que han sido nombradas desde la hnRNP A1 hasta hnRNP U (Figura 8). Las hnRNPs involucradas en el control del *splicing* mejor

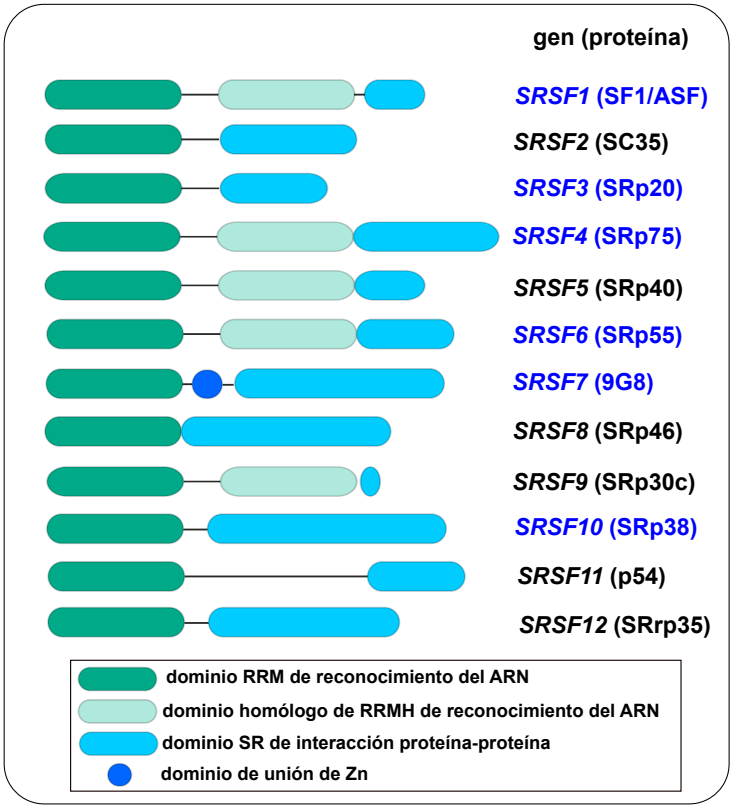

Figura 7. Estructura esquemática de los miembros de la familia de proteínas SR. En color azul se representan aquellas que pueden localizarse en el núcleo y el citoplasma de la célula, mientras que el resto (en negro) se encuentran exclusivamente en el núcleo. Entre paréntesis se referencia el nombre de la proteína.

caracterizadas hasta el momento son la hnRNP A/B y la hnRNP I, también llamada proteína PTB (*polypyrimidine tract-binding protein*). Las hnRNPs tienen una distribución más bien difusa y pueden localizarse tanto en el núcleo como en el citoplasma celular gracias a la presencia en su estructura de una secuencia de localización nuclear y/o dominios que permiten su traslado a citoplasma para cumplir determinadas funciones[209].

11. Desregulación del *splicing* del pre-ARNm

La desregulación del *splicing* del pre-ARNm se ha relacionado ampliamente con las patologías humanas, desde las enfermedades genéticas y neurodegenerativas hasta el cáncer. Se han identificado numerosas alteraciones en las diferentes etapas del *splicing* del pre-ARNm que pueden contribuir a la patogenia de algunas enfermedades.

Concretamente, las mutaciones en los sitios y factores reguladores del *splicing*, específicamente las sustituciones de un solo nucleótido que afectan a los sitios 5'ss y 3'ss, es la mutación más común que afecta al *splicing*. Estas pueden dar lugar a la exclusión de exones del ARNm, la activación de un sitio de *splicing* críptico que en condiciones normales no se utilizaría, o a la retención de intrones (Figura 9). De igual forma, las mutaciones en zonas intrónicas y exónicas pueden

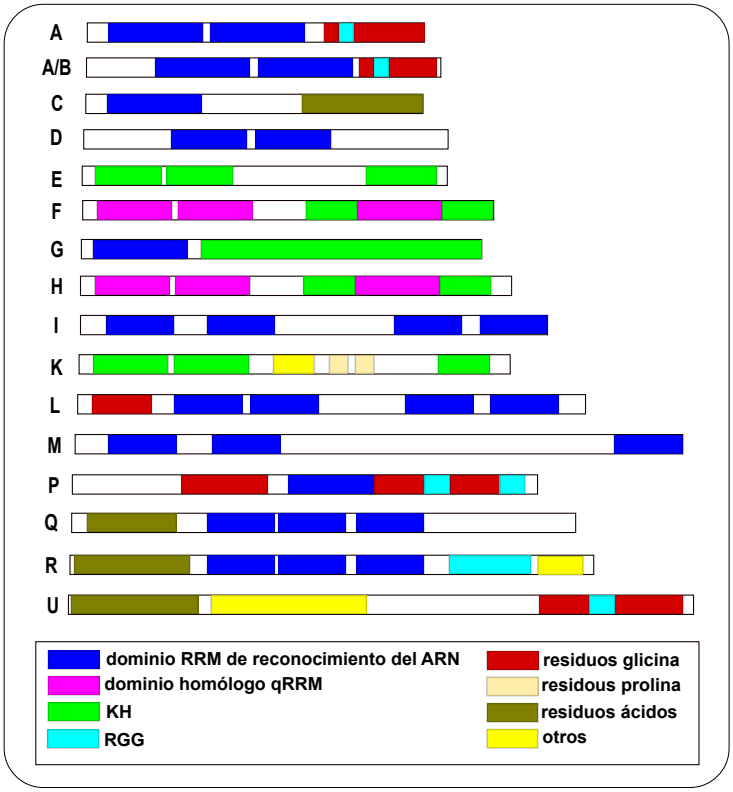

Figura 8. Estructura esquemática de los miembros de la familia de proteínas hnRNPs, donde se muestran los principales dominios de cada uno de los miembros, incluyendo los dominios KH y RGG.

afectar el *splicing* a través de la ganancia o pérdida de sitios reguladores en *cis*, como los ESEs, ESSs, ISEs e ISSs. Este tipo de alteraciones se han identificado asociadas a varias enfermedades como la atrofia muscular espinal[210,211], la fibrosis quística[212], la neuropatía hereditaria llamada disautonomía familiar[213], la distrofia muscular de Duchenne[211,214], la demencia frontotemporal con parkinsonismo-17 (FTDP-17) también conocida como enfermedad de Wilhelmsen-Lynch[215,216], la progeria o síndrome de Hutchinson-Gilford[217], la hipercolesterolemia[218,219], y el cáncer[220,221].

Las mutaciones en genes que codifican para componentes del *spliceosoma* y de la maquinaria del *splicing*, así como aquellas que afectan la biogénesis de las snRNPs, también se han asociado a enfermedades y, particularmente, al cáncer. Las mutaciones en los genes *U2AF1*, *U2AF2*, *SF1*, *SF3A1* y *SF3B1*, cuyas proteínas participan en el reconocimiento del sitio 3'ss en el pre-ARNm, y en la proteína SR, SRSF2, se han detectado en hemopatías como los síndromes mielodisplásicos (SMDs), la leucemia mieloide aguda (LMA), la leucemia linfocítica crónica (LLC) y la leucemia mielomonocítica crónica (LMMC). Pero sin dudas el factor de *splicing* más frecuentemente mutado en cáncer es el *SF3B1*[223], alcanzando frecuencias de hasta un 85 % en los SMD con sideroblastos en anillo (SMD-SA), 6-26 % en la LLC, y 5 % en la LMA y LMMC[224,224–228]. Mutaciones en otros factores de *splicing* como *LUCL7L2*, *PRPF40B*, *SRSF6*, *SRSF1*, *SRSF7*, *TRA2β*, *SRRM2*, *DDX1*, *DDX23*, y *CELF4* también se han identificado en algunas neoplasias hematológicas pero a muy baja frecuencia[229].

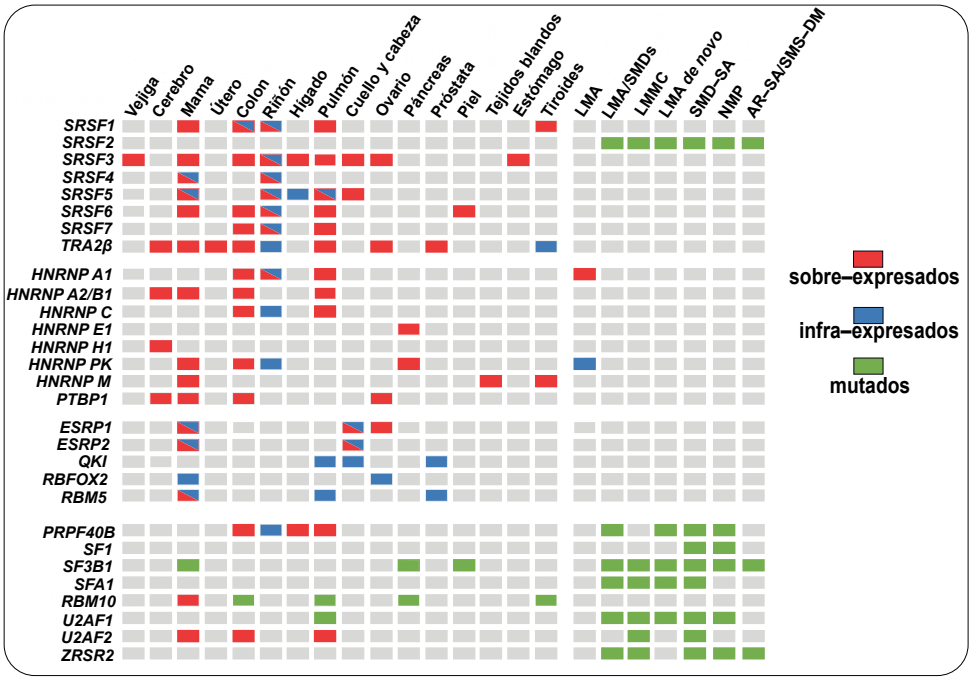

Figura 9. Alteraciones genéticas de los factores del *splicing*. Desregulación de la expresión génica y mutaciones de factores de *splicing* en diferentes tumores humanos. Modificado de Urbanski, Leclair y Anczuków[222].

El *splicing* del pre-ARNm también puede verse alterado por la expresión de los factores de *splicing*. De hecho, más del 70 % de los factores de *splicing* están desregulados a nivel de ARNm en varios cánceres[230–233] (Figura 8). El factor de *splicing* SF2/ASF, fue el primero en reportarse como sobreexpresado en varios tumores sólidos, incluido el de mama y pulmón, debido fundamentalmente a la amplificación de su gen *SRSF1*, evidenciándose su potencial como protooncogén[234]. Además, *SRSF1* es una diana directa de *MYC* y su elevada expresión se ha visto correlacionada con un incremento en la agresividad del tumor, la disminución de la supervivencia y la resistencia a la quimioterapia[234–236].

Las alteraciones en la expresión de los factores del *splicing* repercuten en la expresión y función de sus pre-ARNm dianas. Una evidencia de esto son las alteraciones que se producen en el *splicing* alternativo de los genes diana del propio *SRSF1*, que controlan importantes procesos celulares, como el crecimiento, la supervivencia y la motilidad celulares, así como la muerte celular por apoptosis[222]. *SRSF1* controla el AS de los genes implicados en estas rutas biológicas favoreciendo la producción de isoformas o transcritos de estos genes con propiedades oncogénicas, como por ejemplo *BCL2L1*, *BCL2L11*, *BIN1*, *RPS6KB1*, *MKNK2*, *RON*, *MCL1*, entre otros[237,238] (Figura 10). Por ejemplo, en el caso del gen *RPS6KB1* que codifica para la proteína p85/p70 S6K1, puede dar lugar a 2 isoformas: la isoforma 1 larga, RPS6KB1-1, y la isoforma 2 corta, RPS6KB1-2, debido a la inclusión de los exones alternativos 6a, 6b y 6c. La presencia de un codón de parada en el exón 6c genera una proteína truncada de 31 kDa que tiene el dominio cinasa incompleto. Los altos niveles de la isoforma corta se han detectado en tumores de mama y pulmón, y varios estudios han mostrado su capacidad oncogénica y

contribución en la proliferación celular. Mientras que la isoforma larga tiene una función más de tipo antiproliferativa[234,237,239,240]. *MCL1* es otro de los genes cuyo patrón de *splicing* está regulado por *SRSF1*. Se han descrito 3 isoformas de *MCL1* con funciones opuestas. La isoforma Mcl1-L es antiapoptótica, mientras que las isoformas Mcl1-S y Mcl1-ES favorecen la muerte celular por apoptosis[241,242]. La figura 10 muestra varios ejemplos de expresión de isoformas asociadas a cáncer que son reguladas por diferentes factores de *splicing*, evidenciado el potencial del *splicing* del pre-ARNm como uno de los sellos distintivos de la tumorigénesis[243].

12. Modulación del *splicing* del pre-ARNm como terapia antitumoral

Puesto que las isoformas específicas del AS tienen funciones esenciales en la biología y supervivencia de las células tumorales, y el cáncer presenta una sensibilidad potencialmente mayor a la alteración global de la eficiencia del *splicing* comparado con las células normales, la modulación farmacológica del *splicing* representa una estrategia terapéutica importante. Así, aquellos tumores con alteraciones en genes del *spliceosoma* o con sobreexpresión de isoformas protumorales son más susceptibles de ser abordados terapéuticamente a través de mecanismos que regulen el AS[244–246]. Además, el hecho de que las mutaciones en componentes del *spliceosoma* sean siempre mutuamente excluyentes y se expresen junto al otro alelo en su forma *wild-type*[247], indica que esas células que presentan mutaciones en el *spliceosoma* podrían ser incapaces de tolerar simultáneamente otras alteraciones del *splicing*, y por tanto ser más sensibles a la inhibición farmacológica.

Actualmente existen varios enfoques terapéuticos para modular el *splicing* del pre-ARNm en cáncer así como en otras enfermedades (Figura 11). En este sentido, se han identificado "pequeñas moléculas" con potencial terapéutico que tienen como diana componentes del *spliceosoma*, factores del *splicing*, o los productos del *splicing* como las isoformas.

12.1. Fármacos dirigidos contra componentes del *spliceosoma*

Entre los fármacos que tienen como diana componentes del *spliceosoma* se encuentran 3 familias químicamente distintas, FR901464 (incluye la spliceostatina A/SSA, meayamicina y thailanstatinas A-C), pladienolide B (incluye E7107, H3B-8800 y FD-895) y GEX1 (incluye herboxidieno) que poseen un efecto antiproliferativo o pro-apoptótico *in vitro* en varios modelos murinos de cáncer[248–250]. Estos compuestos se unen a la proteína Sf3b1, bloqueando su conformación en forma abierta, lo que evita el reconocimiento y unión al sitio *branch* (5'ss) del pre-ARNm. La conformación cerrada de Sf3b1 es necesaria para que se produzca el primer paso catalítico del *splicing*. Pero aún no se conoce la razón por la cual estos inhibidores tienen un efecto antitumoral tan potente en vez de provocar una inhibición general del *splicing*. Algunos de estos compuestos se están evaluando actualmente en ensayos clínicos: 1) el H3B-8800, cuya

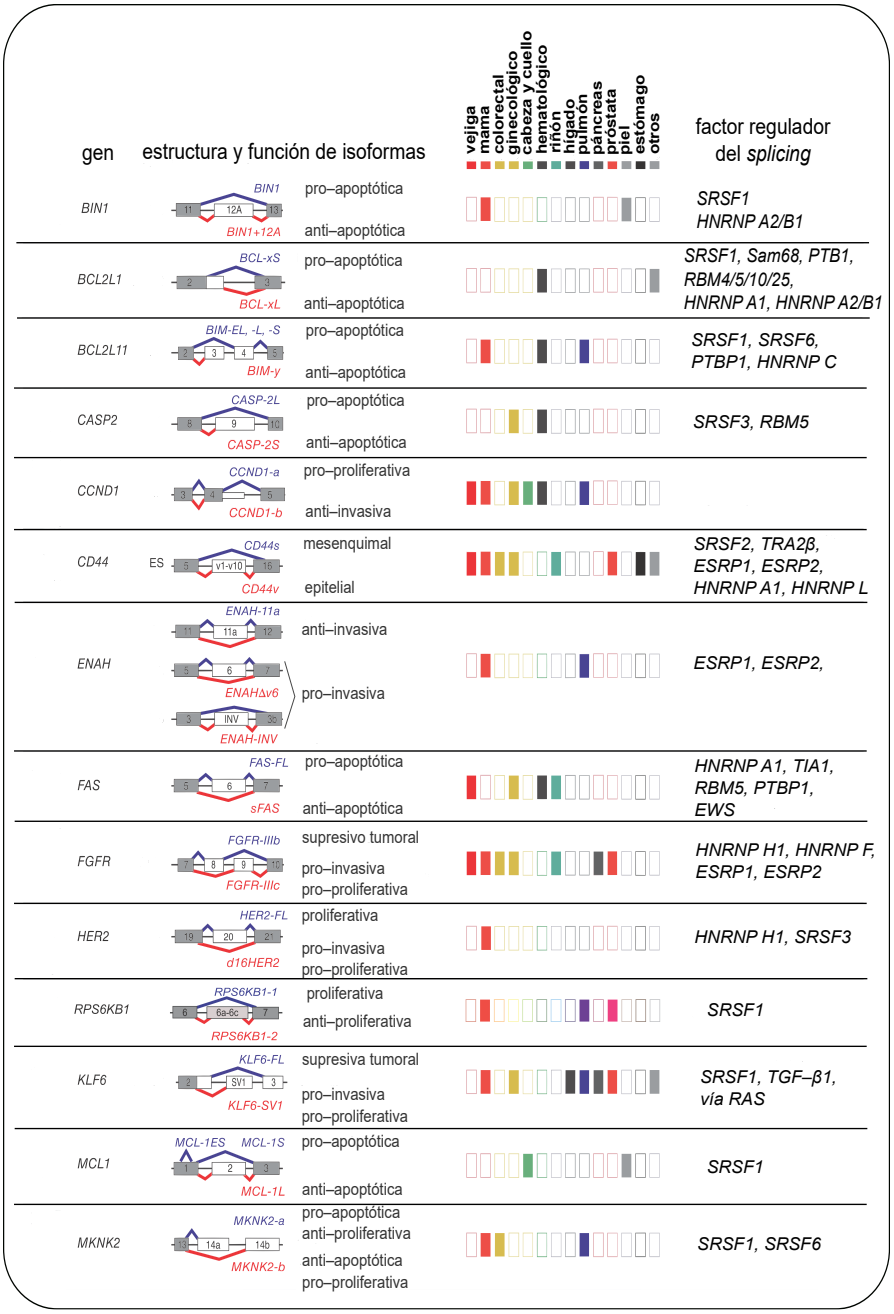

Figura 10. Ejemplos de isoformas asociadas a cáncer. Las cajas coloreadas representan la expresión de las mismas en el cáncer con el que han sido asociadas y a su derecha el factor de *splicing* al que se le ha atribuido la regulación del *splicing* del pre-ARNm del gen. Modificado de Urbanski, Leclair y Anczuków[222].

diana es Sf3b1, en pacientes con SMD, LMA y LMMC (NCT02841540)[251]; 2) el GSK3368715 o EPZ019997[252], un inhibidor de la metiltransferasa 1, *PRMT1*[253], en pacientes con linfoma B difuso de células grandes (LDCG) y tumores sólidos (de páncreas, de pulmón de células no pequeñas y de vejiga) (NCT03666988); 3) dos inhibidores de la metiltransferasa 5, *PRMT5*, GSK3326595[254] en pacientes con tumores sólidos y linfomas no Hodgkin (NCT02783300) y en pacientes con cáncer de mama (NCT04676516), y JNJ-64619178[255] en pacientes con linfoma de

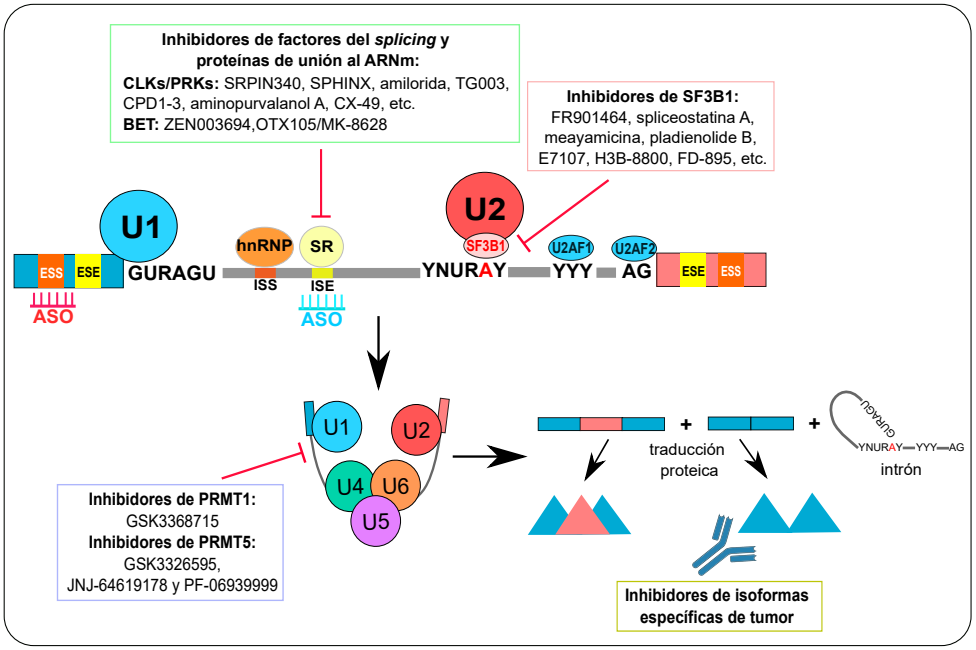

Figura 11. Estrategias terapéuticas para modular el *splicing* del pre-ARNm. Puede ser regulado a diferentes niveles, incluyendo inhibidores de componentes del *spliceosoma* y de factores del *splicing* así como de proteínas de unión al ARN, el uso de oligonucleótidos antisentido (ASO) que induce cambios en los sitios de *splicing*, y el uso de drogas o anticuerpos que inhiben una isoforma proteica específica con funciones diferentes a las canónicas.

células B y tumores sólidos avanzados (NCT03573310); y 4) el PF-06939999, inhibidor también de *PRMT5*[256,257], en pacientes con tumores sólidos en estado avanzado o metastásico (cáncer de pulmón de células no pequeñas, carcinoma de células escamosas de cuello y cabeza, cáncer de esófago, endometrial, cervical y de vejiga) (NCT03854227).

12.2. Fármacos dirigidos contra factores del *splicing* y proteínas de unión al ARNm

Dentro de este grupo de fármacos se encuentran varios compuestos con actividad antitumoral como el NB-506[258], el 4bHWE (4β-hidroxiwitanólido E)[259], la quercetina[260], la amilorida[261,262], las sulfonamidas incluyendo a E7820, indisulam (también llamado E7070 y HY-13650 y tasisulam[263], y los derivados del indol[264,265], entre otros. La actividad antitumoral de alguno de ellos como el NB-506, la amilorida y los derivados del indol se ha visto asociada con la inhibición del *splicing*, bien por la inhibición de las cinasas responsables de la fosforilación de las proteínas SR, o bien por la alteración en el patrón de *splicing* de genes implicados en cáncer favoreciendo la producción de unas isoformas sobre otras.

También dentro de este grupo de drogas se encuentran las llamadas pequeñas moléculas que agrupa a inhibidores de diferentes grupos de proteínas. Por ejemplo, los inhibidores de cinasas *SRPKs*, como SRPIN340 y SPHINX, y de las *CLKs*, como la clorhexidina, el TG003, CPD1-3, la flunarizina y el clotrimazol, entre otros[266–270]. Los inhibidores de la topoisomerasa I, como la

diospirina y sus derivados[271], y los de la fosfoinositol 3-cinasas (PI3K) como la tetrocarcina A[272].

De estos compuestos dirigidos contra factores del *splicing* y proteínas de unión al ARNm, los únicos que se han evaluado en ensayos clínicos son el ZEN003694, en pacientes con cáncer de próstata metastásico resistente a la castración, como único agente (NCT02705469), y en combinación con enzalutamide (NCT02711956), así como en pacientes con cáncer de mama triple negativo en combinación con el talazoparib (NCT03901469); y el OTX105/MK-8628 (también llamado birabresib y MK-8628), en pacientes con tumores sólidos avanzados (NCT02259114)[273,274]. Ambos son inhibidores de bromodominios BET (*Bromodomain and Extra Terminaldomain*)[275,276].

12.3. Otras estrategias terapéuticas dirigidas a la regulación del *splicing* del pre-ARNm

Desde hace unos cuantos años se están explorando y desarrollando otras estrategias completamente diferentes a las mencionadas anteriormente para modular la actividad del *splicing*. Los oligonucleótidos antisentido (ASOs), es un abordaje terapéutico con un potencial enorme, no sólo en cáncer sino en muchas enfermedades[277]. Los ASOs, que se sintetizan químicamente y generalmente presentan una longitud de 12-30 nucleótidos, se diseñaron con el objetivo de unirse al ARN por complementariedad. De hecho, la longitud del ASO determina su especificidad de unión a un único ARN, y de esta forma es capaz de regular las funciones del ARN mediante diferentes mecanismos. En general pueden, o promover la escisión y degradación del ARN o realizar un bloqueo estérico[278]. En el caso del *splicing*, los ASOs se unen a la secuencia del pre-ARNm, específicamente a los sitios o motivos reguladores del *splicing*, evitando su reconocimiento por los factores del *spliceosoma* y los reguladores del *splicing*, y por lo tanto, promueven el cambio de los sitios de *splicing*. También pueden diseñarse para unirse a los sitios ESEs, que inducen la exclusión de un exón a la secuencia del ARNm, y a los sitios ESSs que estimulan la inclusión del exón. La primera terapia correctora del *splicing* que ha usado ASOs ha sido la spinraza™, dirigida a tratar la atrofia muscular[279]. Estudios preclínicos, en líneas celulares y modelos murinos *in vivo* han mostrado que los ASOs pueden ser también aplicables al cáncer. Por ejemplo, la cinasa *MKNK2* puede producir dos isoformas, Mnk2a y Mnk2b, con propiedades antagónicas. Mnk2a actúa como supresor tumoral al favorecer la apoptosis mientras que Mnk2b es un factor de tipo prooncogénico. Se ha diseñado un ASO capaz de mediar el cambio de isoformas y favorecer la expresión de la isoforma Mnk2a sobre la otra. El uso de este ASO inhibió la oncogenicidad de las células de glioblastoma, resensibilizó a las células a la quimioterapia e inhibió el crecimiento de la línea celular de glioblastoma en un modelo murino[280].

13. Isoformas de *TP53*

El gen supresor tumoral y factor de transcripción, *TP53*, localizado en la banda 17p13.1 del cromosoma 17, es probablemente el gen más estudiado en el cáncer, donde su ruta de señalización

se encuentra inactivada con frecuencia. Aunque su disfunción en cáncer está comúnmente asociada a la presencia de mutaciones o deleciones del gen, existen otros mecanismos que pueden atenuar la actividad de este importante supresor tumoral y favorecer la tumorigénesis. En el MM, las mutaciones y deleciones de *TP53* son eventos poco frecuentes en el momento del diagnóstico, si bien su frecuencia aumenta en las recaídas posteriores.

El gen *TP53* comprende 13 exones, 11 constitutivos y 2 alternativos, y se encuentra altamente conservado en los organismos multicelulares[281]. Desde su descubrimiento, p53 se ha considerado una única entidad proteica, pero el avance tecnológico de los últimos 20 años ha permitido la identificación y caracterización de varios transcritos o isoformas de p53. La primera evidencia de la existencia de las isoformas de p53 fue reportada en los años 80, pero no ha sido hasta más de 20 años después cuando se han detectado en diferentes especies, y se ha estudiado su relevancia biológica y clínica[282,283]. Actualmente se sabe que las isoformas de p53 son el resultado de la combinación de: 1) promotores alternativos de inicio de la transcripción, P1 y P2; 2) *splicing* alternativo que retiene un trozo de los intrones 2 y 9; y 3) sitios alternativos de inicio de la traducción proteica[284]. De esta forma se han descrito 12 isoformas proteicas (TAp53α, TAp53β, TAp53γ, Δ40p53α, Δ40p53β, Δ40p53γ, Δ133p53α, Δ133p53β, Δ133p53γ, Δ160p53α, Δ160p53β y Δ160p53γ) codificadas a partir de 9 transcritos de ARNm (Figura 12).

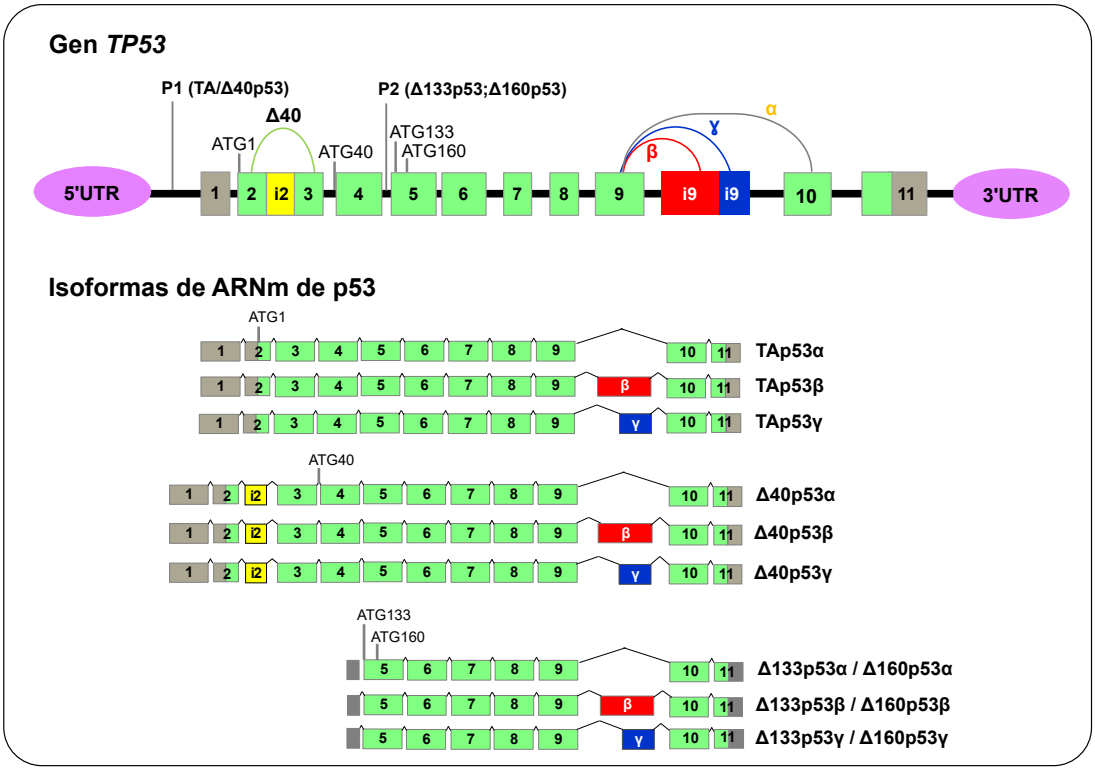

Figura 12. Estructura esquemática del gen *TP53* y de sus isoformas de ARNm. *TP53* tiene 11 exones (codificantes en verde, no codificantes en gris), y puede dar lugar a diferentes transcritos o isoformas debido al uso de promotores alternativos (P1 y P2), a sitios alternativos de inicio de la traducción (ATG1, ATG40, ATG133 y ATG160), y el *splicing* alternativo de los intrones 2 y 9.

El ARNm de p53 que se transcribe usando el promotor P1 codifica para la isoforma

proteica canónica, TAp53α, pero también para la isoforma Δ40p53α si se utiliza el sitio de la traducción alternativo AUG40. Estos transcritos a su vez pueden simultáneamente dar lugar a otras isoformas si se retiene un trozo del intrón 9, generándose o un exón 9β o un exón 9γ, que codifican para TAp53β y/o Δ40p53β, y para TAp53γ y/o Δ40p53γ, respectivamente. Ambos exones 9β y un 9γ contienen un codón de parada de la traducción, por lo que los exones 10 y 11 de las isoformas β y γ no son codificantes. Otro ARNm de p53 puede transcribirse a partir del promotor P1, pero conservando el intrón 2 en su secuencia. La retención de este intrón produce varios codones de parada de la traducción, evitando la obtención del transcrito TAp53α, pero la traducción alternativa en el codón 40 se puede llevar a cabo dando lugar exclusivamente a las isoformas Δ40p53α, Δ40p53β y Δ40p53γ. Los otros seis transcritos de p53 que usan el promotor interno P2 localizado en el intrón 4, pueden iniciar su traducción en el codón 133 o el 160, dando lugar a las isoformas Δ133 y Δ160, respectivamente (Δ133p53α, Δ133p53β, Δ133p53γ y Δ160p53α, Δ160p53β y Δ160p53γ) (Figura 12)[285,285–287].

Las isoformas de *TP53* que comparten la mayor parte de su secuencia pueden agruparse según el mecanismo que dio lugar a su formación, en isoformas α (TAp53α, Δ40p53α, Δ133p53α y Δ160p53α), isoformas β (TAp53β, Δ40p53β, Δ133p53β y Δ160p53β), isoformas γ (TAp53γ, Δ40p53γ, Δ133p53γ y Δ160p53γ), isoformas TA (TAp53α, TAp53β y TAp53γ), isoformas largas (incluye las TAp53α, TAp53β, TAp53γ, y Δ40p53α, Δ40p53β y Δ40p53γ) e isoformas cortas (Δ133p53α, Δ133p53β, Δ133p53γ, Δ160p53α, Δ160p53β y Δ160p53γ).

A nivel proteico, la isoforma TAp53α fue la primera en identificarse. Esta isoforma que se corresponde con la proteína canónica, consta de 393 aminoácidos (aa) con siete dominios funcionales: 1) dos dominios de transactivación (TAD, *transactivation domain*), TAD1 y TAD2 en la región amino terminal (TAD1, 1-42 aa, y TAD2, 43-63 aa), que son requeridos para la función de p53 como factor de transcripción induciendo la expresión de sus genes diana, y para la unión de su principal regulador, Mdm2, que tiene su sitio de unión a p53 en los residuos 13-29; 2) un dominio rico en residuos de prolina (PRD, *proline-rich domain*) (64-92 aa) que puede afectar la estructura tridimensional de la proteína a través de la isomerización de prolinas; 3) un dominio de unión al ADN (DBD, *DNA-binding domain*) (101-292 aa) que es la región más frecuentemente mutada en todos los cánceres humanos, y que es requerido para la activación de la transcripción de sus numerosos genes diana que regulan la proliferación y supervivencia celular; 4) un dominio de localización nuclear (NLS, *nuclear localization signal*) (305-322 aa); 5) un dominio de oligomerización (OD, *oligomerization domain*) (326-356 aa); y 6) un dominio de región básica (364-393 aa) encargada de la regulación negativa del DBD, rico en residuos de lisina, que son modificados postraduccionalmente (fosforilación, metilación, acetilación, ubiquitinación, sumoilación, nedilación, etc.) para regular la actividad y estabilidad de TAp53α[288] (Figura 13).

Las isoformas Δ40, Δ133, y Δ160, carecen de los primeros 39, 132 y 159 aminoácidos, respectivamente. Las variantes Δ40 han perdido el TAD1 pero conservan el resto de la estructura, similares a las variantes TA; mientras que las isoformas Δ133 y Δ160 (isoformas cortas) carecen de ambos dominios TAD y de un trozo del dominio DBD. Estas diferencias estructurales entre

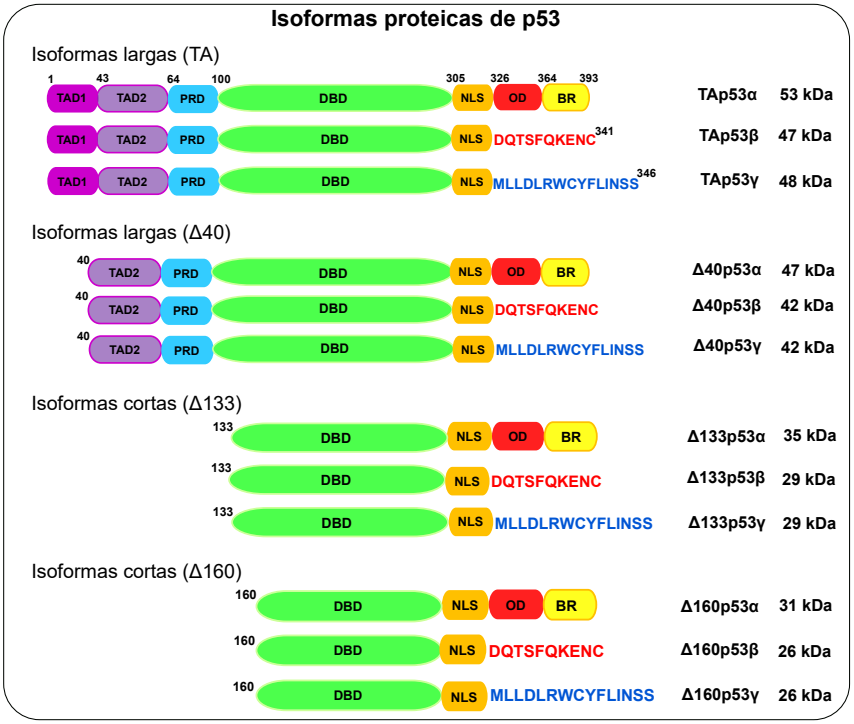

Figura 13. Representación esquemática de las isoformas proteicas de p53. Se muestran los dominios, y los residuos aminoacídicos de inicio y final, en cada una de las isoformas. TAD1: dominio de transactivación 1, [morado]; TAD2: dominio de transactivación 2, [violeta]); PRD: dominio rico en prolinas, [azul]), DBD: dominio de unión al ADN [verde]; NLS: señal de localización nuclear [naranja]; OD: dominio de oligomerización [rojo]; BR: región básica [amarillo]. Se muestran las secuencias específicas de las isoformas β (DQTSFQKENC) y γ (MLLDLRWCYFLINSS), así como el peso molecular de cada isoforma.

las 12 isoformas proteicas de p53 determinan sus funciones.

13.1. Funciones de las isoformas de p53 y su implicación en cáncer

Las funciones de las isoformas de p53 se han investigado mediante la sobreexpresión ectópica y/o silenciamiento de las mismas utilizando diferentes líneas celulares y modelos de animales. Este tipo de experimentos han demostrado que las isoformas de p53 pueden estar involucradas en la regulación del ciclo celular, muerte celular, senescencia, inflamación, invasión, respuesta antioxidante, diferenciación, etc. Estas funciones se han observado no solamente en un contexto biológico sino en diferentes tejidos, tanto en condiciones normales como en un entorno tumoral. De este modo, tras muchos años de investigación se ha establecido que la respuesta celular mediada por p53 es la suma de las actividades intrínsecas no sólo de la isoforma canónica, sino del conjunto de las demás que pueden coexpresarse. Por ello, las alteraciones en la expresión de las isoformas de p53 pueden afectar su vía de señalización y en consecuencia tener un impacto en el cáncer y otras enfermedades. De hecho, en los últimos años varios estudios han demostrado que las isoformas de p53 están diferencialmente expresadas en distintos tipos de cánceres, como el de mama, colon, melanoma, cabeza y cuello, hepático, pulmón, carcinoma renal, glioblastoma y la LMA en comparación con el tejido normal. También se ha descrito una asociación entre la

desregulación de las isoformas de p53 y el pronóstico de los tumores[289–297].

En algunas neoplasias el valor pronóstico de la mutación de *TP53* se acentúa cuando se tiene en cuenta también la expresión de las isoformas de p53. Incluso las isoformas de p53 pueden llegar a anular la ganancia de función del *TP53* mutado. Por ejemplo, la sobreexpresión de la isoforma Δ133p53α en pacientes con cáncer de ovario, o TAp53γ en cáncer de mama, que tienen *TP53* mutado, supera el impacto negativo de la mutación[289,298]. En pacientes con cáncer de ovario seroso o mucinoso con p53 en estado *wild-type* (wt), que expresan la isoforma Δ40p53α tienen un mejor pronóstico clínico que aquellos con p53 wt que no la expresan[298,299].

Todos los hallazgos de los últimos años en torno a las funciones de las isoformas de p53 en diferentes contextos y usando distintas metodologías, han demostrado que sus actividades son dependientes del tipo celular y que puede variar según el escenario molecular. Además, algunas de las isoformas de p53 pueden coexpresarse o ser mutuamente excluyentes.

Es importante señalar también que la mayoría de los estudios de las isoformas de p53 se basan en el análisis a nivel de ARNm mediante PCR cuantitativa en tiempo real y PCR convencional[300], y sólo algún estudio ha analizado algunas isoformas proteicas en un bajo número de muestras de pacientes. El hecho de que las isoformas proteicas difieran entre sí sólo en secuencias concretas que son realmente pequeñas dificulta su análisis individualizado. No obstante, sí que se han logrado producir anticuerpos, algunos disponibles comercialmente, capaces de distinguir algunas de ellas mediante inmunofluorescencia, inmunohistoquímica o *western blot*[301].

Hipótesis de trabajo y Objetivos

El origen del cáncer se ha relacionado tradicionalmente con modificaciones que se producen en la secuencia del ADN de los genomas de las células cancerosas. Sin embargo, la mayoría de los cambios en la expresión de los genes no está aparentemente precedida por una alteración del ADN en forma de mutaciones, anomalías cromosómicas o incluso eventos epigenéticos. En los últimos 30 años el estudio de la expresión génica a escala global se ha utilizado extensamente para caracterizar todo tipo de neoplasias. El desarrollo de los *microarrays* de expresión y más recientemente de la RNA-Seq ha sido clave para disponer de una información detallada de los patrones de expresión génica de los diferentes tumores. En algunas neoplasias, el estudio del perfil de expresión génica ha permitido la identificación de subtipos, ha ayudado a mejorar la estratificación de los pacientes e incluso ha contribuido a llevar a cabo tratamientos más personalizados o dirigidos. No obstante, la mayoría de estos estudios se han centrado en investigar la expresión génica del transcrito canónico, sin tener en cuenta la expresión del resto de los transcritos o isoformas que pueden obtenerse como resultado del *splicing* o procesamiento del pre-ARNm a partir de un mismo gen. En este sentido, actualmente es bien conocido que las diferentes isoformas pueden expresarse de forma desigual a la isoforma canónica y desempeñar funciones distintas, incluso divergentes, interviniendo de forma muy diferente en la patogenia tumoral. De hecho, el *splicing* del pre-ARNm es uno de los mecanismos celulares de regulación postranscripcional más importantes. Puesto que la mayoría de los genes pueden dar lugar a múltiples transcritos una consecuencia de este procesamiento es a veces, incluso, la producción de proteínas con funciones opuestas. Este fenómeno está bien ilustrado en el hecho de que varios de los genes que codifican proteínas implicadas en rutas apoptóticas son capaces de dar lugar a isoformas pro y anti apoptóticas mediante este proceso[222].

La expresión génica se ha analizado minuciosamente en el MM. Los primeros estudios ya mostraron que los perfiles de expresión génica de las CPs tumorales eran claramente diferentes a los de las CPs normales de donantes sanos, y que dentro del grupo de los mielomas se podían encontrar subgrupos moleculares más parecidos a las GMSI, y otros similares a las líneas celulares de MM[302]. Posteriormente, se elaboró una clasificación molecular del MM basada en los perfiles de expresión génica que identificaba siete subgrupos distintos[52]. Estas subentidades moleculares con algunas modificaciones se han confirmado en numerosos estudios posteriores, no solo utilizando *microarrays* de expresión sino también mediante RNA-Seq.

En las neoplasias de CPs, al igual que sucede en otros cánceres, la investigación del *splicing* del pre-ARNm y de la variedad de isoformas generadas mediante este mecanismo, ha sido muy limitada, tanto a nivel del transcriptoma completo como enfocándose en genes particulares. Por este motivo, hemos pensado que resultaría interesante avanzar en el estudio de cómo este mecanismo de regulación postranscripcional puede influir en la patogenia del MM y otras discrasias de células plasmáticas, e incluso averiguar si la modulación farmacológica del *spliceosoma* podría servir como abordaje terapéutico.

Hasta ahora no se ha descrito ninguna alteración cromosómica ni mutación o desregulación significativa de un gen o ruta molecular particular que esté presente en la LCPp, la forma más

agresiva de las neoplasias de CPs, y no lo esté en el MM. Esto indica que otros procesos biológicos pueden ser los responsables de la trasformación de la célula plasmática en una célula tumoral mucho más agresiva e incontrolable que la del MM. La búsqueda de diferencias, tanto en el patrón de *splicing* como en la expresión de las distintas isoformas, entre el MM y la LCPp podría ayudarnos a identificar posibles mecanismos moleculares involucrados en el desarrollo de la LCPp, y que no sean dependientes de la presencia de las alteraciones genéticas ya conocidas.

TP53 es un conocido gen supresor tumoral que ha sido ampliamente estudiado. Concretamente el *splicing* del pre-ARNm es uno de los mecanismos postranscripcionales que ha emergido en los últimos años como uno de los procesos más relevantes en la regulación de p53. Se han descrito al menos 12 isoformas proteicas codificadas a partir de 9 ARNm (TAp53α, TAp53β, TAp53γ, Δ40p53α, Δ40p53β, Δ40p53γ, Δ133p53α, Δ133p53β, Δ133p53γ, Δ160p53α, Δ160p53β y Δ160p53γ). Algunas de las isoformas difieren entre sí en los dominios de transactivación y en el dominio C-terminal, lo que les permite regular diferencialmente la expresión de diferentes genes dianas y ser reguladas también de forma variable por los reguladores de p53. Varios trabajos han demostrado que la alteración de los niveles de expresión de las isoformas de p53 puede inhibir o potenciar su propia actividad como supresor tumoral en diferentes neoplasias y por tanto, influir en su respuesta al tratamiento y pronóstico. La expresión de las isoformas de p53 no se ha investigado aún en el MM. Por este motivo, el análisis de las isoformas de p53, tanto a nivel de proteína como de ARNm, en muestras de pacientes con MM tratados homogéneamente en el marco de un ensayo clínico, podría proporcionar información novedosa de su valor pronóstico.

Actualmente se están desarrollando estrategias terapéuticas dirigidas a modular la maquinaria del *splicing* con resultados esperanzadores. De hecho, existen una serie de fármacos que modifican los patrones de *splicing* del pre-ARNm, cuyo mecanismo de acción es bastante desconocido. Algunos de ellos se están investigando como drogas antitumorales en ensayos clínicos. En este sentido, pensamos que la investigación del efecto de estos agentes en las células mielomatosas sería útil para ampliar el espectro de fármacos con potencial utilidad en el MM y además, para descifrar los mecanismos moleculares del proceso de *splicing* y de su regulación en el MM.

Objetivos:

Objetivo 1: Analizar el transcriptoma de casos de LCPp y de MM que comparten un fondo genético similar y compararlos entre sí.

- Analizar el perfil de expresión génica de muestras de LCPp y compararlo con el de las muestras de MM.
- Explorar los eventos de *splicing* alternativo en las LCPp en relación a los observados en el MM.
- Identificar las isoformas de ARNm diferencialmente expresadas entre la LCPp y el MM.
- Analizar la existencia de sitios reguladores de *splicing* alternativo en ambas neoplasias de CPs mediante análisis bioinformáticos.

Objetivo 2: Evaluar la expresión de las isoformas de p53 en pacientes con MM.

- Identificar y cuantificar las isoformas proteicas de p53 en pacientes con MM.
- Analizar el efecto de la expresión de las isoformas proteicas de p53 en el pronóstico de los pacientes.
- Examinar los patrones de expresión de las isoformas de p53 a nivel de ARNm y compararlo con lo observado a nivel de proteínas.

Objetivo 3: Investigar si la modulación farmacológica del *spliceosoma*, mediante la amilorida, puede servir como abordaje terapéutico en el MM.

- Analizar el efecto citotóxico *in vitro* e *in vivo* de la amilorida en el MM.
- Estudiar el mecanismo de acción de la amilorida en las células del MM.

Resultados

En esta sección se describen las muestras biológicas utilizadas, los materiales y métodos empleados para su estudio, así como los resultados obtenidos en relación con cada uno de los objetivos planteados en este trabajo doctoral.

La presentación de todo ello se recoge en forma de tres artículos científicos originales que han sido publicados como consecuencia del trabajo realizado, los cuales estarán precedidos de un breve resumen en español para facilitar una rápida revisión de su contenido.

La información suplementaria de cada uno de los tres trabajos está disponible en formato electrónico en la página web de la revista, así como en el apartado de **ANEXOS**.

Capítulo 1

ARTÍCULO 1

"Transcriptome analysis reveals significant differences between primary plasma cell leukemia and multiple myeloma even when sharing a similar genetic background"

Elizabeta A. Rojas, Luis A. Corchete, María Victoria Mateos, Ramón García Sanz, Irena Misiewicz-Krzeminska y Norma C. Gutiérrez

Blood Cancer Journal
(2019), 9(12):90
DOI: 10.1038/s41408-019-0253-1

El análisis del transcriptoma revela diferencias significativas entre los pacientes con leucemia de células plasmáticas primaria y con mieloma múltiple que comparten un fondo genético similar

Fundamento: La leucemia de células plasmáticas primaria (LCPp) es una neoplasia poco frecuente y muy agresiva que continúa teniendo un pronóstico infausto. La deleción de 17p se ha observado en aproximadamente el 50 % de las LCPp, mientras que en el MM no excede el 10 % en el momento del diagnóstico. Aunque en el MM la deleción de 17p está asociada con mal pronóstico y enfermedad extramedular, su presencia no le confiere el grado de agresividad observado en la LCPp. El estudio de otros mecanismos que pudieran estar alterados diferencialmente en ambas discrasias, podría proporcionar nuevos datos sobre las diferencias biológicas entre estas dos entidades. Por ello, en este trabajo nos propusimos analizar el transcriptoma de la LCPp y del MM, en presencia de un fondo genético similar.

Metodología: Los estudios del transcriptoma se llevaron a cabo en nueve muestras de pacientes con LCPp y diez con MM. Las muestras fueron seleccionadas de manera que todas tuviesen deleción de 17p y una distribución homogénea del resto de alteraciones citogenéticas entre ambos grupos (deleción de 13q, t(11;14), t(4;14), t(14;16), ganancia de 1q y deleción de 1p). El estudio global del transcriptoma se realizó utilizando los *microarrays* HTAs 2.0 (*human transcriptome arrays*), partiendo del ARN total extraído de las muestras de LCPp y de MM. Se analizó también el estado mutacional del otro alelo de *TP53* mediante secuenciación de Sanger. El análisis de los *microarrays* HTAs se llevó a cabo a tres niveles: expresión diferencial génica, expresión de transcritos y ocurrencia de eventos de *splicing* alternativo. Los resultados obtenidos fueron validados mediante qRT-PCR.

Resultados: La secuenciación de Sanger detectó mutaciones de *TP53* en el 50 % de las muestras de LCPp y en el 30 % de los MM, localizadas la mayoría de ellas en el dominio de unión al ADN de p53 entre los exones 5 y 8, prediciendo una proteína inactiva.

El análisis no supervisado de los HTAs de las 19 muestras permitió distinguir 2 grupos bien diferenciados, el de las LCPp y el de los MM, según la expresión génica. En cambio, el análisis no supervisado de los datos de RNA-seq de una serie de 73 pacientes con MM, pertenecientes al estudio CoMMpass (MMRF), que presentaban todos deleción de 17p no mostró ningún tipo de agrupamiento.

Se encontraron 3 584 genes diferencialmente expresados entre las LCPp y los MM. La mayoría de ellos estaban infraexpresados (3 217 genes) en las LCPp en comparación con los MM. Entre las rutas de señalización afectadas se encontraba el *spliceosoma*, la síntesis de ARNs de transferencia y el procesamiento de proteínas en el retículo endoplasmático y transporte de ARN. El análisis a nivel de isoformas y de eventos de *splicing* mostró que había 20 626 isoformas desreguladas entre ambos grupos y que el evento de *splicing* más frecuente fue la inclusión o exclusión de exones. Además, se detectaron diferencias significativas en la expresión de componentes de la maquinaria del *spliceosoma* entre las LCPp y los MM, tanto a nivel génico

como a nivel de isoformas y de eventos de *splicing*. De hecho, un análisis de identificación de posibles sitios ESEs (*exonic splicing enhancers*) en la secuencia de exones desregulados entre LCPp y MM, mostró que más del 70 % de los exones tenían sitios ESEs de unión para las proteínas SRp40 y SC35, seguidas de SRp30a y SRp20, con 50 % y 42 %, respectivamente.

Los ensayos de qRT-PCR mostraron una correlación positiva estadísticamente significativa con los *microarrays*, a los tres niveles de análisis. Concretamente se confirmó que dos transcritos del gen *IKZF1* estaban infraexpresados en las LCPp, a pesar de que la expresión génica total se mantuvo sin cambios significativos entre ambas discrasias.

Conclusiones: Nuestros datos revelaron diferencias significativas en la expresión de genes, isoformas y eventos de *splicing* entre la LCPp y el MM, en presencia de la deleción de 17p. Estos hallazgos resaltan la relevancia potencial del proceso de *splicing* del pre-ARNm y de la síntesis proteica en la patogénesis de la LCPp.

Rojas et al. *Blood Cancer Journal* (2019)9:90
https://doi.org/10.1038/s41408-019-0253-1

Blood Cancer Journal

ARTICLE Open Access

Transcriptome analysis reveals significant differences between primary plasma cell leukemia and multiple myeloma even when sharing a similar genetic background

Elizabeta A. Rojas[1,2], Luis A. Corchete[1,2], María Victoria Mateos[1,2,3], Ramón García-Sanz[1,2,3,4], Irena Misiewicz-Krzeminska[1,2,5] and Norma C. Gutiérrez[1,2,3,4]

Abstract

Primary plasma cell leukemia (pPCL) is a highly aggressive plasma cell dyscrasia characterised by short remissions and very poor survival. Although the 17p deletion is associated with poor outcome and extramedullary disease in MM, its presence does not confer the degree of aggressiveness observed in pPCL. The comprehensive exploration of isoform expression and RNA splicing events may provide novel information about biological differences between the two diseases. Transcriptomic studies were carried out in nine newly diagnosed pPCL and ten MM samples, all of which harbored the 17p deletion. Unsupervised cluster analysis clearly distinguished pPCL from MM samples. In total 3584 genes and 20033 isoforms were found to be deregulated between pPCL and MM. There were 2727 significantly deregulated isoforms of non-differentially expressed genes. Strangely enough, significant differences were observed in the expression of spliceosomal machinery components between pPCL and MM, in respect of the gene, isoform and the alternative splicing events expression. In summary, transcriptome analysis revealed significant differences in the relative abundance of isoforms between pPCL and MM, even when they both had the 17p deletion. The mRNA processing pathway including RNA splicing machinery emerged as one of the most remarkable mechanisms underlying the biological differences between the two entities.

Introduction

Plasma cell leukemia (PCL) is an uncommon and aggressive plasma cell dyscrasia, characterised by the presence of more than 20% of plasma cells (PCs) and an absolute number of $\geq 2 \times 10^9$/L of PCs in peripheral blood[1,2]. PCL is classified as primary (pPCL) when detected de novo in patients with no evidence of previous multiple myeloma (MM), or as secondary (sPCL) in patients with relapsed or refractory MM that progresses to a leukemic phase[1,3,4]. Around 60% and 40% of PCLs are pPCL and sPCL, respectively[5]. pPCL accounts for less than 3% of all malignant plasma cell disorders[6–8]. As a consequence, the current knowledge regarding the molecular basis of pPCL is quite limited by the small number of cases included in most series.

Various studies have reported that pPCL patients show different clinical and biological features from those of MM. pPCL is associated with a dismal prognosis, whereby median survival is about 10 months. Extramedullary plasmacytomas, renal failure and massive bone marrow infiltration are more frequently observed in pPCL than in MM. Conversely, pPCL exhibits a lower prevalence of bone disease[1,2,9–11].

Cytogenetic studies have shown that pPCL features elevated genomic instability, especially with respect to,

Correspondence: Norma C. Gutiérrez (normagu@usal.es)
[1]Cancer Research Center-IBMCC (USAL-CSIC), Salamanca, Spain
[2]Institute of Biomedical Research of Salamanca (IBSAL), Salamanca, Spain
Full list of author information is available at the end of the article.
These authors contributed equally: Irena Misiewicz-Krzeminska, Norma C. Gutiérrez

karyotypic complexity, and higher prevalence of 17p13 deletions and 1q gains. Of the translocations involving the immunoglobulin heavy chain locus (*IGH*), t(11;14) and t (14;16) are more frequent in pPCL than in MM[11–14]. In recent years, the development of high-throughput technologies has given rise to a detailed knowledge about molecular characteristics of pPCL. Several studies have investigated the gene mutation patterns[15], and differential gene and miRNAs expression profiles[16–20], establishing differences and similarities between pPCL and sPCL, and MM.

Many of the genomic differences detected between pPCL and MM could be attributed to the dissimilar distribution of genetic abnormalities between the two entities[15]. For instance, the overrepresentation of 17p deletions in pPCL could explain some of the differences observed in the molecular and genomic patterns of pPCL and MM. However, a more unfavourable genetic background does not fully explain the ominous prognosis of this plasma cell neoplasm. In fact, although 17p deletion is associated with poor outcome and extramedullary disease in MM, the presence of this abnormality does not confer the degree of aggressiveness observed in pPCL.

We surmised that the comparison of the transcriptome profiles of pPCL and MM cases bearing similar cytogenetic abnormalities could provide valuable insights into new molecular mechanisms responsible for the different clinical outcomes of both diseases, and not reliant on particular chromosomal abnormalities. For this purpose, we analysed the transcriptome of pPCL and MM patients, using samples with 17p deletion and a similar cytogenetic profile, and focusing not only on gene expression profiling previously studied by other authors, but also on isoform expression and alternative splicing patterns.

Materials and methods

For more specific information, see the *Online Supplementary File*.

Patients and samples

Nine patients with newly diagnosed pPCL and ten with newly diagnosed MM were selected for the study based on the presence of 17p deletion. The median age of patients was 61 years (range: 54–89 years) for MM patients and 64 years (range: 45–83 years) for pPCL patients. The research ethics committee of the University Hospital of Salamanca approved the study in accordance with the Declaration of Helsinki principles.

Plasma cells were isolated from bone marrow samples using the AutoMACs immunomagnetic system (Miltenyi Biotec), as previously described[21]. Purity was greater than 95% in all MM and pPCL cases. Interphase fluorescence *in situ* hybridisation studies were performed as previously described[21].

Nucleic acid extraction, quantitative real-time PCR and *TP53* mutation analysis

RNA and DNA were extracted using AllPrep DNA/RNA Mini Kit (Qiagen). RNA integrity was assessed using Agilent 2100 Bioanalyzer. Total RNA (200 ng) was reverse-transcribed to cDNA using the SuperScript First-Strand Synthesis System (Thermo Fisher). Gene expression was evaluated with TaqMan (Applied Biosystems) qRT-PCR assays, and isoform and exon expression were evaluated using SYBR Green (Bio-Rad) qRT-PCR mRNA assays. *PGK1* and *18 S* genes were used as endogenous controls for gene and isoform/exon expressions, respectively, and the relative expression was expressed as $2^{-\Delta Ct}$.

TP53 mutation status was determined using 100 ng of genomic DNA by Sanger sequencing, as previously reported[22].

Human transcriptome arrays

Total RNA was amplified, labelled and hybridised to GeneChip® Human Transcriptome Array 2.0 from Affymetrix. Complete microarray data are available from the Gene Expression Omnibus under accession number GSE131216. Unsupervised multidimensional scaling (MDS) was performed using the Euclidean distance as the distance measure and the group average as the linkage method. Samples in the MDS from the CoMMpass dataset were classified in subgroups using model-based methods from the mclust R package.

Differential expression was analysed using the samr package (v2.0) in R. Gene and isoform level probesets with expression values less than the mean of the microarray antigenomic control expression values in all samples were excluded from further analysis. Genes and isoforms with a value of $q < 0.05$ were considered statistically significant and were selected for the KEGG pathway overrepresentation analysis in the Webgestalt suite[23]. Alternative splicing (AS) analysis was performed using the Affymetrix Transcriptome Analysis Console (TAC) version 4.0.1.36.

Computational RNA-binding site prediction

The SpliceAid database was used to identify potential exonic splicing enhancer (ESE) motifs recognised by human serine/arginine-rich (SR) proteins[24].

Statistical analysis

The significance of differences in experiments was assessed by the two-sided Student's *t* test for unpaired samples. Pearson correlation coefficients were calculated to measure associations between the results of HTA 2.0 and qRT-PCR assays. Fisher's exact tests with two-tailed were calculated using the GraphPad QuickCalcs website: https://www.graphpad.com/quickcalcs/contingency1/. Values of p and q less than 0.05 were considered

statistically significant. All statistical analyses were conducted using IBM SPSS Statistics 22.0 and the SIMFIT v7.0.9 package (Bardsley, University of Manchester, UK).

Results

Genetic abnormalities in pPCL and MM patients

All pPCL and MM samples carried the 17p deletion. A balanced distribution of other genetic abnormalities in the two entities was also taken into account when selecting the samples. Genetic abnormalities analysed by FISH are summarised in Table 1. The frequencies of *IGH* translocations according to 14q32 partners, chromosome 1 abnormalities and 13q deletions are shown in Table 1. Fisher's exact test revealed no statistically significant differences between MM and pPCL (Table 1).

To better characterise the *TP53* status, mutations were analysed in all patients with an available genomic DNA sample (18/19 samples). *TP53* mutations were identified in four of eight pPCLs (50%) and three of ten MM (30%) ($p = 0.63$, Fisher's exact test). Six of the seven identified mutations were missense substitutions (86%), and were localised in the DNA binding domain, distributed between exons 5 and 8. The mutated amino acid residues were in areas with hotspot properties and direct DNA contact site. According to their functionality as transcription factor the missense mutations detected in the seven samples predicted an inactive p53 (Supplementary Table 1).

Differentially expressed genes between pPCL and MM

To investigate the transcriptome signature of pPCL and MM patients, Human Transcriptome Array 2.0 analysis was performed. These microarrays allow us to explore gene expression profile, as well as splicing events and isoform expression, using millions of probes that cover exon–exon splice junctions, and coding and non-coding isoforms.

First, we explored the distribution of the samples in clusters based on similarities in gene expression data using unsupervised multidimensional scaling (MDS). The first component in this analysis clearly separated MM from pPCL samples (Fig. 1a), although two pPCLs were closer to MM samples. We asked whether different clusters could also be identified across a large series of MM cases with del17p. We used RNA-Seq data from 73 MM patients with del17p from the MMRF CoMMpass trial (NCT01454297) to address this question. We found no clusters, but samples were apparently randomly distributed (Supplementary Fig. 1).

Gene expression analysis from HTAs identified a total of 3584 genes differentially expressed between the pPCL and MM groups, of which 367 were overexpressed and 3217 genes were underexpressed in pPCL relative to MM patients (Fig. 1b). The list of the 40 genes with the greatest and least fold change (FC) is shown in Fig. 1c. Functional analysis using the KEGG pathway database revealed statistically significant enrichment for spliceosome, aminoacyl-tRNA biosynthesis, protein processing in endoplasmic reticulum (ER) and RNA transport (Fig. 1d). The heatmap, using only the genes from overrepresented KEGG pathways, distinguished two entities with different gene expression patterns and with a clear prevalence of underexpression in pPCL compared with MM (Supplementary Fig. 2).

Results of gene expression profiling were validated by qRT-PCR. We chose 15 genes, eight components of the spliceosome selected from the functional analysis using KEGG database (*SRSF1, SRSF3, SF3B1, DDX42, DHX15, HNRNPU, THOC1*, and *U2SURP*), and seven genes from the list of the 40 most deregulated genes, whose role in cancer is less well understood (*WARS, AHR, DUSP5, CD79A, GADD45A, GADD45B*, and *PDE4B*). *TP53* gene expression was also quantified. The primers used in these assays are shown in Supplementary Table 2. As shown in Fig. 1e, we observed a high concurrence in the FC direction between HTA and qRT-PCR analysis for all the 16 genes considered. These results also revealed a strong positive and statistically significant correlation ($r = 0.89$, $p < 0.0001$) between the HTA microarray and qRT-PCR results (Fig. 1e).

Table 1 Prevalence of genetic aberrations detected by FISH in pPCL and MM

	pPCL ($n = 9$)	MM ($n = 10$)	*p*-value (Fisher's exact test)
17p del	9/9 (100%)	10/10 (100%)	1.00
13q del	7/9 (78%)	6/10 (60%)	0.63
1q gain	5/9 (56%)	4/10 (40%)	0.65
1p del	2/9 (22%)	1/10 (10%)	0.58
t(11;14)	3/9 (33%)	2/10 (20%)	0.63
t(4;14)	2/9 (33%)	0/10 (0%)	0.21
t(14;16)	1/9 (11%)	0/10 (0%)	0.47

Differentially alternative splicing events in pPCL and MM

Next, we aimed to identify alternative splicing events (ASEs) differentially expressed between pPCL and MM patients. We detected 2873 genes affected by at least one ASE, and the expression of 3303 splicing events (Fig. 2a). The most abundant ASEs were the cassette exon, with 2225 exons included or excluded from mRNAs, followed by alternative 5′ donor site, alternative 3′ acceptor site, and intron retention (Fig. 2a). The differential expression of these four types of ASEs in pPCL relative to MM is shown in Fig. 2b. In this regard, among all ASEs we found a large number of alternatively spliced exons differentially

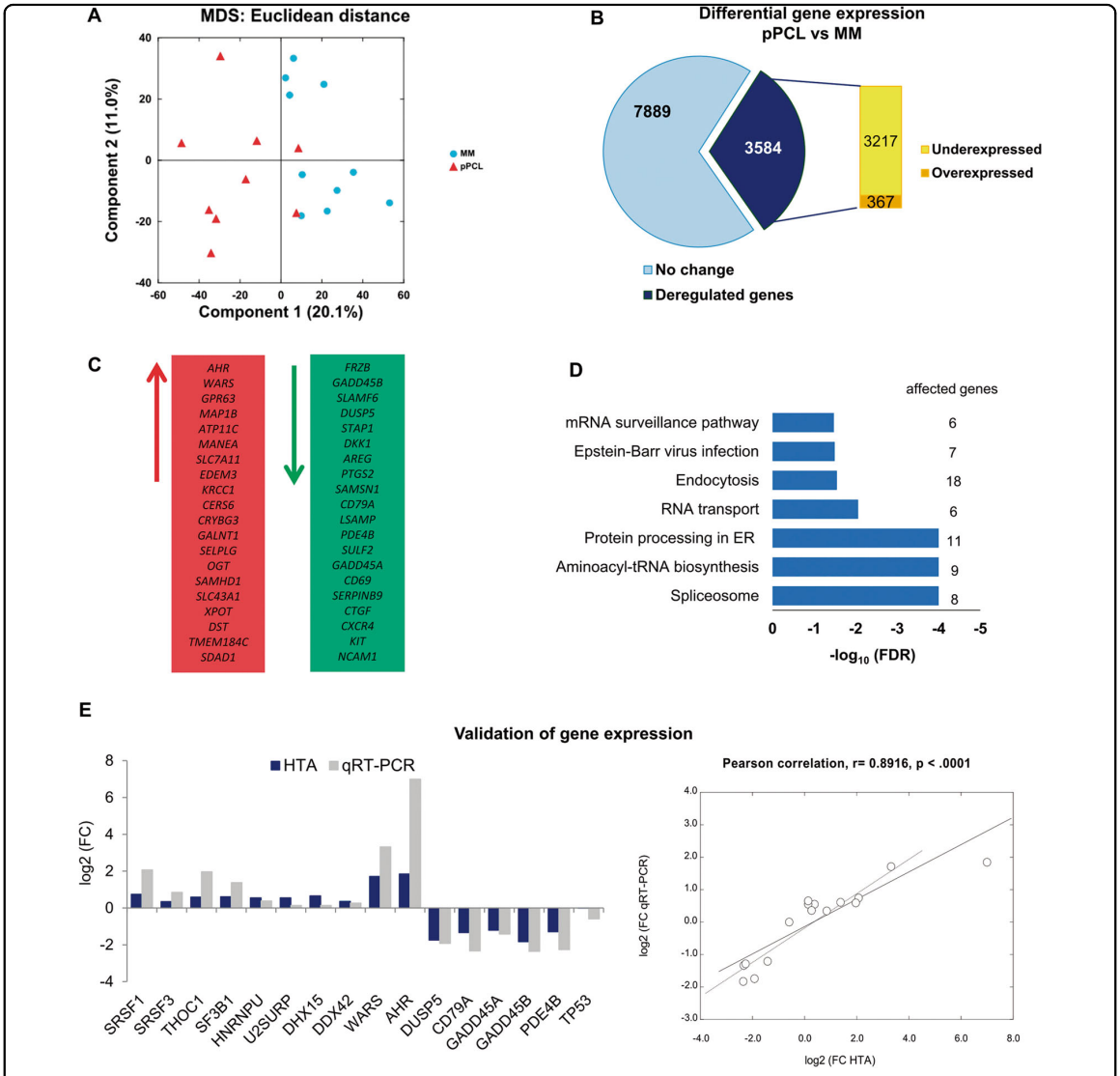

Fig. 1 Gene expression analysis. a Unsupervised analysis of gene expression in MM and pPCL samples using multidimensional scaling (MDS) of 19 samples (9 pPCL and 10 MM) based on the expression of 35,345 genes. Samples appear to be clustered in two groups, based on the Euclidean distance. **b** Differential gene expression of pPCL relative to MM samples using the samr package in R. Genes with positive $\log_2$ FC and $p < 0.05$ were considered overexpressed, and genes with negative $\log_2$ FC and $p < 0.05$ were considered underexpressed, in pPCL compared with MM samples. **c** List of the 40 most deregulated genes: the 20 most overexpressed and the 20 most underexpressed genes in pPCL relative to MM samples. **d** Pathway enrichment analysis at the gene level using Webgestalt suite. The number of affected genes in each pathway is shown. The statistical significance of the enrichment is expressed as $-\log_{10}$ FDR using the Benjamini–Hochberg method. **e** Experimental validation of gene expression of HTA microarray results. The mRNA levels of genes were assessed by qRT-PCR. The results are shown as the magnitude of change ($\log_2$ FC) between pPCL and MM samples, using *18 S* rRNA as the endogenous control gene. The Pearson correlations of gene expression measured by qRT-PCR and by HTAs in pPCL ($n = 9$) and MM ($n = 10$) samples are also shown.

expressed between the two groups (Fig. 2b). KEGG pathway analysis of genes affected by deregulation of alternatively spliced exons, revealed that FoxO signalling, RNA transport, glucagon signalling, phospholipase D signalling and Epstein–Barr virus (EBV) infection pathways were the most significantly enriched (Supplementary Fig. 3).

We validated the differential expression of the cassette exon event of 13 selected genes (*TRA2B, TUBG1, BCL2,*

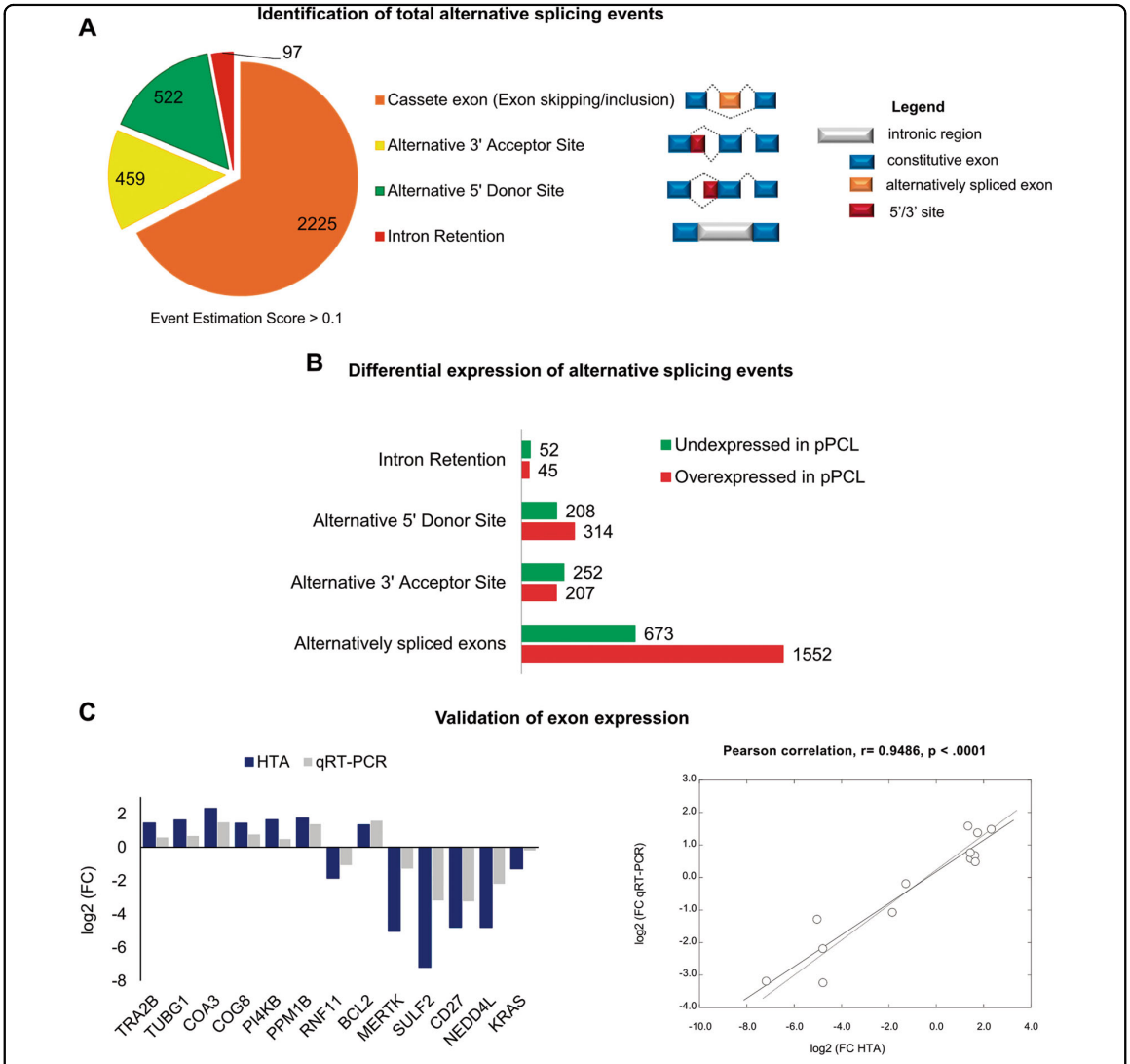

Fig. 2 Alternative splicing analysis. a Analysis of statistically significant alternative splicing events irrespective of gene expression changes between pPCL and MM samples. ASEs were identified using Affymetrix TAC software and classified into four main types of pattern: cassette exon (inclusion or exclusion of exons), alternative 5′ donor site, alternative 3′ acceptor site, and retained introns. Only the events with an event estimation score > 0.1 and an ASE assigned according an absolute splicing index of 2 and exon $p < 0.05$ were considered. **b** Differential ASEs expression of pPCL compared with MM samples using the TAC. ASEs with positive $\log_2$ FC and $p < 0.05$ were considered as overexpressed, and ASEs with negative $\log_2$ FC and $p < 0.05$ were considered as underexpressed, in pPCL compared to MM samples. **c** Experimental validation of exon expression of HTA microarray results. The results are shown as the magnitude of change ($\log_2$ FC) between pPCL and MM samples, using *PGK1* as the endogenous control gene. The Pearson correlation of exon expression measured by qRT-PCR and by HTAs in pPCL ($n = 9$) and MM ($n = 10$) samples are also shown.

COA3, COG8, PI4KB, PPM1B, RNF11, MERTK, SULF2, CD27, KRAS and *NEDD4L*) by qRT-PCR (Supplementary Table 3). The selection criteria were statistically significant exons ($p < 0.05$) with the highest and lowest FC between pPCL and MM, and longer than 70 nucleotides. The primers used for these assays are shown in Supplementary Table 4. Thus, the downregulation of exons of *SULF2, CD27, NEDDL4, RNF11, MERTK* and *KRAS* genes, and the upregulation of exons of *TRA2B, TUBG1, BCL2, COA3, COG8, PI4KB*, and *PPM1B* genes observed in the HTA microarrays of pPCL were validated by qRT-PCR (Supplementary Fig. 4). Furthermore, the

Pearson correlation analysis revealed a strong, positive and statistically significant correlation ($r = 0.9488$, $p < 0.0001$) between HTA microarrays and qRT-PCR results of the 13 selected alternatively spliced exons (Fig. 2c).

It is well known that changes in the expression of different spliceosome genes can affect alternative splicing profile of cancer cells[25–27]. In particular, some of the components of the SR protein family have been shown to be upregulated in various cancers, in which regulate the splicing of many genes. These data strongly emphasise the important role of alternative splicing in tumorigenesis[28,29]. Therefore, we investigated whether the deregulated gene expression of spliceosome components found in pPCL as compared to MM, was correlated with the occurrence of deregulated splicing events detected in this study. We focused on *SRSF1* and *SRSF3* genes, whose overexpression in pPCL was validated by qRT-PCR (as shown in Fig. 1e and Supplementary Fig. 5A). A high correlation between *SRSF1* and *SRSF3* was observed (Supplementary Fig. 5A), which is noteworthy because the expression of *SRSF1* and *SRSF3* genes is mutually regulated and coexpressed in normal and tumour cells, and *SRSF3* is able to regulate the alternative splicing of *SRSF1* gene[30].

We next explored the correlation between *SRSF1* and *SRSF3* genes with the 13 validated exons (Fig. 5b) alternatively spliced and differentially expressed between pPCL and MM (*TRA2B, TUBG1, BCL2, COA3, COG8, PI4KB, PPM1B, RNF11, MERTK, SULF2, CD27, KRAS*, and *NEDD4L*). We found a negative significant correlation between *SRSF1* and the expression of *CD27* exon 2 ($r = -0.71$, $p = 0.0006$), *NEDD4L* exon 3 ($r = -0.55$, $p = 0.0130$) and *RNF11* exon 3 ($r = -0.4755$, $p = 0.0396$) (Supplementary Fig. 5B, C). In the case of *SRSF3*, a negative significant correlation with *CD27* exon 2 ($r = -0.66$, $p = 0.0019$) and *MERTK* exon 3 ($r = -0.5587$, $p = 0.0129$) was also detected (Supplementary Fig. 5B, D).

These results indicate that the alternative splicing of *CD27*, *NEDD4L*, and *RNF11* genes could be regulated by the splicing factor *SRSF1*, and the alternative splicing of *MERTK* and *CD27* genes could be controlled by *SRSF3*.

Differentially expressed isoforms between pPCL and MM

Alternative splicing, carried out by the spliceosome machinery, leads to mRNA isoforms that encode different proteins. Since we had observed differential expression of ASEs between MM and pPCL, we searched for differences in mRNA isoform expression. We identified 20033 deregulated isoforms associated with 6254 gene IDs curated by the HGNC (Hugo Gene Nomenclature Committee), of which 1806 isoforms were overexpressed and 18227 were underexpressed in pPCL patients relative to MM patients (Fig. 3a). The enrichment analysis identified EBV infection, spliceosome and proteasome pathways, among others, as statistically significantly overrepresented KEGG pathways (Fig. 3b). In the unsupervised analysis based on isoform expression, the samples tended to be separated into two groups, as was the case with gene expression analysis (Supplementary Fig. 6).

It should be pointed out that across the entire transcriptome analysis we found significant differences in the expression of the components of the spliceosomal machinery between pPCL and MM. We found 15 spliceosome genes differentially expressed between the two groups. Moreover, 24 spliceosome components displayed differential expression of some of their isoforms, and 36 were affected by AS events (Fig. 4).

In recent years, some studies have reported the advantage of the analysis of isoform expression pattern compared with standard gene expression profiling in cancer research[31,32]. Therefore, we also focused on those

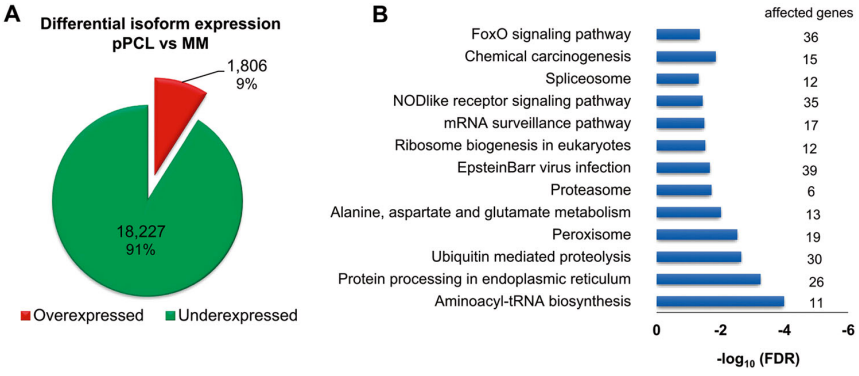

Fig. 3 Differential isoform expression between pPCL and MM samples. a Isoforms with positive $\log_2$ FC and $p < 0.05$ were considered overexpressed, and isoforms with negative $\log_2$ FC and $p < 0.05$ were considered underexpressed. **b** KEGG enrichment analysis based on genes with deregulated isoforms. The statistical significance of the enrichment analysis is expressed as $-\log_{10}$ FDR using the Benjamini–Hochberg method.

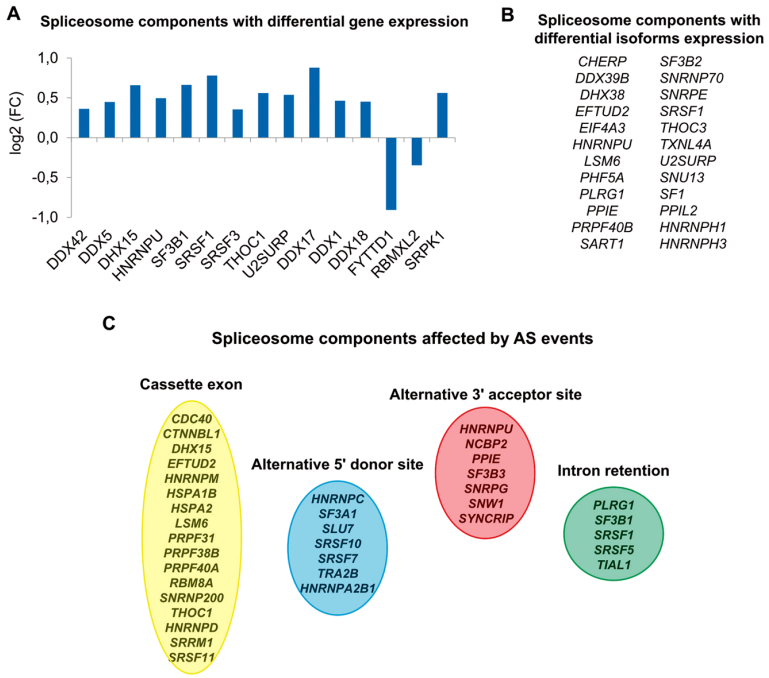

Fig. 4 Deregulation of the spliceosomal machinery between pPCL and MM. Spliceosomal components with differential gene expression ($q < 0.05$) **a** with differential isoform expression ($q < 0.05$) **b** and those affected by alternative splicing events ($q < 0.05$) **c**.

expressed genes (selection criteria for "expressed genes" in Materials and Methods section) that were not differentially expressed, but whose isoforms were differentially expressed. We found 2727 deregulated isoforms belonging to 1249 expressed genes, 1183 of which were coding isoforms (Fig. 5a). A prevalence of underexpressed isoforms in pPCL patients relative to MM was also found.

To validate the differential isoform expression detected by HTA, we focused on the coding isoforms, of which 64 were overexpressed and 1119 underexpressed in pPCL compared to MM patients (Supplementary Fig. 7A). We selected 12 coding isoforms differentially expressed ($q < 0.05$) and distributed according to high, medium and low FC, to be validated by RT-PCR (Supplementary Fig. 7A). In the case of genes with two or three deregulated isoforms a specific sequence was needed in each isoform for primer design. The selected isoforms and the primers used are shown in Supplementary Tables 5 and 6, respectively.

The differential expression of ten of the twelve isoforms tested by qRT-PCR was consistent with the results obtained by HTA (Fig. 5b). Subtle discrepancies were observed for isoforms ENST00000449494 (*RPL10* isoform) and ENST00000612658 (*IKZF1* isoform). A strong, positive and statistically significant correlation ($r = 0.92$, $p < 0.0001$) between the two methods was observed (Fig. 5c).

The overexpressed isoforms ENST00000553436 (*KLC1* gene), ENST00000443588 and ENST00000372393 (*ASS1* gene), and ENST00000340491 (*DLGAP4* gene) are isoforms coding for protein domains, which should be biologically effective and able to exert their function. On the other hand, the isoforms ENST00000413698 and ENST00000646110 (*IKZF1* gene), ENST00000576366 (*RPTOR* gene) and ENST00000413725 (*SF1* gene) are among the underexpressed isoforms, which include regions coding for protein domains whose lack probably lead to loss of some of the protein functions. We were struck in particular by the *IKZF1* gene (Ikaros protein), which was among the genes containing various differentially expressed isoforms. The *IKZF1* gene is composed of eight exons and produces 23 splice variants by alternative splicing, which are differentiated by alternative use of exons and subsequently in their functional domain composition, with distinct biological functions (Supplementary Fig. 6B). Six *IKZF1* isoforms were underexpressed ($q < 0.05$) in the HTA analysis comparing pPCL and MM (Supplementary Fig. 7C). Among the four protein coding isoforms, three could be quantified by qRT-PCR, considering the specific sequences in each isoform. The coding isoforms ENST00000413698 and ENST00000646110 were significantly underexpressed in pPCL ($p < 0.01$) as revealed by qRT-PCR, while the *IKZF1*

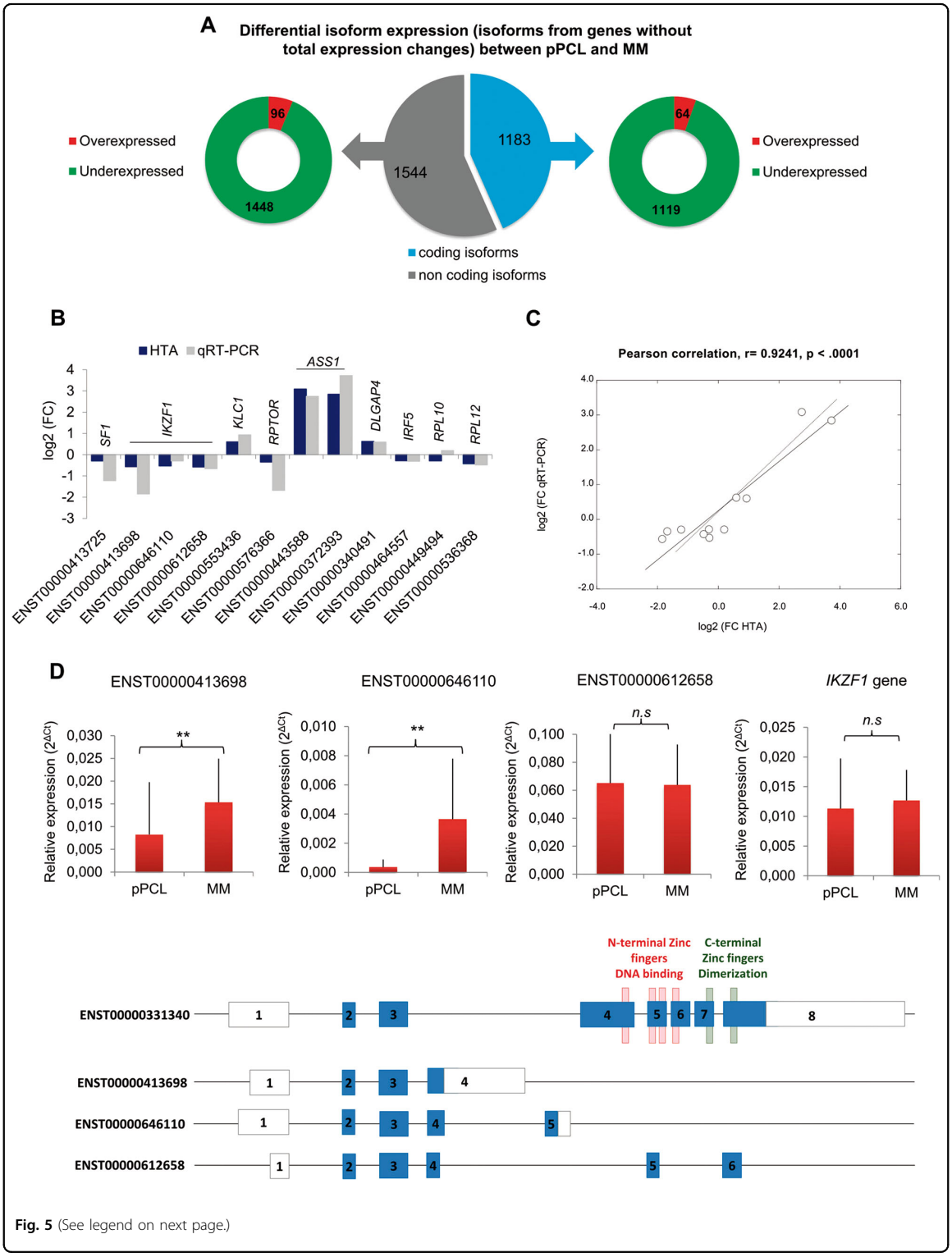

Fig. 5 (See legend on next page.)

(see figure on previous page)

Fig. 5 Identification of differentially expressed isoforms of genes without total expression changes. a Classification of deregulated isoforms according to coding (in blue) and non-coding (in grey) isoforms among the non-differentially expressed genes. The right side shows the coding isoforms that were overexpressed and underexpressed in pPCL relative to MM. The left side shows the non-coding isoforms that were overexpressed and underexpressed in pPCL relative to MM. For both, coding and non-coding isoforms with positive $\log_2$ FC and $p < 0.05$ were considered overexpressed, and isoforms with negative $\log_2$ FC and $p < 0.05$ were considered underexpressed. Genes with a value of $p > 0.05$ were considered not to be differentially expressed. **b** Experimental validation of differential isoform expression from genes without total expression changes in the HTA microarrays. The mRNA levels of isoforms (Ensembl ID) were assessed by qRT-PCR. The results are shown as the $\log_2$ FC between pPCL and MM samples, using the *PGK1* gene as the endogenous control. The expression difference of ten isoforms between pPCL and MM was statistically significant, and the expression difference of ENST00000449494 (*RPL10* isoform) and ENST00000612658 (*IKZF1* isoform) between pPCL and MM were not statistically significant. **c** Pearson correlation of isoform expression measured by qRT-PCR and by HTAs in pPCL ($n = 9$) and MM ($n = 10$) samples. **d** *IKZF1* isoform analysis. The mRNA levels of ENST00000413698, ENST00000646110, ENST00000612658 and *IKZF1* gene were assessed by qRT-PCR. The results are shown as the relative expression (calculated as $2^{-\Delta Ct}$) ± s.d between pPCL and MM samples, using *PGK1* as endogenous control gene. Statistically significant differences between pPCL and MM samples are represented as $^{**}p < 0.01$, $^{*}p < 0.05$ and *n.s.* non-significant (unpaired two-sided *Student's t* test). Schematic representation of the three downregulated *IKZF1* coding isoforms analysed by qRT-PCR in pPCL compared with MM samples is provided below. The longest isoform (ENST00000331340, NM_006060) contains four N-terminal zinc finger motifs (red), and two C-terminal zinc fingers (green). Exons are numbered from 1 to 8. Coding exons are represented by blue boxes and UTR regions by black boxes.

gene expression was equally expressed in both plasma cell dyscrasias, corroborating the HTA results (Fig. 5d). However, we found similar expression of the isoform ENST00000612658 in pPCL and MM (Fig. 5d).

Identification of potential exonic splicing enhancers

Alternative splicing produces different isoforms from a single gene, contributing significantly to proteomic diversity. This process is mediated by the splicing machinery, the spliceosome, which comprises more than 300 splicing factors that bind to specific sequence elements in the pre-mRNA sequence. Among the splice site signals in this sequence, exonic splicing enhancers (ESEs) are short and degenerative sequences that enhance splice-site recognition in constitutively and alternatively spliced exons[33]. ESEs act as binding sites for SR RNA-binding proteins, a family of conserved splicing factors that participate in multiple steps of the spliceosome assembly, during RNA splicing[34]. A broad range of sequences can function as ESEs in a particular context, and distinct SR proteins have different ESE specificities. The development of several resources for identifying ESEs binding sites and the global deregulation of the spliceosomal machinery prompted us to use one of these databases[24] to look for potential ESE motifs recognised by human SR proteins in our transcriptome dataset.

First, we examined exons differentially expressed between pPCL and MM that were validated by qRT-PCR assays. We only considered ESEs with a score of ≥ 5 in the SpliceAid database. The prediction algorithm used identified a very large number of ESEs. The analysis of the 13 exon sequences (*TRA2B, TUBG1, BCL2, COA3, COG8, PI4KB, PPM1B, RNF11, MERTK, SULF2, CD27, KRAS*, and *NEDD4L* genes) based on the SpliceAid database, predicted that all of them had at least one binding site for SR proteins (Fig. 6a). SRp40, SRp30a and SC35 proteins had the highest number of binding sites on the 13 exons, while SRp75 and SRp46 SR proteins had one and zero, respectively (Fig. 6a). These results indicate a possible strong effect of SRp40, SRp30a and SC35 proteins of all the SR proteins involved in the splicing of those pre-mRNAs (with a greater number of binding sites). In fact, SR proteins were overexpressed at the gene level in pPCLs compared with MM patients, although the differences were only statistically significant for *SRSF1* and *SFSF3* (Supplementary Fig. 8).

Secondly, we analysed 104 exons differentially expressed between pPCL and MM that were detected in KEGG pathway analysis of genes affected by inclusion or exclusion of exons (Supplementary Table 6). More than 70% of exons had binding sites for SRp40 and SC35 proteins, followed by SRp30a and SRp20, with 50% and 42%, respectively (Fig. 6b).

Since ESEs can be highly heterogeneous, their composition probably influences the occurrence of pre-mRNA splicing and thereby affects the transcriptome of cells. The higher number of ESEs found using the database indicates that prediction analysis needs to be validated experimentally to identify those that genuinely act by binding to SR proteins in the specific context of pPCL and MM.

Discussion

In this study, we compared the transcriptome profiles of pPCL and MM using samples that shared 17p deletion and a similar pattern of other cytogenetic alterations. These selection criteria allowed us to investigate whether molecular mechanisms other than those associated with the simple predominance of a particular chromosomal abnormality could contribute to determine the dramatic aggressive outcome of pPCL. Using HTA microarrays we were able not only to study the gene expression pattern, as other authors have done, but also to investigate the isoform expression and the impact of alternative splicing on the pathology of these diseases.

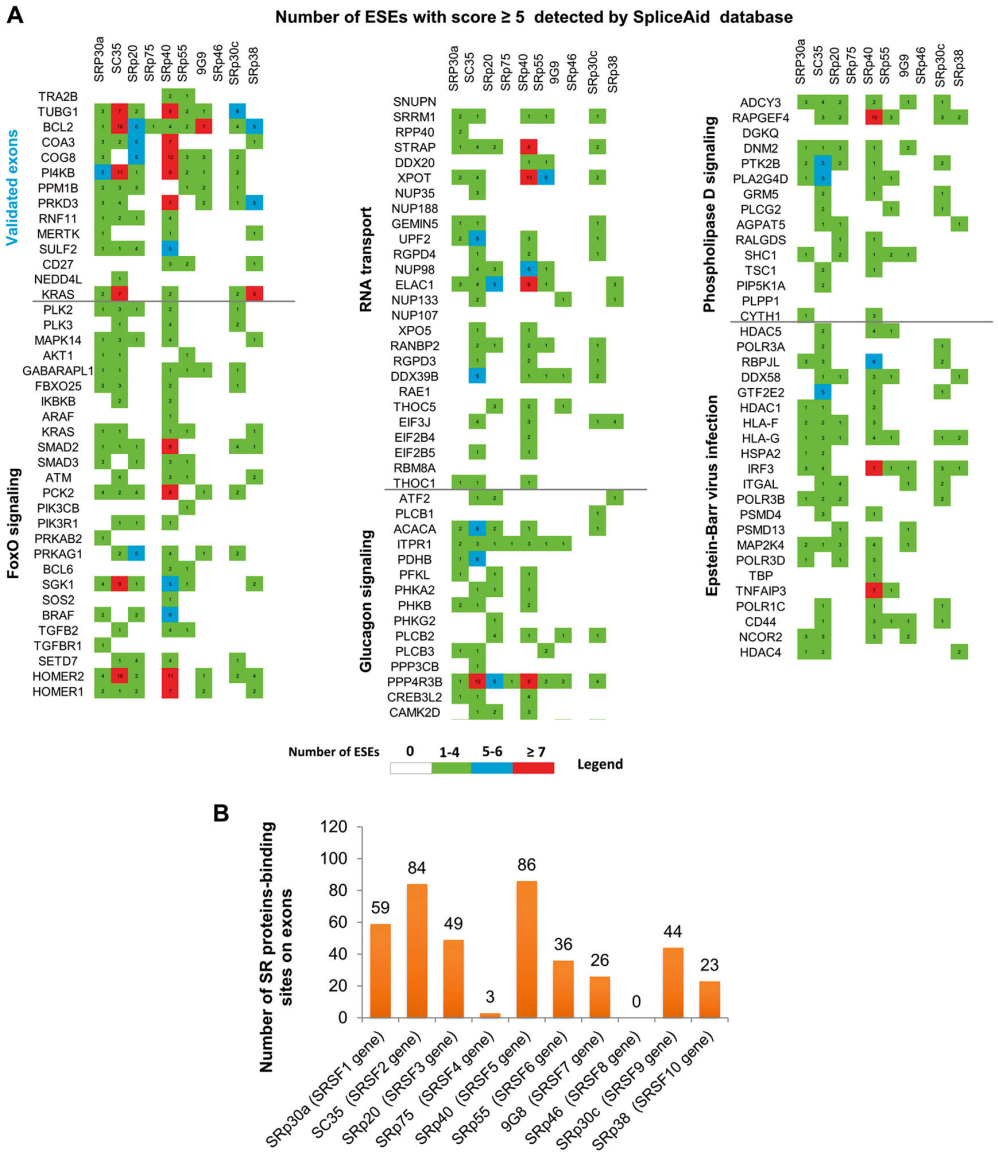

Fig. 6 Predictive identification of exonic splicing enhancers using the SpliceAid database. a Detection of ESEs in the 13 experimentally validated exons with differential expression between pPCL and MM, and on 104 exons with differential expression detected by KEGG pathway analysis affected by inclusion or exclusion of exons. Only the ESEs with a score of ≥5 assigned by the SpliceAid database were considered. The legend refers to the number of ESEs detected per exon for each SR protein. **b** Number of SR protein-binding sites in the 117 exons analysed.

In spite of the similar distribution of cytogenetic alterations in the two groups, the unsupervised analysis based on gene expression data distinguished two differentiated clusters. In contrast, the same kind of analysis using RNA-Seq data from the CoMMpass study did not identify any cluster in the set of MM patients with the 17p deletion. These results suggest that tumour PCs of pPCL have a significantly different transcriptome profile from that observed in the tumour PCs of MM, even though both diseases share the same tumour cells and have similar cytogenetic abnormalities. Indeed, we found a large number of genes that are differentially expressed between pPCL and MM, most of which are underexpressed in pPCL patients. Our results are not

comparable with those of previous studies of gene expression profiling in pPCL and MM patients, since we selected patients with a similar genetic background across the two plasma cell dyscrasias[17]. This probably explains why the gene expression-based pathway enrichment analysis showed seven affected pathways, including the spliceosome, aminoacyl-tRNA biosynthesis and EBV infection, which have not been described before. Nevertheless, *SLAMF6, SULF2, STAP1*, and *AHR* genes, four of the 40 most significantly deregulated genes in pPCL were among the list of 503 genes reported by Todoerti et al.[17] as being differentially expressed between the two groups.

Interestingly, six of the 20 most underexpressed genes founded in pPCL (*FRZB, DKK1, KIT, NCAM1, CTGF*, and *CXCR4*) are commonly associated with the bone marrow microenvironment and bone disease in MM. For example, the expression of the WNT inhibitors, *FRZB* and *DKK1* genes, is associated with osteolytic bone lesions in myeloma patients[35]. In fact, ~80% of MM patients develop osteolytic bone lesions, while in pPCL bone lesions are less frequent[36].

WARS (tryptophanyl-tRNA synthetase) and *AHR* (aryl hydrocarbon receptor) genes were the two most overexpressed genes in pPCL. *WARS* is a housekeeping enzyme that participates in the protein synthesis, catalysing the specific ligation of tRNA with tryptophan[37]. The upregulation of *WARS* has been reported to be included in a high-risk transcriptional signature for pPCL correlated with shorter overall survival[17]. Remarkably, a recent study has demonstrated a novel non-canonical function of *WARS* in antiviral defence, so it is rapidly secreted in response to viral infection, leading to the *in vitro* and *in vivo* inhibition of virus replication[38]. Previous studies have reported high levels of expression of *WARS* in cells infected with human cytomegalovirus, hepatitis B virus, and even in mouse intestines infected with *Cholera vibrio*[39–41]. In our study, an unexpected finding was the deregulation of the EBV infection pathway as revealed by the KEGG analysis for gene, isoform and alternatively spliced exon expressions. In addition, a few studies have reported the use of cellular spliceosome machinery by EBV for the transcription of viral proteins in EBV-infected cells with splicing components[42,43]. We can speculate that the infection with EBV might lead to the overexpression of the *WARS* gene as an antiviral defence of the EBV-infected cells. However, the potential role of this response in the pathogenesis of pPCL is unknown. The *AHR* gene is a cytosolic ligand-activated transcription factor considered as a chemical sensor of xenobiotic-induced carcinogenesis[44]. Several studies have demonstrated that *AHR* is overexpressed and constitutively active, even in the absence of environmental ligands in a range of human tumours, such as cutaneous squamous cell carcinomas[45], breast cancer[46], adult T-cell leukemia[47], pancreatic cancer[48], and human glioma[49]. Recently, *AHR* levels have been inversely associated with survival of MM patients, indicating that *AHR* inhibition may be an attractive therapeutic option for the treatment of this disease[50].

We also investigated alternative splicing events and isoforms expression in pPCL and MM patients. More than 2000 events of alternative splicing, predominantly inclusion or exclusion of exons, were detected. The use of a transcriptome array allowed us to identify more than 1000 deregulated coding isoforms, mostly underexpressed in pPCL, belonging to 658 genes whose expression did not significantly differ between pPCL and MM. Of these, the *SF1* (Splicing Factor 1) gene is a RNA-binding component of the spliceosomal machinery required for the ATP-dependent first step of spliceosome assembly. The deregulated *SF1* isoform is shorter than the canonical one and lacks the essential protein domain expression involved in their RNA binding functions. In this way, the *SF1* isoform is probably unable of efficiently exert its canonical function in spliceosome assembly, irrespective of *SF1* gene expression. We also found two deregulated *ASS1* (Argininosuccinate Synthase 1) isoforms that differs in the number of protein domains and features. The Ass1 protein is one of the enzymes of the urea cycle and catalyses the penultimate step of the arginine biosynthesis pathway. Thereby, *ASS1* gene is critical for the growth of human cancers, due to the role of L-arginine in different aspects of tumour metabolism and the immune system[51,52]. We can reasonably speculate that the overexpression of these two *ASS1* isoforms in pPCL patients could be associated with an increased proliferation of the PCs.

On the other hand, we detected six underexpressed *IKZF1* isoforms in pPCL patients in the HTA data, two of which were validated by qRT-PCR. Ikaros, encoded by the *IKZF1* gene, is a zinc-finger protein essential for lymphocyte development and which is important in MM pathology[53]. Their proteasomal degradation is a critical event in the mechanism of action of immunomodulatory drugs (IMiDs) against MM[54]. The 23 *IKZF1* isoforms produced by alternative splicing are differentiated by the alternative use of exons and subsequently in their functional domain composition, with distinct biological functions. However, only the isoforms that contain at least three of four N-terminal zinc fingers are capable of binding to DNA efficiently, and exert their function as a transcription factor. Nevertheless, the isoforms that contain the C-terminal zinc fingers that are responsible for dimerisation with other Ikaros isoforms and other family members have dominant negative functions by which they interfere with the DNA-binding functions of those proteins, including the inhibition of the activity of the full-length Ikaros protein[55–57]. Interestingly, in this study the

two validated *IKZF1* isoforms are shorter than the canonical isoform and are non-DNA-binding isoforms with a distinct C-terminal compared with the canonical isoform. Likewise, we hypothesised that these two *IKZF1* non-DNA-binding isoforms could also bind to the other members of the zinc-finger protein family through the C-terminal domain and exert a dominant-negative effect by interfering with the activity of those DNA-binding isoforms and, consequently, transcription would not be activated[56,58].

Overall, our results indicate that pPCL is a unique biological entity, and therefore different from MM. Even comparing MM and pPCL cases that share similar cytogenetic alterations, the transcriptome of pPCL is substantially and significantly different from that of MM. This work is the first of its kind to explore the expression of the spliceosomal components and the occurrence of alternative splicing events in pPCL compared with MM samples. Our findings also suggest the existence of a significant connection between alternative splicing deregulation and the molecular features of pPCL, and provide evidence of candidate genes and as yet unidentified pathways that could be pertinent to the biology of pPCL and that could contribute to the more aggressive clinical course of this neoplasm compared with that of MM. A limitation of this study is the small sample size related to the low incidence of pPCL. As such, further research is needed to validate the most relevant findings in other series of pPCL patients with del17p.

Author details
[1]Cancer Research Center-IBMCC (USAL-CSIC), Salamanca, Spain. [2]Institute of Biomedical Research of Salamanca (IBSAL), Salamanca, Spain. [3]Hematology Department, University Hospital of Salamanca, Salamanca, Spain. [4]Centro de Investigación Biomédica en Red de Cáncer (CIBERONC), CB16/12/00233, Salamanca, Spain. [5]National Medicines Institute, Warsaw, Poland

Competing interests
Dr. Mateos reports personal fees from Janssen, Celgene, Amgen, Takeda, Pharmamar, GSK, AbbVie and Adaptive, outside the submitted work. Dr. Garcia-Sanz reports personal fees from Amgen, Janssen, Takeda and Pfizer, outside the submitted work. Dr. Gutiérrez reports honoraria from Janssen outside the submitted work. The other authors declare no conflict of interest.

Funding
This study was partially supported by the Instituto de Salud Carlos III cofinanced by the European Union FEDER funds (PI13/00111 and PI16/01074), Gerencia Regional de Salud, Junta de Castilla y León (BIO/SA57/13) and the Asociación Española Contra el Cáncer (AECC, GCB120981SAN). E.A.R.R. was supported by the Consejería de Educación de Castilla y León and FEDER funds. I.M.K. and L.A.C. were supported by the Sociedad Española de Hematología y Hemoterapia.

Supplementary Information accompanies this paper at (https://doi.org/10.1038/s41408-019-0253-1).

Received: 4 June 2019 Revised: 17 October 2019 Accepted: 29 October 2019
Published online: 20 November 2019

References

1. Albarracin, F., Fonseca, R. Plasma cell leukemia. *Blood Rev.* **25**, 107–112 (2011).
2. Fernández de Larrea, C. et al. Plasma cell leukemia: consensus statement on diagnostic requirements, response criteria and treatment recommendations by the International Myeloma Working Group. *Leukemia* **27**, 780–791 (2013).
3. Kyle, R. A., Maldonado, J. E., Bayrd, E. D. Plasma cell leukemia. Report on 17 cases. *Arch. Intern. Med.* **133**, 813–818 (1974).
4. Noel, P., Kyle, R. A. Plasma cell leukemia: an evaluation of response to therapy. *Am. J. Med.* **83**, 1062–1068 (1987).
5. International Myeloma Working Group. Criteria for the classification of monoclonal gammopathies, multiple myeloma and related disorders: a report of the International Myeloma Working Group. *Br. J. Haematol.* **121**, 749–757 (2003).
6. Gonsalves, W. I. et al. Trends in survival of patients with primary plasma cell leukemia: a population-based analysis. *Blood* **124**, 907–912 (2014).
7. Neri, A. et al. Primary plasma cell leukemia 2.0: advances in biology and clinical management. *Expert Rev. Hematol.* **9**, 1063–1073 (2016).
8. Mina, R., D'Agostino, M., Cerrato, C., Gay, F., Palumbo, A. Plasma cell leukemia: update on biology and therapy. *Leuk. Lymphoma* **58**, 1538–1547 (2017).
9. Ravi, P. et al. Revised diagnostic criteria for plasma cell leukemia: results of a Mayo Clinic study with comparison of outcomes to multiple myeloma. *Blood Cancer J.* **8**, 116 (2018).
10. Simeon, V. et al. Molecular classification and pharmacogenetics of primary plasma cell leukemia: an initial approach toward precision medicine. *Int. J. Mol. Sci.* **16**, 17514–17534 (2015).
11. Tiedemann, R. E. et al. Genetic aberrations and survival in plasma cell leukemia. *Leukemia* **22**, 1044–1052 (2008).
12. Gutiérrez, N. C. et al. Differences in genetic changes between multiple myeloma and plasma cell leukemia demonstrated by comparative genomic hybridization. *Leukemia* **15**, 840–845 (2001).
13. Avet-Loiseau, H. et al. Cytogenetic, interphase, and multicolor fluorescence in situ hybridization analyses in primary plasma cell leukemia: a study of 40 patients at diagnosis, on behalf of the Intergroupe Francophone du Myélome and the Groupe Français de Cytogénétique Hématologique. *Blood* **97**, 822–825 (2001).
14. Mosca, L. et al. Genome-wide analysis of primary plasma cell leukemia identifies recurrent imbalances associated with changes in transcriptional profiles. *Am. J. Hematol.* **88**, 16–23 (2013).
15. Cifola, I. et al. Whole-exome sequencing of primary plasma cell leukemia discloses heterogeneous mutational patterns. *Oncotarget* **6**, 17543–17558 (2015).
16. Usmani, S. Z. et al. Primary plasma cell leukemia: clinical and laboratory presentation, gene-expression profiling and clinical outcome with Total Therapy protocols. *Leukemia* **26**, 2398–2405 (2012).
17. Todoerti, K. et al. Transcriptional characterization of a prospective series of primary plasma cell leukemia revealed signatures associated with tumor progression and poorer outcome. *Clin. Cancer Res.* **19**, 3247–3258 (2013).
18. Lionetti, M. et al. Biological and clinical relevance of miRNA expression signatures in primary plasma cell leukemia. *Clin. Cancer Res.* **19**, 3130–3142 (2013).
19. Todoerti, K. et al. Global methylation patterns in primary plasma cell leukemia. *Leuk. Res.* **73**, 95–102 (2018).
20. Mattioli, M. et al. Gene expression profiling of plasma cell dyscrasias reveals molecular patterns associated with distinct IGH translocations in multiple myeloma. *Oncogene* **24**, 2461–2473 (2005).
21. López-Corral, L. et al. The progression from MGUS to smoldering myeloma and eventually to multiple myeloma involves a clonal expansion of genetically abnormal plasma cells. *Clin. Cancer Res.* **17**, 1692–1700 (2011).
22. Gonzalez, D. et al. Mutational status of the TP53 gene as a predictor of response and survival in patients with chronic lymphocytic leukemia: results from the LRF CLL4 trial. *J. Clin. Oncol.* **29**, 2223–2229 (2011).
23. Wang, J., Vasaikar, S., Shi, Z., Greer, M., Zhang, B. WebGestalt 2017: a more comprehensive, powerful, flexible and interactive gene set enrichment analysis toolkit. *Nucleic Acids Res.* **45**, W130–W137 (2017).
24. Piva, F., Giulietti, M., Nocchi, L., Principato, G. SpliceAid: a database of experimental RNA target motifs bound by splicing proteins in humans. *Bioinf. Oxf. Engl.* **25**, 1211–1213 (2009).

25. Anczuków, O. et al. The splicing factor SRSF1 regulates apoptosis and proliferation to promote mammary epithelial cell transformation. *Nat. Struct. Mol. Biol.* **19**, 220–228 (2012).
26. Anczuków, O. et al. SRSF1-regulated alternative splicing in breast cancer. *Mol. Cell* **60**, 105–117 (2015).
27. DeLigio, J. T. et al. Serine/Arginine-Rich Splicing Factor 3 modulates the alternative splicing of cytoplasmic polyadenylation element binding protein 2. *Mol. Cancer Res.* **17**, 1920–1930 (2019).
28. Das, S., Krainer, A. R. Emerging functions of SRSF1, splicing factor and oncoprotein, in RNA metabolism and cancer. *Mol. Cancer Res.* **12**, 1195–1204 (2014).
29. Karni, R. et al. The gene encoding the splicing factor SF2/ASF is a proto-oncogene. *Nat. Struct. Mol. Biol.* **14**, 185–193 (2007).
30. Ajiro, M., Jia, R., Yang, Y., Zhu, J., Zheng, Z.-M. A genome landscape of SRSF3-regulated splicing events and gene expression in human osteosarcoma U2OS cells. *Nucleic Acids Res.* **44**, 1854–1870 (2016).
31. Zhang, Z., Pal, S., Bi, Y., Tchou, J., Davuluri, R. V. Isoform level expression profiles provide better cancer signatures than gene level expression profiles. *Genome Med.* **5**, 33 (2013).
32. Pal, S. et al. Isoform-level gene signature improves prognostic stratification and accurately classifies glioblastoma subtypes. *Nucleic Acids Res.* **42**, e64 (2014).
33. Blencowe, B. J. Exonic splicing enhancers: mechanism of action, diversity and role in human genetic diseases. *Trends Biochem. Sci.* **25**, 106–110 (2000).
34. Wang, J., Smith, P. J., Krainer, A. R., Zhang, M. Q. Distribution of SR protein exonic splicing enhancer motifs in human protein-coding genes. *Nucleic Acids Res.* **33**, 5053–5062 (2005).
35. van Andel H., Kocemba K. A., Spaargaren M., Pals S. T. Aberrant Wnt signaling in multiple myeloma: molecular mechanisms and targeting options. *Leukemia* (2019). https://doi.org/10.1038/s41375-019-0404-1.
36. van de Donk, N. W. C. J., Lokhorst, H. M., Anderson, K. C. & Richardson, P. G. How I treat plasma cell leukemia. *Blood* **120**, 2376–2389 (2012).
37. Jin, M. Unique roles of tryptophanyl-tRNA synthetase in immune control and its therapeutic implications. *Exp. Mol. Med.* **51**, 1 (2019).
38. Lee H.-C. et al. Released tryptophanyl-tRNA synthetase stimulates innate immune responses against viral infection. *J. Virol.* **93**, (2019). https://doi.org/10.1128/JVI.01291-18.
39. Ellis, C. N. et al. Comparative proteomic analysis reveals activation of mucosal innate immune signaling pathways during cholera. *Infect. Immun.* **83**, 1089–1103 (2015).
40. Wieland, S., Thimme, R., Purcell, R. H., Chisari, F. V. Genomic analysis of the host response to hepatitis B virus infection. *Proc. Natl Acad. Sci. USA* **101**, 6669–6674 (2004).
41. Zhu, H., Cong, J. P., Mamtora, G., Gingeras, T., Shenk, T. Cellular gene expression altered by human cytomegalovirus: global monitoring with oligonucleotide arrays. *Proc. Natl Acad. Sci. USA* **95**, 14470–14475 (1998).
42. Lee, N., Yario, T. A., Gao, J. S., Steitz, J. A. EBV noncoding RNA EBER2 interacts with host RNA-binding proteins to regulate viral gene expression. *Proc. Natl Acad. Sci. USA* **113**, 3221–3226 (2016).
43. Nanni, A. V., Lee, N. Identification of host RNAs that interact with EBV non-coding RNA EBER2. *RNA Biol.* **15**, 1181–1191 (2018).
44. Xue, P., Fu, J., Zhou, Y. The aryl hydrocarbon receptor and tumor immunity. *Front. Immunol.* **9**, 286 (2018).
45. Pan, Z.-Y. et al. Activation and overexpression of the aryl hydrocarbon receptor contribute to cutaneous squamous cell carcinomas: an immunohistochemical study. *Diagn. Pathol.* **13**, 59 (2018).
46. D'Amato, N. C. et al. A TDO2-AhR signaling axis facilitates anoikis resistance and metastasis in triple-negative breast cancer. *Cancer Res.* **75**, 4651–4664 (2015).
47. Hayashibara, T. et al. Possible involvement of aryl hydrocarbon receptor (AhR) in adult T-cell leukemia (ATL) leukemogenesis: constitutive activation of AhR in ATL. *Biochem. Biophys. Res. Commun.* **300**, 128–134 (2003).
48. Koliopanos, A. et al. Increased arylhydrocarbon receptor expression offers a potential therapeutic target for pancreatic cancer. *Oncogene* **21**, 6059–6070 (2002).
49. Gramatzki, D. et al. Aryl hydrocarbon receptor inhibition downregulates the TGF-beta/Smad pathway in human glioblastoma cells. *Oncogene* **28**, 2593–2605 (2009).
50. Bianchi-Smiraglia, A. et al. Inhibition of the aryl hydrocarbon receptor/polyamine biosynthesis axis suppresses multiple myeloma. *J. Clin. Invest.* **128**, 4682–4696 (2018).
51. Szefel, J., Danielak, A., Kruszewski, W. J. Metabolic pathways of L-arginine and therapeutic consequences in tumors. *Adv. Med. Sci.* **64**, 104–110 (2018).
52. Rodriguez, P. C., Quiceno, D. G., Ochoa, A. C. L-arginine availability regulates T-lymphocyte cell-cycle progression. *Blood* **109**, 1568–1573 (2007).
53. Krönke, J. et al. Lenalidomide causes selective degradation of IKZF1 and IKZF3 in multiple myeloma cells. *Science* **343**, 301–305 (2014).
54. Zhu, Y. X. et al. Identification of cereblon-binding proteins and relationship with response and survival after IMiDs in multiple myeloma. *Blood* **124**, 536–545 (2014).
55. Hahm, K. et al. The lymphoid transcription factor LyF-1 is encoded by specific, alternatively spliced mRNAs derived from the Ikaros gene. *Mol. Cell Biol.* **14**, 7111–7123 (1994).
56. Sun, L., Liu, A., Georgopoulos, K. Zinc finger-mediated protein interactions modulate Ikaros activity, a molecular control of lymphocyte development. *EMBO J.* **15**, 5358–5369 (1996).
57. Fedele, P. L. et al. IMiDs prime myeloma cells for daratumumab-mediated cytotoxicity through loss of Ikaros and Aiolos. *Blood* **132**, 2166–2178 (2018).
58. Sun, L. et al. Expression of dominant-negative and mutant isoforms of the antileukemic transcription factor Ikaros in infant acute lymphoblastic leukemia. *Proc. Natl Acad. Sci. USA* **96**, 680–685 (1999).

Capítulo 2

ARTÍCULO 2

"Expression of p53 protein isoforms predicts survival in patients with multiple myeloma"

Elizabeta A. Rojas, Luis A. Corchete, Cristina De Ramón, Patryk Krzeminski, Dalia Quwaider, Ramón García-Sanz, Joaquín Martínez-López, Albert Orio, Laura Rosiño, Joan Bladé, Juan José Lahuerta, Jesús F. San Migue, Marcos González, María Victoria Mateos, Jean-Christophe Bourdon, Irena Misiewicz-Krzeminska y Norma C. Gutiérrez

American Journal of Hematology
(2022), Feb 21
DOI: 10.1002/ajh.26507

La expresión de las isoformas proteicas de p53 predice la supervivencia de los pacientes con mieloma múltiple

Fundamento: La pérdida de la actividad del gen supresor tumoral p53, a través de la deleción de 17p o de la mutación del gen, está asociada con una corta supervivencia y peor pronóstico en el MM. Sin embargo, la desregulación de la vía de p53 abarca un espectro mucho más amplio de alteraciones. Actualmente se sabe que existen al menos 12 isoformas proteicas de p53 codificadas a partir de 9 isoformas de ARNm del gen *TP53*, como resultado de la combinación del *splicing* alternativo, el uso de promotores y/o sitios de inicio de la traducción alternativos. Las isoformas de p53 pueden agruparse en subclases dependiendo del mecanismo que dio lugar a su formación: subclase α, subclase β, subclase γ, subclase TA/Δ40, también llamadas isoformas largas, y subclase Δ133 o isoformas cortas. Aunque la desregulación de la expresión de las isoformas de p53 se ha asociado con el pronóstico en varios tipos de cáncer, hasta ahora no hay estudios que evalúen la expresión de las isoformas de p53 en el MM. Por ello, nos propusimos cuantificar la expresión de las isoformas de p53, tanto a nivel de proteína como de ARNm, en muestras de pacientes con MM, y analizar su valor clínico.

Metodología: Se utilizó la tecnología de nanoinmunoensayo capilar para identificar y cuantificar la expresión de las isoformas proteicas de p53. Para ello se utilizaron 156 muestras de CPs CD138+ purificadas de pacientes con MM de nuevo diagnóstico, incluidos en un ensayo clínico del Grupo Español de Mieloma (PETHEMA/GEM2012). Los anticuerpos primarios utilizados en el estudio fueron: el anticuerpo monoclonal DO-11 cuyo epítopo está presente en el dominio de unión al ADN, y que permite por tanto la detección de todas las isoformas de p53 por su peso molecular; el anticuerpo monoclonal DO-1, cuyo epítopo está situado en el dominio de transactivación 1, sólo presente en las isoformas TA (TAp53α, TAp53β, y TAp53γ); el anticuerpo policlonal A300-249A-T, que es específico de las isoformas α (TAp53α, Δ40p53α, Δ133p53α, y Δ160p53α); y el anticuerpo policlonal KJC8, que es específico de las isoformas β (TAp53β, Δ40p53β, Δ133p53β, y Δ160p53β). El anticuerpo anti-GAPDH, fue utilizado como control endógeno. Todos los datos de expresión de proteínas fueron analizados utilizando el programa Compass™ (ProteinSimple).

La expresión del gen y de las isoformas de p53 a nivel de ARNm fue analizada mediante PCR cuantitativa en tiempo real (qRT-PCR) utilizando oligonucleótidos diseñados, estandarizados y publicados previamente. Se cuantificaron las isoformas α, β, cortas (Δ133/Δ160) y largas (TA/Δ40), además del gen completo. Adicionalmente, para analizar la presencia de mutaciones puntuales del gen *TP53* se secuenciaron sus exones mediante secuenciación de nueva generación (NGS) utilizando el método de captura.

La estimación de las curvas de supervivencia se realizó mediante el método de Kaplan-Meier y su comparación con la prueba de log-rank. La prueba de chi-cuadrado y test de Fisher se utilizó para el análisis de asociación entre las variables categóricas. Todos los análisis estadísticos se llevaron a cabo utilizando los programas SPSS v.22.0, Simfit v.7.5.1 y el paquete R.

Resultados: El 76 % de los pacientes presentaban expresión de la proteína total p53, donde la mayor proporción correspondía a las isoformas largas, detectadas en el 72 % de las muestras, y una menor proporción correspondía a las isoformas cortas, sólo detectadas en el 18 % de los casos. Las isoformas TA se encontraron en el 85 % de los casos: la isoforma TAp53α fue más abundante que TAp53β y TAp53γ. El 15 % de los pacientes no presentaban expresión de las isoformas TA. Por su parte, las isoformas α y β se identificaron en el 85 % y el 52 % de los casos, respectivamente.

Se detectó mayor expresión de las isoformas largas y TAp53β/γ en los pacientes que tenían deleción de 17p. En cambio, la proteína total y el resto de las isoformas no mostraron cambios en su expresión en función de la presencia de deleción de 17p. Además, los pacientes de MM con alto riesgo citogenético expresaron mayores niveles de expresión de TAp53β/γ que aquellos pacientes con riesgo citogenético estándar. El análisis de supervivencia puso de manifiesto que los pacientes con baja y alta expresión de isoformas cortas e isoformas TAp53β/γ, respectivamente, presentaban una supervivencia global (SG) y un tiempo hasta la progresión (SLP) más cortos.

Cuando se analizó la supervivencia de los pacientes combinando el riesgo citogenético con la expresión de las isoformas, se observó que los pacientes con alto riesgo citogenético y alta expresión de las isoformas cortas o baja expresión de la isoforma TAp53β/γ, tuvieron una SG y SLP más largas, comparable a la de los pacientes con riesgo estándar. El mismo análisis considerando las alteraciones citogenéticas individualmente mostró un efecto beneficioso de la expresión de isoformas cortas en el pronóstico de los pacientes con t(4;14) o del(17p). En el análisis multivariante se observó que tanto el alto riesgo citogenético como los altos niveles de expresión de la isoforma TAp53β/γ se mantuvieron como factores pronósticos independientes de la SLP.

Conclusiones: Los cambios en la expresión de las isoformas proteicas cortas y las isoformas TAp53β/γ se asocian con el pronóstico de los pacientes con MM. La estratificación pronóstica de los pacientes basada en las alteraciones citogenéticas mejora notablemente cuando se incluyen los datos de expresión de las isoformas proteicas de p53.

Received: 4 November 2021 | Revised: 21 January 2022 | Accepted: 15 February 2022

DOI: 10.1002/ajh.26507

RESEARCH ARTICLE

AJH WILEY

Expression of p53 protein isoforms predicts survival in patients with multiple myeloma

Elizabeta A. Rojas[1,2] | Luis A. Corchete[1,2] | Cristina De Ramón[1] | Patryk Krzeminski[1,2,3] | Dalia Quwaider[1,2] | Ramón García-Sanz[1,2,4,5] | Joaquín Martínez-López[4,5,6,7] | Albert Oriol[5,8] | Laura Rosiñol[5,9] | Joan Bladé[5,9] | Juan José Lahuerta[5,10] | Jesús F. San Miguel[4,5,11] | Marcos González[1,2,4] | María Victoria Mateos[1,2,4,5] | Jean-Christophe Bourdon[12] | Irena Misiewicz-Krzeminska[1,2,13] | Norma C. Gutiérrez[1,2,4,5]

[1]Hematology Department, University Hospital of Salamanca, IBSAL, Salamanca, Spain

[2]Cancer Research Center-IBMCC (USAL-CSIC), Salamanca, Spain

[3]Department of Nanobiotechnology and Experimental Ecology, Institute of Biology, Warsaw University of Life Sciences, Warsaw, Poland

[4]Centro de Investigación Biomédica en Red de Cáncer (CIBERONC), CB16/12/00233, Salamanca, Spain

[5]Grupo Español de Mieloma (GEM), Barcelona, Spain

[6]Medicine Department, Complutense University, Madrid, Spain

[7]Spanish National Cancer Research Center (CNIO), Madrid, Spain

[8]University Hospital Germans Trias i Pujol, Barcelona, Spain

[9]Hospital Clinic of Barcelona, Instituto de Investigaciones Biomédicas August Pi i Sunyer (IDIBAPS), Barcelona, Spain

[10]Hematology Department, University Hospital 12 de Octubre, Madrid, Spain

[11]Clínica Universidad de Navarra, Centro de Investigaciones Médicas Aplicadas (CIMA), Instituto de Investigación Sanitaria de Navarra (IdiSNA), Pamplona, Spain

[12]School of Medicine, University of Dundee, Dundee, UK

[13]Experimental Hematology Department, Institute of Hematology and Transfusion Medicine, Warsaw, Poland

Correspondence
Norma C. Gutiérrez, Hematology Department, University Hospital of Salamanca, IBSAL, Paseo San Vicente, 58-182, Salamanca 37007, Spain.
Email: normagu@usal.es

Funding information
The Instituto de Salud Carlos III, European Union FEDER funds, Grant Numbers: PI16/01074 and PI19/00674; The Asociación Española Contra el Cáncer, Grant Number: AECC, PROYE20047GUTI; National Science Centre, Poland, Grant Number: UMO-2019/35/B/NZ5/02824; The Consejería de Educación de Castilla y León and FEDER funds; AECC, Grant Number: CLJUN18010DERA.

Abstract

Loss and/or mutation of the *TP53* gene are associated with short survival in multiple myeloma, but the p53 landscape goes far beyond. At least 12 p53 protein isoforms have been identified as a result of a combination of alternative splicing, alternative promoters and/or alternative transcription site starts, which are grouped as α, β, γ, from transactivation domain (TA), long, and short isoforms. Nowadays, there are no studies evaluating the expression of p53 isoforms and its clinical relevance in multiple myeloma (MM). We used capillary nanoimmunoassay to quantify the expression of p53 protein isoforms in CD138-purified samples from 156 patients with newly diagnosed MM who were treated as part of the PETHEMA/GEM2012 clinical trial and investigated their prognostic impact.

Irena Misiewicz-Krzeminska and Norma C. Gutiérrez contributed equally to this study.

Quantitative real-time polymerase chain reaction was used to corroborate the results at RNA levels. Low and high levels of expression of short and TAp53β/γ isoforms, respectively, were associated with adverse prognosis in MM patients. Multivariate Cox models identified high levels of TAp53β/γ (hazard ratio [HR], 4.49; $p < .001$) and high-risk cytogenetics (HR, 2.69; $p < .001$) as independent prognostic factors associated with shorter time to progression. The current cytogenetic-risk classification was notably improved when expression levels of p53 protein isoforms were incorporated, whereby high-risk MM expressing high levels of short isoforms had significantly longer survival than high-risk patients with low levels of these isoforms. This is the first study that demonstrates the prognostic value of p53 isoforms in MM patients, providing new insights on the role of p53 protein dysregulation in MM biology.

1 | INTRODUCTION

Loss and/or mutation of the *TP53* gene are associated with short survival in multiple myeloma (MM). *TP53* mutations are uncommon at diagnosis, being present in less than 8% of cases, and deletion of the 17p13 chromosomal region, del(17p), has been identified in approximately 10% of newly diagnosed MM patients.[1,2] Although del(17p) has been routinely examined in the clinical setting for many years and *TP53* mutations are considered in present-day genetic studies, the p53 landscape covers a far wider range of phenomena than just *TP53* deletions and mutations.[3,4] Therefore, the study of other deregulations of the p53 pathway, particularly those that trigger defective p53 activity, are also important.[3–6]

The discovery of an alternative promoter in the *TP53* gene in 2005 led to the identification and characterization of p53 isoforms.[7] This finding has had a profound impact on our perspective on the p53 pathway and the ways of researching p53 tumor suppressor activity. The *TP53* gene expresses at least twelve p53 protein isoforms that are encoded by nine p53 mRNAs: TAp53α, TAp53β, TAp53γ, Δ40p53α, Δ40p53β, Δ40p53γ, Δ133p53α, Δ133p53β, Δ133p53γ, Δ160p53α, Δ160p53β, and Δ160p53γ proteins. The p53 isoforms arise from the combination of alternative promoter usage (proximal and internal promoters), alternative initiation codons (ATG1, ATG40, ATG133 and ATG160), and/or alternative splicing of introns 2 (Δ40) and/or 9 (α, β, γ) (Figures 1A and S6A,B). They can be grouped into subclasses or variants, such as the α, β, γ, from transactivation domain (TA), Δ40, and Δ133/Δ160 variants, based on the molecular mechanisms that lead to their formation (Figures S1D and S6A,B). The 12 p53 protein isoforms share a common region of the DNA-binding domain (DBD) but have different transactivation and oligomerization domains that allow them to differentially regulate the expression of p53 target genes and, at the same time, to be distinctively modulated by their negative regulators, like the Mdm2 and Mdm4 proteins.[7–11]

Several studies have demonstrated that p53 isoforms are differentially expressed in human cancers and that they affect the prognosis of some of these tumors. *TP53* deletions have been associated with low levels of p53 gene and protein expression in MM, using microarrays and immunohistochemistry, respectively.[3,12,13] Moreover, haploinsufficiency of p53 has been functionally demonstrated in MM cell lines[3] and a low level of expression of *TP53* gene has been associated with inferior outcome in MM patients. However, no studies have so far evaluated the expression of p53 isoforms and its clinical significance in MM.[8,14–16]

In this study, we investigated for the first time the relative expression of p53 isoforms in MM at the protein and mRNA levels. Using samples from homogeneously treated MM patients, we found that the differential expression of short and TA p53 isoforms influenced survival. In addition, incorporating expression levels of p53 isoforms improved the current cytogenetic-risk classification.

2 | MATERIALS AND METHODS

2.1 | Primary samples

A total of 156 protein samples from newly diagnosed MM patients enrolled in the clinical trial GEM2012 (NCT01916252) were included in the study. Although 458 patients were evaluated in this trial, fewer than 40% of the purified MM samples had sufficient material available to enable proteins and nucleic acids to be extracted. Details of the GEM2012 trial and sample processing have been previously reported.[17,18]

Baseline characteristics of patients for whom data were available are summarized in Table S1. No statistically significant differences between the present cohorts and the whole series from the GEM2012 trial ($N = 458$) were observed.

Fluorescence in situ hybridization (FISH) studies to detect *IGH* rearrangements, 17p and 1p deletions, and 1q gains were available for

all patients. Cytogenetic abnormalities were distributed as expected, based on previously published data. The high-risk cytogenetic group included those patients with t(4;14), t(14;16), and/or 17p deletion (del17p), according to International Myeloma Working Group criteria.[19] The median follow-up of the GEM2012 patients in this study was 72 months (range, 32–88 months). At the end of their follow-up, 68 patients (47%) had progressed, and 34 patients (23%) had died.

2.2 | Protein extraction and capillary electrophoresis immunoassay

Proteins were extracted simultaneously with genomic DNA and RNA by ice-cold acetone precipitation, as previously described.[20] The total protein assay was used to quantify protein concentration using WES™ system (ProteinSimple). Capillary electrophoresis immunoassay (CNIA) analysis, also called Simple Western, was performed using a WES

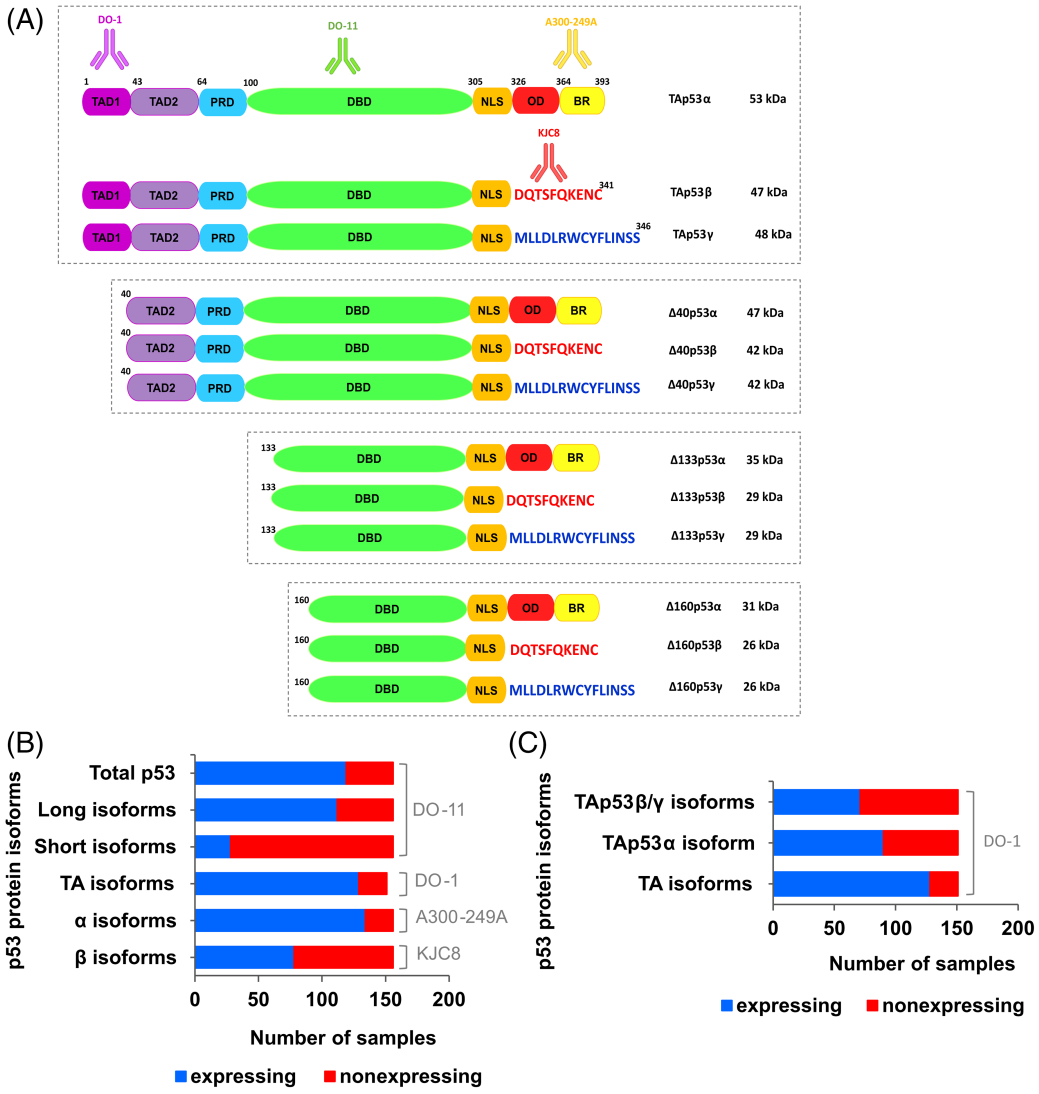

FIGURE 1 Schematic representation of human p53 protein isoforms, and the region containing the epitope for the p53 antibodies used in this study. (A) The main domains of p53 protein isoforms and their locations are represented by colors and amino acid (aa) numbering, respectively. The C-terminal sequences specific to the β (DQTSFQKENC) and γ (MLLDLRWCYFLINSS) variants are also shown. The molecular weight of each p53 isoform protein is indicated. The α, β, TA, long, and short protein isoforms are specifically recognized by A300-249A, KJC8, DO-1, and DO-11, respectively. (B) Number of MM patients with and without expression of each p53 isoform. (C) Number of MM patients with and without expression of TA isoforms, differentiating the two bands at 55–57 and 60–63 kDa that correspond to the TAp53α and TAp53β/γ isoforms, respectively. BR, basic region, aa 364–393 (yellow); DBD, DNA-binding domain, aa 101–292 (green); NLS, nuclear localization signal, aa 305–322 (orange); OD, oligomerization domain, aa 326–356 (red); PRD, proline-rich domain, aa 64–92 (blue); TAD1, transactivation domain 1, aa 1–42 (purple); TAD2: transactivation domain 2, aa 43–63 (violet) [Color figure can be viewed at wileyonlinelibrary.com]

machine (ProteinSimple, San Jose, CA) in accordance with the manufacturer's protocols and as previously described.[20,21] The primary antibodies used in the study were: mouse monoclonal DO-11 (BioRad; MCA1704, aa 181–190), whose epitope is present in the common region DBD and allows detection of all p53 protein isoforms; mouse monoclonal DO-1 (Santa Cruz Biotechnology; sc-126, aa 11–25), whose epitope is situated in the transactivation domain 1 that is present only in the TAp53α, TAp53β, and TAp53γ protein isoforms; rabbit polyclonal anti-p53 A300-249A-T (Bethyl Laboratories, Inc.; aa 375–393), which is specific to the α isoforms (TAp53α, Δ40p53α, Δ133p53α, and Δ160p53α); and anti-GAPDH (Cell Signaling; rabbit mAb #2118), which was used as the endogenous control. The rabbit polyclonal KJC8 antibody, which is specific to the β isoforms (TAp53β, Δ40p53β, Δ133p53β, and Δ160p53β), was provided by Prof. J-C. Bourdon (aa 331–341).[7]

All protein data were analyzed with Compass™ software (ProteinSimple), qualitatively at first, using the virtual blots (analogous to the images of the long-established western blot) that show the protein band with the expected size and also quantitatively, measuring the chemiluminescence peaks (peak area) that correspond to the expression of a particular protein. The protein expression was reported as relative to the endogenous control, GAPDH.

A more detailed protocol of the relative quantification of protein by CNIA has been reported previously.[18,20,21]

2.3 | Plasmids and transfection

We used the null-p53 JJN3 myeloma cells nucleotransfected with the specific expression vectors as positive controls for the p53α, p53β, p53γ, and Δ133p53α protein isoforms based on their migration profiles (Figure S1A–C). The commercial expression plasmids containing each isoform were obtained from Origene: p53β isoform (NM_001126114) SC322987, p53γ isoform (NM_001126113) SC322990, and Δ133p53α isoform (NM_001126115) SC322927. The pcDNA3 p53 WT, which codes for the canonical p53α, was a gift from David Meek (Addgene plasmid # 69003).[22] For transient protein expression, the null-p53 JJN3 myeloma cell line was nucleofected with 1 μg of each plasmid using the X005 program of the Amaxa II nucleofector (Lonza Bioscience). The proteins were collected 24 h post-transfection.

2.4 | Nucleic acid extraction and quantitative real-time polymerase chain reaction analysis

Total RNA was extracted from all samples using the AllPrep DNA/RNA Mini Kit (Qiagen). RNA integrity was assessed using Agilent 2100 Bioanalyzer (Agilent Technologies), and samples with an RNA integrity number (RIN) ≥ 6 were used. Total RNA (200 ng) was reverse-transcribed to cDNA using the SuperScript First-Strand Synthesis System, which uses oligo (dT) (Thermo Fisher). *TP53* isoforms (α, β, short [Δ133/Δ160] and long [TA/Δ40] isoforms) (Figure S6A,B) were examined by quantitative real-time polymerase chain reaction (qRT-PCR), as previously described.[23] We also measured the expression of the *TP53* gene, detected at a region of mRNA common to all isoforms. The *PGK1* gene was used as the endogenous control. Samples with a Ct value ≥35 were considered as not expressed. Values of ΔCt, defined as Ct (housekeeping gene) − Ct (target gene), were also calculated.

2.5 | Next-generation sequencing

Genomic DNA samples were purified before sequencing using Genomic DNA Clean & Concentrator TM-10 (Zymo Research, Irvine, CA). Generation of libraries was carried out by target enrichment SeqCap EZ Choice gene panel (Roche NimbleGen Inc., Madison, WI) that included the coding sequence of *TP53* gene, which was designed by NimbleDesign platform. The resulting pool (48-plex) underwent high-throughput paired-end (101 bp) sequencing on an Illumina MiSeq System with 1500-fold coverage. Sequence alignment and variant calling was performed using MiSeq Reporter software (Illumina Inc.). Annotation of resulting variant call files (.vcfs) was performed with BaseSpace Variant Interpreter software, filtering out single nucleotide variants (SNVs) and small insertions/deletions with <100X reads and variant allele frequency (VAF) of < 10%.

2.6 | Statistical analysis

All statistical analyses were carried out with IBM SPSS Statistics 26.0 (IBM Corp., Armonk, NY), the Simfit package (W.G. Bardsley, University of Manchester, Manchester, UK; v7.0.9 Academic 32 bit), and R work packages. The Mann–Whitney *U* test was used to analyze the continuous variables.

For survival analyses, probabilities of overall survival (OS) and survival without progression (abbreviated to TTP) were assessed for each isoform using the Kaplan–Meier estimator. Patients who were not enrolled in the GEM2014 maintenance protocol after completing the GEM2012 clinical trial and who had not progressed, relapsed, or died were excluded from these analyses. The TTP was defined as the time from MM diagnosis to the day of disease progression. The survival curves of the isoform groups were compared using the log-rank test. The Cutoff Finder R package was used to determine the optimal cutoff for all survival analyses, which was defined as the most significant split discriminating between long and short survival when testing all possible cutoffs using the log-rank test.

After checking that the assumptions of proportional hazards held using Schoenfeld residuals and that there was no significant multicollinearity, multivariable Cox regression models were fitted considering a set of covariates with clinical and biological interest. Thus, the models included conventional covariates such as high-risk cytogenetics, age at diagnosis (years), International Staging System (ISS) stage (III vs. I/II), elevated lactate dehydrogenase (LDH), plasmacytoma occurrence, and protein isoforms expression previously

dichotomized by the Cutoff Finder R package. All these predictor covariates were entered into the regression equation together. These multivariable analyses were performed in R with the survival and car packages and associated forest plots were depicted using the survminer package. The relative contribution of the covariates to the Cox models was assessed by estimation of the proportion of the χ^2 statistic accruing from each covariate using the rms package; the higher the value of the statistic, the greater the contribution of the covariate to the model.

3 | RESULTS

3.1 | Expression patterns of p53 protein isoforms in MM

The expression of the p53 protein isoforms, α isoforms (TAp53α, Δ40p53α, Δ133p53α, and Δ160p53α); β isoforms (TAp53β, Δ40p53β, Δ133p53β, and Δ160p53β); TA isoforms (from transactivation domain: TAp53α, TAp53β, and TAp53γ); long (includes TA and Δ40: TAp53α, TAp53β, TAp53γ, Δ40p53α, Δ40p53β, and Δ40p53γ) and short isoforms (Δ133 and Δ160: Δ133/Δ160 α, β, and γ), as well as the total p53 protein, was assessed in the 156 MM samples by capillary nanoimmunoelectrophoresis using the specific antibodies (Figures 1A and S1A–D, Table S2).

The qualitative analysis of CNIA assays showed expression of the total p53 protein in 119/156 (76%) MM samples using the DO-11 antibody, which recognizes identical epitopes present in all the p53 protein isoforms. Based on the migration profile and the recognition pattern of this antibody, we observed that the major proportion of the total p53 protein corresponded to the long isoforms, which were detected in 112 of the 156 MM samples (72%), and the minor proportion corresponded to the short isoforms, which were only present in 28 of the 156 MM samples (18%) (Figure 1B).

The TA protein isoforms were detected in 128/151 MM samples (85%) using the DO-1 antibody, whose epitope is present in the transactivation domain 1 (TAD1, aa 20 to 25) (Figure 1A). Among the TA isoforms, we were able to distinguish the TAp53α band at 60–63 kDa in 90/151 (60%) samples, and the bands corresponding to TAp53β and TAp53γ, which were observed merged as a single band at 55–57 kDa in 71/151 MM samples (47%). Twenty-three patients (15%) did not show any of those isoforms (Figure 1C). The α and β protein isoforms were identified in 132/156 (85%) and 81/156 (52%) samples, respectively, as measured by the antibodies A300-249A and KJC8, which were specific to each isoform (Figure 1B).

The quantitative analysis revealed a high level of variability in the expression of all the p53 protein isoforms analyzed (Figure S1E). The expression of long isoforms was the most homogeneous, while the TAp53β/γ and α isoforms showed the greatest variability, as indicated by their higher coefficients of variation (Figure S1F).

3.2 | Relationship between p53 protein isoforms and cytogenetic abnormalities

We next analyzed the association between the expression of p53 protein isoforms and the cytogenetic features of MM patients. We found no statistically significant differences in the level of expression of total p53 protein between MM patients with and without del(17p). In contrast, we detected significant differences in the expression of long and TAp53β/γ isoforms between the two groups (Figure 2). We also noticed that none of the 14 patients with del(17p) expressed short isoforms (Figure 2). The expression of α and β protein isoforms was similar in all patients, irrespective of the presence of del(17p). The analysis considering the mutation status of *TP53* showed comparable results. We found that the expression levels of TA isoforms were significantly higher in patients with mutated *TP53* gene than in those with nonmutated gene. No significant associations between the expression of the other p53 protein isoforms and the presence of *TP53* mutations were found (Figure S2).

On the other hand, no differences in the expression of any of the p53 protein isoforms analyzed and the total p53 protein were found to be associated with the presence of the gain of 1q, del(1p) or t(4;14). Since the limited number of patients with specific high-risk cytogenetic abnormalities may preclude the identification of significant differences, we also analyzed the relationship between the levels of p53 protein isoforms and cytogenetic alterations, grouping them into high- and standard-risk categories. We found statistically significant differences in the expression levels of TAp53β/γ isoforms between the two cytogenetic groups. High-cytogenetic-risk patients expressed TAp53β/γ isoforms significantly more strongly than did standard-risk patients (Figure 2). No differences in the expression of the other p53 isoforms and total p53 protein were found in either cytogenetic-risk group.

3.3 | Effect of the expression of p53 protein isoforms on MM patient survival

High levels of the short p53 isoforms were accompanied by a reduction of 75% (HR = 0.25, $p = .004$) in the risk of progression and an 88% (HR = 0.124, $p = .014$) drop in the risk of mortality (Figure 3A). Conversely, high levels of TA isoforms were associated with shorter TTP and OS (HR = 2.02, $p = .008$ and HR = 2.39, $p = .018$, respectively) (Figure S3A). Nevertheless, only the high level of expression of TAp53β/γ isoforms, but not of TAp53α, was associated with negative effects on TTP and OS (HR = 3.58, $p < .001$ and HR = 2.38, $p = .022$, respectively) (Figures 3B and S3B). The expression levels of α and β variants, as well as levels of total p53 protein had no influence on the survival of MM patients (Figure S3C).

We further explored the impact of expression levels of p53 protein isoforms on the survival of MM patients according to the cytogenetic abnormalities. In the present cohort, MM patients bearing at least one high-risk cytogenetic lesion, as well as those with the 17p deletion, had significantly shorter survival than those patients without these abnormalities, as described in previous studies (Figure S4A).

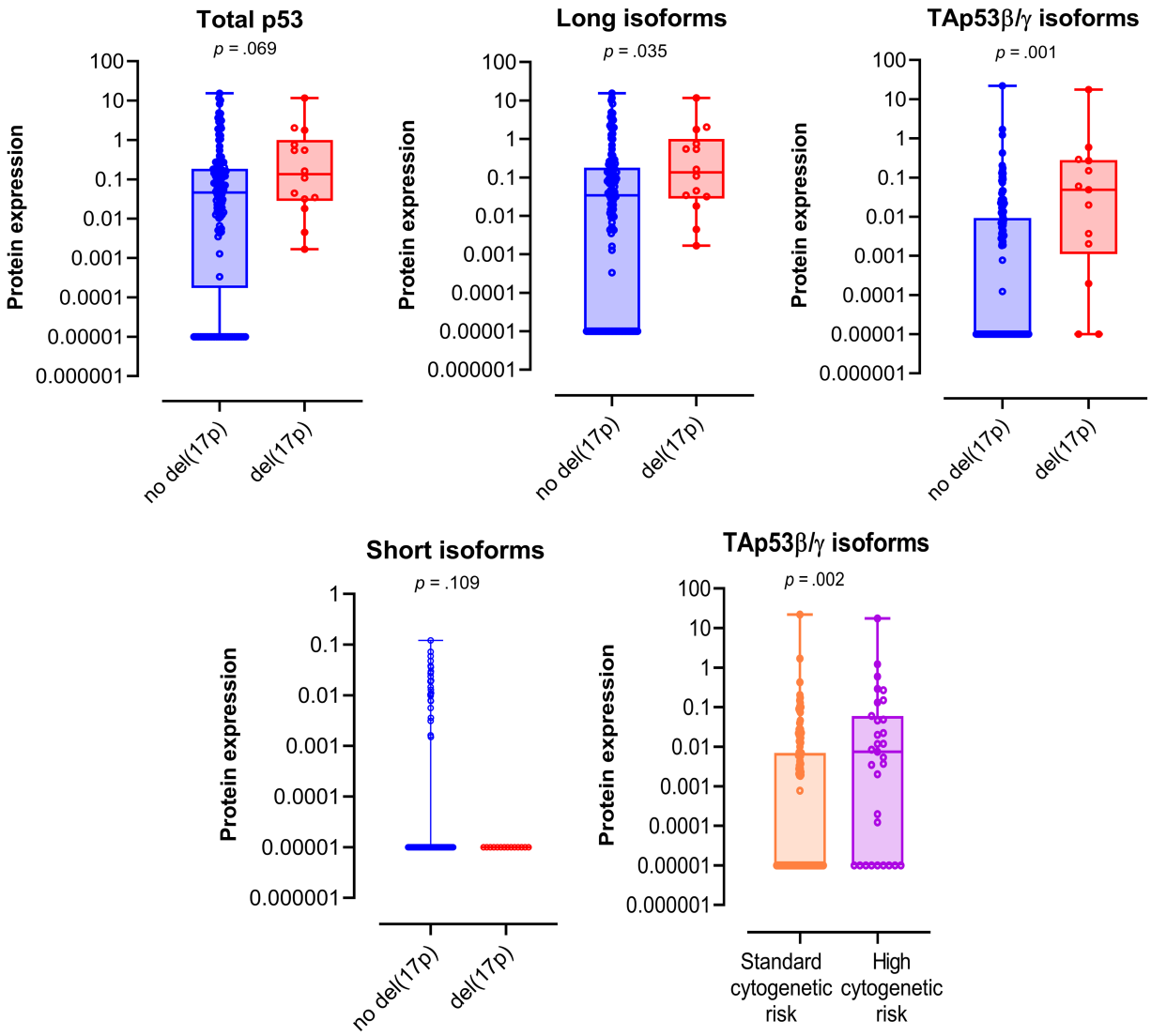

FIGURE 2 Association of p53 protein isoforms with deletion of 17p and with standard and high cytogenetic risk. Distribution of the expression of total p53 protein, long, TAp53β/γ and short isoforms, based on the presence or absence of the 17p deletion. Expression levels of the TAp53β/γ in MM patients with standard and high cytogenetic risk. The statistically significant differences between groups were determined by the Mann–Whitney *U* test (*p* values indicated) [Color figure can be viewed at wileyonlinelibrary.com]

When the cytogenetic-risk groups were analyzed with respect to the expression of p53 isoforms two different survival categories were identified within the high-risk group. Thus, MM patients with high-risk cytogenetics and a high level of expression of short p53 isoforms had significantly longer TTP and OS, which were comparable to those attained by standard-risk patients (Figure 4A). However, the effect of the TAp53β/γ isoforms, and long isoforms were the opposite, in such way that MM patients with high-risk cytogenetics and low-level expression of TAp53β/γ or long isoforms had longer TTP and OS, similar to those patients with standard risk as demonstrated by FISH (Figures 4B and S4B). These results indicate that high levels of short isoforms, and low levels of TAp53β/γ and long protein isoforms allow the identification of a subset of MM patients with high cytogenetic risk that showed a better prognosis than expected. Interestingly, a positive influence of the short p53 isoforms was also observed when t(4;14) or del(17p) were considered separately (Figure S5A). Furthermore, within the MM cases with t(4;14) the high levels of expression of TAp53β/γ and long p53 isoforms distinguished a group of patients with significantly shorter TTP and OS (Figure S5B).

In the full multivariate Cox model for TTP, including p53 protein isoform expression and the conventional variables of proven prognostic impact on MM, we observed that high-risk cytogenetics and high expression levels of TAp53β/γ isoforms remained independent prognostic factors (HR = 4.49, $p < .001$ and HR = 2.69, $p < .001$,

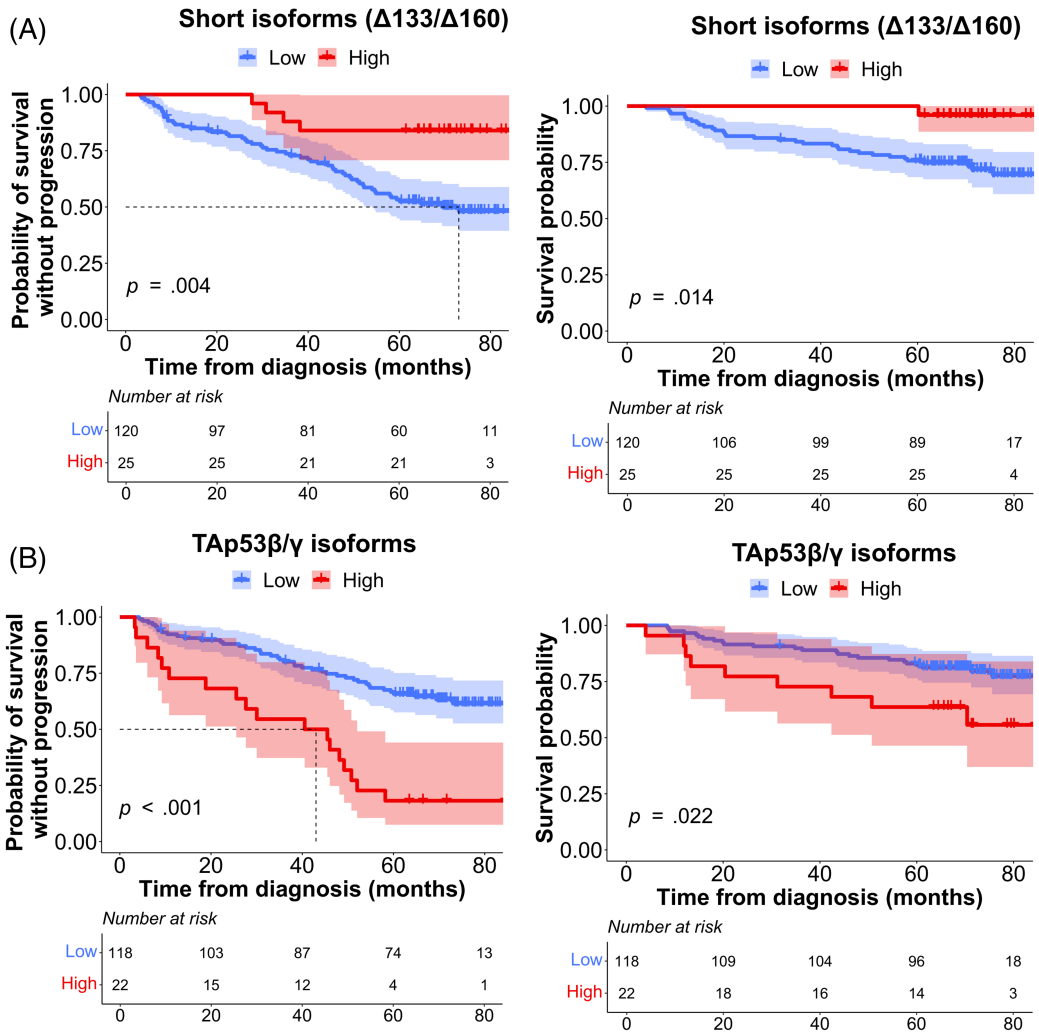

FIGURE 3 Probability of survival without progression and of overall survival of MM patients by level of p53 protein isoforms. (A) TTP and OS probabilities in patients with high levels of short isoforms. (B) TTP and OS probability according to the expression of TAp53β/γ isoforms. The log-rank (Mantel–Cox) test *p* values are shown. MM, multiple myeloma; OS, overall survival; TA, transactivation domain; TTP, survival without progression [Color figure can be viewed at wileyonlinelibrary.com]

respectively). High-risk cytogenetics and the age at diagnosis retained their independent value in predicting adverse OS (Figure 4C). The analysis of the contribution of the variables showed that high-risk cytogenetics explained 28% and 44% of the variation in TTP and OS, respectively. Significantly, the expression levels of TAp53β/γ isoforms explained 41% of the variation in TTP (Figure S5C).

3.4 | Expression patterns of p53 isoforms at the mRNA level in MM

mRNA was available from 109 of the 156 MM samples. We quantified the p53 isoforms by qRT-PCR using a well-established approach,[23] selecting the p53 mRNA variants that were homologous with those identified at the protein level by CNIA, that is to say, the α, β, short (Δ133/Δ160), and long (TA/Δ40) isoforms (Figure S6A,B). The main limitation of this approach is the difficulty to quantify each specific isoform individually.[23] Therefore, our analysis of mRNA isoforms was limited to identifying the group of six long isoforms and the three TA isoforms were not distinguished. We also measured the expression of the *TP53* gene, detected at a region of mRNA common to all isoforms. Samples with a Ct value ≥35 were considered as not expressed.

The *TP53* gene and α isoforms were expressed in all the 109 MM samples. The long isoforms were only absent from one MM sample, while the short isoforms were the least frequently expressed, only in 72/109 (67%) MM samples, similar to the p53 protein isoforms levels (Figure S6C). We wondered whether the low expression of the short isoform detected in our cohort could be corroborated in another set of MM patients. We took advantage of the availability of RNA-Seq data from 780 MM patients included in the MMRF CoMMpass trial

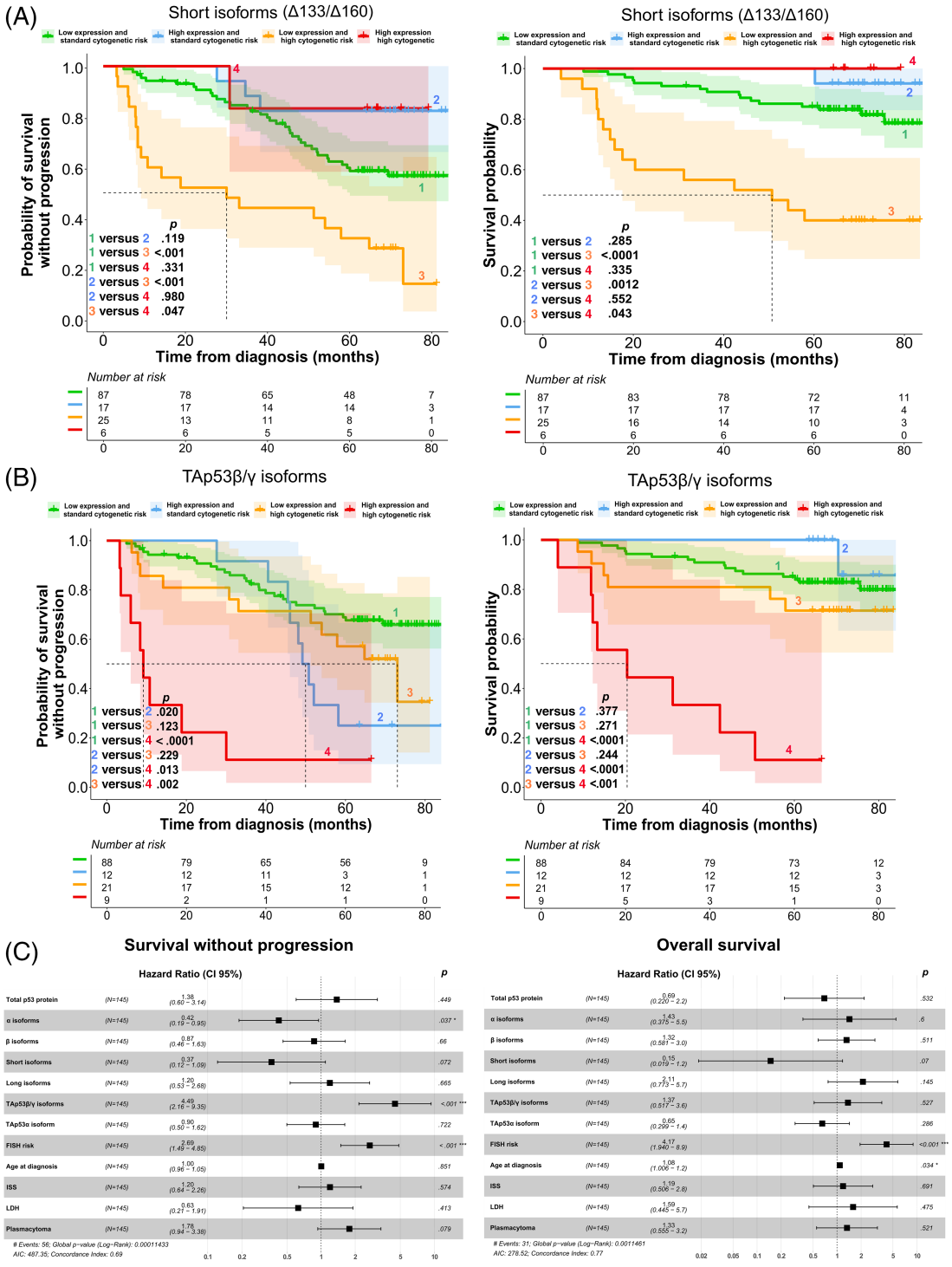

FIGURE 4 Probability of survival without progression and of overall survival of MM patients by cytogenetic risk and level of p53 protein isoforms, simultaneously. Analysis of MM patients with standard and high cytogenetic risk in combination with high and low expression levels of short (A) and TAp53β/γ (B) protein isoforms. The log-rank (Mantel–Cox) test *p* values are shown. (C) Forest plot of multivariate models with probabilities for each factor associated with TTP and OS of patients, based on the expression level of the studied p53 protein isoforms and age at diagnosis (years), ISS III versus I/II, high-level LDH, plasmacytoma and high versus standard cytogenetic risk ($N = 145$). 95% Confidence intervals are indicated in parentheses. MM samples with missing values were excluded from the model. ISS, International Staging System; LDH, lactate dehydrogenase; MM, multiple myeloma; TA, transactivation domain; TTP, survival without progression [Color figure can be viewed at wileyonlinelibrary.com]

(NCT01454297) to address this question. Even using a different approach to quantify mRNA, such as RNA-Seq, we observed that the number of MM patients expressing short mRNA isoforms was significantly lower than that expressing long mRNA isoforms (Figure S6D).

The univariate survival analysis using qRT-PCR data from mRNA revealed similar results to those observed at the protein level. MM patients with high levels of short isoform expression had statistically significant longer TTP and OS (median not reached) compared with patients with lower levels (HR = 0.50, $p = .021$ and HR = 0.31, $p = .005$, respectively) (Figure S6E). However, unlike p53 protein, the low levels of the *TP53* gene were associated with a shorter OS (HR = 0.27, $p < .001$) but had no impact on the TTP of MM patients (Figure S6F). Nevertheless, the expression of the α and β isoforms did not affect the survival of patients, similarly to what was noted at the protein level.

4 | DISCUSSION

We have investigated for the first time the expression of p53 isoforms at the protein and mRNA levels and analyzed their putative impact on the outcome of a large cohort of homogeneously treated MM patients. Currently, most of the information regarding expression of p53 isoforms in tumors is based on mRNA levels quantified by reverse transcription PCR. In fact, the quantification of p53 isoforms using classical western blot assays would need a significant amount of protein, which is not available for most of the cases. Our previous implementation of the capillary nanoimmunoassay platform for protein quantification in the clinical setting[18,20] allowed us to explore the hitherto unknown general landscape of p53 protein isoform expression in MM. Although this technology is highly effective analyzing low protein amounts, the genetic studies included in the evaluation of MM patients at diagnosis consume the entire sample in many cases.

We found total p53 protein to be expressed in more than 70% of MM samples, with the greater contribution of long than short isoforms, the latter being detected in very few samples. The TA protein isoforms were also expressed in most patients. Although qRT-PCR was able to detect expression of *TP53* gene in all the MM patients, and of p53 mRNA isoforms in the majority of cases, short mRNA isoforms were the least frequently expressed subclass, as observed at the protein level.

The short isoforms, also known as N-terminally truncated variants (the Δ133 and Δ160 variants), lack the first 132 amino acids, including a small part of the DBD. The integrity of the DBD is essential to the transcriptional factor functions of TAp53α, through which it can bind to the p53 DNA consensus recognition element (RE) present in the promoters of its target genes.[24,25] The absence of TAD1, TAD2, and a portion of the DBD from the short protein isoform structure entails the lack of sensitivity to proteasomal degradation and the absence of specific transactivation activity that characterize the TAp53α isoform. The Δ133p53α isoform not only is defective in promoting apoptosis, but also acts dominant-negatively toward TAp53α, inhibiting p53-mediated apoptosis.[7] Some studies have shown abnormal expression of short mRNA isoforms in tumor cells relative to normal tissues. In addition, a negative impact of the short mRNA isoforms on the outcome of oncological patients has also been reported.[7,26–33] In contrast to these findings, we observed a significant positive influence on MM patient prognosis of a high level of expression of the short p53 isoforms, quantified at the protein or mRNA level. However, the impact of the short isoforms on prognosis differs depending on the tumor type. For example, the Δ133p53β expression has been associated with adverse prognosis in breast cancer,[27] while with better prognosis in mutant p53 ovarian cancer.[28,31] Recently, the co-expression of the p53 isoforms has been shown to differentially regulate the p53-POLι-dependent DNA damage tolerance (DDT) pathway.[34] However, since only 12 MM patients with co-expression of TAp53α and short isoforms were identified, we can speculate that, in this particular cancer, it is less likely that the short isoforms are affecting the DDT pathway. Accordingly, it can be said that there is little information about the quantification of short isoforms in hematological cancers, and their functions are not completely understood.

The TA isoforms (TAp53α, TAp53β, and TAp53γ) possess the entire N-terminal domain, which contains the two independent transactivation domains (TAD1 and TAD2), but a different C-terminal. TAp53α, which is the canonical p53 protein and the most abundant p53 isoform, contains the complete C-terminal region, including the oligomerization domain (aa 326–356) and the basic domain (aa 364–393), but the TAp53β and TAp53γ isoforms are C-terminally truncated variants. These structural differences determine their differential functions. Our cohort featured a higher level of expression of TAp53α than of TAp53β/γ proteins. We also noted a negative impact of the high level of expression of TAp53β/γ proteins on the survival of MM patients. These data are consistent with another study of acute myeloid leukemia patients in which high levels of TAp53α and low levels of TAp53β/γ were associated with a greater sensitivity to valproic acid treatment.[35] Elevated TAp53γ mRNA levels have also been associated with reduced progression-free survival in uterine serous carcinoma.[36] However, opposite results showing an association between low levels of TAp53β and TAp53γ mRNAs and worse prognosis have also been reported.[14,37] In more than 10 years of intensive research, several studies have displayed the differential and aberrant expression of C-terminally truncated variants in various cancers. Nonetheless, their properties remain controversial, as shown in several apparently contradictory reports[7,14–16,26,38–40] that do not provide enough and clear evidence for defining the TAp53β/γ functions. For example, a significant increase in p21 and BAX promoter activities was found to be enhanced by overexpression of the TAp53α isoform, but not by the overexpression of TAp53β and TAp53γ.[41] Moreover, an *in vivo* study revealed that the TAp53β and TAp53γ isoforms significantly increased the tumor growth of H1299 cells.[42] Although the discrepancies among these studies cannot easily be explained, it seems most plausible that the functions of the TAp53β and TAp53γ isoforms are dependent on the cellular and tissue context.

It was of particular note that considering the expression levels of p53 isoforms made it possible to refine the prognostic significance of the cytogenetic-risk classification. Thus, high-cytogenetic-risk patients who expressed low levels of short p53 isoforms or high levels of TA/long p53 isoforms had shorter survival than expected, while the survival of the group of high-cytogenetic-risk patients expressing high levels of short

p53 isoforms or low levels of TA/long p53 isoforms was comparable to that of patients with standard cytogenetic risk. These results were also observed when each of the high-risk cytogenetic alterations was analyzed in conjunction with the expression of p53 protein isoforms.

In conclusion, short and TAp53β/γ protein isoform expression is associated with the clinical outcome of MM patients, and the prognostic stratification of MM patients is notably improved when cytogenetic risk is combined with their expression levels. These novel findings broaden the spectrum of the known actions of the p53 protein affecting MM outcome beyond the well-known unfavorable prognosis of deletions and/or mutations of the *TP53* gene.

ACKNOWLEDGMENTS

The authors would like to thank Isabel Isidro, Teresa Prieto, and Vanesa Gutierrez for their technical assistance with MM cell purification and FISH analysis; Phil Mason and Andrés García for their help in reviewing the English language of the manuscript.

CONFLICT OF INTERESTS

Dr García-Sanz reports receiving personal fees from Amgen, Janssen, Takeda, and Pfizer, and receives honoraria from Pharmacyclics, research funding from Hospira, and travel accommodation from Celgene, unconnected with the submitted work. Dr Martínez-López has consulting and advisory roles with Novartis, Celgene, Janssen, and Bristol-Myers Squibb, receives speakers' bureau compensation from Novartis, Celgene, Janssen, and Bristol-Myers Squibb, and receives research funding from Novartis, Celgene, Janssen, and Bristol-Myers Squibb (institutional). Dr Oriol has consulting and advisory roles with Amgen and Janssen-Cilag, Amgen, and receives research funding from Janssen (institutional). Dr Bladé receives honoraria from Celgene, Janssen, and Amgen. Dr Lahuerta has consulting and advisory roles with Janssen-Cilag and Celgene. Dr San Miguel has consulting and advisory roles with Amgen, Bristol-Myers Squibb, Celgene, Janssen, MSD, Novartis, Takeda, and Roche. Dr Rosiñol receives honoraria from Janssen, Celgene, Amgen, Takeda, Sanofi, GSK, and Karyofarm. Dr Mateos receives honoraria and speakers' bureau compensation from Janssen and Celgene, Onyx, Takeda, Novartis, and Bristol-Myers Squibb, unconnected with the submitted work. Dr Gutiérrez receives honoraria from Janssen unconnected with the submitted work. The other authors declare no conflicts of interest.

AUTHOR CONTRIBUTIONS

Elizabeta A. Rojas conceived the idea and designed the study, developed, and performed qRT-PCR and CNIA experiments, analyzed data, prepared the figures and wrote the manuscript; Luis A. Corchete analyzed the clinical data, supervised the statistical analysis and participated in the preparation of figures; Cristina De Ramón performed next-generation sequencing experiments, analyzed the clinical data, and participated in the preparation of tables; Patryk Krzeminski carried out the nucleofection assays for generation of positive controls; Dalia Quwaider assisted with laboratory experiments; Ramón García-Sanz, Joaquín Martínez-López, Albert Oriol, Laura Rosiñol, Joan Bladé, Juan José Lahuerta, Jesús F. San Miguel, Marcos González, María Victoria Mateos, and Norma C. Gutiérrez provided patient samples and clinical data and were responsible for obtaining informed consent from patients. Jean-Christophe Bourdon provided antibodies, contributed to the data interpretation, and provided support with conceptual issues; Irena Misiewicz-Krzeminska designed the study, developed and performed CNIA experiments, analyzed protein data, prepared figures, and supervised the whole study; Norma C. Gutiérrez conceived the idea and designed the study, participated in the writing of the manuscript, supervised the whole study, and provided funding. All authors reviewed critically and approved the manuscript.

DATA AVAILABILITY STATEMENT

All data generated during this study are included in this published article and its supplementary information files. The raw data analyzed during the current study available from the corresponding author on reasonable request.

ORCID

Elizabeta A. Rojas https://orcid.org/0000-0002-2541-7254
Luis A. Corchete https://orcid.org/0000-0003-4577-8599
Cristina De Ramón https://orcid.org/0000-0002-8167-6410
Patryk Krzeminski https://orcid.org/0000-0002-0526-9135
Joaquín Martínez-López https://orcid.org/0000-0001-7908-0063
Irena Misiewicz-Krzeminska https://orcid.org/0000-0002-4206-8586
Norma C. Gutiérrez https://orcid.org/0000-0001-5834-9510

REFERENCES

1. Lodé L, Eveillard M, Trichet V, et al. Mutations in TP53 are exclusively associated with del(17p) in multiple myeloma. *Haematologica*. 2010;95(11):1973-1976. doi:10.3324/haematol.2010.023697
2. Cardona-Benavides IJ, de Ramón C, Gutiérrez NC. Genetic abnormalities in multiple myeloma: prognostic and therapeutic implications. *Cells*. 2021;10(2):336. doi:10.3390/cells10020336
3. Teoh PJ, Chung TH, Sebastian S, et al. p53 Haploinsufficiency and functional abnormalities in multiple myeloma. *Leukemia*. 2014;28(10):2066-2074. doi:10.1038/leu.2014.102
4. Shah V, Sherborne AL, Walker BA, et al. Prediction of outcome in newly diagnosed myeloma: a meta-analysis of the molecular profiles of 1905 trial patients. *Leukemia*. 2018;32(1):102-110. doi:10.1038/leu.2017.179
5. Fonseca R, Blood E, Rue M, et al. Clinical and biologic implications of recurrent genomic aberrations in myeloma. *Blood*. 2003;101(11):4569-4575. doi:10.1182/blood-2002-10-3017
6. Cohen YC, Saranga A, Gatt ME, et al. Treatment patterns and clinical outcomes in high-risk newly diagnosed multiple myeloma patients carrying the 17p deletion: An observational multi-center retrospective study. *Am J Hematol*. 2018;93(6):810-815. doi:10.1002/ajh.25098
7. Bourdon JC, Fernandes K, Murray-Zmijewski F, et al. p53 isoforms can regulate p53 transcriptional activity. *Genes Dev*. 2005;19(18):2122-2137. doi:10.1101/gad.1339905
8. Surget S, Khoury MP, Bourdon JC. Uncovering the role of p53 splice variants in human malignancy: a clinical perspective. *Onco Targets Ther*. 2013;7:57-68. doi:10.2147/OTT.S53876
9. Hafner A, Bulyk ML, Jambhekar A, Lahav G. The multiple mechanisms that regulate p53 activity and cell fate. *Nat Rev Mol Cell Biol*. 2019;20(4):199-210. doi:10.1038/s41580-019-0110-x
10. Joruiz SM, Bourdon JC. p53 Isoforms: Key Regulators of the Cell Fate Decision. *Cold Spring Harb Perspect Med*. 2016;6(8):a026039. doi:10.1101/cshperspect.a026039

11. Honda R, Tanaka H, Yasuda H. Oncoprotein MDM2 is a ubiquitin ligase E3 for tumor suppressor p53. *FEBS Lett*. 1997;420(1):25-27. doi:10.1016/s0014-5793(97)01480-4
12. Xiong W, Wu X, Starnes S, et al. An analysis of the clinical and biologic significance of TP53 loss and the identification of potential novel transcriptional targets of TP53 in multiple myeloma. *Blood*. 2008;112(10):4235-4246. doi:10.1182/blood-2007-10-119123
13. Chang H, Yeung J, Qi C, Xu W. Aberrant nuclear p53 protein expression detected by immunohistochemistry is associated with hemizygous P53 deletion and poor survival for multiple myeloma. *Br J Haematol*. 2007;138(3):324-329. doi:10.1111/j.1365-2141.2007.06649.x
14. Bourdon JC, Khoury MP, Diot A, et al. p53 mutant breast cancer patients expressing p53γ have as good a prognosis as wild-type p53 breast cancer patients. *Breast Cancer Res*. 2011;13(1):R7. doi:10.1186/bcr2811
15. Anensen N, Oyan AM, Bourdon JC, Kalland KH, Bruserud O, Gjertsen BT. A distinct p53 protein isoform signature reflects the onset of induction chemotherapy for acute myeloid leukemia. *Clin Cancer Res*. 2006;12(13):3985-3992. doi:10.1158/1078-0432.CCR-05-1970
16. Boldrup L, Bourdon JC, Coates PJ, Sjöström B, Nylander K. Expression of p53 isoforms in squamous cell carcinoma of the head and neck. *Eur J Cancer*. 2007;43(3):617-623. doi:10.1016/j.ejca.2006.10.019
17. Rosiñol L, Oriol A, Rios R, et al. Bortezomib, lenalidomide, and dexamethasone as induction therapy prior to autologous transplant in multiple myeloma. *Blood*. 2019;134(16):1337-1345. doi:10.1182/blood.2019000241
18. Misiewicz-Krzeminska I, de Ramón C, Corchete LA, et al. Quantitative expression of Ikaros, IRF4, and PSMD10 proteins predicts survival in VRD-treated patients with multiple myeloma. *Blood Adv*. 2020;4(23):6023-6033. doi:10.1182/bloodadvances.2020002711
19. Rajkumar SV, Dimopoulos MA, Palumbo A, et al. International Myeloma Working Group updated criteria for the diagnosis of multiple myeloma. *Lancet Oncol*. 2014;15(12):e538-e548. doi:10.1016/S1470-2045(14)70442-5
20. Misiewicz-Krzeminska I, Corchete LA, Rojas EA, et al. A novel nano-immunoassay method for quantification of proteins from CD138-purified myeloma cells: biological and clinical utility. *Haematologica*. 2018;103(5):880-889. doi:10.3324/haematol.2017.181628
21. Misiewicz-Krzeminska I, Isidro I, Gutiérrez N. Capillary nano-immunoassay for quantification of proteins from CD138-purified myeloma cells. *Bio Protocol*. 2019;9(12). doi:10.21769/BioProtoc.3267
22. Loughery J, Cox M, Smith LM, Meek DW. Critical role for p53-serine 15 phosphorylation in stimulating transactivation at p53-responsive promoters. *Nucleic Acids Res*. 2014;42(12):7666-7680. doi:10.1093/nar/gku501
23. Khoury MP, Marcel V, Fernandes K, Diot A, Lane DP, Bourdon JC. Detecting and quantifying p53 isoforms at mRNA level in cell lines and tissues. *Methods Mol Biol*. 2013;962:1-14. doi:10.1007/978-1-62703-236-0_1
24. Laptenko O, Prives C. Transcriptional regulation by p53: one protein, many possibilities. *Cell Death Differ*. 2006;13(6):951-961. doi:10.1038/sj.cdd.4401916
25. Harms KL, Chen X. The functional domains in p53 family proteins exhibit both common and distinct properties. *Cell Death Differ*. 2006;13(6):890-897. doi:10.1038/sj.cdd.4401904
26. Fujita K, Mondal AM, Horikawa I, et al. p53 isoforms Delta133p53 and p53beta are endogenous regulators of replicative cellular senescence. *Nat Cell Biol*. 2009;11(9):1135-1142. doi:10.1038/ncb1928
27. Gadea G, Arsic N, Fernandes K, et al. TP53 drives invasion through expression of its Δ133p53β variant. *Elife*. 2016;5:e14734. doi:10.7554/eLife.14734
28. Hofstetter G, Berger A, Schuster E, et al. Δ133p53 is an independent prognostic marker in p53 mutant advanced serous ovarian cancer. *Br J Cancer*. 2011;105(10):1593-1599. doi:10.1038/bjc.2011.433
29. Nutthasirikul N, Limpaiboon T, Leelayuwat C, Patrakitkomjorn S, Jearanaikoon P. Ratio disruption of the Δ133p53 and TAp53 isoform equilibrium correlates with poor clinical outcome in intrahepatic cholangiocarcinoma. *Int J Oncol*. 2013;42(4):1181-1188. doi:10.3892/ijo.2013.1818
30. Nutthasirikul N, Hahnvajanawong C, Techasen A, et al. Targeting the Δ133p53 isoform can restore chemosensitivity in 5-fluorouracil-resistant cholangiocarcinoma cells. *Int J Oncol*. 2015;47(6):2153-2164. doi:10.3892/ijo.2015.3188
31. Bischof K, Knappskog S, Hjelle SM, et al. Influence of p53 isoform expression on survival in high-grade serous ovarian cancers. *Sci Rep*. 2019;9(1):5244. doi:10.1038/s41598-019-41706-z
32. Ozretić P, Hanžić N, Proust B, et al. Expression profiles of p53/p73, NME and GLI families in metastatic melanoma tissue and cell lines. *Sci Rep*. 2019;9(1):12470. doi:10.1038/s41598-019-48882-y
33. Kazantseva M, Mehta S, Eiholzer RA, et al. The Δ133p53β isoform promotes an immunosuppressive environment leading to aggressive prostate cancer. *Cell Death Dis*. 2019;10(9):631. doi:10.1038/s41419-019-1861-1
34. Guo Y, Rall-Scharpf M, Bourdon JC, Wiesmüller L, Biber S. p53 isoforms differentially impact on the POLι dependent DNA damage tolerance pathway. *Cell Death Dis*. 2021;12(10):941. doi:10.1038/s41419-021-04224-3
35. Haaland I, Hjelle SM, Reikvam H, et al. p53 protein isoform profiles in AML: correlation with distinct differentiation stages and response to epigenetic differentiation therapy. *Cells*. 2021;10(4):833. doi:10.3390/cells10040833
36. Bischof K, Knappskog S, Stefansson I, et al. High expression of the p53 isoform γ is associated with reduced progression-free survival in uterine serous carcinoma. *BMC Cancer*. 2018;18(1):684. doi:10.1186/s12885-018-4591-3
37. Avery-Kiejda KA, Morten B, Wong-Brown MW, Mathe A, Scott RJ. The relative mRNA expression of p53 isoforms in breast cancer is associated with clinical features and outcome. *Carcinogenesis*. 2014;35(3):586-596. doi:10.1093/carcin/bgt411
38. Courtois S, Verhaegh G, North S, et al. DeltaN-p53, a natural isoform of p53 lacking the first transactivation domain, counteracts growth suppression by wild-type p53. *Oncogene*. 2002;21(44):6722-6728. doi:10.1038/sj.onc.1205874
39. Avery-Kiejda KA, Zhang XD, Adams LJ, et al. Small molecular weight variants of p53 are expressed in human melanoma cells and are induced by the DNA-damaging agent cisplatin. *Clin Cancer Res*. 2008;14(6):1659-1668. doi:10.1158/1078-0432.CCR-07-1422
40. Oh L, Hainaut P, Blanchet S, Ariffin H. Expression of p53 N-terminal isoforms in B-cell precursor acute lymphoblastic leukemia and its correlation with clinicopathological profiles. *BMC Cancer*. 2020;20(1):110. doi:10.1186/s12885-020-6599-8
41. Marcel V, Fernandes K, Terrier O, Lane DP, Bourdon JC. Modulation of p53β and p53γ expression by regulating the alternative splicing of TP53 gene modifies cellular response. *Cell Death Differ*. 2014;21(9):1377-1387. doi:10.1038/cdd.2014.73
42. Silden E, Hjelle SM, Wergeland L, et al. Expression of TP53 isoforms p53β or p53γ enhances chemosensitivity in TP53(null) cell lines. *PLoS One*. 2013;8(2):e56276. doi:10.1371/journal.pone.0056276

SUPPORTING INFORMATION

Additional supporting information may be found in the online version of the article at the publisher's website.

How to cite this article: Rojas EA, Corchete LA, De Ramón C, et al. Expression of p53 protein isoforms predicts survival in patients with multiple myeloma. *Am J Hematol*. 2022;97(6):700-710. doi:10.1002/ajh.26507

Capítulo 3

ARTÍCULO 3

"Amiloride, an old diuretic drug, is a potential therapeutic agent for multiple myeloma"

Elizabeta A. Rojas, Luis Antonio Corchete, Laura San-Segundo, Juan F. Martínez-Blanch, Francisco M. Codoñer, Teresa Paíno, Noemí Puig, Ramón García-Sanz, María Victoria Mateos, Enrique M. Ocio, Irena Misiewicz-Krzeminska y Norma C. Gutiérrez

Clinical Cancer Research
(2017), 23(21): 6602-6615
DOI: 10.1158/1078-0432.CCR-17-0678

La amilorida, un antiguo diurético, es un agente terapéutico potencial para el mieloma múltiple

Fundamento: El mieloma múltiple (MM) continúa siendo una enfermedad incurable. Los pacientes con MM se caracterizan por presentar sucesivas recaídas que son cada vez más resistentes a los fármacos administrados. Por lo tanto, a pesar de los avances en el conocimiento de su patogénesis y del desarrollo de fármacos dirigidos a mecanismos moleculares específicos, sigue siendo necesaria la investigación de otros agentes terapéuticos con actividad antitumoral para poder abordar las sucesivas recaídas. En este trabajo se analiza si la amilorida, un fármaco de tipo diurético aprobado para el tratamiento de la hipertensión y el edema asociado a la insuficiencia cardíaca, puede ser utilizado como una droga antimieloma.

Metodología: Se utilizaron nueve líneas celulares de MM (NCI-H929, JJN3, KMS12-BM, KMS12-PE, RPMI-8226, U-266, MM1S, MM1R y RPMI-LR5), y 18 muestras de médula ósea (MO) de pacientes con MM, para estudiar la citotoxicidad *in vitro* y el mecanismo de acción de la amilorida. Además, cuatro muestras de MO completas de donantes sanos fueron empleadas para evaluar la citotoxicidad de la amilorida *ex vivo*, y un modelo murino de xenoinjerto de MM (65 ratones) para evaluar la citotoxicidad de la amilorida *in vivo*.

La viabilidad y proliferación celulares se evaluaron mediante ensayos de bromuro de 3-(4,5-dimetiltiazol-2-ilo)-2,5-difeniltetrazol (MTT) y ensayos de CellTiter-Glo. La muerte celular fue analizada mediante citometría de flujo con doble marcaje con Anexina V y ioduro de propidio. La despolarización de la membrana mitocondrial y el ciclo celular se midieron mediante citometría de flujo utilizando un marcaje con DilC1(5) y con ioduro de propidio, respectivamente. La actividad de las caspasas 3/7, 8 y 9 se analizó mediante ensayos de luminiscencia.

Se utilizó un panel de 5 anticuerpos para evaluar la citotoxicidad de la amilorida en las poblaciones celulares de MO, junto con el marcaje de anexina V [linfocitos T (CD3+), linfocitos B (CD19+), células NK (CD56+/CD3−), y granulocitos (SSChigh/CD45+dim)]. Para evaluar la citotoxicidad de la amilorida en las CPs patológicas se utilizaron junto con el marcaje de anexina V tres marcadores, CD38, CD45 y CD56 o CD19, dependiendo del fenotipo específico de cada paciente. Los mecanismos de acción de la amilorida fueron investigados mediante experimentos de RNA-Seq, qRT-PCR, *western blot* y ensayos de inmunofluorescencia.

Resultados: La amilorida provocó la muerte celular por apoptosis en el panel de líneas celulares de MM, así como en el modelo murino de xenoinjerto, sin toxicidad sistémica asociada al tratamiento. Se observó un efecto sinérgico al combinar la amilorida con dexametasona, melfalán, lenalidomida, y pomalidomida. Los experimentos de RNA-Seq mostraron un elevado número de isoformas, eventos de *splicing* alternativo y componentes de la maquinaria del *spliceosoma* alterados después del tratamiento con la amilorida. La inhibición de la viabilidad celular se detectó simultáneamente a la inhibición de la maquinaria del *splicing*. La inducción de apoptosis por la amilorida fue independiente de que p53 estuviese en su forma *wild-type* o mutado.

Conclusiones: Los resultados obtenidos demuestran una potente actividad antimieloma

de la amilorida y proporcionan las bases para considerar a la amilorida una alternativa terapéutica para los pacientes con MM refractarios o en recaída, especialmente para aquellos que presentan deleción o mutación de p53 que sean resistentes a los tratamientos actuales.

Cancer Therapy: Preclinical

Clinical Cancer Research

Amiloride, An Old Diuretic Drug, Is a Potential Therapeutic Agent for Multiple Myeloma

Elizabeta A. Rojas[1,2], Luis Antonio Corchete[1,2,3], Laura San-Segundo[1,2], Juan F. Martínez-Blanch[4], Francisco M. Codoñer[4], Teresa Paíno[1,2], Noemí Puig[1,2,3], Ramón García-Sanz[1,2,3], María Victoria Mateos[1,2,3], Enrique M. Ocio[1,2,3], Irena Misiewicz-Krzeminska[1,2,5], and Norma C. Gutiérrez[1,2,3]

Abstract

Purpose: The search for new drugs that control the continuous relapses of multiple myeloma is still required. Here, we report for the first time the potent antimyeloma activity of amiloride, an old potassium-sparing diuretic approved for the treatment of hypertension and edema due to heart failure.

Experimental Design: Myeloma cell lines and primary samples were used to evaluate cytotoxicity of amiloride. *In vivo* studies were carried out in a xenograft mouse model. The mechanisms of action were investigated using RNA-Seq experiments, qRT-PCR, immunoblotting, and immunofluorescence assays.

Results: Amiloride-induced apoptosis was observed in a broad panel of multiple myeloma cell lines and in a xenograft mouse model. Moreover, amiloride also had a synergistic effect when combined with dexamethasone, melphalan, lenalidomide, and pomalidomide. RNA-Seq experiments showed that amiloride not only significantly altered the level of transcript isoforms and alternative splicing events, but also deregulated the spliceosomal machinery. In addition, disruption of the splicing machinery in immunofluorescence studies was associated with the inhibition of myeloma cell viability after amiloride exposure. Although amiloride was able to induce apoptosis in myeloma cells lacking p53 expression, activation of p53 signaling was observed in wild-type and mutated *TP53* cells after amiloride exposure. On the other hand, we did not find a significant systemic toxicity in mice treated with amiloride.

Conclusions: Overall, our results demonstrate the antimyeloma activity of amiloride and provide a mechanistic rationale for its use as an alternative treatment option for relapsed multiple myeloma patients, especially those with 17p deletion or *TP53* mutations that are resistant to current therapies. *Clin Cancer Res; 23(21); 6602–15. ©2017 AACR.*

Introduction

Despite improvements in the survival of multiple myeloma patients thanks to the introduction of novel therapeutic agents (1, 2), it remains an incurable disease (3). Multiple myeloma initially responds to chemotherapy but relapse and chemoresistance usually occur (4), so subsequent recurrences are part of its natural history. Therefore, the search for new drugs that control the disease continues to be required.

Great efforts to develop new agents against multiple myeloma have been made in recent years, to the extent that a wide array of new agents with different mechanisms of action have recently been approved. These include new mAbs, proteasome inhibitors, immunomodulatory drugs and histone deacetylase inhibitors, among others (5). However, their approval processes required several years of research and major investment. An interesting alternative by which this long process might be shortened is the drug-repositioning approach, which involves using old drugs approved for noncancerous diseases (6). One of the advantages of this strategy is that the pharmacokinetic and pharmacodynamic properties and toxicity profiles tend to be well known. The diuretic drug, amiloride, is one such agent.

Amiloride is a potassium-sparing diuretic that has been employed clinically for more than three decades in the treatment of hypokalemia, hypertension, edema and congestive heart failure (7). Some studies demonstrated its significant antitumor and antimetastasis activities that were initially associated with the inhibition of Na^+/H^+ exchangers (8). Recently, amiloride was found to modify alternative splicing (AS) in various human cancer cells (9). Pre-mRNA alternative splicing is a highly regulated process, and numerous studies have demonstrated its aberrations to be associated with cancer, tumor progression, and metastasis. This mechanism has recently gained attention as a potential therapeutic target for cancer due to the differential splicing patterns identified in tumor cells and metastatic tumor populations (10–14).

In this study, we evaluated for the first time the antimyeloma (anti-multiple myeloma) effect of amiloride using *in vitro, ex vivo*, and *in vivo* models. We found that amiloride had potent activity against a broad panel of multiple myeloma cell lines regardless of

[1]Cancer Research Center-IBMCC (USAL-CSIC), Salamanca, Spain. [2]Institute of Biomedical Research of Salamanca (IBSAL), Salamanca, Spain. [3]Hematology Department, University Hospital of Salamanca, Spain. [4]Lifesequencing S.L., Valencia, Spain. [5]National Medicines Institute, Warsaw, Poland.

Note: Supplementary data for this article are available at Clinical Cancer Research Online (http://clincancerres.aacrjournals.org/).

I. Misiewicz-Krzeminska and N.C. Gutiérrez contributed equally to this article.

Corresponding Author: Norma C. Gutiérrez, Department of Hematology, University Hospital of Salamanca, Paseo San Vicente, 58-182, Salamanca 37007, Spain. Phone: 349-2329-1384; Fax: 349-2329-4624; E-mail: normagu@usal.es

doi: 10.1158/1078-0432.CCR-17-0678

Translational Relevance

The investigation of novel therapeutic agents is needed to manage the multiple relapses arising from resistant clones in multiple myeloma. In this study, we demonstrate for the first time the antimyeloma activity of amiloride, a very well-known drug used in the treatment of hypokalemia, hypertension, and edema. This finding together with the manageable toxicity profile of amiloride provide the rationale for conducting clinical trials that support the repositioning of this old drug for the treatment of multiple myeloma. Moreover, our results showed that multiple myeloma cells either with WT or mutated *TP53* were highly sensitive to amiloride, which makes this drug an attractive candidate for high-risk myeloma patients with *TP53* abnormalities.

TP53 status. In addition, RNA-Seq experiments showed a strong alteration of spliceosome functionality. These encouraging findings, in conjunction with the manageable toxicity profiles of amiloride, provide a framework for evaluating its utility in clinical trials.

Materials and Methods

Reagents and multiple myeloma cells

The human myeloma cell lines, NCI-H929, MM1S, MM1R, and U266 were acquired from ATCC, RPMI-8226, KMS12-BM, KMS12-PE, and JJN3 from DMSZ (Deutsche Sammlung von Mikroorganismen and Zellkulturen). RPMI-LR5 cell line was kindly provided by Dr. W.S. Dalton (Moffitt Cancer Center, Tampa, FL). All cell lines were cultured in RPMI1640 medium supplemented with 10% FBS and antibiotics (Gibco). Cells were routinely checked for the presence of mycoplasma with MycoAlert kit (Lonza). Cell line identity was confirmed periodically by STR analysis with PowerPlex 16 HS System kit (Promega) and online STR matching analysis (www.dsmz.de/fp/cgi-bin/str.html). All multiple myeloma samples from patients and cells from healthy donors were cultured in AIMV medium supplemented with 20% FBS (Thermo Fisher Scientific). $CD138^+$ plasma cells from bone marrow samples of 8 patients with multiple myeloma were isolated using an autoMACS separation system (Miltenyi-Biotec). Clinical information of the patients included in the study is summarized in Supplementary Materials.

Amiloride and melphalan were purchased from Sigma-Aldrich, bortezomib was from LC Laboratories, dexamethasone was from Merck KGaA, and lenalidomide and pomalidomide from Selleckchem. All multiple myeloma patients as well as healthy donors involved in the study provided written informed consent in accordance with the Helsinki Declaration. The research ethics committee of the University Hospital of Salamanca approved the study.

Cell viability assays

Cell viability and proliferation were evaluated using CellTiter-Glo (Promega) and 3 (4,5-dimethylthiazol-2-yl)-2,5-diphenyltetrazolium bromide (MTT) colorimetric assay (Sigma-Aldrich), respectively, as described previously (15, 16). Synergism between amiloride and other drugs was evaluated with CalcuSyn software (Biosoft; ref. 17; Supplementary Material).

Apoptosis and cell-cycle assays

Apoptosis using Annexin V-FITC/propidium iodide (PI) double staining, mitochondrial membrane depolarization using DilC1(5) (Immunostep) and cell-cycle analysis, were performed by flow cytometry using Infinicyt software (Cytognos S.L.), as described previously (15). Caspases-3/7, 8, and 9 activities were evaluated by Caspase Glo 3/7, Caspase-Glo 8, and Caspase-Glo 9 assays (Promega), respectively, according to the manufacturer's protocol.

***Ex vivo* analysis of cytotoxicity in freshly total bone marrow cells**

The experiments with patient's cells were performed in total bone marrow samples from patients with multiple myeloma. Immediately after extraction, total bone marrow samples were lysed with ammonium chloride to remove red blood cells (erythrocytes); the remaining white blood cells were maintained for 48 hours in AIMV medium supplemented with 20% FBS (Thermo Fisher Scientific) in the absence or presence of different concentrations of amiloride. Then, the activity of amiloride was investigated on plasma cells (PC) and on the main bone marrow cell populations separately. To evaluate the cytotoxicity of amiloride on PCs, samples were analyzed using Annexin V (Immunostep) in combination with three markers that allowed for the identification of pathologic PCs present in the sample. With that aim, we used a fix combination of two mAbs (CD38 and CD45) plus a third one, chosen depending on the specific phenotype of each patient's clonal plasma cells (usually CD56 or CD19). The cells were incubated for 15 minutes at room temperature in the dark. A total of 5×10^5 cells were acquired on a FACSCanto II flow cytometer (BD Biosciences). Finally, apoptosis was analyzed in pathologic PCs (gated on $CD38^{++}$ and $CD56^{+/-}$, or $CD19^{+/-}$ and FSC/SSC) using the Infinicyt software. Annexin V–positive events among the target populations were considered apoptotic cells.

Amiloride cytotoxicity on the other bone marrow cell populations, that is B and T lymphocytes, NK cells and granulocytes, was assessed with the same aforementioned protocol described, but including a panel of 5 antibodies in combination with Annexin V to identify T lymphocytes ($CD3^+$), B lymphocytes ($CD19^+$), NK cells ($CD56^+/CD3^-$), and granulocytes ($SSC^{high}/CD45+^{dim}$). Among each of these populations separately, we identified as apoptotic the percentage being Annexin V positive using the Infinicyt software.

Multiple myeloma xenograft murine model

All animal experiments were performed according to the institutional guidelines and the protocol previously approved by the ethical committee of the University of Salamanca (Salamanca, Spain). For the human subcutaneous plasmacytoma model, 65 CB17-SCID mice (The Jackson Laboratory) were subcutaneously inoculated into the right flank with 3×10^6 MM1S cells in 100 μL of RPMI1640 medium and 100 μL of Matrigel (BD Biosciences). Treatment was initiated immediately after tumor cell inoculation and mice were randomized to the following treatment cohorts, each of five animals: vehicle-alone PBS (C); amiloride, 10 mg/kg (A10); amiloride, 15 mg/kg (A15); dexamethasone, 0.5 mg/kg (D); melphalan, 2.5 mg/kg (M), dexamethasone + melphalan (DM); dexamethasone + amiloride, 10 mg/kg (DA10); melphalan + amiloride, 10 mg/kg (MA10); dexamethasone + melphalan + amiloride, 10 mg/kg (DMA10); dexamethasone + amiloride, 15 mg/kg (DA15); melphalan + amiloride, 15 mg/kg (MA15);

and dexamethasone + melphalan + amiloride, 15 mg/kg (DMA15). Amiloride was administered orally daily, and dexamethasone and melphalan intraperitoneally (i.p.) two days a week. Tumor burden estimation and toxicity monitoring were performed as described previously (18).

To estimate survival, mice were sacrificed when the diameter of their tumor reached 2 cm or when they became moribund. Time to endpoint (TTE) was estimated from the day of treatment initiation. For *in vivo* mechanistic studies, six and four mice, respectively, were subcutaneously inoculated in the right flank with 3×10^6 MM1S cells and 3×10^6 RPMI cells. When the tumor attained a large volume, mice were randomized to receive the vehicle-alone PBS (control group) or amiloride (20 mg/kg) orally for two consecutive days. On the third day, mice were sacrificed and the tumors retrieved for analysis.

RNA sequencing

Poly A^+ RNA from KMS12-BM and JJN3 cells untreated or treated with amiloride (0.1 mmol/L and 0.4 mmol/L, respectively) for 24 hours was isolated and prepared for RNA sequencing (RNA-Seq). Libraries were constructed following a TruSeq Stranded mRNA Sample Preparation Guide (Illumina). The final cDNA library was sequenced using Illumina HiSeq 2500 in combination of 100 Paired-End at Lifesequencing S.L. (Supplementary Material).

RNA-Seq analysis

Paired-end FASTQ files for 12 samples were used in the RNA-Seq analyses. We analyzed the data in three stages: gene expression, isoform level, and splicing events. First, in the analysis of differential expression at the gene level, the genes were considered to be differentially expressed for an absolute n-fold change (FC) of $\geq$2 and a false discovery rate (FDR) of <0.05. Second, in the analysis of isoform level, we focused on the isoforms with an absolute value of FC $\geq$ 2 and that corresponded to genes without altered total expression. The criteria used to assign genes as "no-change" were FDR > 0.05 and an absolute value of FC < 2, when the DESeq2 package was applied. Third, differential alternative splicing events were detected using rMATS version 3.0.9 (19), classifying these events into five major types of pattern: skipped exon (SE), alternative 5′ splice site (A5SS), alternative 3′ splice site (A3SS), mutually exclusive exons (MXE), and retained introns (RI). rMATS also calculates the difference in the ratio of these events between two conditions, and produces an estimate of the FDR. Finally, all the enrichment analyses were conducted using the Webgestalt web tool (20), employing the Gene Ontology and KEGG databases as data sources. The dataset is available at the Gene Expression Omnibus (GEO) repository (http://www.ncbi.nlm.nih.gov/geo) under the accession number GSE95077.

Further details are provided in the Supplementary Material.

RNA extraction and quantitative real-time PCR analysis

RNA was extracted using the RNeasy Plus Mini kit (Qiagen). The RNA integrity was assessed with an Agilent 2100 Bioanalyzer (Agilent Technologies). Total RNA (1 μg) was reverse-transcribed to cDNA using High-Capacity cDNA Reverse Transcription Kit (Applied Biosystems). Gene expression was quantified by TaqMan qRT-PCR mRNA assays (Applied Biosystems) and normalized relative to 18S5 using the $2^{-\Delta C_t}$ method.

Immunoblotting and immunofluorescence analysis

Western blot methods and the preparation of protein lysates have been described elsewhere (15). The sources of the mAbs are described in the Supplementary Material.

For immunofluorescence, cells were fixed in 4% paraformaldehyde, permeabilized with 0.25% Triton X-100/PBS, stained with primary mouse anti-SC35 (Abcam) and goat anti-mouse IgG (H+L) secondary antibody, and Alexa Fluor 488 conjugate (Thermo Fisher Scientific). Fluorescence was measured under a Leica confocal microscope.

Statistical analysis

All statistical analyses were carried out with IBM SPSS Statistics 22.0 (IBM Corp.) and the Simfit package (W.G. Bardsley, University of Manchester, Manchester, UK; v7.0.9 Academic 32-bit, http://www.simfit.org.uk/). *P* values were corrected for multiple testing using the FDR, with values of <0.05 being considered to be statistically significant. Differences in the *in vitro* experiments are expressed as the mean ± SD of at least three determinations and were assessed by the two-sided Student *t* test or the Mann–Whitney *U* test. Differences in tumor volumes between groups were evaluated fitting an exponential regression model and the regression parameters were compared using a *t* test for unequal variances. Survival curves were plotted using the Kaplan–Meier method, and compared using the log-rank test.

Results

Amiloride is cytotoxic for multiple myeloma and potentiates the efficacy of various antimyeloma agents

Amiloride exhibited potent *in vitro* antimultiple myeloma activity in a dose- and time-dependent manner, as demonstrated in a panel of seven myeloma cell lines with a wide range of cytogenetic abnormalities and p53 status (Supplementary Table S1; Supplementary Fig. S1A). The viability was significantly reduced in both the *TP53* wild-type (WT; H929, MM1S) and the mutated *TP53* cell lines (KMS12-BM, KMS12-PE, U-266, and RPMI-8226) after exposure to amiloride ($P < 0.01$; Fig. 1A), although viability reduction in the p53-null cell line JJN3 required a higher dose and a longer time course ($P < 0.01$). The antimultiple myeloma effect of amiloride was also observed in melphalan- and dexamethasone-resistant cell lines, RPMI-LR5 and MM1R, respectively (Supplementary Fig. S2A).

In the *ex vivo* study using bone marrow cells from 10 patients with multiple myeloma (six newly diagnosed and four relapsed/refractory), we observed significant apoptosis induction in plasma cells, even in three patients bearing deletion of 17p, with minor cytotoxicity toward B and T lymphocytes, NK cells, and neutrophils (Fig. 1B). Myeloma cell cytotoxicity of amiloride was also confirmed on isolated $CD138^+$ plasma cells from eight multiple myeloma patients (Supplementary Fig. S1B). Interestingly, amiloride did not induced cytotoxicity on normal plasma cells from healthy donors (Supplementary Fig. S1C).

Next, we evaluated the cytotoxicity of double combinations of amiloride with melphalan and dexamethasone, employing a constant ratio between them. Subsequent isobologram analysis revealed a combination index (CI) in the synergistic range for the double combinations of amiloride with dexamethasone or melphalan, ranging from 0.2 to 0.8, depending on the doses

and cell lines used (Fig. 1C; Supplementary Fig. S2B). Furthermore, amiloride overcame the melphalan and dexamethasone resistance of RPMI-LR5 and MM1R, respectively (Supplementary Fig. S2C and S2D). Amiloride was also combined with new agents such as lenalidomide, pomalidomide and bortezomib. A significant synergism was observed between amiloride and lenalidomide or pomalidomide plus dexamethasone (Fig. 1D and E). In contrast, the combination of amiloride with bortezomib was antagonistic in all cell lines tested (Supplementary Fig. S2E).

To test whether amiloride was able to inhibit the protective effect of the bone marrow microenvironment, MM1S-luc cells were cocultured with mesenchymal stem cells (MSC) from six multiple myeloma patients and treated with increasing concentrations of amiloride for 48 hours. Despite the proliferative advantage to multiple myeloma cells conferred by MSCs, amiloride abrogated the protective effect conferring by MSCs. In contrast, MSCs were resistant to the cytotoxic effect of amiloride (Supplementary Fig. S3).

Amiloride induces apoptosis and enhances mitochondrial depolarization

To elucidate the mechanisms leading to the decrease of cell growth induced by amiloride, we analyzed cell cycle and apoptosis in multiple myeloma cell lines treated with increasing concentrations of the drug (0.1–1.0 mmol/L). Amiloride induced significant apoptosis after 24 and 48 hours in H929, KMS12-BM and JJN3 cell lines (Fig. 2A; Supplementary Fig. S4A), as well as in MM1S, U-266 and RPMI cell lines after 48 hours (Supplementary Fig. S4B). The apoptosis induction was dose-dependent in all cell lines, with the highest levels in the KMS12-BM cell line, even at 0.1 mmol/L after 24 hours of treatment (Fig. 2A). It is of particular note that the apoptosis induced by amiloride was also observed in cells with del(17p) or *TP53* mutations (JJN3 and KMS12-BM, respectively). No significant effect of amiloride on cell cycle was observed (Supplementary Fig. S5).

To evaluate the involvement of mitochondria in cell death, the membrane potential ($\Delta\psi_m$) was measured. Amiloride caused a decrease in $\Delta\psi_m$, particularly significantly in KMS12-BM, H929, and RPMI-8226 cells (Fig. 2B; Supplementary Fig. S6). Using a luminescent-proteolytic assay, we observed that the caspases 3/7, 8, and 9 were significantly activated in all the cell lines tested (Fig. 2C; Supplementary Fig. S7A). The involvement of a caspase-independent mechanism was also observed, as Z-VAD-FMK, a pan-caspase inhibitor, was able to inhibit caspase-3/7 activity, but unable to inhibit apoptosis induced by amiloride (Supplementary Fig. S7B).

***In vivo* antimyeloma efficacy of amiloride**

We evaluated the *in vivo* efficacy of amiloride (A) in monotherapy and in combination with melphalan (M) and dexamethasone (D). As to the best of our knowledge, there are no data concerning the antitumor efficacy of amiloride in the animal model used here, we evaluated two doses of amiloride (10 mg/kg and 15 mg/kg). Treatment of MM1S-inoculated CB17-SCID mice with a double or triple combination of A (regardless of the A dose applied), together with D and/or M, enhanced tumor growth inhibition, although the differences were only statistically significant for the combinations DA10, DA15, and DMA15 (Fig. 3A; Supplementary Fig. S8A). With respect to survival, we observed a significant improvement in TTE in the group of mice treated with the double combinations, DA10 and MA10, and the triple combination, DMA10, compared with the D, M, and DM groups, respectively ($P < 0.05$; Fig. 3B). The mice treated with the triple combination DMA10 had a median overall survival (OS) of 115 days compared with 99 days for the combination DM ($P < 0.05$; Fig. 3B). The double combinations, DA15 and MA15, also showed a statistically significant benefit ($P < 0.01$) in terms of OS compared with the single drugs (Supplementary Fig. S8B). The triple combination DMA15 also had a longer OS (median, 110 days) than the double combination DM (median, 99 days), although the difference was not statistically significant ($P = 0.053$; Supplementary Fig. S8B). No significant toxicity, measured as body weight loss, was observed in the mice receiving combinations with amiloride (Supplementary Fig. S8C).

Amiloride induces gene and transcript isoforms expression changes

To determine the molecular basis of the anti-myeloma activity of amiloride, we performed RNA-Seq analysis in KMS12-BM and JJN3 cell lines, the most and the least sensitive, respectively, at the beginning of apoptosis (15%–25% cell death, assessed by CellTiter-Glo luminescent assays) after amiloride treatment. The study design is shown in Supplementary Fig. S9. RNA-Seq data were analyzed at three levels: gene, isoform and splicing events. Although there were clearly more deregulated genes in KMS12-BM (almost 5,000) than in the JJN3 cell line (almost 1,000; Fig. 4A), significant enrichment of functional categories, such as metabolic, MAPK, and Jak–STAT signaling pathways, and endocytosis (Supplementary Fig. S10A), were found among the genes deregulated in both cell lines after amiloride treatment. The analysis of differential expression at the isoform level identified a similar number of deregulated transcript isoforms (over 15,000) in both cell lines (Supplementary Fig. S10B).

Next, we focused our analysis on those genes with a total expression that was not differentially modified after amiloride treatment, but whose transcript isoforms were differentially expressed. We found a considerable number of genes that were significantly deregulated at the isoform but not the gene level in both cell lines (Fig. 4B). Among the most significantly enriched pathways with deregulated transcript isoforms, in both cell lines, were those of the spliceosome, apoptosis, metabolic pathways, and those associated with protein-processing in ER, oxidative phosphorylation, cell cycle, RNA transport, and endocytosis (Fig. 4C). Transcript isoforms belonging to different components of the spliceosome and that are involved in the assembly and regulation of the spliceosomal machinery were significantly deregulated after amiloride treatment (Supplementary Table S3). For example, the transcript ENST00000269601, which encodes the canonical protein TXNL4A, is upregulated in myeloma cells treated with amiloride, whereas the transcript ENST00000588162, which encodes a smaller protein, was only expressed in untreated cells. Notably, the p53 pathway was only highly enriched in p53-expressing cell line, KMS12-BM, but not in the p53-null cell line, JJN3 (Fig. 4C; Supplementary Table S4).

Finally, using Multivariate Analysis of Transcript Splicing software we identified thousands of alternative splicing (AS) events in both cell lines after amiloride exposure (Fig. 4D). Most of the significant AS events (FDR < 0.05) involved genes whose total

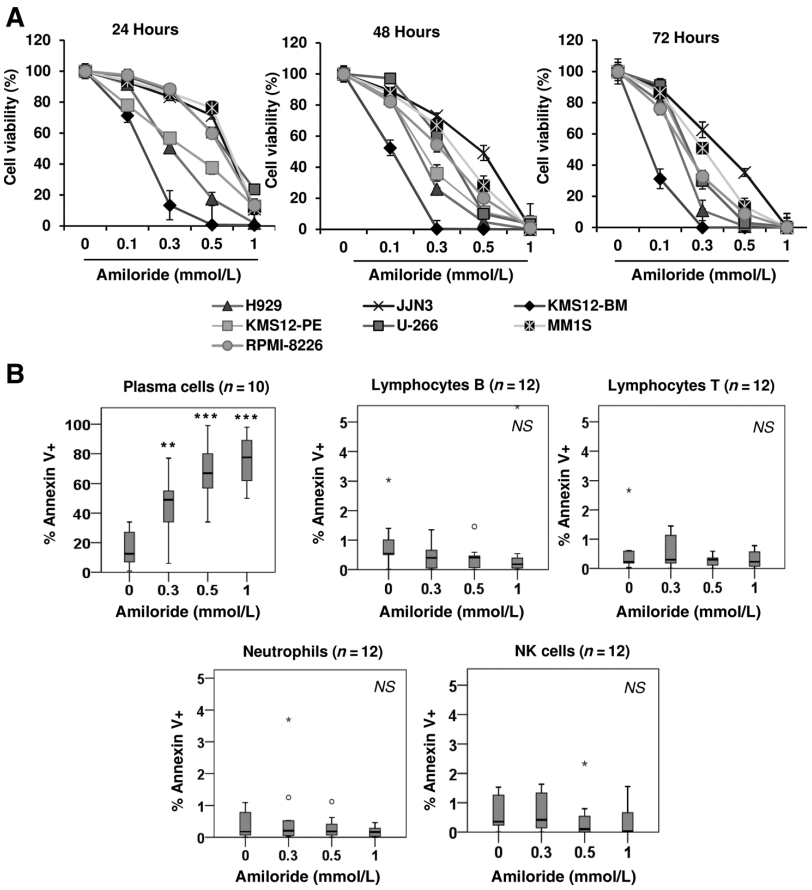

Figure 1.

Antimyeloma activity of amiloride in *in vitro* and *ex vivo* studies. **A,** The indicated multiple myeloma cell lines were incubated with increasing concentrations of amiloride for 24, 48, and 72 hours. Cell viability was analyzed by CellTiter-Glo luminescent assays. The average luminescent values of the untreated control samples were taken as 100%. Results are the means of three independent experiments. The statistically significant differences between untreated and treated cell lines were determined with Student *t* test. **B,** Bone marrow cells from patients with multiple myeloma, were treated *ex vivo* with increasing concentrations of amiloride for 48 hours. After the incubation period, cells were stained with the combination of Annexin V-FITC and three mAbs (CD45-PerCP-Cy5.5, CD38-APC and CD56 or CD19-PE) for the analysis of apoptosis in plasma cells. A panel of five antibodies in combination with Annexin V was used for the analysis of apoptosis in T and B lymphocytes, NK cells, and granulocytes. Results are presented as the percentage of Annexin V-positive cells. Statistically significant differences are represented as ***, FDR < 0.001 and **, FDR < 0.01 (Mann–Whitney *U* test). (*Continued on the following page.*)

expression was not modified by amiloride, indicating that the deregulation of alternative splicing could be a specific mechanism of action of amiloride. The most common AS event in both cell lines was the SE, which is the most common splice event in mammalian pre-mRNAs.

Amiloride modulates alternative splicing machinery

Given that RNA-Seq results showed deregulation of alternative splicing and spliceosome components in myeloma cells, we next evaluated whether the antimyeloma effect of amiloride was associated with modulation of the splicing machinery. The immunofluorescent staining for the SR (serine/arginine-rich) protein SC35 demonstrated the amiloride-induced modulation of the splicing machinery in myeloma cells with distinct *TP53* status. Thus, the modulation of the splicing machinery was accompanied by a reduction in cell viability in the H929 and JJN3 cell lines (Fig. 5). In both settings, the number of speckles was reduced but the remaining speckles increased in size and intensity. This finding was confirmed *in vivo* (Supplementary Fig. S11A) using xenografts inoculated with other multiple myeloma cell lines. Structural changes of the nuclear speckles induced by amiloride were also observed in $CD138^+$ cells from one newly diagnosed multiple myeloma patient (Supplementary Fig. S11B). In addition, mRNA levels of the spliceosome

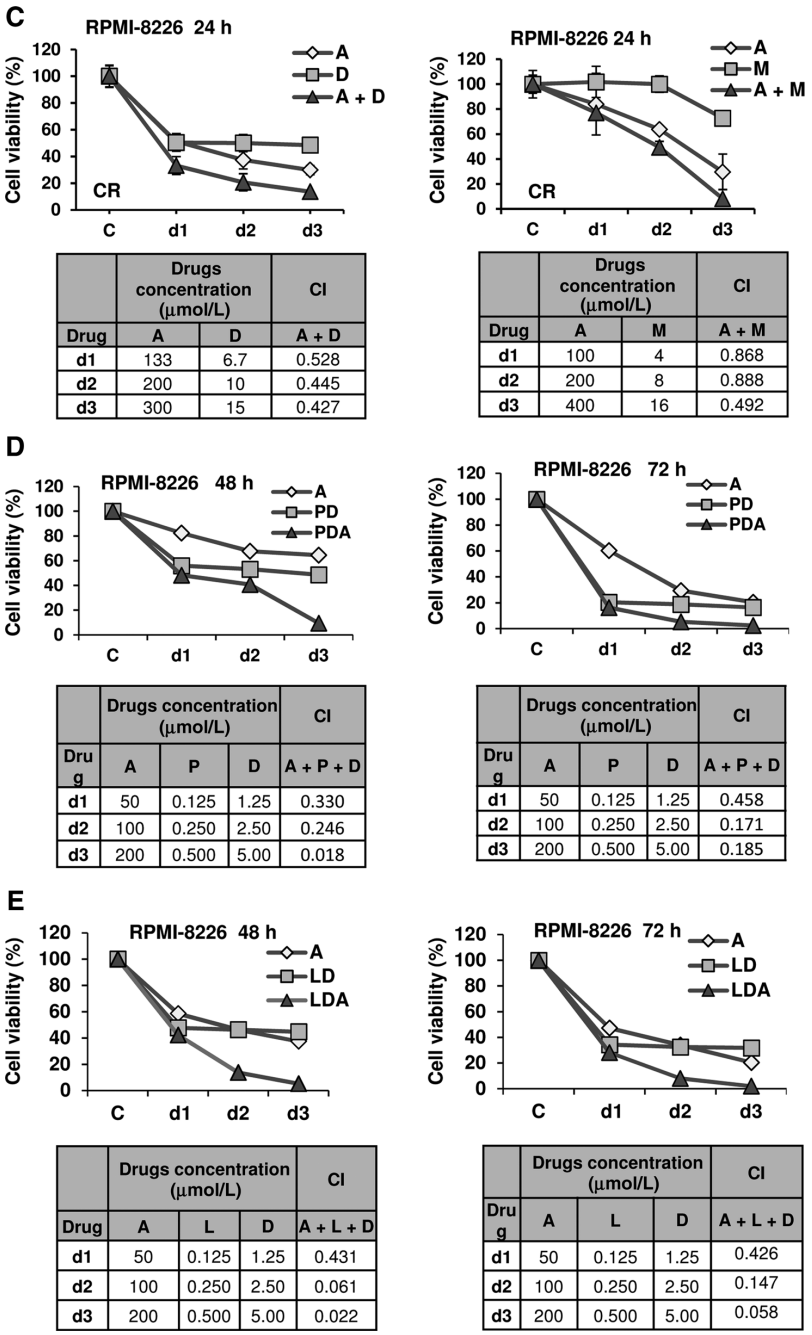

	Drugs concentration (μmol/L)		CI
Drug	A	D	A + D
d1	133	6.7	0.528
d2	200	10	0.445
d3	300	15	0.427

	Drugs concentration (μmol/L)		CI
Drug	A	M	A + M
d1	100	4	0.868
d2	200	8	0.888
d3	400	16	0.492

	Drugs concentration (μmol/L)			CI
Drug	A	P	D	A + P + D
d1	50	0.125	1.25	0.330
d2	100	0.250	2.50	0.246
d3	200	0.500	5.00	0.018

	Drugs concentration (μmol/L)			CI
Drug	A	P	D	A + P + D
d1	50	0.125	1.25	0.458
d2	100	0.250	2.50	0.171
d3	200	0.500	5.00	0.185

	Drugs concentration (μmol/L)			CI
Drug	A	L	D	A + L + D
d1	50	0.125	1.25	0.431
d2	100	0.250	2.50	0.061
d3	200	0.500	5.00	0.022

	Drugs concentration (μmol/L)			CI
Drug	A	L	D	A + L + D
d1	50	0.125	1.25	0.426
d2	100	0.250	2.50	0.147
d3	200	0.500	5.00	0.058

Figure 1.

(*Continued.*) RPMI-8226 cell line was treated with the indicated double combinations of amiloride with melphalan or dexamethasone (**C**) and triple combinations with pomalidomide or lenalidomide plus dexamethasone (**D**, **E**). Cell viability was assessed by MTT assay, as represented in the graphs. The combination indexes (CI) were calculated with the CalcuSyn software. CIs of <0.3, 0.3–0.7, 0.7–0.85, 0.85–0.90, 0.90–1.10, and >1.10 indicate strong synergism, synergism, moderate synergism, slight synergism, additive effect, and antagonism, respectively. C, control; A, amiloride; D, dexamethasone; M, melphalan; P, pomalidomide; L, lenalidomide; d1, d2, and d3, drug concentrations used in the study; CR, constant ratio.

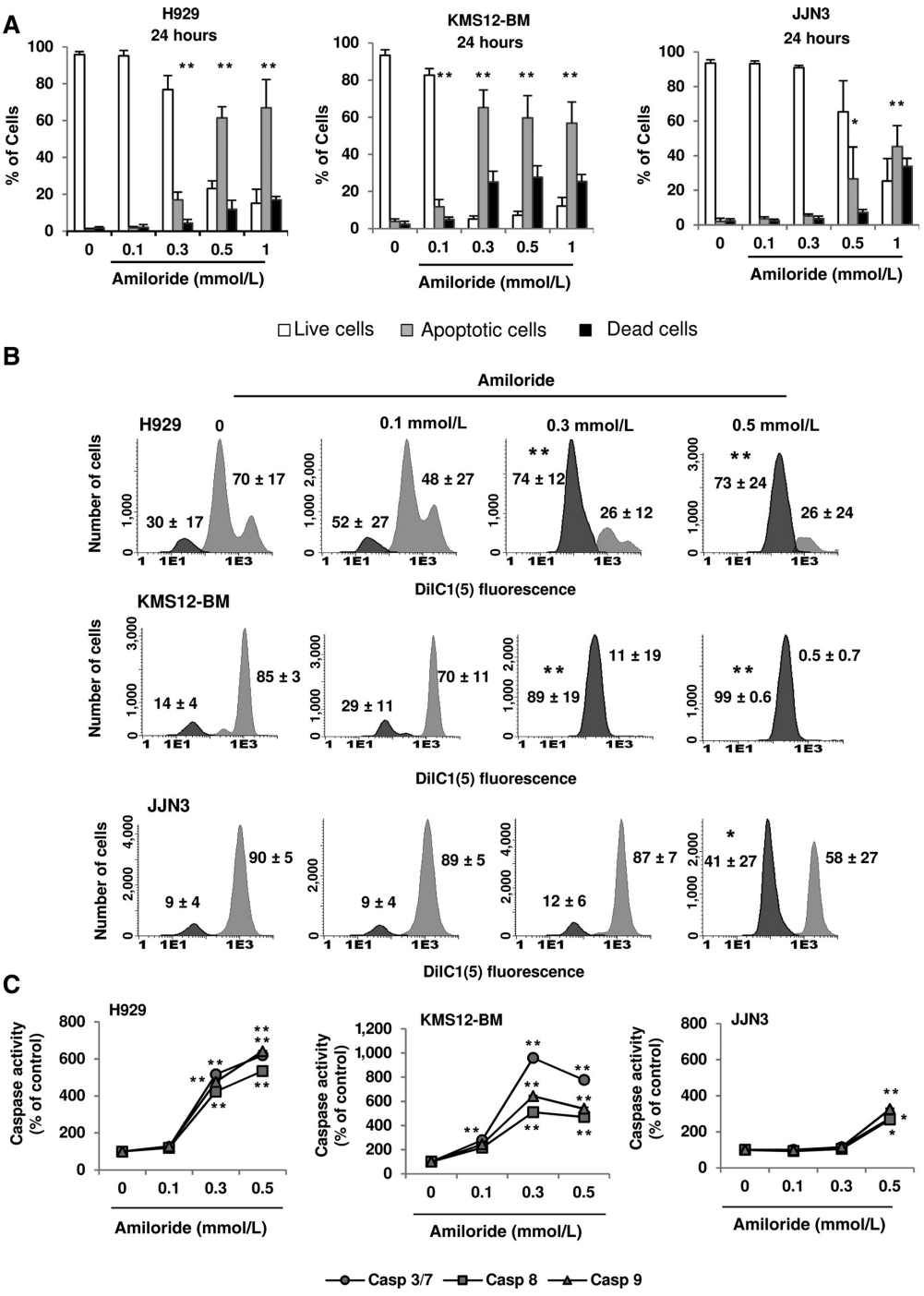

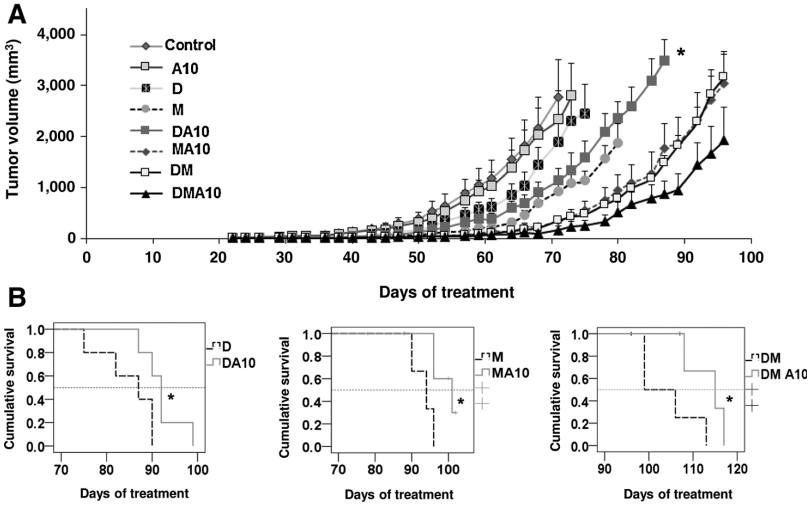

Figure 3.

The triple and double combination of dexamethasone and melphalan with amiloride displays superior anti-multiple myeloma activity and improves median survival compared with single agents and double combinations in a subcutaneous plasmacytoma model. CB17-SCID mice subcutaneously inoculated with 3×10^6 MM1S cells in the right flank were randomized to receive vehicle, amiloride (10 mg/kg, oral, daily), dexamethasone (0.5 mg/kg, i.p., 2 days per week), melphalan (2.5 mg/kg, i.p., 2 days per week) in monotherapy and the respective double and triple combinations ($n = 5$/group). **A,** Evolution of tumor volumes of the plasmacytomas. Statistical differences between groups were evaluated fitting an exponential regression model and the regression parameters were compared using a *t* test for unequal variances. Bars indicate SEM. **B,** Kaplan–Meier curves representing the survival of each treatment group. Mice were sacrificed when their tumor diameters reached 2 cm or when they became moribund. Statistically significant differences were analyzed by the log-rank test, and are represented as *, $P < 0.05$.

components (SNRNP27, SRSF4, SF3B1, LSM3, LSM14A, PRPF3, and PRPF4) were significantly overexpressed in myeloma cells from patients after amiloride treatment (Supplementary Fig. S11C). Altogether, these results suggest the potential association between the antimyeloma activity of amiloride and the modulation of spliceosomal machinery.

Antimyeloma activity of amiloride is associated with functional p53 signaling

Our results showed that multiple myeloma cells either with WT or mutated *TP53* were highly sensitive to amiloride, although higher doses and longer exposure to amiloride were required for p53-null cells. Moreover, pathway enrichment analysis from RNA-Seq data in mutated *TP53* cells revealed a subset of deregulated transcript isoforms involved in the p53 pathway. These findings suggest an activation of p53 signaling pathway in multiple myeloma cells after treatment with amiloride. To test this hypothesis, we used qRT-PCR to measure the expression of p53 targets, such as *BAK1*, *BBC3*, *TNFRSF10B*, *FAS*, *CDKN1B*, and *CDKN1A* in multiple myeloma cell lines with different *TP53* status. We observed a normal functional p53 response in the WT/WT cell line (MM1S), whereas p53 signaling was abrogated in JJN3 cells with no basal p53 expression (Fig. 6A). Interestingly, the mutated *TP53* cell lines (KMS12-BM and U-266) also showed overexpression of p53 targets. Similar results were found by RNA-Seq data analysis (Supplementary Fig. S12). The activation of p53 signaling pathway was confirmed in $CD138^+$ cells from eight multiple myeloma patients after treatment with amiloride (Supplementary Fig. S13)

The cell lines with mutated *TP53* showed deregulation of p53 targets after treatment with amiloride, so we decided to confirm the involvement of p53 in amiloride-induced cytotoxicity of multiple myeloma cells. The functionality of p53 signaling pathway in mutated *TP53* cell lines was confirmed using p53 activity inhibitors: pifithrin-α (PFTα), a reversible inhibitor of p53-mediated apoptosis and p53-dependent gene transcription (21), and pifithrin-μ (PFTμ), an inhibitor of the p53–Bcl-xL interaction that directly inhibits p53 binding to mitochondria (22). Amiloride cytotoxicity was reduced in WT and mutated *TP53* multiple myeloma cell lines when used with p53 inhibitors. As expected, the inhibitors had no effect on the death of JJN3 cells, which lack p53 expression (Fig. 6B). These results imply that p53 signaling

Figure 2.

Amiloride induces apoptosis, activates caspases, and deregulates mitochondrial potential in multiple myeloma cell lines. H929, JJN3, and KMS12-BM cells were treated with increasing concentrations of amiloride for 24 hours. **A,** The induction of apoptosis was analyzed by flow cytometry after Annexin-V/PI staining. **B,** Mitochondrial membrane depolarization was examined by flow cytometry after DiIC1(5) staining. **C,** The activity of caspase-8, caspase-9, and caspase-3/7 was analyzed by luminescent caspase assays. Results are expressed as the mean ± SD of three independent experiments. Statistically significant differences between untreated and treated cell lines are represented as **, $P < 0.01$ and *, $P < 0.05$ (Student *t* test).

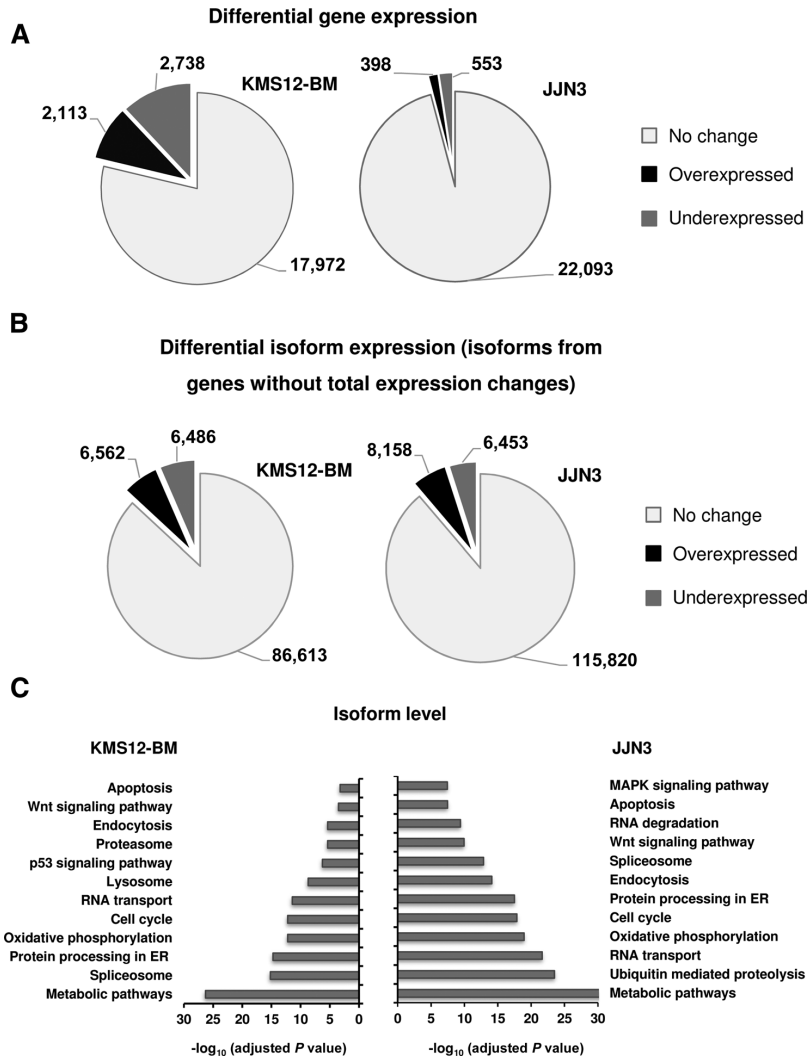

Figure 4.
Amiloride induces gene and isoform expression changes and modulates alternative splicing. RNA sequencing analysis was conducted on Poly A+ RNA from KMS12-BM and JJN3 cell lines, treated, or untreated with amiloride (0.1 mmol/L and 0.4 mmol/L, respectively) for 24 hours. **A,** Distribution of differentially expressed genes induced by amiloride (overexpressed with FC $\geq$ 2 and FDR < 0.05; underexpressed with FC $\leq$ -2 and FDR < 0.05 and not deregulated genes), identified using the DESeq2 R package. **B,** Distribution of differentially expressed transcript isoforms contained in genes without expression changes, identified using Cuffdiff. Only the isoforms that have a |FC|$\geq$ 2 were considered as differentially expressed. **C,** Summary of the biologically relevant pathways among the top 50 significantly enriched pathways in KEGG enrichment analysis for amiloride-deregulated isoforms detected in KMS12-BM (left) and JJN3 (right) cell lines. Statistical significance of the enrichment is expressed as -log10 (Benjamini–Hochberg adjusted *P* value). (*Continued on the following page.*)

has an important role in amiloride-induced apoptosis of multiple myeloma cells that express either WT or mutated *TP53*. On the other hand, the involvement of a mechanism other than p53 signaling activation would explain the antimyeloma effect of amiloride on p53-null cells.

Discussion

In this study, we demonstrate for the first time the antimyeloma activity of amiloride, an antihypertensive drug, through two novel mechanisms of action, spliceosome deregulation and p53 signaling pathway activation. Initially, we observed potent *in vitro* antimyeloma activity of amiloride, both in *TP53* wild-type and mutated *TP53* cells. Even in p53-null cells, viability was reduced by using higher doses and longer exposures. The *ex vivo* study of myeloma cells from patients indicated that amiloride induced cytotoxicity in plasma cells, including three cases bearing deletion of 17p, whereas viability of other bone marrow cell populations was not affected. Furthermore, amiloride in combination with dexamethasone and melphalan was clearly synergic *in vitro*. A synergic effect was also observed when amiloride was combined with lenalidomide or pomalidomide plus dexamethasone. In this context, amiloride has been described as potentiating synergistically the antiproliferative effect of other drugs like imatinib, the first-line therapy for patients with chronic myeloid leukemia (CML; refs. 23, 24). However, we did not find synergism between amiloride and bortezomib, which could limit the use of amiloride in bortezomib-based induction regimens.

The induction of apoptosis by amiloride in CML was accompanied by the increase in levels of caspases 9 and 3. Our results

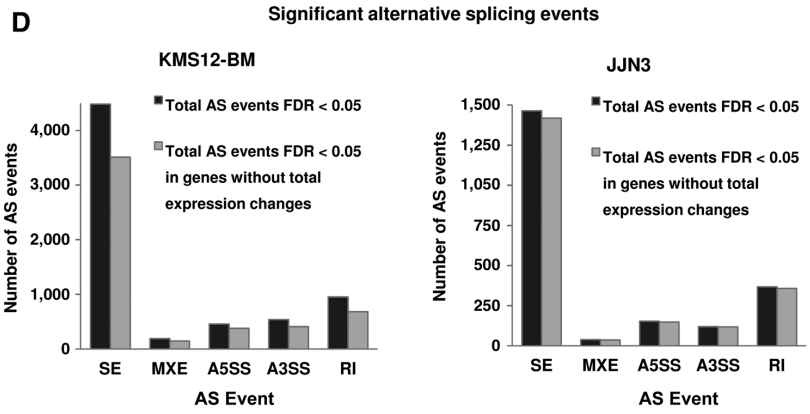

	SE	MXE	A5SS	A3SS	RI		SE	MXE	A5SS	A3SS	RI
Total AS events FDR < 0.05	4484	192	458	539	953		1465	39	154	120	369
Total AS events FDR < 0.05 in genes without total expression changes	3512 (78%)	145 (76%)	379 (83%)	408 (76%)	684 (72%)		1419 (97%)	37 (95%)	148 (96%)	118 (98%)	358 (97%)

Figure 4.
(*Continued.*) **D,** Alternative splicing events in genes without expression changes were detected using rMATS and classified into five main types of pattern: skipped exon (SE), mutually exclusive exons (MXE), alternative 5′ splice site (A5SS), alternative 3′ splice site (A3SS), and retained introns (RI). rMATS also calculates the difference in the ratio of these events between two conditions, producing a false discovery rate.

showed that the apoptosis induced by amiloride was mediated by both caspase-dependent and caspase-independent mechanisms, which is consistent with other studies in glioblastoma and breast tumor cells (25–27). Moreover, we observed increased survival of mice bearing human subcutaneous plasmacytomas treated with double or triple combinations including amiloride compared with treatment with melphalan and/or dexamethasone.

The anticancer effect of amiloride has previously been described in several tumors, using *in vitro* and *in vivo* models (9, 23–33). There is evidence for multiple mechanisms of action of amiloride, including TRAIL-induced cytotoxicity associated with the PI3K-Akt pathway (24, 28, 30, 33) and alternative splicing deregulation of apoptotic genes (9, 23, 28). The RNA-Seq allowed us to study its mechanism of action in myeloma cells more extensively. In fact, RNA-Seq analysis in two cell lines with distinct patterns of response to the drug, the most and the least sensitive, revealed that amiloride significantly altered the level of transcript isoforms and the alternative splicing events. It should be pointed out that the significant impact on the differential expression of isoforms from genes whose total expression was not changed. In other words, the traditional gene expression profiling would have overlooked the substantial modifications of more than 10,000 transcript isoforms by amiloride treatment. These results are consistent with the reported advantage of the analysis at the genome-wide isoform level compared with gene expression in cancer research (34, 35).

One of the most significantly enriched pathways in the analysis of differentially expressed isoforms after amiloride treatment was spliceosome. We found that amiloride induced a general deregulation of spliceosomal machinery at the gene and transcript isoform levels that affected the early and late stages of spliceosome assembly and several spliceosome-associated proteins, including the catalytic steps of the splicing. These findings, together with the large quantity of total transcript isoforms modified by amiloride, prompted us to investigate further the influence of amiloride in the pre-mRNA splicing machinery. The small nuclear ribonucleoproteins (snRNP) and splicing factors, like the SR protein family, are organized in nuclear speckles (36). The changes in protein SC35-staining speckles are used as a marker for the disruption of the splicing machinery (37–40). Upon the inhibition of the splicing machinery, the number of nuclear speckles decreases but those remaining increase in size and intensity (36, 41). Using this marker, after amiloride treatment, we identified a similar pattern of nuclear speckle modifications that was associated with cell viability inhibition. This finding indicates that amiloride provokes the disruption of the splicing machinery and that this could, in turn, induce cytotoxicity.

The RNA-Seq analysis at the transcript isoform level also identified the p53 pathway as one of the most significantly enriched functional categories. Remarkably, the p53 pathway was highly overexpressed only in the cell line expressing mutated *TP53*, and not in the p53-null cell line. In addition, upregulation of p53 targets was observed in WT and mutated *TP53* myeloma cells treated with amiloride. These results, together with the fact that the inhibition of p53 protein activity prevents amiloride-induced cell death, even in two mutated *TP53* cell lines, demonstrate that amiloride-induced apoptosis in myeloma cells is dependent on p53 activation and is independent of the mutational status of *TP53*. Apart from that, the reduction in cell viability in the amiloride-treated p53-null cell line supports the notion that other mechanisms independent of p53, such as the

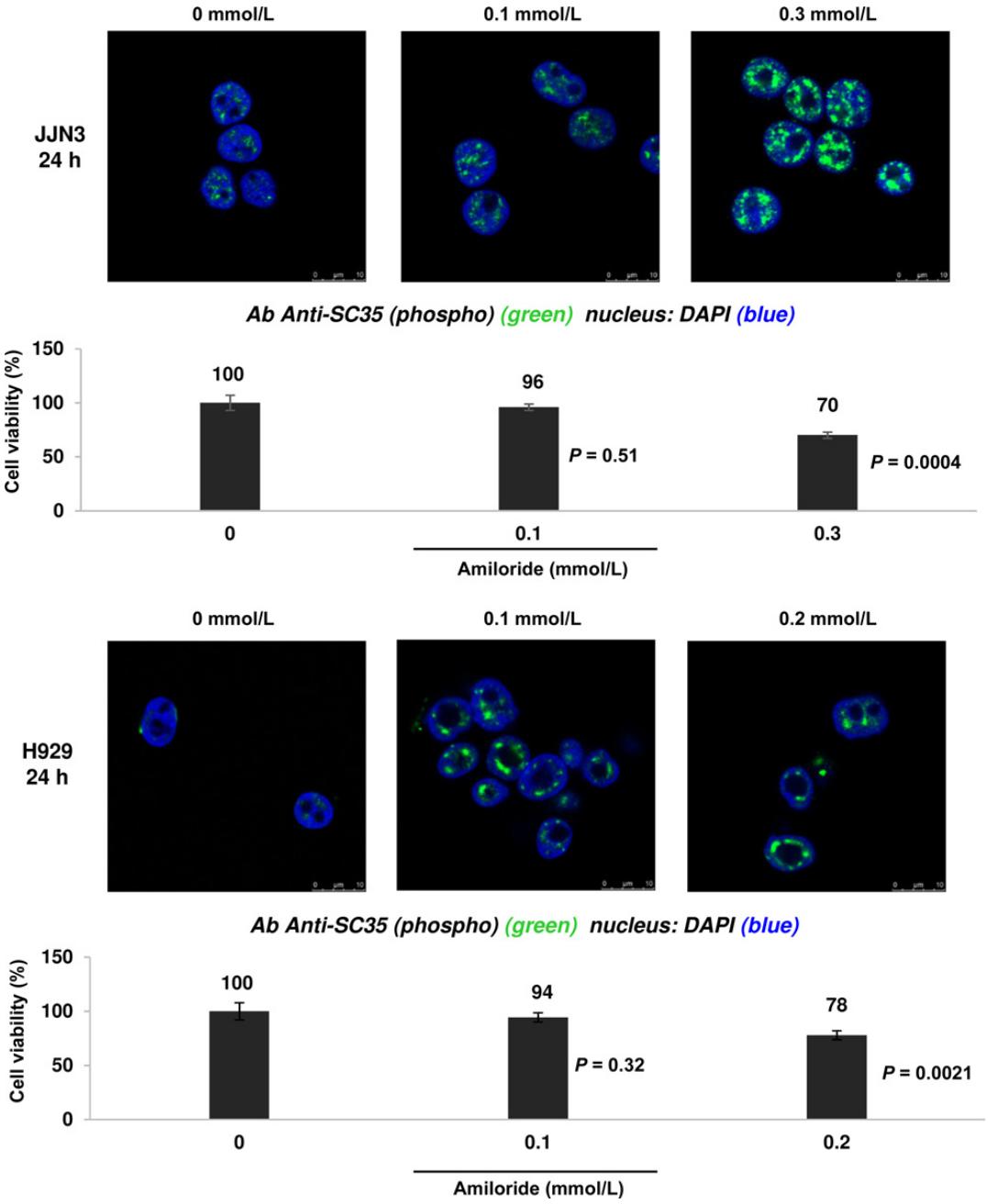

Figure 5.

Amiloride affects the pre-mRNA splicing machinery in myeloma cells *in vitro*, independently of *TP53* status. H929 (*TP53* WT) and JJN3 (*TP53* null) cells were treated with increasing concentrations of amiloride. SC35-staining nuclear speckles were detected by immunofluorescence after 24 hours. Cell viability was analyzed by CellTiter-Glo luminescent assays and expressed as the mean ± SD. Statistically significant differences between amiloride-treated and untreated cells are presented. *P* values were assessed by the two-sided Student *t* test.

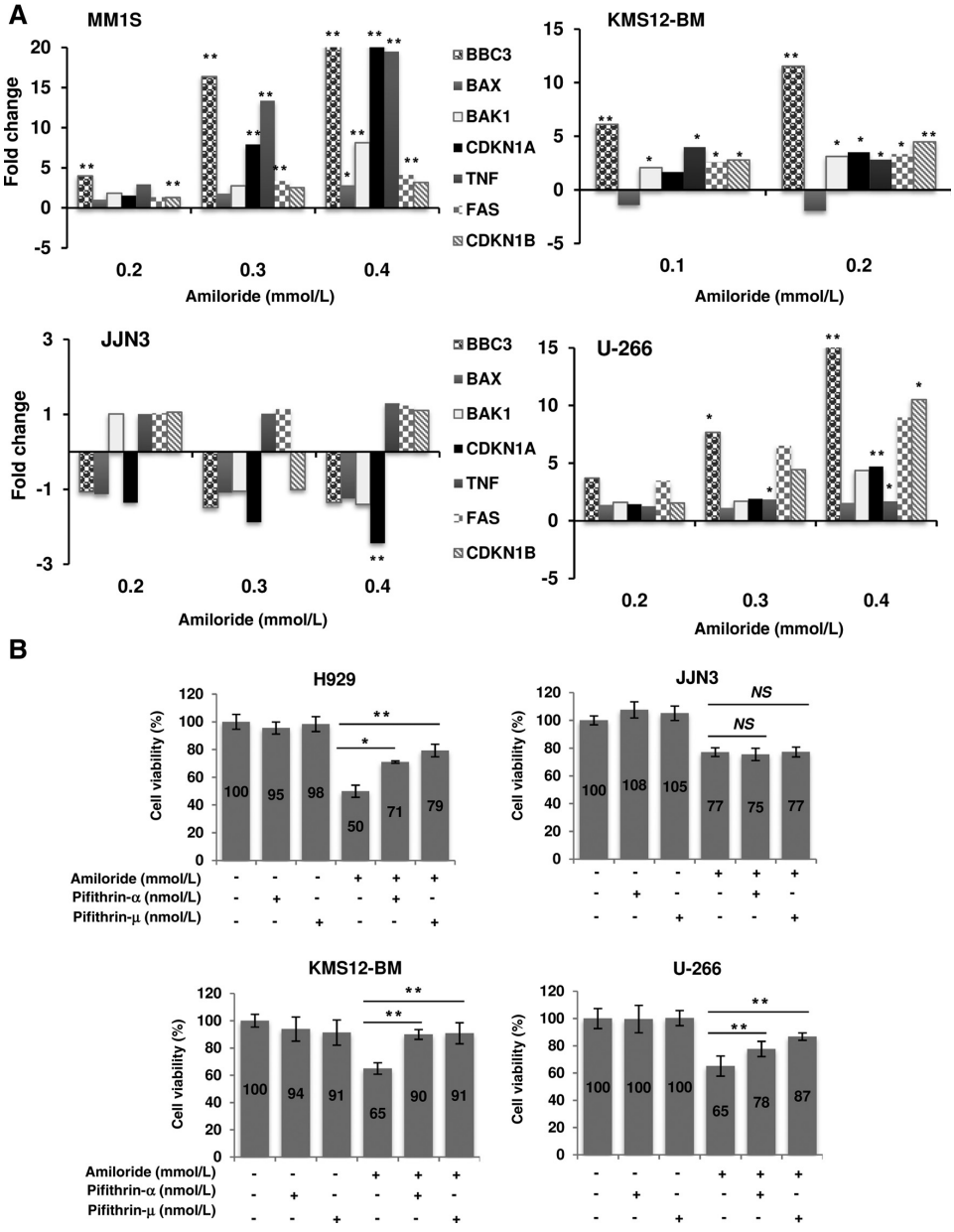

Figure 6.

The p53 signaling pathway is activated in *TP53* WT and MUT, but not in p53-null multiple myeloma cells. **A,** MM1S, KMS12-BM, JJN3, and U-266 cells were treated with increasing concentrations of amiloride. mRNA levels of *BBC3* (*PUMA*), *BAX, BAK1, CDKN1A* (*p21*), *CDKN1B, TNFRSF10B*, and *FAS* (*CD95*), were assessed by qRT-PCR 24 hours after amiloride treatment. The results are shown as the magnitude of change between treated and untreated cells and correspond to the average of three experiments after normalization with 18S rRNA. Statistically significant differences between untreated and treated cell lines are represented as **, $P < 0.01$ and *, $P < 0.05$ (Student *t* test). **B,** Cell viability upon amiloride (KMS12-BM at 0.1 mmol/L; H929 at 0.2 mmol/L; JJN3 and U-266 at 0.3 mmol/L), pifithrin-α (10 nmol/L) or pifithrin-μ (2.5 nmol/L) treatment was analyzed by CellTiter-Glo luminescent assays, 24 hours after amiloride treatment. Results are the mean of at least three independent experiments. Asterisks indicate statistically significant differences between amiloride-treated cells and amiloride-pifithrin-α/μ-treated cells; **, $P < 0.01$; *, $P < 0.05$; *N.S.*, no significant (Student *t* test).

spliceosomal machinery disruption observed in JJN3 cell line, are involved in amiloride activity.

Amiloride has been used for many years as adjuvant treatment with thiazide diuretics in congestive heart failure and hypertension (42–45). Here, we demonstrate for the first time the therapeutic potential of amiloride in multiple myeloma. The concentration of amiloride used in the *in vivo* experiments is higher than that commonly used as a potassium-sparing diuretic, suggesting that a higher dose would be needed to produce the anti-multiple myeloma effect. The toxicity profile of this drug is very well known and the main side effect is hyperkalemia, which could be the main factor that limits the use of amiloride as an antimyeloma drug. To minimize this risk, a careful electrolyte monitoring along with the coadministration of a kaliuretic agent or the use of new oral agents for the hyperkalemia treatment, such as patiromer calcium (46–48) and ZS-9 (zirconium cyclosilicate; refs. 48–50), could be required. Moreover, attempts to develop amiloride analogues that show reduced diuretic and antikaliuretic effects retaining or enhancing anticancer activity are currently underway in different laboratories. On the other hand, as reported in other studies (23, 32), we did not find any significant systemic toxicity in the mice treated with amiloride, and the viability of the lymphocyte population either from multiple myeloma patients or healthy donors was not affected, even at the highest dose.

Our results also revealed that the antimyeloma activity of amiloride was mediated through spliceosome modulation and involved the p53 pathway. In fact, p53 signaling was activated after amiloride exposure, independently of the mutational status of *TP53*. On the other hand, amiloride was also able to induce apoptosis in myeloma cells that did not express p53.

In conclusion, these findings together with the possibility of combining amiloride with melphalan, dexamethasone, or lenalidomide or pomalidomide, support the initiation of clinical trials including amiloride for patients with relapsed and refractory multiple myeloma, particularly for those with 17p deletion or *TP53* mutations who display a poor prognosis.

Disclosure of Potential Conflicts of Interest

No potential conflicts of interest were disclosed.

Authors' Contributions

Conception and design: E.A. Rojas, I. Misiewicz-Krzeminska, N.C. Gutiérrez
Development of methodology: E.A. Rojas, J.F. Martínez-Blanch, I. Misiewicz-Krzeminska
Acquisition of data (provided animals, acquired and managed patients, provided facilities, etc.): E.A. Rojas, L. San-Segundo, J.F. Martínez-Blanch, F.M. Codoñer, T. Paíno, N. Puig, M. Victoria Mateos, N.C. Gutiérrez
Analysis and interpretation of data (e.g., statistical analysis, biostatistics, computational analysis): E.A. Rojas, L.A. Corchete, J.F. Martínez-Blanch, F.M. Codoñer, T. Paíno, N. Puig, E.M. Ocio, N.C. Gutiérrez
Writing, review, and/or revision of the manuscript: E.A. Rojas, L.A. Corchete, F.M. Codoñer, N. Puig, R. García-Sanz, M. Victoria Mateos, E.M. Ocio, I. Misiewicz-Krzeminska, N.C. Gutiérrez
Administrative, technical, or material support (i.e., reporting or organizing data, constructing databases): N. Puig, R. García-Sanz, N.C. Gutiérrez
Study supervision: R. García-Sanz, I. Misiewicz-Krzeminska, N.C. Gutiérrez

Acknowledgments

The authors thank Isabel Isidro, Teresa Prieto, Vanesa Gutiérrez, Irene Aires, and José Pérez for their technical assistance; Lorena González for the help with the assays of the combinations of antimyeloma drugs; Mercedes Garayoa for the help with MSC studies; and Phil Mason for his help in reviewing the English language of the manuscript.

Grant Support

This study was partially supported by the Instituto de Salud Carlos III-Cofinanciación with funding from FEDER (PI13/00111 and PI16/01074), Asociación Española Contra el Cáncer (AECC, GCB120981SAN), Gerencia Regional de Salud, Junta de Castilla y León (BIO/SA57/13 and BIO/SA22/15), and the INNOCAMPUS Program (CEI10-1-0010). I. Misiewicz-Krzeminska was supported by a Black Swan Research Initiative® grant from the International Myeloma Foundation. L.A. Corchete was supported by a grant from the Fundación Española de Hematología y Hemoterapia.

The costs of publication of this article were defrayed in part by the payment of page charges. This article must therefore be hereby marked *advertisement* in accordance with 18 U.S.C. Section 1734 solely to indicate this fact.

Received March 8, 2017; revised June 30, 2017; accepted July 28, 2017; published OnlineFirst August 8, 2017.

References

1. Kumar SK, Rajkumar SV, Dispenzieri A, Lacy MQ, Hayman SR, Buadi FK, et al. Improved survival in multiple myeloma and the impact of novel therapies. Blood 2008;111:2516–20.
2. Kumar SK, Dispenzieri A, Lacy MQ, Gertz MA, Buadi FK, Pandey S, et al. Continued improvement in survival in multiple myeloma: changes in early mortality and outcomes in older patients. Leukemia 2014;28:1122–8.
3. Mateos M-V, Ocio EM, Paiva B, Rosiñol L, Martínez-López J, Bladé J, et al. Treatment for patients with newly diagnosed multiple myeloma in 2015. Blood Rev 2015;29:387–403.
4. Kumar SK, Lee JH, Lahuerta JJ, Morgan G, Richardson PG, Crowley J, et al. Risk of progression and survival in multiple myeloma relapsing after therapy with IMiDs and bortezomib: a multicenter international myeloma working group study. Leukemia 2012;26:149–57.
5. Rajan AM, Kumar S. New investigational drugs with single-agent activity in multiple myeloma. Blood Cancer J 2016;6:e451.
6. Würth R, Thellung S, Bajetto A, Mazzanti M, Florio T, Barbieri F. Drug-repositioning opportunities for cancer therapy: novel molecular targets for known compounds. Drug Discov Today 2016;21:190–9.
7. Tang CM, Presser F, Morad M. Amiloride selectively blocks the low threshold (T) calcium channel. Science 1988;240:213–5.
8. Slepkov ER, Rainey JK, Sykes BD, Fliegel L. Structural and functional analysis of the Na+/H+ exchanger. Biochem J 2007;401:623–33.
9. Chang J-G, Yang D-M, Chang W-H, Chow L-P, Chan W-L, Lin H-H, et al. Small molecule amiloride modulates oncogenic RNA alternative splicing to devitalize human cancer cells. PLoS One 2011;6:e18643.
10. Tazi J, Bakkour N, Stamm S. Alternative splicing and disease. Biochim Biophys Acta 2009;1792:14–26.
11. Wang G-S, Cooper TA. Splicing in disease: disruption of the splicing code and the decoding machinery. Nat Rev Genet 2007;8:749–61.
12. Cartegni L, Chew SL, Krainer AR. Listening to silence and understanding nonsense: exonic mutations that affect splicing. Nat Rev Genet 2002;3:285–98.
13. Venables JP. Aberrant and alternative splicing in cancer. Cancer Res 2004;64:7647–54.
14. Kim E, Goren A, Ast G. Insights into the connection between cancer and alternative splicing. Trends Genet 2008;24:7–10.
15. Misiewicz-Krzeminska I, Sarasquete ME, Quwaider D, Krzeminski P, Ticona FV, Paíno T, et al. Restoration of microRNA-214 expression reduces growth of myeloma cells through positive regulation of P53 and inhibition of DNA replication. Haematologica 2013;98:640–8.
16. Maiso P, Carvajal-Vergara X, Ocio EM, López-Pérez R, Mateo G, Gutiérrez N, et al. The histone deacetylase inhibitor LBH589 is a potent antimyeloma agent that overcomes drug resistance. Cancer Res 2006;66:5781–9.

17. Chou T-C. Drug combination studies and their synergy quantification using the Chou-Talalay method. Cancer Res 2010;70:440–6.
18. Ocio EM, Vilanova D, Atadja P, Maiso P, Crusoe E, Fernández-Lázaro D, et al. In vitro and in vivo rationale for the triple combination of panobinostat (LBH589) and dexamethasone with either bortezomib or lenalidomide in multiple myeloma. Haematologica 2010;95:794–803.
19. Shen S, Park JW, Lu Z, Lin L, Henry MD, Wu YN, et al. rMATS: robust and flexible detection of differential alternative splicing from replicate RNA-Seq data. Proc Natl Acad Sci U S A 2014;111:E5593–5601.
20. Wang J, Duncan D, Shi Z, Zhang B. WEB-based GEne SeT AnaLysis Toolkit (WebGestalt): update 2013. Nucleic Acids Res 2013;41:W77–83.
21. Farah IO, Begum RA, Ishaque AB. Differential protection and transactivation of P53, P21, Bcl2, PCNA, cyclin G, and MDM2 genes in rat liver and the HepG2 cell line upon exposure to pifithrin. Biomed Sci Instrum 2007;43:116–21.
22. Hagn F, Klein C, Demmer O, Marchenko N, Vaseva A, Moll UM, et al. BclxL changes conformation upon binding to wild-type but not mutant p53 DNA binding domain. J Biol Chem 2010;285:3439–50.
23. Chang W-H, Liu T-C, Yang W-K, Lee C-C, Lin Y-H, Chen T-Y, et al. Amiloride modulates alternative splicing in leukemic cells and resensitizes Bcr-AblT315I mutant cells to imatinib. Cancer Res 2011;71:383–92.
24. Zheng Y, Yang H, Li T, Zhao B, Shao T, Xiang X, et al. Amiloride sensitizes human pancreatic cancer cells to erlotinib in vitro through inhibition of the PI3K/AKT signaling pathway. Acta Pharmacol Sin 2015;36:614–26.
25. Leon LJ, Pasupuleti N, Gorin F, Carraway KL. A cell-permeant amiloride derivative induces caspase-independent, AIF-mediated programmed necrotic death of breast cancer cells. PLoS One 2013;8:e63038.
26. Hegde M, Roscoe J, Cala P, Gorin F. Amiloride kills malignant glioma cells independent of its inhibition of the sodium-hydrogen exchanger. J Pharmacol Exp Ther 2004;310:67–74.
27. Harley W, Floyd C, Dunn T, Zhang X-D, Chen T-Y, Hegde M, et al. Dual inhibition of sodium-mediated proton and calcium efflux triggers non-apoptotic cell death in malignant gliomas. Brain Res 2010;1363:159–69.
28. Tang J-Y, Chang H-W, Chang J-G. Modulating roles of amiloride in irradiation-induced antiproliferative effects in glioblastoma multiforme cells involving Akt phosphorylation and the alternative splicing of apoptotic genes. DNA Cell Biol 2013;32:504–10.
29. Yang X, Wang D, Dong W, Song Z, Dou K. Suppression of Na+/H + exchanger 1 by RNA interference or amiloride inhibits human hepatoma cell line SMMC-7721 cell invasion. Med Oncol Northwood 2011;28:385–90.
30. Cho Y-L, Lee K-S, Lee S-J, Namkoong S, Kim Y-M, Lee H, et al. Amiloride potentiates TRAIL-induced tumor cell apoptosis by intracellular acidification-dependent Akt inactivation. Biochem Biophys Res Commun 2005; 326:752–8.
31. Sparks RL, Pool TB, Smith NK, Cameron IL. Effects of amiloride on tumor growth and intracellular element content of tumor cells in vivo. Cancer Res 1983;43:73–7.
32. Matthews H, Ranson M, Kelso MJ. Anti-tumour/metastasis effects of the potassium-sparing diuretic amiloride: an orally active anti-cancer drug waiting for its call-of-duty? Int J Cancer 2011;129:2051–61.
33. Kim KM, Lee YJ. Amiloride augments TRAIL-induced apoptotic death by inhibiting phosphorylation of kinases and phosphatases associated with the P13K-Akt pathway. Oncogene 2005;24:355–66.
34. Zhang C, Li H-R, Fan J-B, Wang-Rodriguez J, Downs T, Fu X-D, et al. Profiling alternatively spliced mRNA isoforms for prostate cancer classification. BMC Bioinformatics 2006;7:202.
35. Zhang Z, Pal S, Bi Y, Tchou J, Davuluri RV. Isoform level expression profiles provide better cancer signatures than gene level expression profiles. Genome Med 2013;5:33.
36. Shepard PJ, Hertel KJ. The SR protein family. Genome Biol 2009; 10:242.
37. Kotake Y, Sagane K, Owa T, Mimori-Kiyosue Y, Shimizu H, Uesugi M, et al. Splicing factor SF3b as a target of the antitumor natural product pladienolide. Nat Chem Biol 2007;3:570–5.
38. Kaida D, Motoyoshi H, Tashiro E, Nojima T, Hagiwara M, Ishigami K, et al. Spliceostatin A targets SF3b and inhibits both splicing and nuclear retention of pre-mRNA. Nat Chem Biol 2007;3:576–83.
39. Allende-Vega N, Dayal S, Agarwala U, Sparks A, Bourdon J-C, Saville MK. p53 is activated in response to disruption of the pre-mRNA splicing machinery. Oncogene 2013;32:1–14.
40. Ghosh G, Adams JA. Phosphorylation mechanism and structure of serine-arginine protein kinases. FEBS J 2011;278:587–97.
41. Spector DL, Lamond AI. Nuclear speckles. Cold Spring Harb Perspect Biol 2011;3:a000646.
42. Fuchs SC, Poli-de-Figueiredo CE, Figueiredo Neto JA, Scala LCN, Whelton PK, Mosele F, et al. Effectiveness of chlorthalidone plus amiloride for the prevention of hypertension: the PREVER-Prevention Randomized Clinical Trial. J Am Heart Assoc 2016;5:04248.
43. Andersen H, Hansen PBL, Bistrup C, Nielsen F, Henriksen JE, Jensen BL. Significant natriuretic and antihypertensive action of the epithelial sodium channel blocker amiloride in diabetic patients with and without nephropathy. J Hypertens 2016;34:1621–9.
44. Oxlund CS, Buhl KB, Jacobsen IA, Hansen MR, Gram J, Henriksen JE, et al. Amiloride lowers blood pressure and attenuates urine plasminogen activation in patients with treatment-resistant hypertension. J Am Soc Hypertens 2014;8:872–81.
45. Fuchs FD, Scala LCN, Vilela-Martin JF, de Mello RB, Mosele F, Whelton PK, et al. Effectiveness of chlorthalidone/amiloride versus losartan in patients with stage I hypertension: results from the PREVER-treatment randomized trial. J Hypertens 2016;34:798–806.
46. Weir MR, Bakris GL, Bushinsky DA, Mayo MR, Garza D, Stasiv Y, et al. Patiromer in patients with kidney disease and hyperkalemia receiving RAAS inhibitors. N Engl J Med 2015;372:211–21.
47. Bakris GL, Pitt B, Weir MR, Freeman MW, Mayo MR, Garza D, et al. Effect of patiromer on serum potassium level in patients with hyperkalemia and diabetic kidney disease: The AMETHYST-DN Randomized Clinical Trial. JAMA 2015;314:151–61.
48. Henneman A, Guirguis E, Grace Y, Patel D, Shah B. Emerging therapies for the management of chronic hyperkalemia in the ambulatory care setting. Am J Health Syst Pharm 2016;73:33–44.
49. Linder KE, Krawczynski MA, Laskey D. Sodium zirconium cyclosilicate (ZS-9): a novel agent for the treatment of hyperkalemia. Pharmacotherapy 2016;36:923–33.
50. Packham DK, Kosiborod M. Pharmacodynamics and pharmacokinetics of sodium zirconium cyclosilicate [ZS-9] in the treatment of hyperkalemia. Expert Opin Drug Metab Toxicol 2016;12:567–73.

Discusión general

El cáncer es una enfermedad genética que agrupa una serie de entidades caracterizadas por un crecimiento y una proliferación celulares incontrolables. Las células tumorales aprenden a evadir la muerte celular y adquieren otras capacidades biológicas durante el desarrollo de los tumores, los llamados *hallmarks* del cáncer[303]. Entre ellos, los cambios en la expresión génica que experimenta la célula tumoral han sido extensamente estudiados a lo largo de los años. Sin embargo, durante mucho tiempo se ha considerado que los genes sólo producían un único ARNm y este a su vez una única proteína. Hoy día sabemos que la mayoría de los genes pueden dar lugar a distintos ARNm maduros y distintas proteínas a través del proceso de *splicing* alternativo del pre-ARNm. Los avances tecnológicos han permitido estudiar cómo ocurre este complejo procesamiento de una molécula de pre-ARNm, así como las proteínas que participan en él y lo regulan. Pero el *splicing* del pre-ARNm no sólo afecta a más del 95 % de los genes sino que además puede afectar la regulación de múltiples procesos biológicos. Es evidente que este importante mecanismo de regulación postranscripcional es responsable de la alta complejidad y heterogeneidad a nivel de transcriptoma y proteoma celular, por lo que no resulta sorprendente que su alteración esté muy ligada a cáncer. De hecho, en la actualidad se están desarrollando numerosas estrategias terapéuticas dirigidas a regular y corregir las alteraciones propias de este mecanismo celular en distintas enfermedades, incluido el cáncer.

El **primer trabajo** de la presente tesis doctoral se centró en comparar el transcriptoma de la LCPp con el del MM, en presencia de un fondo genético similar. La CP tumoral es aparentemente la misma en ambas neoplasias de CP, sin embargo, las diferencias en el comportamiento clínico y la respuesta terapéutica son muy acentuadas. El estudio de otros mecanismos biológicos no explorados hasta el momento que pudieran estar alterados diferencialmente entre ambas discrasias podría ayudar a entender por qué las LCPp tienen un comportamiento significativamente más agresivo que los MM. Una de las razones que se ha esgrimido en este sentido es que en las LCPp se concentran las alteraciones genéticas de alto riesgo, de forma aislada o en combinación, en mucha mayor medida que en el MM. Con el fin de eliminar el sesgo introducido por la distribución diferente de las alteraciones genéticas entre las LCPp y los MM, a la hora de comparar su expresión génica global, abordamos el estudio seleccionando casos de MM y de LCPp que presentaban alteraciones genéticas similares. Así, tanto los pacientes con MM como con LCPp tenían deleción de 17p y una distribución muy parecida del resto de alteraciones citogenéticas. Este diseño constituye uno de los planteamientos diferenciales respecto a los utilizados en los trabajos anteriores en los que se comparaba el perfil de expresión génica de ambas neoplasias de CP. La otra innovación de este estudio fue la utilización de *microarrays* de transcriptoma (HTA, *Human Transcriptome Array*) que permiten analizar no sólo el patrón de expression génica estudiado previamente por otros autores[61,304,305], sino también explorar por primera vez la expresión de isoformas y el impacto del *splicing* alternativo del pre-ARNm.

El análisis no supervisado de los HTAs basado en la expresión génica nos permitió diferenciar dos grupos, uno de ellos contenía los casos de LCPp y el otro, los de MM. Este hallazgo sugería que el transcriptoma de las LCPp se diferenciaba con claridad de el del MM,

incluso habiendo seleccionado casos con alteraciones genéticas similares. En cambio, un análisis semejante utilizando datos de RNA-Seq provenientes de 73 pacientes con MM que tenían deleción de 17p incluidos en el estudio CoMMpass no identificó ninguna agrupación de muestras. Este resultado indica que el hecho de que todos los MM portaran la deleción de 17p determinaba un perfil de expresión génica parecido entre ellos, y que si había otras características genómicas distintas entre los MM con deleción de 17p no eran lo suficientemente consistentes como para que un análisis de *clustering* identificara agrupaciones.

El análisis supervisado a nivel génico confirmó las diferencias entre los casos de LCPp y MM, ya que se detectaron más de 3 000 genes infraexpresados y alrededor de 300 genes sobreexpresados en la LCPp en comparación con el MM. Las vías del *spliceosoma* y del procesamiento del ARNm estuvieron entre las más desreguladas entre ambas discrasias. La desregulación de estas vías no se había descrito previamente, probablemente debido a los criterios de selección de los pacientes, anteriormente mencionados. El análisis de la expresión de las isoformas y de los eventos de *splicing* alternativo en la LCPp y el MM confirmó la afectación de las vías del *splicing* de pre-ARNm, ya que se detectaron cambios significativos de expresión en componentes del *spliceosoma*, como el factor de *splicing* 1 (*SF1*), y desregulación de exones que tenían sitios de unión para las proteínas de regulación del *splicing*.

Encontramos que el gen *WARS*, que codifica para una enzima que participa en la síntesis proteica, y el gen *AHR*, un factor de transcripción citoplasmático, fueron los dos genes significativamente más sobreexpresados en los casos de LCPp. Este hallazgo unido a la desregulación detectada de la vía de señalización de infección por el virus de Epstein Barr (EBV) a nivel génico, de isoformas y de eventos de *splicing* alternativo en los casos de LCPp, nos resultó particularmente interesante. Algunos trabajos previos han reportado elevados niveles de expresión de *WARS* en células humanas infectadas con diferentes virus[306–308], así como el uso de la maquinaria celular del *spliceosoma* por el EBV para la trascripción de sus proteínas virales en las células infectadas[309,310], sugiriendo que *WARS* podría tener una función importante en la defensa antiviral tras la infección con el EBV[311]. *AHR* por su parte, es conocido también por ser un regulador de la inmunidad antiviral[312,313] y recientes evidencias sugieren su efecto en la iniciación, progresión e invasión de las células tumorales[314]. Otros estudios han demostrado la sobreexpresión y activación constitutiva de *AHR* en varios cánceres, incluido el MM donde su elevada expresión se asoció con una menor supervivencia de los pacientes[315]. Se podría hipotetizar que la infección con el EBV podría estimular un incremento en los niveles de *WARS* y *AHR* en la LCPp como parte de la defensa antiviral de las células infectadas.

La investigación de las isoformas a nivel global puede aportar, como hemos visto en el primer trabajo, información pasada por alto cuando los estudios de expresión sólo se centran en el transcrito de ARNm canónico o constitutivo. Asimismo, el análisis pormenorizado de las isoformas generadas por el *splicing* alternativo en genes particulares ha ayudado a entender la importancia de este mecanismo en la regulación postranscripcional. En la última década se ha estudiado y descrito el *splicing* alternativo de muchos genes asociados a distintas enfermedades

que puede dar lugar a isoformas variadas con funciones distintas o incluso opuestas. Es el caso de algunas que estimulan la invasión celular y la diseminación metastásica en cáncer como la isoforma CD44v que incluye en su secuencia exones que normalmente se excluyen del ARNm canónico. Se ha demostrado que otras contribuyen a la generación de resistencias a los fármacos como la isoforma proteica d16HER2, que resulta de la exclusión del exón 20 de la secuencia del ARNm de HER2. Curiosamente, la expresión de d16HER2 en cáncer de mama disminuye la sensibilidad al anticuerpo anti-HER2, trastuzumab, al inhibir la apoptosis que induce este anticuerpo mediante la sobreexpresión de Bcl-2 y la activación de la cinasa Src[316,317].

El gen *TP53* también da lugar a diversas isoformas, aunque estas han sido poco analizadas, a pesar de que se trata de uno de los genes más estudiados del genoma ya que su disfunción e inactivación tienen un papel central en la patogenia del cáncer y en su respuesta terapéutica. Las isoformas de p53 se han estudiado sobre todo en el cáncer de mama, en el que la sobreexpresión de algunas de ellas[284] se ha asociado con peor pronóstico[318]. Es el caso, por ejemplo, de la isoforma Δ40p53α que se ha encontrado sobreexpresada significativamente en el tejido tumoral de mama respecto del tejido normal, especialmente en aquellos casos de cáncer de mama tripe negativo[318], y también de la isoforma Δ133p53β que promueve la invasión en cáncer de mama y de colon, independientemente de que p53 esté mutado o no[319].

En el MM no se han realizado estudios dirigidos a evaluar la expresión de las isoformas de *TP53*. Teniendo en cuenta la importancia de las alteraciones de este gen en el pronóstico del MM, en el **segundo trabajo**, nos planteamos analizar la expresión de las isoformas de p53 y evaluar su impacto en el pronóstico de los pacientes. Para ello se utilizaron muestras de pacientes con MM de nuevo diagnóstico incluidos en el ensayo clínico GEM2012. La expresión de las isoformas tanto de forma global como para un gen particular se ha analizado casi siempre a nivel del ARNm, bien con técnicas de *microarrays* o RNA-Seq, en el primer caso, o con PCR cuantitativa, en el segundo. Sin embargo, lo ideal sería cuantificar los niveles de las isoformas proteicas, aun sabiendo la dificultad que entraña conseguir muestra suficiente para analizar las proteínas, especialmente en el MM en el que la purificación de las muestras mediante selección de CD138 resulta en concentraciones muy limitadas de proteína. En este trabajo se ha utilizado por primera vez la tecnología de inmunoelectroforesis capilar (CNIA) en el análisis de la expresión proteica de cinco subclases de isoformas de p53 (isoformas α, isoformas β, isoformas TA, isoformas largas e isoformas cortas). Esta metodología nos permitió cuantificar proteínas partiendo de cantidades muy reducidas de muestra. Además, se analizó mediante PCR cuantitativa en tiempo real (qRT-PCR) la expresión a nivel de ARNm de estas mismas cinco subclases de isoformas. Las isoformas cortas también llamadas isoformas N-terminal truncadas carecen de los dos dominios de transactivación (TAD1 y TAD2) y de un trozo del dominio de unión al ADN (DBD), por lo que son distintas a las isoformas largas, no solo estructural sino funcionalmente también. Dentro de las llamadas isoformas TA, mientras que la isoforma canónica, TAp53α, posee el dominio de oligomerización y región básica completos, las isoformas TAp53β y TAp53γ son isoformas con el C-terminal truncado. Tal como ocurre con las isoformas cortas, las diferencias estructurales entre

estas isoformas TA determinan sus funciones diferenciales.

En líneas generales los resultados de la cuantificación de las isoformas de p53 a nivel proteico y de ARNm fueron bastante congruentes. No obstante, mientras que la qRT-PCR mostró expresión del gen *TP53* en todos los pacientes con MM, la proteína p53 fue detectada en aproximadamente el 70 % de las muestras de MM. Tanto a nivel de proteína como de ARNm, las isoformas largas y las cortas fueron las más y las menos expresadas, respectivamente.

Nuestros resultados también muestran que aquellos pacientes con elevada expresión de las isoformas cortas presentan mejor pronóstico que aquellos con nula o baja expresión, tanto a nivel de proteína como de ARNm. El hecho de que algunos trabajos hayan observado un impacto negativo de las isoformas cortas en la evolución de los pacientes[284,298,319–322] indica que la función de las isoformas cortas y su impacto en el pronóstico podría depender del tipo de cáncer, y evidencia también la necesidad de más estudios que profundicen en las funciones de las isoformas de p53 que no están definidas del todo.

Aunque la isoforma canónica TAp53α, estaba sobreexpresada en un mayor número de pacientes con MM que las isoformas TAp53β y TAp53γ, solamente estas últimas, y no la isoforma canónica, tuvieron una repercusión negativa en la supervivencia. Estos resultados son consistentes con algunos estudios previos[323,324], pero discrepan de otros[289,318]. ¿El hecho de que una isoforma se exprese mucho en un tumor respecto al tejido normal implicaría que puede tener una función importante en la patogenia de la enfermedad? Los estudios existentes son controvertidos pero refuerzan la hipótesis de que las funciones de las isoformas de p53 son muy dependientes del tipo y contexto celulares.

Uno de los hallazgos más destacados de nuestro estudio fue encontrar que los niveles de expresión proteica de las isoformas de p53 mejoraban significativamente la estratificación pronóstica basada en las alteraciones citogenéticas de los pacientes con MM. Así, dentro del grupo de pacientes de alto riesgo citogenético, la alta expresión de las isoformas cortas o la baja de las isoformas TA y largas identificó un grupo de pacientes con una supervivencia más larga.

Desde hace varios años se están desarrollando estrategias terapéuticas basadas en la regulación del proceso del *splicing* alternativo del pre-ARNm. Además, la secuenciación masiva de nueva generación ha permitido identificar genes de la maquinaria del *splicing* y del *spliceosoma* frecuentemente mutados, lo que les convierte en dianas atractivas para su regulación farmacológica. Nuestros resultados han mostrado que este importante proceso celular se encuentra desregulado diferencialmente entre el MM y la LCPp, y que las isoformas de p53 tienen valor pronóstico en los pacientes con MM. En este contexto, en el **tercer trabajo** nos planteamos investigar si la modulación farmacológica del *spliceosoma* puede servir como abordaje terapéutico en el MM.

Existe una amplia variedad de fármacos dirigidos contra componentes del *spliceosoma*, algunos de los cuales están siendo evaluados en ensayos clínicos, como el ZEN003694 y OTX105/MK-8628. Concretamente nos pareció interesante analizar la actividad antimieloma de la amilorida, un diurético comúnmente utilizado en el tratamiento de la hipertensión y el edema

producido por la insuficiencia cardiaca. Este fármaco ya había sido evaluado previamente en otras neoplasias en las que se había detectado que simultáneamente a su efecto antitumoral alteraba el *splicing* de distintos genes involucrados en apoptosis y proliferación celular[261,262]. En nuestro estudio utilizamos un panel de nueve líneas celulares de MM, un modelo murino de xenoinjerto, y muestras de MO de pacientes con MM, tanto de nuevo diagnóstico como refractarios o en recaída, para evaluar la actividad antimieloma de la amilorida así como su mecanismo de acción en el MM.

Los estudios *in vitro* en el panel de líneas celulares con dosis crecientes de la amilorida mostraron una potente actividad antimieloma. Este resultado fue observado también en los ensayos *ex vivo*, utilizando células mielomatosas de pacientes. La citotoxicidad producida por el fármaco fue específica de las células plasmáticas y no afectó al resto de poblaciones de la MO. Además, se detectó un efecto sinérgico significativo cuando se combinó la amilorida con distintos fármacos que tienen una actividad antimieloma contrastada, como la dexametasona, el melfalán, la lenalidomida y la pomalidomida. Adicionalmente, la eficacia de la amilorida *in vivo* fue evaluada en el modelo murino de xenoinjerto en el que se observó una elevada eficacia en combinación doble y triple con la dexametasona y con el melfalán. De forma llamativa, en nuestro estudio la amilorida no fue sinérgica con el bortezomib, lo cual podría limitar su uso en aquellos regímenes terapéuticos basados en el bortezomib. La actividad antitumoral de la amilorida se había descrito previamente en otros tipos de cánceres como la leucemia mieloide crónica[261], en el cáncer de páncreas[325] donde también se reportó su sinergismo con el erlotinib, y en cáncer de mama[326] y glioblastomas[327,328].

Aunque los estudios realizados en este trabajo doctoral demostraron la actividad antimieloma de la amilorida, teníamos especial interés en comprobar también si contribuía a este efecto la capacidad de la amilorida de modular el *spliceosoma*. Para profundizar en el mecanismo de acción de la amilorida en el MM se realizaron experimentos de RNA-Seq en dos líneas de MM, la más y la menos sensible al fármaco. El análisis del transcriptoma reveló que la amilorida producía una desregulación global de la maquinaria del *spliceosoma* y del proceso del *splicing*, afectando la expresión, a nivel génico y de isoformas, de proteínas cruciales en el ensamblaje del *spliceosoma* que participan en los pasos catalíticos del *splicing*, como *SNRPC*, *SF3A2*, *U2AF1*, *EIF4A3*, *SRSF1* y *SRSF10*. Para corroborar la inhibición de la maquinaria del *splicing* se analizó el tamaño y el número de los llamados focos o puntos nucleares (*nuclear speckles*) tras la exposición a la amilorida. Los *nuclear speckles* son estructuras nucleares enriquecidas de factores del *spliceosoma* que participan en el *splicing* del pre-ARNm[329]. El incremento del tamaño y de la intensidad de estos *nuclear speckles* se usa comúnmente como marcador de la alteración del *splicing*[330–333]. Los experimentos de microscopía fluorescente mostraron que la inhibición de la viabilidad celular en el MM tras la exposición a la amilorida ocurría de forma simultánea a la inhibición de la maquinaria del *splicing*, indicando que la citotoxicidad de la amilorida podría ser una consecuencia de la inhibición del *splicing*.

El análisis de la RNA-Seq también mostró que la vía de señalización de p53 fue una de

las más alteradas tras el tratamiento con la amilorida. Curiosamente las líneas celulares con p53 mutado también presentaron un incremento en la expresión de dianas de p53, igualmente que las líneas con p53 *wild-type*, pero al contrario de la línea celular con pérdida de *TP53*. Estos resultaron sugieren que la apoptosis inducida por la amilorida en las células de MM es dependiente de la activación de la ruta de p53, pero independiente del estatus mutacional de p53. Sin embargo, el hecho de que en la línea celular con deleción de 17p, JJN3, también se haya observado una disminución de la viabilidad celular sin afectar la expresión de las dianas de p53, implica que existen otros mecanismos adicionales independientes de p53 responsables de la actividad antimieloma de la amilorida, como pudiera ser la inhibición de la maquinaria del *splicing* demostrada en este trabajo. De hecho, los experimentos *ex vivo* en muestras de pacientes con MM refractarios y/o con deleción de p53, mostraron que la amilorida también induce una reducción significativa en la viabilidad de las células plasmáticas.

En resumen, los hallazgos encontrados en la presente tesis doctoral corroboran el interés de estudiar en el MM y otras gammapatías monoclonales el mecanismo del *splicing* del pre-ARNm y la expresión de las isoformas que genera. Por un lado, el análisis global de la expresión génica y de sus isoformas en las LCPp demuestra que su evolución clínica, tan distinta a la del MM, podría estar relacionada con las diferencias encontradas en el proceso de *splicing* alternativo del pre-ARNm entre las dos entidades. Por otro lado, el análisis más detallado de las isoformas proteicas que se generan en el procesamiento de un gen concreto, como es el supresor tumoral *TP53*, ha servido para revelar que existe una expresión diferencial de las isoformas proteicas de p53 entre las muestras de MM con influencia en la supervivencia de los pacientes. Y lo que es más importante, la expresión de algunas de estas isoformas permite identificar pacientes que siendo de alto riesgo citogenético tendrían una supervivencia similar a los pacientes con riesgo citogenético estándar. Finalmente, hemos demostrado la actividad antimieloma de la amilorida, un agente bien conocido por su actividad diurética y antihipertensiva. En estos momentos en que el reposicionamiento terapéutico está adquiriendo especial interés, este resultado podría ser considerado a la hora de plantear ensayos clínicos que incluyan la amilorida en el tratamiento de pacientes con MM en recaída o refractarios, especialmente los que tengan disfunciones del gen *TP53*.

Conclusiones

En relación con el capítulo 1, orientado al análisis del transcriptoma de la leucemia de células plasmáticas primaria (LCPp):

1) Las células plasmáticas (CPs) tumorales de la LCPp tienen un perfil transcriptómico significativamente diferente al observado en las CPs del MM, aun compartiendo las mismas alteraciones citogenéticas.

2) En la LCPp prevalece un patrón de infraexpresión de genes y de isoformas, en relación a lo observado en el MM.

3) El proceso de *splicing* del pre-ARNm y la maquinaria del *spliceosoma* son las vías biológicas significativamente más desreguladas entre la LCPp y el MM, tanto a nivel génico como a nivel de isoformas y de eventos de *splicing*.

En relación con el capítulo 2, centrado en el estudio de las isoformas de p53 a nivel de proteína y de ARNm en pacientes con MM:

1) Las isoformas largas de p53, y más concretamente las isoformas TA, presentan niveles altos de expresión en el MM, mientras que las isoformas cortas se expresan en un grupo muy reducido de pacientes con MM.

2) La expresión disminuida de las isoformas cortas de p53 y la expresión aumentada de las isoformas TAp53β/γ se asocian a una supervivencia más corta de los pacientes con MM menores de 65 años tratados con el esquema VRd (bortezomib, lenalidomida y dexametasona) y trasplante autólogo de progenitores hematopoyéticos.

3) La cuantificación de las isoformas de p53 en los pacientes con MM mejora la estratificación pronóstica basada en el riesgo citogenético. Los pacientes con alto riesgo citogenético y expresión elevada de las isoformas cortas o expresión disminuida de las isoformas TAp53β/γ, presentan una supervivencia más prolongada, comparable a la de los pacientes de riesgo estándar.

En relación con el capítulo 3, dirigido a la investigación de la modulación farmacológica del *spliceosoma* como posible abordaje terapéutico en el MM:

1) La amilorida presenta una potente actividad antimieloma *in vitro*, *ex vivo* e *in vivo*, sin provocar toxicidad sistémica en el modelo de ratón.

2) La reducción de la viabilidad de las líneas celulares de mieloma es simultánea a la inhibición de la maquinaria del *splicing*.

3) La apoptosis inducida por la amilorida en las células de mieloma depende de la activación de p53 y es independiente del estado mutacional de *TP53*.

4) La amilorida muestra un efecto antimieloma sinérgico con la dexametasona, el melfalán, la lenalidomida y la pomalidomida.

Referencias bibliográficas

Referencias bibliográficas

[1] R. A. Kyle, T. M. Therneau, S. V. Rajkumar, *et al.* Prevalence of monoclonal gammopathy of undetermined significance. *N. Engl. J. Med.*, 354(13): 1362–1369, 2006. [DOI: 10.1056/NEJMoa054494] [*PubMed* ID: 16571879]. [Citado en p. 3]

[2] S. V. Rajkumar, O. Landgren, y M. V. Mateos. Smoldering multiple myeloma. *Blood*, 125(20): 3069–3075, 2015. [*PubMed Central* ID: PMC4432003] [DOI: 10.1182/blood-2014-09-568899] [*PubMed* ID: 25838344]. [Citado en p. 3]

[3] R. A. Kyle, E. D. Remstein, T. M. Therneau, *et al.* Clinical course and prognosis of smoldering (asymptomatic) multiple myeloma. *N. Engl. J. Med.*, 356(25): 2582–2590, 2007. [DOI: 10.1056/NEJMoa070389] [*PubMed* ID: 17582068]. [Citado en p. 3]

[4] S. V. Rajkumar, G. Merlini, y J. F. San Miguel. Haematological cancer: Redefining myeloma. *Nat. Rev. Clin. Oncol.*, 9(9): 494–496, 2012. [DOI: 10.1038/nrclinonc.2012.128] [*PubMed* ID: 22850755]. [Citado en p. 3]

[5] M. Ho, A. Patel, C. Y. Goh, *et al.* Changing paradigms in diagnosis and treatment of monoclonal gammopathy of undetermined significance (MGUS) and smoldering multiple myeloma (SMM). *Leukemia*, 34(12): 3111–3125, 2020. [DOI: 10.1038/s41375-020-01051-x] [*PubMed* ID: 33046818]. [Citado en p. 3]

[6] S. V. Rajkumar, M. A. Dimopoulos, A. Palumbo, *et al.* International Myeloma Working Group updated criteria for the diagnosis of multiple myeloma. *Lancet Oncol.*, 15(12): e538–548, 2014. [DOI: 10.1016/S1470-2045(14)70442-5] [*PubMed* ID: 25439696]. [Citado en pp. 3 y 4]

[7] C. Fernández de Larrea, R. A. Kyle, B. G. Durie, *et al.* Plasma cell leukemia: consensus statement on diagnostic requirements, response criteria and treatment recommendations by the International Myeloma Working Group. *Leukemia*, 27(4): 780–791, 2013. [*PubMed Central* ID: PMC4112539] [DOI: 10.1038/leu.2012.336] [*PubMed* ID: 23288300]. [Citado en p. 5]

[8] P. Noel y R. A. Kyle. Plasma cell leukemia: an evaluation of response to therapy. *Am. J. Med.*, 83(6): 1062–1068, 1987. [DOI: 10.1016/0002-9343(87)90942-9] [*PubMed* ID: 3503574]. [Citado en p. 5]

[9] W. I. Gonsalves, S. V. Rajkumar, R. S. Go, *et al.* Trends in survival of patients with primary plasma cell leukemia: a population-based analysis. *Blood*, 124(6): 907–912, 2014. [*PubMed Central* ID: PMC4126330] [DOI: 10.1182/blood-2014-03-565051] [*PubMed* ID: 24957143]. [Citado en p. 5]

[10] R. E. Tiedemann, N. Gonzalez-Paz, R. A. Kyle, *et al.* Genetic aberrations and survival in plasma cell leukemia. *Leukemia*, 22(5): 1044–1052, 2008. [*PubMed Central* ID: PMC3893817] [DOI: 10.1038/leu.2008.4] [*PubMed* ID: 18216867]. [Citado en pp. 5, 7, 9, y 12]

[11] Renata Bezdekova, Tomas Jelinek, Romana Kralova, *et al.* Necessity of flow cytometry assessment of circulating plasma cells and its connection with clinical characteristics of primary and secondary plasma cell leukaemia. *Br. J. Haematol.*, 195(1): 95–107, 2021. [DOI: 10.1111/bjh.17713]. [Citado en p. 5]

[12] R. A. Kyle, J. E. Maldonado, y E. D. Bayrd. Plasma cell leukemia. Report on 17 cases. *Arch. Intern. Med.*, 133(5): 813–818, 1974. [DOI: 10.1001/archinte.133.5.813] [*PubMed* ID: 4821776]. [Citado en p. 5]

[13] G. An, X. Qin, C. Acharya, *et al.* Multiple myeloma patients with low proportion of circulating plasma cells had similar survival with primary plasma cell leukemia patients. *Ann. Hematol.*, 94(2): 257–264, 2015. [DOI: 10.1007/s00277-014-2211-0] [*PubMed* ID: 25231928]. [Citado en p. 5]

[14] M. Granell, X. Calvo, A. Garcia-Guiñón, *et al.* Prognostic impact of circulating plasma cells in patients with multiple myeloma: implications for plasma cell leukemia definition. *Haematologica*, 102(6): 1099–1104, 2017. [*PubMed Central* ID: PMC5451342] [DOI: 10.3324/haematol.2016.158303] [*PubMed* ID: 28255016]. [Citado en p. 5]

[15] W. I. Gonsalves, S. V. Rajkumar, A. Dispenzieri, *et al.* Quantification of circulating clonal plasma cells via multiparametric flow cytometry identifies patients with smoldering multiple myeloma at high risk of progression. *Leukemia*, 31(1): 130–135, 2017. [*PubMed Central* ID: PMC5244483] [DOI: 10.1038/leu.2016.205] [*PubMed* ID: 27457702]. [Citado en p. 5]

[16] C. Fernández de Larrea, R. Kyle, L. Rosiñol, *et al.* Primary plasma cell leukemia: consensus definition by the International Myeloma Working Group according to peripheral blood plasma cell percentage. *Blood Cancer J.*, 11(12): 192, 2021. [*PubMed Central* ID: PMC8640034] [DOI: 10.1038/s41408-021-00587-0] [*PubMed* ID: 34857730]. [Citado en p. 5]

[17] C. P. Chaulagain, M. J. Diacovo, A. Van, *et al.* Management of Primary Plasma Cell Leukemia Remains Challenging Even in the Era of Novel Agents. *Clin. Med. Insights Blood Disord.*, 14: 2634853521999389, 2021. [*PubMed Central* ID: PMC7917418] [DOI: 10.1177/2634853521999389] [*PubMed* ID: 33716516]. [Citado en p. 5]

[18] R. Mina, M. D'Agostino, C. Cerrato, *et al.* Plasma cell leukemia: update on biology and therapy. *Leuk. Lymphoma*, 58(7): 1538–1547, 2017. [DOI: 10.1080/10428194.2016.1250263] [*PubMed* ID: 27819179]. [Citado en p. 5]

[19] V. H. Jimenez-Zepeda y V. J. Dominguez-Martinez. Plasma cell leukemia: a highly aggressive monoclonal gammopathy with a very poor prognosis. *Int. J. Hematol.*, 89(3): 259–268, 2009. [DOI: 10.1007/s12185-009-0288-3] [*PubMed* ID: 19326058]. [Citado en p. 5]

[20] A. Jurczyszyn, J. Radocha, J. Davila, *et al.* Prognostic indicators in primary plasma cell leukaemia: a multicentre retrospective study of 117 patients. *Br. J. Haematol.*, 180(6): 831–839, 2018. [DOI: 10.1111/bjh.15092] [*PubMed* ID: 29315478]. [Citado en p. 5]

[21] G. Ramsingh, P. Mehan, J. Luo, *et al.* Primary plasma cell leukemia: a Surveillance, Epidemiology, and End Results database analysis between 1973 and 2004. *Cancer*, 115(24): 5734–5739, 2009. [DOI: 10.1002/cncr.24700] [*PubMed* ID: 19877113]. [Citado en p. 5]

[22] W. M. Kuehl y P. L. Bergsagel. Multiple myeloma: evolving genetic events and host interactions. *Nat. Rev. Cancer*, 2(3): 175–187, 2002. [DOI: 10.1038/nrc746] [*PubMed* ID: 11990854]. [Citado en p. 5]

[23] B. A. Walker, C. P. Wardell, A. Murison, *et al.* APOBEC family mutational signatures are associated with poor prognosis translocations in multiple myeloma. *Nat. Commun.*, 6: 6997, 2015. [*PubMed Central* ID: PMC4568299] [DOI: 10.1038/ncomms7997] [*PubMed* ID: 25904160]. [Citado en pp. 6 y 10]

[24] G. J. Morgan, B. A. Walker, y F. E. Davies. The genetic architecture of multiple myeloma. *Nat. Rev. Cancer*, 12(5): 335–348, 2012. [DOI: 10.1038/nrc3257] [*PubMed* ID: 22495321]. [Citado en pp. 6 y 11]

[25] W. J. Chng, R. P. Ketterling, y R. Fonseca. Analysis of genetic abnormalities provides insights into genetic evolution of hyperdiploid myeloma. *Genes Chromosomes Cancer*, 45(12): 1111–1120, 2006. [DOI: 10.1002/gcc.20375] [*PubMed* ID: 16955468]. [Citado en pp. 6 y 7]

[26] H. Avet-Loiseau, M. Attal, L. Campion, *et al.* Long-term analysis of the IFM 99 trials for myeloma: cytogenetic abnormalities [t(4;14), del(17p), 1q gains] play a major role in defining long-term survival. *J. Clin. Oncol.*, 30(16): 1949–1952, 2012. [DOI: 10.1200/JCO.2011.36.5726] [*PubMed* ID: 22547600]. [Citado en p. 7]

[27] G. An, Y. Xu, L. Shi, *et al.* Chromosome 1q21 gains confer inferior outcomes in multiple myeloma treated with bortezomib but copy number variation and percentage of plasma cells involved have no additional prognostic value. *Haematologica*, 99(2): 353–359, 2014. [*PubMed Central* ID: PMC3912967] [DOI: 10.3324/haematol.2013.088211] [*PubMed* ID: 24213147]. [Citado en p. 7]

[28] R. Fonseca, S. A. Van Wier, W. J. Chng, *et al.* Prognostic value of chromosome 1q21 gain by fluorescent in situ hybridization and increase CKS1B expression in myeloma. *Leukemia*, 20(11): 2034–2040, 2006. [DOI: 10.1038/sj.leu.2404403] [*PubMed* ID: 17024118]. [Citado en p. 7]

[29] L. Shi, S. Wang, M. Zangari, *et al.* Over-expression of CKS1B activates both MEK/ERK and JAK/STAT3 signaling pathways and promotes myeloma cell drug-resistance. *Oncotarget*, 1(1): 22–33, 2010. [*PubMed Central* ID: PMC2949973] [DOI: 10.18632/oncotarget.105] [*PubMed* ID: 20930946]. [Citado en p. 7]

[30] S. P. Treon, P. Maimonis, D. Bua, *et al.* Elevated soluble MUC1 levels and decreased anti-MUC1 antibody levels in patients with multiple myeloma. *Blood*, 96(9): 3147–3153, 2000. [*PubMed* ID: 11049996]. [Citado en p. 7]

[31] S. Legartova, J. Krejci, A. Harnicarova, *et al.* Nuclear topography of the 1q21 genomic region and Mcl-1 protein levels associated with pathophysiology of multiple myeloma. *Neoplasma*, 56(5): 404–413, 2009. [DOI: 10.4149/neo_2009_05_404] [*PubMed* ID: 19580342]. [Citado en p. 7]

[32] J. D. Shaughnessy, P. Qu, S. Usmani, *et al.* Pharmacogenomics of bortezomib test-dosing identifies hyperexpression of proteasome genes, especially PSMD4, as novel high-risk feature in myeloma treated with Total Therapy 3. *Blood*, 118(13): 3512–3524, 2011. [*PubMed Central* ID: PMC3186329] [DOI: 10.1182/blood-2010-12-328252] [*PubMed* ID: 21628408]. [Citado en p. 7]

[33] J. Inoue, T. Otsuki, A. Hirasawa, *et al.* Overexpression of PDZK1 within the 1q12-q22 amplicon is likely to be associated with drug-resistance phenotype in multiple myeloma. *Am. J. Pathol.*, 165(1): 71–81, 2004. [*PubMed Central* ID: PMC1618545] [DOI: 10.1016/S0002-9440(10)63276-2] [*PubMed* ID: 15215163]. [Citado en p. 7]

[34] B. A. Walker, P. E. Leone, L. Chiecchio, *et al.* A compendium of myeloma-associated chromosomal copy number abnormalities and their prognostic value. *Blood*, 116(15): 56–65, 2010. [DOI: 10.1182/blood-2010-04-279596] [*PubMed* ID: 20616218]. [Citado en p. 7]

[35] K. D. Boyd, F. M. Ross, B. A. Walker, *et al.* Mapping of chromosome 1p deletions in myeloma identifies FAM46C at 1p12 and CDKN2C at 1p32.3 as being genes in regions associated with adverse survival. *Clin. Cancer Res.*, 17(24): 7776–7784, 2011. [*PubMed Central* ID: PMC5751883] [DOI: 10.1158/1078-0432.CCR-11-1791] [*PubMed* ID: 21994415]. [Citado en p. 7]

[36] L. López-Corral, M. E. Sarasquete, S. Beà, *et al.* SNP-based mapping arrays reveal high genomic complexity in monoclonal gammopathies, from MGUS to myeloma status. *Leukemia*, 26(12): 2521–2529, 2012. [DOI: 10.1038/leu.2012.128] [*PubMed* ID: 22565645]. [Citado en p. 7]

[37] B. Hebraud, X. Leleu, V. Lauwers-Cances, *et al.* Deletion of the 1p32 region is a major independent prognostic factor in young patients with myeloma: the IFM experience on 1195 patients. *Leukemia*, 28(3): 675–679, 2014. [*PubMed Central* ID: PMC6140327] [DOI: 10.1038/leu.2013.225] [*PubMed* ID: 23892719]. [Citado en p. 7]

[38] B. A. Walker, K. Mavrommatis, C. P. Wardell, *et al.* Identification of novel mutational drivers reveals oncogene dependencies in multiple myeloma. *Blood*, 132(6): 587–597, 2018. [*PubMed Central* ID: PMC6097138] [DOI: 10.1182/blood-2018-03-840132] [*PubMed* ID: 29884741]. [Citado en p. 7]

[39] H. Avet-Louseau, A. Daviet, S. Sauner, y R. Bataille. Chromosome 13 abnormalities in multiple myeloma are mostly monosomy 13. *Br. J. Haematol.*, 111(4): 1116–1117, 2000. [DOI: 10.1046/j.1365-2141.2000.02488.x] [*PubMed* ID: 11227093]. [Citado en p. 7]

[40] R. Fonseca, M. M. Oken, D. Harrington, *et al.* Deletions of chromosome 13 in multiple myeloma identified by interphase FISH usually denote large deletions of the q arm or monosomy. *Leukemia*, 15(6): 981–986, 2001. [DOI: 10.1038/sj.leu.2402125] [*PubMed* ID: 11417487]. [Citado en p. 7]

[41] E. M. Boyle, S. Deshpande, R. Tytarenko, *et al.* The molecular make up of smoldering myeloma highlights the evolutionary pathways leading to multiple myeloma. *Nat. Commun.*, 12(1): 293, 2021. [*PubMed Central* ID: PMC7804406] [DOI: 10.1038/s41467-020-20524-2] [*PubMed* ID: 33436579]. [Citado en p. 7]

[42] W. J. Chng, S. A. Van Wier, G. J. Ahmann, *et al.* A validated FISH trisomy index demonstrates the hyperdiploid and nonhyperdiploid dichotomy in MGUS. *Blood*, 106(6): 2156–2161, 2005. [*PubMed Central* ID: PMC1895145] [DOI: 10.1182/blood-2005-02-0761] [*PubMed* ID: 15920009]. [Citado en p. 7]

[43] M. A. Chapman, M. S. Lawrence, J. J. Keats, *et al.* Initial genome sequencing and analysis of multiple myeloma. *Nature*, 471(7339): 467–472, 2011. [*PubMed Central* ID: PMC3560292] [DOI: 10.1038/nature09837] [*PubMed* ID: 21430775]. [Citado en p. 7]

[44] N. Bolli, H. Avet-Loiseau, D. C. Wedge, *et al.* Heterogeneity of genomic evolution and mutational profiles in multiple myeloma. *Nat. Commun.*, 5: 2997, 2014. [*PubMed Central* ID: PMC3905727] [DOI: 10.1038/ncomms3997] [*PubMed* ID: 24429703]. [Citado en p. 7]

[45] V. Yellapantula, M. Hultcrantz, E. H. Rustad, *et al.* Comprehensive detection of recurring genomic abnormalities: a targeted sequencing approach for multiple myeloma. *Blood Cancer J.*, 9(12): 101, 2019. [*PubMed Central* ID: PMC6906304] [DOI: 10.1038/s41408-019-0264-y] [*PubMed* ID: 31827071]. [Citado en p. 7]

[46] J. G. Lohr, P. Stojanov, S. L. Carter, *et al.* Widespread genetic heterogeneity in multiple myeloma: implications for targeted therapy. *Cancer Cell*, 25(1): 91–101, 2014. [*PubMed Central* ID: PMC4241387] [DOI: 10.1016/j.ccr.2013.12.015] [*PubMed* ID: 24434212]. [Citado en p. 7]

[47] B. A. Walker, E. M. Boyle, C. P. Wardell, *et al.* Mutational Spectrum, Copy Number Changes, and Outcome: Results of a Sequencing Study of Patients With Newly Diagnosed Myeloma. *J. Clin. Oncol.*, 33(33): 3911–3920, 2015. [*PubMed Central* ID: PMC6485456] [DOI: 10.1200/JCO.2014.59.1503] [*PubMed* ID: 26282654]. [Citado en p. 7]

[48] B. A. Walker, K. Mavrommatis, C. P. Wardell, *et al.* A high-risk, Double-Hit, group of newly diagnosed myeloma identified by genomic analysis. *Leukemia*, 33(1): 159–170, 2019. [*PubMed Central* ID: PMC6326953] [DOI: 10.1038/s41375-018-0196-8] [*PubMed* ID: 29967379]. [Citado en p. 7]

[49] A. B. Herrero, D. Quwaider, L. A. Corchete, *et al.* FAM46C controls antibody production by the polyadenylation of immunoglobulin mRNAs and inhibits cell migration in multiple myeloma. *J. Cell Mol. Med.*, 24(7): 4171–4182, 2020. [*PubMed Central* ID: PMC7171423] [DOI: 10.1111/jcmm.15078] [*PubMed* ID: 32141701]. [Citado en p. 8]

[50] S. Manier, K. Z. Salem, J. Park, *et al.* Genomic complexity of multiple myeloma and its clinical implications. *Nat. Rev. Clin. Oncol.*, 14(2): 100–113, 2017. [DOI: 10.1038/nrclinonc.2016.122] [*PubMed* ID: 27531699]. [Citado en pp. 8, 10, y 11]

[51] P. L. Bergsagel, W. M. Kuehl, F. Zhan, *et al.* Cyclin D dysregulation: an early and unifying pathogenic event in multiple myeloma. *Blood*, 106(1): 296–303, 2005. [*PubMed Central* ID: PMC1895118] [DOI: 10.1182/blood-2005-01-0034] [*PubMed* ID: 15755896]. [Citado en p. 8]

[52] F. Zhan, Y. Huang, S. Colla, *et al.* The molecular classification of multiple myeloma. *Blood*, 108(6): 2020–2028, 2006. [*PubMed Central* ID: PMC1895543] [DOI: 10.1182/blood-2005-11-013458] [*PubMed* ID: 16728703]. [Citado en pp. 8, 9, y 37]

[53] P. Liebisch, C. Wendl, A. Wellmann, *et al.* High incidence of trisomies 1q, 9q, and 11q in multiple myeloma: results from a comprehensive molecular cytogenetic analysis. *Leukemia*, 17(12): 2535–2537, 2003. [DOI: 10.1038/sj.leu.2403153] [*PubMed* ID: 14523465]. [Citado en p. 9]

[54] T. Guglielmelli, E. Giugliano, S. Cappia, *et al.* Frequency and distribution of trisomy 11 in multiple myeloma patients: relation with overexpression of CCND1 and t(11;14). *Cancer Genet. Cytogenet.*, 173(1): 51–56, 2007. [DOI: 10.1016/j.cancergencyto.2006.09.017] [*PubMed* ID: 17284370]. [Citado en p. 9]

[55] I. Misiewicz-Krzeminska, M. E. Sarasquete, C. Vicente-Dueñas, *et al.* Post-transcriptional Modifications Contribute to the Upregulation of Cyclin D2 in Multiple Myeloma. *Clin. Cancer Res.*, 22(1): 207–217, 2016. [DOI: 10.1158/1078-0432.CCR-14-2796] [*PubMed* ID: 26341922]. [Citado en p. 9]

[56] H. Handa, Y. Murakami, R. Ishihara, *et al.* The Role and Function of microRNA in the Pathogenesis of Multiple Myeloma. *Cancers (Basel)*, 11(11), 2019. [*PubMed Central* ID: PMC6896016] [DOI: 10.3390/cancers11111738] [*PubMed* ID: 31698726]. [Citado en p. 9]

[57] I. Misiewicz-Krzeminska, P. Krzeminski, L. A. Corchete, *et al.* Factors Regulating microRNA Expression and Function in Multiple Myeloma. *Noncoding RNA*, 5(1), 2019. [*PubMed Central* ID: PMC6468559] [DOI: 10.3390/ncrna5010009] [*PubMed* ID: 30259358]. [Citado en p. 9]

[58] N. C. Gutiérrez, M. E. Sarasquete, I. Misiewicz-Krzeminska, *et al.* Deregulation of microRNA expression in the different genetic subtypes of multiple myeloma and correlation with gene expression profiling. *Leukemia*, 24(3): 629–637, 2010. [DOI: 10.1038/leu.2009.274] [*PubMed* ID: 20054351]. [Citado en p. 9]

[59] E. A. Rojas y N. C. Gutiérrez. Genomics of Plasma Cell Leukemia. *Cancers (Basel)*, 14(6), 2022. [*PubMed Central* ID: PMC8946729] [DOI: 10.3390/cancers14061594] [*PubMed* ID: 35326746]. [Citado en p. 9]

[60] N. C. Gutiérrez, J. M. Hernández, J. L. García, *et al.* Differences in genetic changes between multiple myeloma and plasma cell leukemia demonstrated by comparative genomic hybridization. *Leukemia*, 15(5): 840–845, 2001. [DOI: 10.1038/sj.leu.2402116] [*PubMed* ID: 11368447]. [Citado en p. 9]

[61] L. Mosca, P. Musto, K. Todoerti, *et al.* Genome-wide analysis of primary plasma cell leukemia identifies recurrent imbalances associated with changes in transcriptional profiles. *Am. J. Hematol.*, 88(1): 16–23, 2013. [DOI: 10.1002/ajh.23339] [*PubMed* ID: 23044976]. [Citado en pp. 9 y 105]

[62] H. Chang, X. Qi, J. Yeung, *et al.* Genetic aberrations including chromosome 1 abnormalities and clinical features of plasma cell leukemia. *Leuk Res.*, 33(2): 259–262, 2009. [DOI: 10.1016/j.leukres.2008.06.027] [*PubMed* ID: 18676019]. [Citado en pp. 9 y 12]

[63] T. Yu, Y. Xu, G. An, *et al.* Primary Plasma Cell Leukemia: Real-World Retrospective Study of 46 Patients From a Single-Center Study in China. *Clin. Lymphoma Myeloma Leuk.*, 20(10): e652–e659, 2020. [DOI: 10.1016/j.clml.2020.05.014] [*PubMed* ID: 32624447]. [Citado en p. 9]

[64] C. Schinke, E. M. Boyle, C. Ashby, *et al.* Genomic analysis of primary plasma cell leukemia reveals complex structural alterations and high-risk mutational patterns. *Blood Cancer J.*, 10(6): 70, 2020. [*PubMed Central* ID: PMC7303180] [DOI: 10.1038/s41408-020-0336-z] [*PubMed* ID: 32555163]. [Citado en p. 9]

[65] T. Cazaubiel, X. Leleu, A. Perrot, *et al.* Primary plasma cell leukemias displaying t(11;14) have specific genomic, transcriptional, and clinical features. *Blood*, 139(17): 2666–2672, 2022. [DOI: 10.1182/blood.2021014968] [*PubMed* ID: 35171994]. [Citado en pp. 9 y 12]

[66] H. Avet-Loiseau, A. Daviet, C. Brigaudeau, *et al.* Cytogenetic, interphase, and multicolor fluorescence in situ hybridization analyses in primary plasma cell leukemia: a study of 40 patients at diagnosis, on behalf of the Intergroupe Francophone du Myélome and the Groupe Français de Cytogénétique Hématologique. *Blood*, 97(3): 822–825, 2001. [DOI: 10.1182/blood.v97.3.822] [*PubMed* ID: 11157506]. [Citado en p. 9]

[67] L. Chiecchio, G. P. Dagrada, H. E. White, *et al.* Frequent upregulation of MYC in plasma cell leukemia. *Genes Chromosomes Cancer*, 48(7): 624–636, 2009. [DOI: 10.1002/gcc.20670] [*PubMed* ID: 19396865]. [Citado en p. 9]

[68] K. Todoerti, E. Taiana, N. Puccio, *et al.* Transcriptomic Analysis in Multiple Myeloma and Primary Plasma Cell Leukemia with t(11;14) Reveals Different Expression Patterns with Biological Implications in Venetoclax Sensitivity. *Cancers (Basel)*, 13(19), 2021. [*PubMed Central* ID: PMC8508148] [DOI: 10.3390/cancers13194898] [*PubMed* ID: 34638381]. [Citado en p. 9]

[69] H. Avet-Loiseau, F. Gerson, F. Magrangeas, *et al.* Rearrangements of the c-myc oncogene are present in 15human multiple myeloma tumors. *Blood*, 98(10): 3082–3086, 2001. [DOI: 10.1182/blood.v98.10.3082] [*PubMed* ID: 11698294]. [Citado en pp. 9 y 12]

[70] S. Bezieau, M. C. Devilder, H. Avet-Loiseau, *et al.* High incidence of N and K-Ras activating mutations in multiple myeloma and primary plasma cell leukemia at diagnosis. *Hum. Mutat.*, 18(3): 212–224, 2001. [DOI: 10.1002/humu.1177] [*PubMed* ID: 11524732]. [Citado en p. 9]

[71] Titouan Cazaubiel, Laure Buisson, Sabrina Maheo, *et al.* The Genomic and Transcriptomic Landscape of Plasma Cell Leukemia. *Blood*, 136: 48–49, 2020. [DOI: 10.1182/blood-2020-139340]. [Citado en pp. 9, 10, y 12]

[72] M. Lionetti, M. Barbieri, M. Manzoni, *et al.* Molecular spectrum of TP53 mutations in plasma cell dyscrasias by next generation sequencing: an Italian cohort study and overview of the literature. *Oncotarget*, 7(16): 21353–21361, 2016. [*PubMed Central* ID: PMC5008290] [DOI: 10.18632/oncotarget.7241] [*PubMed* ID: 26870891]. [Citado en p. 9]

[73] I. Cifola, M. Lionetti, E. Pinatel, *et al.* Whole-exome sequencing of primary plasma cell leukemia discloses heterogeneous mutational patterns. *Oncotarget*, 6(19): 17543–17558, 2015. [*PubMed Central* ID: PMC4627327] [DOI: 10.18632/oncotarget.4028] [*PubMed* ID: 26046463]. [Citado en p. 9]

[74] J. R. Mikhael, D. Dingli, V. Roy, *et al.* Management of newly diagnosed symptomatic multiple myeloma: updated Mayo Stratification of Myeloma and Risk-Adapted Therapy (mSMART) consensus guidelines 2013. *Mayo. Clin. Proc.*, 88(4): 360–376, 2013. [DOI: 10.1016/j.mayocp.2013.01.019] [*PubMed* ID: 23541011]. [Citado en p. 10]

[75] H. Avet-Loiseau, F. Malard, L. Campion, *et al.* Translocation t(14;16) and multiple myeloma: is it really an independent prognostic factor? *Blood*, 117(6): 2009–2011, 2011. [DOI: 10.1182/blood-2010-07-295105] [*PubMed* ID: 20962323]. [Citado en p. 10]

[76] R. Fonseca, P. L. Bergsagel, J. Drach, *et al.* International Myeloma Working Group molecular classification of multiple myeloma: spotlight review. *Leukemia*, 23(12): 2210–2221, 2009. [*PubMed Central* ID: PMC2964268] [DOI: 10.1038/leu.2009.174] [*PubMed* ID: 19798094]. [Citado en p. 10]

[77] H. Avet-Loiseau, M. Attal, P. Moreau, *et al.* Genetic abnormalities and survival in multiple myeloma: the experience of the Intergroupe Francophone du Myélome. *Blood*, 109(8): 3489–3495, 2007. [DOI: 10.1182/blood-2006-08-040410] [*PubMed* ID: 17209057]. [Citado en p. 10]

[78] R. Fonseca, E. Blood, M. Rue, *et al.* Clinical and biologic implications of recurrent genomic aberrations in myeloma. *Blood*, 101(11): 4569–4575, 2003. [DOI: 10.1182/blood-2002-10-3017] [*PubMed* ID: 12576322]. [Citado en p. 10]

[79] J. Drach, J. Ackermann, E. Fritz, *et al.* Presence of a p53 gene deletion in patients with multiple myeloma predicts for short survival after conventional-dose chemotherapy. *Blood*, 92(3): 802–809, 1998. [*PubMed* ID: 9680348]. [Citado en p. 10]

[80] J. Ouyang, X. Gou, Y. Ma, *et al.* Prognostic value of 1p deletion for multiple myeloma: a meta-analysis. *Int. J. Lab. Hematol.*, 36(5): 555–565, 2014. [DOI: 10.1111/ijlh.12189] [*PubMed* ID: 24460694]. [Citado en p. 10]

[81] T. M. Schmidt, B. G. Barwick, N. Joseph, *et al.* Gain of Chromosome 1q is associated with early progression in multiple myeloma patients treated with lenalidomide, bortezomib, and dexamethasone. *Blood Cancer J.*, 9(12): 94, 2019. [*PubMed Central* ID: PMC6877577] [DOI: 10.1038/s41408-019-0254-0] [*PubMed* ID: 31767829]. [Citado en p. 10]

[82] I. Hanamura. Gain/Amplification of Chromosome Arm 1q21 in Multiple Myeloma. *Cancers (Basel)*, 13(2), 2021. [*PubMed Central* ID: PMC7827173] [DOI: 10.3390/cancers13020256] [*PubMed* ID: 33445467]. [Citado en p. 10]

[83] S. K. Kumar, V. Rajkumar, R. A. Kyle, *et al.* Multiple myeloma. *Nat. Rev. Dis. Primers*, 3: 17046, 2017. [DOI: 10.1038/nrdp.2017.46] [*PubMed* ID: 28726797]. [Citado en p. 10]

[84] K. D. Boyd, F. M. Ross, L. Chiecchio, *et al.* A novel prognostic model in myeloma based on co-segregating adverse FISH lesions and the ISS: analysis of patients treated in the MRC Myeloma IX trial. *Leukemia*, 26(2): 349–355, 2012. [*PubMed Central* ID: PMC4545515] [DOI: 10.1038/leu.2011.204] [*PubMed* ID: 21836613]. [Citado en p. 12]

[85] C. S. Mitsiades, N. S. Mitsiades, N. C. Munshi, *et al.* The role of the bone microenvironment in the pathophysiology and therapeutic management of multiple myeloma: interplay of growth factors, their receptors and stromal interactions. *Eur. J. Cancer.*, 42(11): 1564–1573, 2006. [DOI: 10.1016/j.ejca.2005.12.025] [*PubMed* ID: 16765041]. [Citado en p. 12]

[86] S. K. Kumar, S. V. Rajkumar, A. Dispenzieri, *et al.* Improved survival in multiple myeloma and the impact of novel therapies. *Blood*, 111(5): 2516–2520, 2008. [*PubMed Central* ID: PMC2254544] [DOI: 10.1182/blood-2007-10-116129] [*PubMed* ID: 17975015]. [Citado en pp. 12 y 13]

[87] M. A. Dimopoulos, S. Delimpasi, E. Katodritou, *et al.* Significant improvement in the survival of patients with multiple myeloma presenting with severe renal impairment after the introduction of novel agents. *Ann. Oncol.*, 25(1): 195–200, 2014. [DOI: 10.1093/annonc/mdt483] [*PubMed* ID: 24356630]. [Citado en p. 12]

[88] R. Fonseca, S. Abouzaid, M. Bonafede, *et al.* Trends in overall survival and costs of multiple myeloma, 2000-2014. *Leukemia*, 31(9): 1915–1921, 2017. [*PubMed Central* ID: PMC5596206] [DOI: 10.1038/leu.2016.380] [*PubMed* ID: 28008176]. [Citado en p. 12]

[89] C. Röllig, S. Knop, y M. Bornhäuser. Multiple myeloma. *Lancet*, 385(9983): 2197–2208, 2015. [DOI: 10.1016/S0140-6736(14)60493-1] [*PubMed* ID: 25540889]. [Citado en p. 13]

[90] L. W. Huang, W. Bacon, C. Cirrincione, *et al.* Efficacy and safety of high-dose chemotherapy with autologous stem cell transplantation in senior versus younger adults with newly diagnosed multiple myeloma. *Hematol. Oncol.*, 35(4): 752–759, 2017. [*PubMed Central* ID: PMC5949235] [DOI: 10.1002/hon.2379] [*PubMed* ID: 28105753]. [Citado en p. 13]

[91] C. Straka, P. Liebisch, H. Salwender, *et al.* Autotransplant with and without induction chemotherapy in older multiple myeloma patients: long-term outcome of a randomized trial. *Haematologica*, 101(11): 1398–1406, 2016. [*PubMed Central* ID: PMC5394869] [DOI: 10.3324/haematol.2016.151860] [*PubMed* ID: 27662018]. [Citado en p. 13]

[92] H. W. Auner, L. Garderet, y N. Kröger. Autologous haematopoietic cell transplantation in elderly patients with multiple myeloma. *Br. J. Haematol.*, 171(4): 453–462, 2015. [DOI: 10.1111/bjh.13608] [*PubMed* ID: 26213240]. [Citado en p. 13]

[93] S. K. Kumar, A. Dispenzieri, M. Q. Lacy, *et al.* Continued improvement in survival in multiple myeloma: changes in early mortality and outcomes in older patients. *Leukemia*, 28(5): 1122–1128, 2014. [*PubMed Central* ID: PMC4000285] [DOI: 10.1038/leu.2013.313] [*PubMed* ID: 24157580]. [Citado en p. 13]

[94] P. Moreau, S. K. Kumar, J. San Miguel, *et al.* Treatment of relapsed and refractory multiple myeloma: recommendations from the International Myeloma Working Group. *Lancet Oncol.*, 22(3): e105–e118, 2021. [DOI: 10.1016/S1470-2045(20)30756-7] [*PubMed* ID: 33662288]. [Citado en p. 13]

[95] P. J. Teoh y W. J. Chng. CAR T-cell therapy in multiple myeloma: more room for improvement. *Blood Cancer J.*, 11(4): 84, 2021. [*PubMed Central* ID: PMC8085238] [DOI: 10.1038/s41408-021-00469-5] [*PubMed* ID: 33927192]. [Citado en pp. 13 y 16]

[96] Y. Yang, Y. Li, H. Gu, *et al.* Emerging agents and regimens for multiple myeloma. *J. Hematol. Oncol.*, 13(1): 150, 2020. [*PubMed Central* ID: PMC7654052] [DOI: 10.1186/s13045-020-00980-5] [*PubMed* ID: 33168044]. [Citado en p. 13]

[97] A. J. Cowan, D. J. Green, M. Kwok, *et al.* Diagnosis and Management of Multiple Myeloma: A Review. *JAMA*, 327(5): 464–477, 2022. [DOI: 10.1001/jama.2022.0003] [*PubMed* ID: 35103762]. [Citado en p. 13]

[98] P. Moreau, R. Misbahi, N. Milpied, *et al.* Long-term results (12 years) of high-dose therapy in 127 patients with de novo multiple myeloma. *Leukemia*, 16(9): 1838–1843, 2002. [DOI: 10.1038/sj.leu.2402613] [*PubMed* ID: 12200701]. [Citado en p. 13]

[99] T. J. McElwain y R. L. Powles. High-dose intravenous melphalan for plasma-cell leukaemia and myeloma. *Lancet*, 2(8354): 822–824, 1983. [DOI: 10.1016/s0140-6736(83)90739-0] [*PubMed* ID: 6137651]. [Citado en p. 13]

[100] R. Alexanian, B. Barlogie, y D. Dixon. High-dose glucocorticoid treatment of resistant myeloma. *Ann. Intern. Med.*, 105(1): 8–11, 1986. [DOI: 10.7326/0003-4819-105-1-8] [*PubMed* ID: 3717812]. [Citado en p. 13]

[101] K. Zervas, M. A. Dimopoulos, E. Hatzicharissi, *et al.* Primary treatment of multiple myeloma with thalidomide, vincristine, liposomal doxorubicin and dexamethasone (T-VAD doxil): a phase II multicenter study. *Ann. Oncol.*, 15(1): 134–138, 2004. [DOI: 10.1093/annonc/mdh026] [*PubMed* ID: 14679133]. [Citado en p. 13]

[102] N. Grzasko, G. Charlinski, M. Morawska, *et al.* Bendamustine-Based Regimens as Salvage Therapy in Refractory/Relapsed Multiple Myeloma Patients: A Retrospective Real-Life Analysis by the Polish Myeloma Group. *J. Clin. Med.*, 10(23), 2021. [*PubMed Central* ID: PMC8658377] [DOI: 10.3390/jcm10235504] [*PubMed* ID: 34884206]. [Citado en p. 13]

[103] F. Gay, A. Günther, M. Offidani, *et al.* Carfilzomib, bendamustine, and dexamethasone in patients with advanced multiple myeloma: The EMN09 phase 1/2 study of the European Myeloma Network. *Cancer*, 127(18): 3413–3421, 2021. [DOI: 10.1002/cncr.33647] [*PubMed* ID: 34181755]. [Citado en p. 13]

[104] C. R. Berkers, M. Verdoes, E. Lichtman, *et al.* Activity probe for in vivo profiling of the specificity of proteasome inhibitor bortezomib. *Nat. Methods*, 2(5): 357–362, 2005. [DOI: 10.1038/nmeth759] [*PubMed* ID: 15846363]. [Citado en p. 13]

[105] D. Chauhan, Z. Tian, B. Zhou, *et al.* In vitro and in vivo selective antitumor activity of a novel orally bioavailable proteasome inhibitor MLN9708 against multiple myeloma cells. *Clin. Cancer Res.*, 17(16): 5311–5321, 2011. [*PubMed Central* ID: PMC3156932] [DOI: 10.1158/1078-0432.CCR-11-0476] [*PubMed* ID: 21724551]. [Citado en p. 13]

[106] D. J. Kuhn, Q. Chen, P. M. Voorhees, *et al.* Potent activity of carfilzomib, a novel, irreversible inhibitor of the ubiquitin-proteasome pathway, against preclinical models of multiple myeloma. *Blood*, 110(9): 3281–3290, 2007. [*PubMed Central* ID: PMC2200918] [DOI: 10.1182/blood-2007-01-065888] [*PubMed* ID: 17591945]. [Citado en p. 13]

[107] S. Ito. Proteasome Inhibitors for the Treatment of Multiple Myeloma. *Cancers (Basel)*, 12(2), 2020. [*PubMed Central* ID: PMC7072336] [DOI: 10.3390/cancers12020265] [*PubMed* ID: 31979059]. [Citado en p. 13]

[108] P. Moreau, P. G. Richardson, M. Cavo, *et al.* Proteasome inhibitors in multiple myeloma: 10 years later. *Blood*, 120(5): 947–959, 2012. [*PubMed Central* ID: PMC4123429] [DOI: 10.1182/blood-2012-04-403733] [*PubMed* ID: 22645181]. [Citado en p. 13]

[109] S. P. E. Jayaweera, S. P. Wanigasinghe Kanakanamge, D. Rajalingam, y G. N. Silva. Carfilzomib: A Promising Proteasome Inhibitor for the Treatment of Relapsed and Refractory Multiple Myeloma. *Front. Oncol.*, 11: 740796, 2021. [*PubMed Central* ID: PMC8631731] [DOI: 10.3389/fonc.2021.740796] [*PubMed* ID: 34858819]. [Citado en p. 13]

[110] K. Lagrue, A. Carisey, D. J. Morgan, *et al.* Lenalidomide augments actin remodeling and lowers NK-cell activation thresholds. *Blood*, 126(1): 50–60, 2015. [*PubMed Central* ID: PMC4551357] [DOI: 10.1182/blood-2015-01-625004] [*PubMed* ID: 26002964]. [Citado en p. 14]

[111] R. LeBlanc, T. Hideshima, L. P. Catley, *et al.* Immunomodulatory drug costimulates T cells via the B7-CD28 pathway. *Blood*, 103(5): 1787–1790, 2004. [DOI: 10.1182/blood-2003-02-0361] [*PubMed* ID: 14512311]. [Citado en p. 14]

[112] S. Andhavarapu y V. Roy. Immunomodulatory drugs in multiple myeloma. *Expert Rev. Hematol.*, 6(1): 69–82, 2013. [DOI: 10.1586/ehm.12.62] [*PubMed* ID: 23373782]. [Citado en p. 14]

[113] A. Lopez-Girona, D. Mendy, T. Ito, *et al.* Cereblon is a direct protein target for immunomodulatory and antiproliferative activities of lenalidomide and pomalidomide. *Leukemia*, 26(11): 2326–2335, 2012. [*PubMed Central* ID: PMC3496085] [DOI: 10.1038/leu.2012.119] [*PubMed* ID: 22552008]. [Citado en p. 14]

[114] T. Ito y H. Handa. Cereblon and its downstream substrates as molecular targets of immunomodulatory drugs. *Int. J. Hematol.*, 104(3): 293–299, 2016. [DOI: 10.1007/s12185-016-2073-4] [*PubMed* ID: 27460676]. [Citado en p. 14]

[115] G. Charlinski, D. H. Vesole, y A. Jurczyszyn. Rapid Progress in the Use of Immunomodulatory Drugs and Cereblon E3 Ligase Modulators in the Treatment of Multiple Myeloma. *Cancers (Basel)*, 13(18), 2021. [*PubMed Central* ID: PMC8468542] [DOI: 10.3390/cancers13184666] [*PubMed* ID: 34572892]. [Citado en p. 14]

[116] Niels WCJ van de Donk, Rakesh Popat, Jeremy Larsen, *et al.* First results of iberdomide (IBER; CC-220) in combination with dexamethasone (DEX) and daratumumab (DARA) or bortezomib (BORT) in patients with relapsed/refractory multiple myeloma (RRMM). *Blood*, 136: 16–17, 2020. [Citado en p. 14]

[117] D. W. Rasco, K. P. Papadopoulos, M. Pourdehnad, *et al.* A First-in-Human Study of Novel Cereblon Modulator Avadomide (CC-122) in Advanced Malignancies. *Clin. Cancer Res.*, 25(1): 90–98, 2019. [DOI: 10.1158/1078-0432.CCR-18-1203] [*PubMed* ID: 30201761]. [Citado en p. 14]

[118] Paul G Richardson, Enrique Ocio, Noopur S Raje, *et al.* CC-92480, a Potent, Novel Cereblon E3 Ligase Modulator (CELMoD) Agent, in Combination with Dexamethasone (DEX) and Bortezomib (BORT) in Patients (pts) with Relapsed/Refractory Multiple Myeloma (RRMM): Preliminary Results from the Phase 1/2 Study CC-92480-MM-002. *Blood*, 138: 2731, 2021. [DOI: 10.1182/blood-2021-147812]. [Citado en p. 14]

[119] M. Zhao, M. Hu, Y. Chen, *et al.* Cereblon modulator CC-885 induces CRBN-dependent ubiquitination and degradation of CDK4 in multiple myeloma. *Biochem. Biophys. Res. Commun.*, 549: 150–156, 2021. [DOI: 10.1016/j.bbrc.2021.02.110] [*PubMed* ID: 33676183]. [Citado en p. 14]

[120] S. Grosicki, M. Simonova, I. Spicka, *et al.* Once-per-week selinexor, bortezomib, and dexamethasone versus twice-per-week bortezomib and dexamethasone in patients with multiple myeloma (BOSTON): a randomised, open-label, phase 3 trial. *Lancet*, 396(10262): 1563–1573, 2020. [DOI: 10.1016/S0140-6736(20)32292-3] [*PubMed* ID: 33189178]. [Citado en p. 14]

[121] A. Chari, D. T. Vogl, M. Gavriatopoulou, *et al.* Oral Selinexor-Dexamethasone for Triple-Class Refractory Multiple Myeloma. *N. Engl. J. Med.*, 381(8): 727–738, 2019. [DOI: 10.1056/NEJMoa1903455] [*PubMed* ID: 31433920]. [Citado en p. 14]

[122] J. F. San-Miguel, V. T. Hungria, S. S. Yoon, *et al.* Panobinostat plus bortezomib and dexamethasone versus placebo plus bortezomib and dexamethasone in patients with relapsed or relapsed and refractory multiple myeloma: a multicentre, randomised, double-blind phase 3 trial. *Lancet Oncol.*, 15(11): 1195–1206, 2014. [DOI: 10.1016/S1470-2045(14)70440-1] [*PubMed* ID: 25242045]. [Citado en p. 14]

[123] E. M. Ocio y J. F. San Miguel. The DAC system and associations with multiple myeloma. *Invest. New Drugs*, 28(Supplement 1): 28–35, 2010. [*PubMed Central* ID: PMC3003792] [DOI: 10.1007/s10637-010-9589-x] [*PubMed* ID: 21120582]. [Citado en p. 14]

[124] E. D. Deeks. Venetoclax: First Global Approval. *Drugs*, 76(9): 979–987, 2016. [DOI: 10.1007/s40265-016-0596-x] [*PubMed* ID: 27260335]. [Citado en p. 14]

[125] A. J. Souers, J. D. Leverson, E. R. Boghaert, *et al.* ABT-199, a potent and selective BCL-2 inhibitor, achieves antitumor activity while sparing platelets. *Nat. Med.*, 19(2): 202–208, 2013. [DOI: 10.1038/nm.3048] [*PubMed* ID: 23291630]. [Citado en p. 14]

[126] S. Kumar, J. L. Kaufman, C. Gasparetto, *et al.* Efficacy of venetoclax as targeted therapy for relapsed/refractory t(11;14) multiple myeloma. *Blood*, 130(22): 2401–2409, 2017. [DOI: 10.1182/blood-2017-06-788786] [*PubMed* ID: 29018077]. [Citado en p. 15]

[127] N. J. Bahlis, M. A. Dimopoulos, D. J. White, *et al.* Daratumumab plus lenalidomide and dexamethasone in relapsed/refractory multiple myeloma: extended follow-up of POLLUX, a randomized, open-label, phase 3 study. *Leukemia*, 34(7): 1875–1884, 2020. [*PubMed Central* ID: PMC7326710] [DOI: 10.1002/cncr.31680] [*PubMed* ID: 32001798]. [Citado en p. 15]

[128] A. Palumbo, A. Chanan-Khan, K. Weisel, *et al.* Daratumumab, Bortezomib, and Dexamethasone for Multiple Myeloma. *N. Engl. J. Med.*, 375(8): 754–766, 2016. [DOI: 10.1056/NEJMoa1606038] [*PubMed* ID: 27557302]. [Citado en p. 15]

[129] M. V. Mateos, P. Sonneveld, V. Hungria, *et al.* Daratumumab, Bortezomib, and Dexamethasone Versus Bortezomib and Dexamethasone in Patients With Previously Treated Multiple Myeloma: Three-year Follow-up of CASTOR. *Clin. Lymphoma Myeloma Leuk.*, 20(8): 509–518, 2020. [DOI: 10.1016/j.clml.2019.09.623] [*PubMed* ID: 32482541]. [Citado en p. 15]

[130] M. A. Dimopoulos, A. Oriol, H. Nahi, *et al.* Daratumumab, Lenalidomide, and Dexamethasone for Multiple Myeloma. *N. Engl. J. Med.*, 375(14): 1319–1331, 2016. [DOI: 10.1056/NEJMoa1607751] [*PubMed* ID: 27705267]. [Citado en p. 15]

[131] H. M. Lokhorst, T. Plesner, J. P. Laubach, *et al.* Targeting CD38 with Daratumumab Monotherapy in Multiple Myeloma. *N. Engl. J. Med.*, 373(13): 1207–1219, 2015. [DOI: 10.1056/NEJMoa1506348] [*PubMed* ID: 26308596]. [Citado en p. 15]

[132] S. Lonial, B. M. Weiss, S. Z. Usmani, *et al.* Daratumumab monotherapy in patients with treatment-refractory multiple myeloma (SIRIUS): an open-label, randomised, phase 2 trial. *Lancet*, 387(10027): 1551–1560, 2016. [DOI: 10.1016/S0140-6736(15)01120-4] [*PubMed* ID: 26778538]. [Citado en p. 15]

[133] T. Martin, R. Baz, D. M. Benson, *et al.* A phase 1b study of isatuximab plus lenalidomide and dexamethasone for relapsed/refractory multiple myeloma. *Blood*, 129(25): 3294–3303, 2017. [*PubMed Central* ID: PMC5482100] [DOI: 10.1182/blood-2016-09-740787] [*PubMed* ID: 28483761]. [Citado en p. 15]

[134] M. S. Raab, M. Engelhardt, A. Blank, *et al.* MOR202, a novel anti-CD38 monoclonal antibody, in patients with relapsed or refractory multiple myeloma: a first-in-human, multicentre, phase 1-2a trial. *Lancet Haematol.*, 7(5): e381–e394, 2020. [DOI: 10.1016/S2352-3026(19)30249-2] [*PubMed* ID: 32171061]. [Citado en p. 15]

[135] M. Gentile, G. Specchia, D. Derudas, *et al.* Elotuzumab, lenalidomide, and dexamethasone as salvage therapy for patients with multiple myeloma: Italian, multicenter, retrospective clinical experience with 300 cases outside of controlled clinical trials. *Haematologica*, 106(1): 291–294, 2021. [*PubMed Central* ID: PMC7776255] [DOI: 10.3324/haematol.2019.241513] [*PubMed* ID: 32107338]. [Citado en p. 15]

[136] K. Suzuki, K. Sunami, K. Ohashi, *et al.* Randomized phase 3 study of elotuzumab for relapsed or refractory multiple myeloma: ELOQUENT-2 Japanese patient subanalysis. *Blood Cancer J.*, 7(3): e540, 2017. [*PubMed Central* ID: PMC5380903] [DOI: 10.1038/bcj.2017.18] [*PubMed* ID: 28282035]. [Citado en p. 15]

[137] M. A. Dimopoulos, D. Dytfeld, S. Grosicki, *et al.* Elotuzumab plus Pomalidomide and Dexamethasone for Multiple Myeloma. *N. Engl. J. Med.*, 379(19): 1811–1822, 2018. [DOI: 10.1056/NEJMoa1805762] [*PubMed* ID: 30403938]. [Citado en p. 15]

[138] A. Chiu, W. Xu, B. He, *et al.* Hodgkin lymphoma cells express TACI and BCMA receptors and generate survival and proliferation signals in response to BAFF and APRIL. *Blood*, 109(2): 729–739, 2007. [*PubMed Central* ID: PMC1785096] [DOI: 10.1182/blood-2006-04-015958] [*PubMed* ID: 16960154]. [Citado en p. 15]

[139] D. T. Avery, S. L. Kalled, J. I. Ellyard, *et al.* BAFF selectively enhances the survival of plasmablasts generated from human memory B cells. *J. Clin. Invest.*, 112(2): 286–297, 2003. [*PubMed Central* ID: PMC164292] [DOI: 10.1172/JCI18025] [*PubMed* ID: 12865416]. [Citado en p. 15]

[140] B. P. O'Connor, V. S. Raman, L. D. Erickson, *et al.* BCMA is essential for the survival of long-lived bone marrow plasma cells. *J. Exp. Med.*, 199(1): 91–98, 2004. [*PubMed Central* ID: PMC1887725] [DOI: 10.1084/jem.20031330] [*PubMed* ID: 14707116]. [Citado en p. 15]

[141] Y. T. Tai, X. F. Li, I. Breitkreutz, *et al.* Role of B-cell-activating factor in adhesion and growth of human multiple myeloma cells in the bone marrow microenvironment. *Cancer Res.*, 66(13): 6675–6682, 2006. [DOI: 10.1158/0008-5472.CAN-06-0190] [*PubMed* ID: 16818641]. [Citado en p. 15]

[142] J. O. Claudio, E. Masih-Khan, H. Tang, *et al.* A molecular compendium of genes expressed in multiple myeloma. *Blood*, 100(6): 2175–2186, 2002. [DOI: 10.1182/blood-2002-01-0008] [*PubMed* ID: 12200383]. [Citado en p. 15]

[143] S. Ailawadhi, K. R. Kelly, R. A. Vescio, *et al.* A Phase I Study to Assess the Safety and Pharmacokinetics of Single-agent Lorvotuzumab Mertansine (IMGN901) in Patients with Relapsed and/or Refractory CD-56-positive Multiple Myeloma. *Clin. Lymphoma Myeloma Leuk.*, 19(1): 29–34, 2019. [*PubMed Central* ID: PMC9059793] [DOI: 10.1016/j.clml.2018.08.018] [*PubMed* ID: 30340993]. [Citado en p. 15]

[144] C. L. Abrahams, X. Li, M. Embry, *et al.* Targeting CD74 in multiple myeloma with the novel, site-specific antibody-drug conjugate STRO-001. *Oncotarget*, 9(102): 37700–37714, 2018. [*PubMed Central* ID: PMC6340874] [DOI: 10.18632/oncotarget.26491] [*PubMed* ID: 30701025]. [Citado en p. 15]

[145] P. Sapra, R. Stein, J. Pickett, *et al.* Anti-CD74 antibody-doxorubicin conjugate, IMMU-110, in a human multiple myeloma xenograft and in monkeys. *Clin. Cancer Res.*, 11(14): 5257–5264, 2005. [DOI: 10.1158/1078-0432.CCR-05-0204] [*PubMed* ID: 16033844]. [Citado en p. 15]

[146] H. Tamura, M. Ishibashi, T. Yamashita, *et al.* Marrow stromal cells induce B7-H1 expression on myeloma cells, generating aggressive characteristics in multiple myeloma. *Leukemia*, 27(2): 464–472, 2013. [DOI: 10.1038/leu.2012.213] [*PubMed* ID: 22828443]. [Citado en p. 15]

[147] Y. Chang, Y. Jiang, Y. Chen, *et al.* Bone marrow PD-1 positive T cells reflect tumor mass and prognosis in multiple myeloma. *Int. J. Clin. Exp. Pathol.*, 11(1): 304–313, 2018. [*PubMed Central* ID: PMC6957957] [*PubMed* ID: 9414264]. [Citado en p. 15]

[148] M. V. Mateos, R. Z. Orlowski, E. M. Ocio, *et al.* Pembrolizumab combined with lenalidomide and low-dose dexamethasone for relapsed or refractory multiple myeloma: phase I KEYNOTE-023 study. *Br. J. Haematol.*, 186(5): e117–e121, 2019. [DOI: 10.1111/bjh.15946] [*PubMed* ID: 31090915]. [Citado en p. 15]

[149] T. Jelinek, B. Paiva, y R. Hajek. Update on PD-1/PD-L1 Inhibitors in Multiple Myeloma. *Front. Immunol.*, 9: 2431, 2018. [*PubMed Central* ID: PMC6250817] [DOI: 10.3389/fimmu.2018.02431] [*PubMed* ID: 30505301]. [Citado en p. 15]

[150] Christie PM Verkleij, Monique C Minnema, Okke de Weerdt, *et al.* Efficacy and safety of nivolumab combined with daratumumab with or without low-dose cyclophosphamide in relapsed/refractory multiple myeloma; interim analysis of the phase 2 Nivo-Dara study. *Blood*, 134: 1879, 2019. [DOI: 10.1182/blood-2019-124339]. [Citado en p. 15]

[151] N. C. Smits y C. L. Sentman. Bispecific T-Cell Engagers (BiTEs) as Treatment of B-Cell Lymphoma. *J. Clin. Oncol.*, 34(10): 1131–1133, 2016. [*PubMed Central* ID: PMC5085271] [DOI: 10.1200/JCO.2015.64.9970] [*PubMed* ID: 26884583]. [Citado en p. 15]

[152] M. Mack, G. Riethmüller, y P. Kufer. A small bispecific antibody construct expressed as a functional single-chain molecule with high tumor cell cytotoxicity. *Proc. Natl. Acad. Sci. U.S.A.*, 92(15): 7021–7025, 1995. [*PubMed Central* ID: PMC41463] [DOI: 10.1073/pnas.92.15.7021] [*PubMed* ID: 7624362]. [Citado en p. 16]

[153] S. Hipp, Y. T. Tai, D. Blanset, *et al.* A novel BCMA/CD3 bispecific T-cell engager for the treatment of multiple myeloma induces selective lysis in vitro and in vivo. *Leukemia*, 31(8): 1743–1751, 2017. [DOI: 10.1038/leu.2016.388] [*PubMed* ID: 28025583]. [Citado en p. 16]

[154] R. L. Goldstein, A. Goyos, C. M. Li, *et al.* AMG 701 induces cytotoxicity of multiple myeloma cells and depletes plasma cells in cynomolgus monkeys. *Blood Adv.*, 4(17): 4180–4194, 2020. [*PubMed Central* ID: PMC7479952] [DOI: 10.1182/bloodadvances.2020002565] [*PubMed* ID: 32886754]. [Citado en p. 16]

[155] Luciano J. Costa, Sandy W. Wong, Arancha Bermúdez, *et al.* First Clinical Study of the B-Cell Maturation Antigen (BCMA) 2+1 T Cell Engager (TCE) CC-93269 in Patients (Pts) with Relapsed/Refractory Multiple Myeloma (RRMM): Interim Results of a Phase 1 Multicenter Trial. *Blood*, 134(Supplement 1): 143–143, 2019. [DOI: 10.1182/blood-2019-122895]. [Citado en p. 16]

[156] K. Pillarisetti, S. Edavettal, M. Mendonça, *et al.* A T-cell-redirecting bispecific G-protein-coupled receptor class 5 member D x CD3 antibody to treat multiple myeloma. *Blood*, 135(15): 1232–1243, 2020. [*PubMed Central* ID: PMC7146017] [DOI: 10.1182/blood.2019003342] [*PubMed* ID: 32040549]. [Citado en p. 16]

[157] J. Atamaniuk, A. Gleiss, E. Porpaczy, *et al.* Overexpression of G protein-coupled receptor 5D in the bone marrow is associated with poor prognosis in patients with multiple myeloma. *Eur J. Clin. Invest.*, 42(9): 953–960, 2012. [DOI: 10.1111/j.1365-2362.2012.02679.x] [*PubMed* ID: 22591013]. [Citado en p. 16]

[158] Deepu Madduri, Saad Z Usmani, Sundar Jagannath, *et al.* Results from CARTITUDE-1: a phase 1b/2 study of JNJ-4528, a CAR-T cell therapy directed against B-cell maturation antigen (BCMA), in patients with relapsed and/or refractory multiple myeloma (R/R MM). *Blood*, 134: 577, 2019. [DOI: 10.1182/blood-2019-121731]. [Citado en p. 16]

[159] J. G. Berdeja, D. Madduri, S. Z. Usmani, *et al.* Ciltacabtagene autoleucel, a B-cell maturation antigen-directed chimeric antigen receptor T-cell therapy in patients with relapsed or refractory multiple myeloma (CARTITUDE-1): a phase 1b/2 open-label study. *Lancet*, 398(10297): 314–324, 2021. [DOI: 10.1016/S0140-6736(21)00933-8] [*PubMed* ID: 34175021]. [Citado en p. 16]

[160] L. Mikkilineni y J. N. Kochenderfer. CAR T cell therapies for patients with multiple myeloma. *Nat. Rev. Clin. Oncol.*, 18(2): 71–84, 2021. [DOI: 10.1038/s41571-020-0427-6] [*PubMed* ID: 32978608]. [Citado en p. 16]

[161] M. Greaves y C. C. Maley. Clonal evolution in cancer. *Nature*, 481(7381): 306–313, 2012. [*PubMed Central* ID: PMC3367003] [DOI: 10.1038/nature10762] [*PubMed* ID: 22258609]. [Citado en p. 17]

[162] J. Eder, R. Sedrani, y C. Wiesmann. The discovery of first-in-class drugs: origins and evolution. *Nat. Rev. Drug Discov.*, 13(8): 577–587, 2014. [DOI: 10.1038/nrd4336] [*PubMed* ID: 25033734]. [Citado en p. 17]

[163] O. J. Wouters, M. McKee, y J. Luyten. Estimated Research and Development Investment Needed to Bring a New Medicine to Market, 2009-2018. *JAMA*, 323(9): 844–853, 2020. [*PubMed Central* ID: PMC7054832] [DOI: 10.1001/jama.2020.1166] [*PubMed* ID: 32125404]. [Citado en p. 17]

[164] M. N. Patel, M. D. Halling-Brown, J. E. Tym, *et al.* Objective assessment of cancer genes for drug discovery. *Nat. Rev. Drug Discov.*, 12(1): 35–50, 2013. [DOI: 10.1038/nrd3913] [*PubMed* ID: 23274470]. [Citado en p. 17]

[165] P. Pantziarka, C. Verbaanderd, V. Sukhatme, *et al.* ReDO_DB: the repurposing drugs in oncology database. *Ecancermedicalscience*, 12: 886, 2018. [*PubMed Central* ID: PMC6345075] [DOI: 10.3332/ecancer.2018.886] [*PubMed* ID: 30679953]. [Citado en p. 17]

[166] S. M. Corsello, J. A. Bittker, Z. Liu, *et al.* The Drug Repurposing Hub: a next-generation drug library and information resource. *Nat. Med.*, 23(4): 405–408, 2017. [*PubMed Central* ID: PMC5568558] [DOI: 10.1038/nm.4306] [*PubMed* ID: 28388612]. [Citado en p. 17]

[167] S. Singhal, J. Mehta, R. Desikan, *et al.* Antitumor activity of thalidomide in refractory multiple myeloma. *N. Engl. J. Med.*, 341(21): 1565–1571, 1999. [DOI: 10.1056/NEJM199911183412102] [*PubMed* ID: 10564685]. [Citado en p. 17]

[168] A. Palumbo, T. Facon, P. Sonneveld, *et al.* Thalidomide for treatment of multiple myeloma: 10 years later. *Blood*, 111(8): 3968–3977, 2008. [DOI: 10.1182/blood-2007-10-117457] [*PubMed* ID: 18245666]. [Citado en p. 17]

[169] P. M. Fayers, A. Palumbo, C. Hulin, *et al.* Thalidomide for previously untreated elderly patients with multiple myeloma: meta-analysis of 1685 individual patient data from 6 randomized clinical trials. *Blood*, 118(5): 1239–1247, 2011. [DOI: 10.1182/blood-2011-03-341669] [*PubMed* ID: 21670471]. [Citado en p. 17]

[170] A Waage, AP Palumbo, P Fayers, *et al.* MP versus MPT for previously untreated elderly patients with multiple myeloma: A meta-analysis of 1,682 individual patient data from six randomized clinical trials. *J. Clin. Oncol.*, 28(Supplement 15): 8130–8130, 2010. [DOI: 10.1200/jco.2010.28.15_-suppl.8130]. [Citado en p. 17]

[171] F. Hitz, M. Kraus, T. Pabst, *et al.* Nelfinavir and lenalidomide/dexamethasone in patients with lenalidomide-refractory multiple myeloma. A phase I/II Trial (SAKK 39/10). *Blood Cancer J.*, 9(9): 70, 2019. [*PubMed Central* ID: PMC6711992] [DOI: 10.1038/s41408-019-0228-2] [*PubMed* ID: 31455773]. [Citado en p. 18]

[172] N. Toloczko-Iwaniuk, D. Dziemianczyk-Pakiela, B. K. Nowaszewska, *et al.* Celecoxib in Cancer Therapy and Prevention - Review. *Curr. Drug Targets*, 20(3): 302–315, 2019. [DOI: 10.2174/1389450119666180803121737] [*PubMed* ID: 30073924]. [Citado en p. 18]

[173] P. Baumann, S. Mandl-Weber, A. Völkl, *et al.* Dihydroorotate dehydrogenase inhibitor A771726 (leflunomide) induces apoptosis and diminishes proliferation of multiple myeloma cells. *Mol. Cancer Ther.*, 8(2): 366–375, 2009. [DOI: 10.1158/1535-7163.MCT-08-0664] [*PubMed* ID: 19174558]. [Citado en p. 18]

[174] J. Longo, P. Smirnov, Z. Li, *et al.* The mevalonate pathway is an actionable vulnerability of t(4;14)-positive multiple myeloma. *Leukemia*, 35(3): 796–808, 2021. [*PubMed Central* ID: PMC7359767] [DOI: 10.4103/ijmr.IJMR_672_18] [*PubMed* ID: 32665698]. [Citado en p. 18]

[175] C. Lam, I. D. Ferguson, M. C. Mariano, *et al.* Repurposing tofacitinib as an anti-myeloma therapeutic to reverse growth-promoting effects of the bone marrow microenvironment. *Haematologica*, 103(7): 1218–1228, 2018. [*PubMed Central* ID: PMC6029548] [DOI: 10.3324/haematol.2017.174482] [*PubMed* ID: 29622655]. [Citado en p. 18]

[176] V. Haberle y A. Stark. Eukaryotic core promoters and the functional basis of transcription initiation. *Nat. Rev. Mol. Cell Biol.*, 19(10): 621–637, 2018. [*PubMed Central* ID: PMC6205604] [DOI: 10.1038/s41580-018-0028-8] [*PubMed* ID: 29946135]. [Citado en p. 18]

[177] L. M. Gallego-Paez, M. C. Bordone, A. C. Leote, *et al.* Alternative splicing: the pledge, the turn, and the prestige : The key role of alternative splicing in human biological systems. *Hum. Genet.*, 136(9): 1015–1042, 2017. [*PubMed Central* ID: PMC5602094] [DOI: 10.1007/s00439-017-1790-y] [*PubMed* ID: 28374191]. [Citado en pp. 18 y 21]

[178] F. E. Baralle y J. Giudice. Alternative splicing as a regulator of development and tissue identity. *Nat. Rev. Mol. Cell Biol.*, 18(7): 437–451, 2017. [*PubMed Central* ID: PMC6839889] [DOI: 10.1038/nrm.2017.27] [*PubMed* ID: 28488700]. [Citado en pp. 18 y 21]

[179] Z. Frankenstein, J. Sperling, R. Sperling, y M. Eisenstein. A unique spatial arrangement of the snRNPs within the native spliceosome emerges from in silico studies. *Structure*, 20(6): 1097–1106, 2012. [*PubMed Central* ID: PMC3372696] [DOI: 10.1016/j.str.2012.03.022] [*PubMed* ID: 22578543]. [Citado en p. 19]

[180] N. Behzadnia, M. M. Golas, K. Hartmuth, *et al.* Composition and three-dimensional EM structure of double affinity-purified, human prespliceosomal A complexes. *EMBO J.*, 26(6): 1737–1748, 2007. [*PubMed Central* ID: PMC1829389] [DOI: 10.1038/sj.emboj.7601631] [*PubMed* ID: 17332742]. [Citado en p. 18]

[181] S. Bessonov, M. Anokhina, C. L. Will, *et al.* Isolation of an active step I spliceosome and composition of its RNP core. *Nature*, 452(7189): 846–850, 2008. [DOI: 10.1038/nature06842] [*PubMed* ID: 18322460]. [Citado en p. 18]

[182] J. Deckert, K. Hartmuth, D. Boehringer, *et al.* Protein composition and electron microscopy structure of affinity-purified human spliceosomal B complexes isolated under physiological conditions. *Mol. Cell Biol.*, 26(14): 5528–5543, 2006. [*PubMed Central* ID: PMC1592722] [DOI: 10.1128/MCB.00582-06] [*PubMed* ID: 16809785]. [Citado en p. 18]

[183] D. Frendewey y W. Keller. Stepwise assembly of a pre-mRNA splicing complex requires U-snRNPs and specific intron sequences. *Cell*, 42(1): 355–367, 1985. [DOI: 10.1016/s0092-8674(85)80131-8] [*PubMed* ID: 3160483]. [Citado en p. 18]

[184] M. Aebi, H. Hornig, R. A. Padgett, *et al.* Sequence requirements for splicing of higher eukaryotic nuclear pre-mRNA. *Cell*, 47(4): 555–565, 1986. [DOI: 10.1016/0092-8674(86)90620-3] [*PubMed* ID: 3779836]. [Citado en p. 18]

[185] U. Vijayraghavan, R. Parker, J. Tamm, *et al.* Mutations in conserved intron sequences affect multiple steps in the yeast splicing pathway, particularly assembly of the spliceosome. *EMBO J.*, 5(7): 1683–1695, 1986. [*PubMed Central* ID: PMC1166995] [DOI: 10.1002/j.1460-2075.1986.tb04412.x] [*PubMed* ID: 3017708]. [Citado en p. 18]

[186] A. I. Lamond, M. M. Konarska, y P. A. Sharp. A mutational analysis of spliceosome assembly: evidence for splice site collaboration during spliceosome formation. *Genes Dev.*, 1(6): 532–543, 1987. [DOI: 10.1101/gad.1.6.532] [*PubMed* ID: 2824284]. [Citado en p. 18]

[187] S. C. Bonnal, I. López-Oreja, y J. Valcárcel. Roles and mechanisms of alternative splicing in cancer - implications for care. *Nat. Rev. Clin. Oncol.*, 17(8): 457–474, 2020. [DOI: 10.1101/542506] [*PubMed* ID: 32303702]. [Citado en p. 19]

[188] C. Cretu, J. Schmitzová, A. Ponce-Salvatierra, *et al.* Molecular Architecture of SF3b and Structural Consequences of Its Cancer-Related Mutations. *Mol. Cell*, 64(2): 307–319, 2016. [DOI: 10.1016/j.molcel.2016.08.036] [*PubMed* ID: 27720643]. [Citado en p. 20]

[189] R. Bai, R. Wan, C. Yan, *et al.* spliceosome before activation. *Science*, 360(6396): 1423–1429, 2018. [DOI: 10.1126/science.aau0325] [*PubMed* ID: 29794219]. [Citado en p. 20]

[190] B. Kastner, C. L. Will, H. Stark, y R. Lührmann. Structural Insights into Nuclear pre-mRNA Splicing in Higher Eukaryotes. *Cold Spring Harb. Perspect. Biol.*, 11(11), 2019. [*PubMed Central* ID: PMC6824238] [DOI: 10.1101/cshperspect.a032417] [*PubMed* ID: 30765414]. [Citado en p. 20]

[191] R. Wan, R. Bai, y Y. Shi. Molecular choreography of pre-mRNA splicing by the spliceosome. *Curr. Opin. Struct. Biol.*, 59: 124–133, 2019. [DOI: 10.1016/j.sbi.2019.07.010] [*PubMed* ID: 31476650]. [Citado en p. 20]

[192] S. M. Berget, C. Moore, y P. A. Sharp. Spliced segments at the 5' terminus of adenovirus 2 late mRNA. *Proc. Natl. Acad. Sci. U.S.A.*, 74(8): 3171–3175, 1977. [*PubMed Central* ID: PMC431482] [DOI: 10.1073/pnas.74.8.3171] [*PubMed* ID: 269380]. [Citado en p. 21]

[193] L. T. Chow, R. E. Gelinas, T. R. Broker, y R. J. Roberts. An amazing sequence arrangement at the 5' ends of adenovirus 2 messenger RNA. *Cell*, 12(1): 1–8, 1977. [DOI: 10.1016/0092-8674(77)90180-5] [*PubMed* ID: 902310]. [Citado en p. 21]

[194] Z. Wang y C. B. Burge. Splicing regulation: from a parts list of regulatory elements to an integrated splicing code. *RNA*, 14(5): 802–813, 2008. [*PubMed Central* ID: PMC2327353] [DOI: 10.1261/rna.876308] [*PubMed* ID: 18369186]. [Citado en p. 22]

[195] J. Y. Wu y T. Maniatis. Specific interactions between proteins implicated in splice site selection and regulated alternative splicing. *Cell*, 75(6): 1061–1070, 1993. [DOI: 10.1016/0092-8674(93)90316-i] [*PubMed* ID: 8261509]. [Citado en p. 22]

[196] J. D. Kohtz, S. F. Jamison, C. L. Will, *et al.* Protein-protein interactions and 5'-splice-site recognition in mammalian mRNA precursors. *Nature*, 368(6467): 119–124, 1994. [DOI: 10.1038/368119a0] [*PubMed* ID: 8139654]. [Citado en p. 22]

[197] N. Kataoka, J. L. Bachorik, y G. Dreyfuss. Transportin-SR, a nuclear import receptor for SR proteins. *J. Cell Biol.*, 145(6): 1145–1152, 1999. [*PubMed Central* ID: PMC2133142] [DOI: 10.1083/jcb.145.6.1145] [*PubMed* ID: 10366588]. [Citado en p. 22]

[198] D. Longman, I. L. Johnstone, y J. F. Cáceres. Functional characterization of SR and SR-related genes in Caenorhabditis elegans. *EMBO J.*, 19(7): 1625–1637, 2000. [*PubMed Central* ID: PMC310231] [DOI: 10.1093/emboj/19.7.1625] [*PubMed* ID: 10747030]. [Citado en p. 23]

[199] D. N. Richardson, M. F. Rogers, A. Labadorf, *et al.* Comparative analysis of serine/arginine-rich proteins across 27 eukaryotes: insights into sub-family classification and extent of alternative splicing. *PLoS One*, 6(9): e24542, 2011. [*PubMed Central* ID: PMC3173450] [DOI: 10.1371/journal.pone.0024542] [*PubMed* ID: 21935421]. [Citado en p. 23]

[200] J. C. Long y J. F. Caceres. The SR protein family of splicing factors: master regulators of gene expression. *Biochem. J.*, 417(1): 15–27, 2009. [DOI: 10.1042/BJ20081501] [*PubMed* ID: 19061484]. [Citado en p. 23]

[201] L. Twyffels, C. Gueydan, y V. Kruys. Shuttling SR proteins: more than splicing factors. *FEBS J.*, 278(18): 3246–3255, 2011. [DOI: 10.1111/j.1742-4658.2011.08274.x] [*PubMed* ID: 21794093]. [Citado en p. 23]

[202] J. M. Howard y J. R. Sanford. The RNAissance family: SR proteins as multifaceted regulators of gene expression. *Wiley Interdiscip. Rev. RNA*, 6(1): 93–110, 2015. [*PubMed Central* ID: PMC4268343] [DOI: 10.1002/wrna.1260] [*PubMed* ID: 25155147]. [Citado en p. 23]

[203] P. J. Shepard y K. J. Hertel. The SR protein family. *Genome Biol.*, 10(10): 242, 2009. [*PubMed Central* ID: PMC2784316] [DOI: 10.1186/gb-2009-10-10-242] [*PubMed* ID: 19857271]. [Citado en p. 23]

[204] Z. Zhou y X. D. Fu. Regulation of splicing by SR proteins and SR protein-specific kinases. *Chromosoma*, 122(3): 191–207, 2013. [*PubMed Central* ID: PMC3660409] [DOI: 10.1007/s00412-013-0407-z] [*PubMed* ID: 23525660]. [Citado en p. 23]

[205] J. F. Gui, W. S. Lane, y X. D. Fu. A serine kinase regulates intracellular localization of splicing factors in the cell cycle. *Nature*, 369(6482): 678–682, 1994. [DOI: 10.1038/369678a0] [*PubMed* ID: 8208298]. [Citado en p. 23]

[206] H. Y. Wang, W. Lin, J. A. Dyck, *et al.* SRPK2: a differentially expressed SR protein-specific kinase involved in mediating the interaction and localization of pre-mRNA splicing factors in mammalian cells. *J. Cell Biol.*, 140(4): 737–750, 1998. [*PubMed Central* ID: PMC2141757] [DOI: 10.1083/jcb.140.4.737] [*PubMed* ID: 9472028]. [Citado en p. 23]

[207] K. Colwill, T. Pawson, B. Andrews, *et al.* The Clk/Sty protein kinase phosphorylates SR splicing factors and regulates their intranuclear distribution. *EMBO J.*, 15(2): 265–275, 1996. [*PubMed Central* ID: PMC449941] [*PubMed* ID: 8617202]. [Citado en p. 23]

[208] F. Rossi, E. Labourier, T. Forné, *et al.* Specific phosphorylation of SR proteins by mammalian DNA topoisomerase I. *Nature*, 381(6577): 80–82, 1996. [DOI: 10.1038/381080a0] [*PubMed* ID: 8609994]. [Citado en p. 23]

[209] S. Piñol-Roma y G. Dreyfuss. Shuttling of pre-mRNA binding proteins between nucleus and cytoplasm. *Nature*, 355(6362): 730–732, 1992. [DOI: 10.1038/355730a0] [*PubMed* ID: 1371331]. [Citado en p. 24]

[210] C. L. Lorson, E. Hahnen, E. J. Androphy, y B. Wirth. A single nucleotide in the SMN gene regulates splicing and is responsible for spinal muscular atrophy. *Proc. Natl. Acad. Sci. U.S.A.*, 96(11): 6307–6311, 1999. [*PubMed Central* ID: PMC26877] [DOI: 10.1073/pnas.96.11.6307] [*PubMed* ID: 10339583]. [Citado en p. 25]

[211] N. J. Abreu y M. A. Waldrop. Overview of gene therapy in spinal muscular atrophy and Duchenne muscular dystrophy. *Pediatr. Pulmonol.*, 56(4): 710–720, 2021. [DOI: 10.1002/ppul.25055] [*PubMed* ID: 32886442]. [Citado en p. 25]

[212] F. Pagani, M. Raponi, y F. E. Baralle. Synonymous mutations in CFTR exon 12 affect splicing and are not neutral in evolution. *Proc. Natl. Acad. Sci. U.S.A.*, 102(18): 6368–6372, 2005. [*PubMed Central* ID: PMC1088389] [DOI: 10.1073/pnas.0502288102] [*PubMed* ID: 15840711]. [Citado en p. 25]

[213] E. C. Ibrahim, M. M. Hims, N. Shomron, *et al.* Weak definition of IKBKAP exon 20 leads to aberrant splicing in familial dysautonomia. *Hum. Mutat.*, 28(1): 41–53, 2007. [DOI: 10.1002/humu.20401] [*PubMed* ID: 16964593]. [Citado en p. 25]

[214] R. Benchaouir, V. Robin, y A. Goyenvalle. Gene and splicing therapies for neuromuscular diseases. *Front. Biosci.-Landmark*, 20(8): 1190–1233, 2015. [DOI: 10.2741/4367] [*PubMed* ID: 25961553]. [Citado en p. 25]

[215] M. Hutton, C. L. Lendon, P. Rizzu, *et al.* Association of missense and 5'-splice-site mutations in tau with the inherited dementia FTDP-17. *Nature*, 393(6686): 702–705, 1998. [DOI: 10.1038/31508] [*PubMed* ID: 9641683]. [Citado en p. 25]

[216] A. Grover, H. Houlden, M. Baker, *et al.* 5' splice site mutations in tau associated with the inherited dementia FTDP-17 affect a stem-loop structure that regulates alternative splicing of exon 10. *J. Biol. Chem.*, 274(21): 15134–15143, 1999. [DOI: 10.1074/jbc.274.21.15134] [*PubMed* ID: 10329720]. [Citado en p. 25]

[217] P. Scaffidi y T. Misteli. Reversal of the cellular phenotype in the premature aging disease Hutchinson-Gilford progeria syndrome. *Nat. Med.*, 11(4): 440–445, 2005. [*PubMed Central* ID: PMC1351119] [DOI: 10.1038/nm1204] [*PubMed* ID: 15750600]. [Citado en p. 25]

[218] S. Calandra, P. Tarugi, y S. Bertolini. Altered mRNA splicing in lipoprotein disorders. *Curr Opin Lipidol*, 22(2): 93–99, 2011. [DOI: 10.1097/MOL.0b013e3283426ebc] [*PubMed* ID: 21157333]. [Citado en p. 25]

[219] L. F. Reeskamp, M. L. Hartgers, J. Peter, *et al.* A Deep Intronic Variant in LDLR in Familial Hypercholesterolemia. *Circ. Genom. Precis. Med.*, 11(12): e002385, 2018. [DOI: 10.1161/CIRCGEN.118.002385] [*PubMed* ID: 30562117]. [Citado en p. 25]

[220] F. Supek, B. Miñana, J. Valcárcel, *et al.* Synonymous mutations frequently act as driver mutations in human cancers. *Cell*, 156(6): 1324–1335, 2014. [DOI: 10.1016/j.cell.2014.01.051] [*PubMed* ID: 24630730]. [Citado en p. 25]

[221] S. Diederichs, L. Bartsch, J. C. Berkmann, *et al.* The dark matter of the cancer genome: aberrations in regulatory elements, untranslated regions, splice sites, non-coding RNA and synonymous mutations. *EMBO Mol. Med.*, 8(5): 442–457, 2016. [*PubMed Central* ID: PMC5126213] [DOI: 10.15252/emmm.201506055] [*PubMed* ID: 26992833]. [Citado en p. 25]

[222] L. M. Urbanski, N. Leclair, y O. Anczuków. Alternative-splicing defects in cancer: Splicing regulators and their downstream targets, guiding the way to novel cancer therapeutics. *Wiley Interdiscip. Rev. RNA*, 9(4): e1476, 2018. [*PubMed Central* ID: PMC6002934] [DOI: 10.1002/wrna.1476] [*PubMed* ID: 29693319]. [Citado en pp. 26, 28, y 37]

[223] O. Anczuków y A. R. Krainer. Splicing-factor alterations in cancers. *RNA*, 22(9): 1285–1301, 2016. [*PubMed Central* ID: PMC4986885] [DOI: 10.1261/rna.057919.116] [*PubMed* ID: 27530828]. [Citado en p. 25]

[224] K. Yoshida, M. Sanada, Y. Shiraishi, *et al.* Frequent pathway mutations of splicing machinery in myelodysplasia. *Nature*, 478(7367): 64–69, 2011. [DOI: 10.1038/nature10496] [*PubMed* ID: 21909114]. [Citado en p. 25]

[225] E. Papaemmanuil, M. Cazzola, J. Boultwood, *et al.* Somatic SF3B1 mutation in myelodysplasia with ring sideroblasts. *N. Engl. J. Med.*, 365(15): 1384–1395, 2011. [*PubMed Central* ID: PMC3322589] [DOI: 10.1056/NEJMoa1103283] [*PubMed* ID: 21995386]. [Citado en p. 25]

[226] V. Quesada, L. Conde, N. Villamor, *et al.* Exome sequencing identifies recurrent mutations of the splicing factor SF3B1 gene in chronic lymphocytic leukemia. *Nat Genet*, 44(1): 47–52, 2011. [DOI: 10.1038/ng.1032] [*PubMed* ID: 22158541]. [Citado en p. 25]

[227] D. Rossi, A. Bruscaggin, V. Spina, *et al.* Mutations of the SF3B1 splicing factor in chronic lymphocytic leukemia: association with progression and fludarabine-refractoriness. *Blood*, 118(26): 6904–6908, 2011. [*PubMed Central* ID: PMC3245210] [DOI: 10.1182/blood-2011-08-373159] [*PubMed* ID: 22039264]. [Citado en p. 25]

[228] L. Wang, M. S. Lawrence, Y. Wan, *et al.* SF3B1 and other novel cancer genes in chronic lymphocytic leukemia. *N. Engl. J. Med.*, 365(26): 2497–2506, 2011. [*PubMed Central* ID: PMC3685413] [DOI: 10.1056/NEJMoa1109016] [*PubMed* ID: 22150006]. [Citado en p. 25]

[229] A. Kurtovic-Kozaric, B. Przychodzen, J. Singh, *et al.* PRPF8 defects cause missplicing in myeloid malignancies. *Leukemia*, 29(1): 126–136, 2015. [*PubMed Central* ID: PMC4214909] [DOI: 10.1038/leu.2014.144] [*PubMed* ID: 24781015]. [Citado en p. 25]

[230] H. Dvinge, E. Kim, O. Abdel-Wahab, y R. K. Bradley. RNA splicing factors as oncoproteins and tumour suppressors. *Nat. Rev. Cancer*, 16(7): 413–430, 2016. [*PubMed Central* ID: PMC5094465] [DOI: 10.1038/nrc.2016.51] [*PubMed* ID: 27282250]. [Citado en p. 26]

[231] E. Sebestyén, B. Singh, B. Miñana, *et al.* Large-scale analysis of genome and transcriptome alterations in multiple tumors unveils novel cancer-relevant splicing networks. *Genome Res.*, 26(6): 732–744, 2016. [*PubMed Central* ID: PMC4889968] [DOI: 10.1101/gr.199935.115] [*PubMed* ID: 27197215]. [Citado en p. 26]

[232] A. Sveen, S. Kilpinen, A. Ruusulehto, *et al.* Aberrant RNA splicing in cancer; expression changes and driver mutations of splicing factor genes. *Oncogene*, 35(19): 2413–2427, 2016. [DOI: 10.1038/onc.2015.318] [*PubMed* ID: 26300000]. [Citado en p. 26]

[233] R. I. Skotheim y M. Nees. Alternative splicing in cancer: noise, functional, or systematic? *Int J Biochem Cell Biol*, 39(7-8): 1432–1449, 2007. [DOI: 10.1016/j.biocel.2007.02.016] [*PubMed* ID: 17416541]. [Citado en p. 26]

[234] R. Karni, E. de Stanchina, S. W. Lowe, *et al.* The gene encoding the splicing factor SF2/ASF is a proto-oncogene. *Nat Struct Mol Biol*, 14(3): 185–193, 2007. [*PubMed Central* ID: PMC4595851] [DOI: 10.1038/nsmb1209] [*PubMed* ID: 17310252]. [Citado en pp. 26 y 27]

[235] S. Das, O. Anczuków, M. Akerman, y A. R. Krainer. Oncogenic splicing factor SRSF1 is a critical transcriptional target of MYC. *Cell Rep.*, 1(2): 110–117, 2012. [*PubMed Central* ID: PMC3334311] [DOI: 10.1016/j.celrep.2011.12.001] [*PubMed* ID: 22545246]. [Citado en p. 26]

[236] O. Anczuków, M. Akerman, A. Cléry, *et al.* SRSF1-Regulated Alternative Splicing in Breast Cancer. *Mol. Cell*, 60(1): 105–117, 2015. [*PubMed Central* ID: PMC4597910] [DOI: 10.1016/j.molcel.2015.09.005] [*PubMed* ID: 26431027]. [Citado en p. 26]

[237] O. Anczuków, A. Z. Rosenberg, M. Akerman, *et al.* The splicing factor SRSF1 regulates apoptosis and proliferation to promote mammary epithelial cell transformation. *Nat Struct Mol Biol*, 19(2): 220–228, 2012. [*PubMed Central* ID: PMC3272117] [DOI: 10.1038/nsmb.2207] [*PubMed* ID: 22245967]. [Citado en pp. 26 y 27]

[238] J. X. Du, Y. H. Luo, S. J. Zhang, *et al.* Splicing factor SRSF1 promotes breast cancer progression via oncogenic splice switching of PTPMT1. *J. Exp. Clin. Cancer Res.*, 40(1): 171, 2021. [*PubMed Central* ID: PMC8122567] [DOI: 10.1186/s13046-021-01978-8] [*PubMed* ID: 33992102]. [Citado en p. 26]

[239] V. Ben-Hur, P. Denichenko, Z. Siegfried, *et al.* S6K1 alternative splicing modulates its oncogenic activity and regulates mTORC1. *Cell Rep.*, 3(1): 103–115, 2013. [*PubMed Central* ID: PMC5021319] [DOI: 10.1016/j.celrep.2012.11.020] [*PubMed* ID: 23273915]. [Citado en p. 27]

[240] H. Mei, Y. Wang, J. Fan, y Z. Lin. Alternative splicing of S6K1 promotes non-small cell lung cancer survival. *Tumour. Biol.*, 37(10): 13369–13376, 2016. [DOI: 10.1007/s13277-016-5253-1] [*PubMed* ID: 27460085]. [Citado en p. 27]

[241] J. Bae, C. P. Leo, S. Y. Hsu, y A. J. Hsueh. MCL-1S, a splicing variant of the antiapoptotic BCL-2 family member MCL-1, encodes a proapoptotic protein possessing only the BH3 domain. *J. Biol. Chem.*, 275(33): 25255–25261, 2000. [DOI: 10.1074/jbc.M909826199] [*PubMed* ID: 10837489]. [Citado en p. 27]

[242] C. D. Bingle, R. W. Craig, B. M. Swales, *et al.* Exon skipping in Mcl-1 results in a bcl-2 homology domain 3 only gene product that promotes cell death. *J. Biol. Chem.*, 275(29): 22136–22146, 2000. [DOI: 10.1074/jbc.M909572199] [*PubMed* ID: 10766760]. [Citado en p. 27]

[243] M. Ladomery. Aberrant alternative splicing is another hallmark of cancer. *Int. J. Cell Biol.*, 2013: 463786, 2013. [*PubMed Central* ID: PMC3786539] [DOI: 10.1155/2013/463786] [*PubMed* ID: 24101931]. [Citado en p. 27]

[244] S. J. Harper y D. O. Bates. VEGF-A splicing: the key to anti-angiogenic therapeutics? *Nat. Rev. Cancer*, 8(11): 880–887, 2008. [*PubMed Central* ID: PMC2613352] [DOI: 10.1038/nrc2505] [*PubMed* ID: 18923433]. [Citado en p. 27]

[245] H. R. Christofk, M. G. Vander Heiden, M. H. Harris, *et al.* The M2 splice isoform of pyruvate kinase is important for cancer metabolism and tumour growth. *Nature*, 452(7184): 230–233, 2008. [DOI: 10.1038/nature06734] [*PubMed* ID: 18337823]. [Citado en p. 27]

[246] T. Y. Hsu, L. M. Simon, N. J. Neill, *et al.* The spliceosome is a therapeutic vulnerability in MYC-driven cancer. *Nature*, 525(7569): 384–388, 2015. [*PubMed Central* ID: PMC4831063] [DOI: 10.1038/nature14985] [*PubMed* ID: 26331541]. [Citado en p. 27]

[247] S. C. Lee, K. North, E. Kim, *et al.* Synthetic Lethal and Convergent Biological Effects of Cancer-Associated Spliceosomal Gene Mutations. *Cancer Cell*, 34(2): 225–241, 2018. [*PubMed Central* ID: PMC6373472] [DOI: 10.1016/j.ccell.2018.07.003] [*PubMed* ID: 30107174]. [Citado en p. 27]

[248] T. R. Webb, A. S. Joyner, y P. M. Potter. The development and application of small molecule modulators of SF3b as therapeutic agents for cancer. *Drug Discov Today*, 18(1-2): 43–49, 2013. [*PubMed Central* ID: PMC3596818] [DOI: 10.1016/j.drudis.2012.07.013] [*PubMed* ID: 22885522]. [Citado en p. 27]

[249] S. Bonnal, L. Vigevani, y J. Valcárcel. The spliceosome as a target of novel antitumour drugs. *Nat. Rev. Drug Discov.*, 11(11): 847–859, 2012. [DOI: 10.1038/nrd3823] [*PubMed* ID: 23123942]. [Citado en p. 27]

[250] K. C. Nicolaou, D. Rhoades, y S. M. Kumar. Total Syntheses of Thailanstatins A-C, Spliceostatin D, and Analogues Thereof. Stereodivergent Synthesis of Tetrasubstituted Dihydro- and Tetrahydropyrans and Design, Synthesis, Biological Evaluation, and Discovery of Potent Antitumor Agents. *J. Am. Chem. Soc.*, 140(26): 8303–8320, 2018. [DOI: 10.1021/jacs.8b04634] [*PubMed* ID: 29943984]. [Citado en p. 27]

[251] M. Seiler, A. Yoshimi, R. Darman, *et al.* H3B-8800, an orally available small-molecule splicing modulator, induces lethality in spliceosome-mutant cancers. *Nat. Med.*, 24(4): 497–504, 2018. [*PubMed Central* ID: PMC6730556] [DOI: 10.1038/nm.4493] [*PubMed* ID: 29457796]. [Citado en p. 28]

[252] A. Fedoriw, S. R. Rajapurkar, S. O'Brien, *et al.* Anti-tumor Activity of the Type I PRMT Inhibitor, GSK3368715, Synergizes with PRMT5 Inhibition through MTAP Loss. *Cancer Cell*, 36(1): 100–114, 2019. [DOI: 10.1016/j.ccell.2019.05.014] [*PubMed* ID: 31257072]. [Citado en p. 28]

[253] J. Tang, A. Frankel, R. J. Cook, *et al.* PRMT1 is the predominant type I protein arginine methyltransferase in mammalian cells. *J. Biol. Chem.*, 275(11): 7723–7730, 2000. [DOI: 10.1074/jbc.275.11.7723] [*PubMed* ID: 10713084]. [Citado en p. 28]

[254] S. V. Gerhart, W. A. Kellner, C. Thompson, *et al.* Activation of the p53-MDM4 regulatory axis defines the anti-tumour response to PRMT5 inhibition through its role in regulating cellular splicing. *Sci. Rep.*, 8(1): 9711, 2018. [*PubMed Central* ID: PMC6018746] [DOI: 10.1038/s41598-018-28002-y] [*PubMed* ID: 29946150]. [Citado en p. 28]

[255] D. Brehmer, L. Beke, T. Wu, *et al.* Discovery and Pharmacological Characterization of JNJ-64619178, a Novel Small-Molecule Inhibitor of PRMT5 with Potent Antitumor Activity. *Mol. Cancer Ther.*, 20(12): 2317–2328, 2021. [DOI: 10.1158/1535-7163.MCT-21-0367] [*PubMed* ID: 34583982]. [Citado en p. 28]

[256] K. Jensen-Pergakes, J. Tatlock, K. A. Maegley, *et al.* SAM-Competitive PRMT5 Inhibitor PF-06939999 Demonstrates Antitumor Activity in Splicing Dysregulated NSCLC with Decreased Liability of Drug Resistance. *Mol. Cancer Ther.*, 21(1): 3–15, 2022. [DOI: 10.1158/1535-7163.MCT-21-0620] [*PubMed* ID: 34737197]. [Citado en p. 29]

[257] H. Lin, M. Wang, Y. W. Zhang, *et al.* Discovery of Potent and Selective Covalent Protein Arginine Methyltransferase 5 (PRMT5) Inhibitors. *ACS Med. Chem. Lett.*, 10(7): 1033–1038, 2019. [*PubMed Central* ID: PMC6627734] [DOI: 10.1021/acsmedchemlett.9b00074] [*PubMed* ID: 31312404]. [Citado en p. 29]

[258] B. Pilch, E. Allemand, M. Facompré, *et al.* Specific inhibition of serine- and arginine-rich splicing factors phosphorylation, spliceosome assembly, and splicing by the antitumor drug NB-506. *Cancer Res.*, 61(18): 6876–6884, 2001. [*PubMed* ID: 11559564]. [Citado en p. 29]

[259] C. C. Lee, W. H. Chang, Y. S. Chang, *et al.* 4β-Hydroxywithanolide E Modulates Alternative Splicing of Apoptotic Genes in Human Hepatocellular Carcinoma Huh-7 Cells. *Sci. Rep.*, 7(1): 7290, 2017. [*PubMed Central* ID: PMC5544667] [DOI: 10.1038/s41598-017-07472-6] [*PubMed* ID: 28779122]. [Citado en p. 29]

[260] R. Tummala, W. Lou, A. C. Gao, y N. Nadiminty. Quercetin Targets hnRNPA1 to Overcome Enzalutamide Resistance in Prostate Cancer Cells. *Mol. Cancer Ther.*, 16(12): 2770–2779, 2017. [*PubMed Central* ID: PMC5716891] [DOI: 10.1158/1535-7163.MCT-17-0030] [*PubMed* ID: 28729398]. [Citado en p. 29]

[261] W. H. Chang, T. C. Liu, W. K. Yang, *et al.* Amiloride modulates alternative splicing in leukemic cells and resensitizes Bcr-AblT315I mutant cells to imatinib. *Cancer Res.*, 71(2): 383–392, 2011. [DOI: 10.1158/0008-5472.CAN-10-1037] [*PubMed* ID: 21224352]. [Citado en pp. 29 y 109]

[262] J. G. Chang, D. M. Yang, W. H. Chang, *et al.* Small molecule amiloride modulates oncogenic RNA alternative splicing to devitalize human cancer cells. *PLoS One*, 6(6): e18643, 2011. [*PubMed Central* ID: PMC3111415] [DOI: 10.1371/journal.pone.0018643] [*PubMed* ID: 21694768]. [Citado en pp. 29 y 109]

[263] T. Uehara, Y. Minoshima, K. Sagane, *et al.* Selective degradation of splicing factor CAPERα by anticancer sulfonamides. *Nat. Chem. Biol.*, 13(6): 675–680, 2017. [DOI: 10.1038/nchembio.2363] [*PubMed* ID: 28437394]. [Citado en p. 29]

[264] J. Soret, N. Bakkour, S. Maire, *et al.* Selective modification of alternative splicing by indole derivatives that target serine-arginine-rich protein splicing factors. *Proc. Natl. Acad. Sci. U.S.A.*, 102(24): 8764–8769, 2005. [*PubMed Central* ID: PMC1150812] [DOI: 10.1073/pnas.0409829102] [*PubMed* ID: 15939885]. [Citado en p. 29]

[265] C. Ghigna, M. De Toledo, S. Bonomi, *et al.* Pro-metastatic splicing of Ron proto-oncogene mRNA can be reversed: therapeutic potential of bifunctional oligonucleotides and indole derivatives. *RNA Biol.*, 7(4): 495–503, 2010. [DOI: 10.4161/rna.7.4.12744] [*PubMed* ID: 20864806]. [Citado en p. 29]

[266] R. P. Siqueira, é. d. e. A. Barbosa, M. D. Polêto, *et al.* Potential Antileukemia Effect and Structural Analyses of SRPK Inhibition by N-(2-(Piperidin-1-yl)-5-(Trifluoromethyl)Phenyl)Isonicotinamide (SRPIN340). *PLoS One*, 10(8): e0134882, 2015. [*PubMed Central* ID: PMC4526641] [DOI: 10.1371/journal.pone.0134882] [*PubMed* ID: 26244849]. [Citado en p. 29]

[267] D. O. Bates, J. C. Morris, S. Oltean, y L. F. Donaldson. Pharmacology of Modulators of Alternative Splicing. *Pharmacol. Rev.*, 69(1): 63–79, 2017. [*PubMed Central* ID: PMC5226212] [DOI: 10.1124/pr.115.011239] [*PubMed* ID: 28034912]. [Citado en p. 29]

[268] I. Younis, M. Berg, D. Kaida, *et al.* Rapid-response splicing reporter screens identify differential regulators of constitutive and alternative splicing. *Mol. Cell Biol.*, 30(7): 1718–1728, 2010. [*PubMed Central* ID: PMC2838070] [DOI: 10.1128/MCB.01301-09] [*PubMed* ID: 20123975]. [Citado en p. 29]

[269] M. Sakuma, K. Iida, y M. Hagiwara. Deciphering targeting rules of splicing modulator compounds: case of TG003. *BMC Mol. Biol.*, 16: 16, 2015. [*PubMed Central* ID: PMC4580995] [DOI: 10.1186/s12867-015-0044-6] [*PubMed* ID: 26400733]. [Citado en p. 29]

[270] K. Iwai, M. Yaguchi, K. Nishimura, *et al.* Anti-tumor efficacy of a novel CLK inhibitor via targeting RNA splicing and MYC-dependent vulnerability. *EMBO Mol. Med.*, 10(6), 2018. [*PubMed Central* ID: PMC5991599] [DOI: 10.15252/emmm.201708289] [*PubMed* ID: 29769258]. [Citado en p. 29]

[271] J. Tazi, N. Bakkour, J. Soret, *et al.* Selective inhibition of topoisomerase I and various steps of spliceosome assembly by diospyrin derivatives. *Mol. Pharmacol.*, 67(4): 1186–1194, 2005. [DOI: 10.1124/mol.104.007633] [*PubMed* ID: 15625279]. [Citado en p. 30]

[272] K. A. Effenberger, V. K. Urabe, y M. S. Jurica. Modulating splicing with small molecular inhibitors of the spliceosome. *Wiley Interdiscip. Rev. RNA*, 8(2), 2017. [*PubMed Central* ID: PMC5253128] [DOI: 10.1002/wrna.1381] [*PubMed* ID: 27440103]. [Citado en p. 30]

[273] J. Lewin, J. C. Soria, A. Stathis, *et al.* Phase Ib Trial With Birabresib, a Small-Molecule Inhibitor of Bromodomain and Extraterminal Proteins, in Patients With Selected Advanced Solid Tumors. *J. Clin. Oncol.*, 36(30): 3007–3014, 2018. [DOI: 10.1200/JCO.2018.78.2292] [*PubMed* ID: 29733771]. [Citado en p. 30]

[274] R. Vázquez, M. E. Riveiro, L. Astorgues-Xerri, *et al.* The bromodomain inhibitor OTX015 (MK-8628) exerts anti-tumor activity in triple-negative breast cancer models as single agent and in combination with everolimus. *Oncotarget*, 8(5): 7598–7613, 2017. [*PubMed Central* ID: PMC5352346] [DOI: 10.18632/oncotarget.13814] [*PubMed* ID: 27935867]. [Citado en p. 30]

[275] I. A. Asangani, K. Wilder-Romans, V. L. Dommeti, *et al.* BET Bromodomain Inhibitors Enhance Efficacy and Disrupt Resistance to AR Antagonists in the Treatment of Prostate Cancer. *Mol. Cancer Res.*, 14(4): 324–331, 2016. [*PubMed Central* ID: PMC4834259] [DOI: 10.1158/1541-7786.MCR-15-0472] [*PubMed* ID: 26792867]. [Citado en p. 30]

[276] Laura Tsujikawa, Karen Norek, Cyrus Calosing, *et al.* Abstract LB-038: Preclinical development and clinical validation of a whole blood pharmacodynamic marker assay for the BET bromodomain inhibitor ZEN-3694 in metastatic castration-resistant prostate cancer (mCRPC) patients. *Cancer Res.*, 77(Supplement 13): LB–038, 2017. [DOI: 10.1158/1538-7445.AM2017-LB-038]. [Citado en p. 30]

[277] C. F. Bennett y E. E. Swayze. RNA targeting therapeutics: molecular mechanisms of antisense oligonucleotides as a therapeutic platform. *Annu. Rev. Pharmacol. Toxicol.*, 50: 259–293, 2010. [DOI: 10.1146/annurev.pharmtox.010909.105654] [*PubMed* ID: 20055705]. [Citado en p. 30]

[278] C. F. Bennett. Therapeutic Antisense Oligonucleotides Are Coming of Age. *Annu. Rev. Med.*, 70: 307–321, 2019. [DOI: 10.1146/annurev-med-041217-010829] [*PubMed* ID: 30691367]. [Citado en p. 30]

[279] L. Wan y G. Dreyfuss. Splicing-Correcting Therapy for SMA. *Cell*, 170(1): 5, 2017. [DOI: 10.1016/j.cell.2017.06.028] [*PubMed* ID: 28666123]. [Citado en p. 30]

[280] M. Mogilevsky, O. Shimshon, S. Kumar, *et al.* Modulation of MKNK2 alternative splicing by splice-switching oligonucleotides as a novel approach for glioblastoma treatment. *Nucleic Acids Res.*, 46(21): 11396–11404, 2018. [*PubMed Central* ID: PMC6265459] [DOI: 10.1093/nar/gky921] [*PubMed* ID: 30329087]. [Citado en p. 30]

[281] D. P. Lane, C. F. Cheok, C. Brown, *et al.* Mdm2 and p53 are highly conserved from placozoans to man. *Cell Cycle*, 9(3): 540–547, 2010. [DOI: 10.4161/cc.9.3.10516] [*PubMed* ID: 20081368]. [Citado en p. 31]

[282] G. Matlashewski, P. Lamb, D. Pim, *et al.* Isolation and characterization of a human p53 cDNA clone: expression of the human p53 gene. *EMBO J.*, 3(13): 3257–3262, 1984. [*PubMed Central* ID: PMC557846] [DOI: 10.1002/j.1460-2075.1984.tb02287.x] [*PubMed* ID: 6396087]. [Citado en p. 31]

[283] D. Wolf, N. Harris, N. Goldfinger, y V. Rotter. Isolation of a full-length mouse cDNA clone coding for an immunologically distinct p53 molecule. *Mol. Cell Biol.*, 5(1): 127–132, 1985. [*PubMed Central* ID: PMC366686] [DOI: 10.1128/mcb.5.1.127-132.1985] [*PubMed* ID: 2580227]. [Citado en p. 31]

[284] J. C. Bourdon, K. Fernandes, F. Murray-Zmijewski, *et al.* p53 isoforms can regulate p53 transcriptional activity. *Genes Dev.*, 19(18): 2122–2137, 2005. [*PubMed Central* ID: PMC1221884] [DOI: 10.1101/gad.1339905] [*PubMed* ID: 16131611]. [Citado en pp. 31, 107, y 108]

[285] S. Courtois, G. Verhaegh, S. North, *et al.* DeltaN-p53, a natural isoform of p53 lacking the first transactivation domain, counteracts growth suppression by wild-type p53. *Oncogene*, 21(44): 6722–6728, 2002. [DOI: 10.1038/sj.onc.1205874] [*PubMed* ID: 12360399]. [Citado en p. 32]

[286] V. Marcel, S. Perrier, M. Aoubala, *et al.* Δ160p53 is a novel N-terminal p53 isoform encoded by Δ133p53 transcript. *FEBS Lett.*, 584(21): 4463–4468, 2010. [DOI: 10.1016/j.febslet.2010.10.005] [*PubMed* ID: 20937277]. [Citado en p. 32]

[287] S. M. Joruiz y J. C. Bourdon. p53 Isoforms: Key Regulators of the Cell Fate Decision. *Cold Spring Harb. Perspect. Med.*, 6(8), 2016. [*PubMed Central* ID: PMC4968168] [DOI: 10.1101/cshperspect.a026039] [*PubMed* ID: 26801896]. [Citado en p. 32]

[288] T. Anbarasan y J. C. Bourdon. The Emerging Landscape of p53 Isoforms in Physiology, Cancer and Degenerative Diseases. *Int. J. Mol. Sci.*, 20(24), 2019. [*PubMed Central* ID: PMC6941119] [DOI: 10.3390/ijms20246257] [*PubMed* ID: 31835844]. [Citado en p. 32]

[289] J. C. Bourdon, M. P. Khoury, A. Diot, *et al.* p53 mutant breast cancer patients expressing p53γ have as good a prognosis as wild-type p53 breast cancer patients. *Breast Cancer Res.*, 13(1): R7, 2011. [*PubMed Central* ID: PMC3109573] [DOI: 10.1186/bcr2811] [*PubMed* ID: 21251329]. [Citado en pp. 34 y 108]

[290] M. Kazantseva, R. A. Eiholzer, S. Mehta, *et al.* Elevation of the TP53 isoform Δ133p53β in glioblastomas: an alternative to mutant p53 in promoting tumor development. *J. Pathol.*, 246(1): 77–88, 2018. [*PubMed Central* ID: PMC6120556] [DOI: 10.1002/path.5111] [*PubMed* ID: 29888503]. [Citado en p. 34]

[291] A. Tadijan, F. Precazzini, N. Hanžić, *et al.* Altered Expression of Shorter p53 Family Isoforms Can Impact Melanoma Aggressiveness. *Cancers (Basel)*, 13(20), 2021. [*PubMed Central* ID: PMC8533715] [DOI: 10.3390/cancers13205231] [*PubMed* ID: 34680379]. [Citado en p. 34]

[292] K. A. Avery-Kiejda, X. D. Zhang, L. J. Adams, *et al.* Small molecular weight variants of p53 are expressed in human melanoma cells and are induced by the DNA-damaging agent cisplatin. *Clin. Cancer Res.*, 14(6): 1659–1668, 2008. [DOI: 10.1158/1078-0432.CCR-07-1422] [*PubMed* ID: 18310316]. [Citado en p. 34]

[293] W. Song, S. W. Huo, J. J. Lü, *et al.* Expression of p53 isoforms in renal cell carcinoma. *Chin. Med. J. (Engl.)*, 122(8): 921–926, 2009. [*PubMed* ID: 19493415]. [Citado en p. 34]

[294] L. Boldrup, J. C. Bourdon, P. J. Coates, *et al.* Expression of p53 isoforms in squamous cell carcinoma of the head and neck. *Eur. J. Cancer.*, 43(3): 617–623, 2007. [*PubMed Central* ID: PMC3523263] [DOI: 10.1016/j.ejca.2006.10.019] [*PubMed* ID: 17215121]. [Citado en p. 34]

[295] R. Takahashi, C. Giannini, J. N. Sarkaria, *et al.* p53 isoform profiling in glioblastoma and injured brain. *Oncogene*, 32(26): 3165–3174, 2013. [*PubMed Central* ID: PMC3904233] [DOI: 10.1038/onc.2012.322] [*PubMed* ID: 22824800]. [Citado en p. 34]

[296] N. Anensen, A. M. Oyan, J. C. Bourdon, *et al.* A distinct p53 protein isoform signature reflects the onset of induction chemotherapy for acute myeloid leukemia. *Clin. Cancer Res.*, 12(13): 3985–3992, 2006. [DOI: 10.1158/1078-0432.CCR-05-1970] [*PubMed* ID: 16818696]. [Citado en p. 34]

[297] S. Surget, M. P. Khoury, y J. C. Bourdon. Uncovering the role of p53 splice variants in human malignancy: a clinical perspective. *OncoTargets Ther.*, 7: 57–68, 2013. [*PubMed Central* ID: PMC3872270] [DOI: 10.2147/OTT.S53876] [*PubMed* ID: 24379683]. [Citado en p. 34]

[298] G. Hofstetter, A. Berger, E. Schuster, *et al.* Δ133p53 is an independent prognostic marker in p53 mutant advanced serous ovarian cancer. *Br. J. Cancer*, 105(10): 1593–1599, 2011. [*PubMed Central* ID: PMC3242533] [DOI: 10.1038/bjc.2011.433] [*PubMed* ID: 22009029]. [Citado en pp. 34 y 108]

[299] G. Hofstetter, A. Berger, R. Berger, *et al.* The N-terminally truncated p53 isoform Δ40p53 influences prognosis in mucinous ovarian cancer. *Int. J. Gynecol. Cancer*, 22(3): 372–379, 2012. [DOI: 10.1097/IGC.0b013e31823ca031] [*PubMed* ID: 22246403]. [Citado en p. 34]

[300] M. P. Khoury, V. Marcel, K. Fernandes, *et al.* Detecting and quantifying p53 isoforms at mRNA level in cell lines and tissues. *Methods Mol. Biol.*, 962: 1–14, 2013. [DOI: 10.1007/978-1-62703-236-0_1] [*PubMed* ID: 23150433]. [Citado en p. 34]

[301] V. Marcel, M. P. Khoury, K. Fernandes, *et al.* Detecting p53 isoforms at protein level. *Methods Mol. Biol.*, 962: 15–29, 2013. [DOI: 10.1007/978-1-62703-236-0_2] [*PubMed* ID: 23150434]. [Citado en p. 34]

[302] F. Zhan, J. Hardin, B. Kordsmeier, *et al.* Global gene expression profiling of multiple myeloma, monoclonal gammopathy of undetermined significance, and normal bone marrow plasma cells. *Blood*, 99(5): 1745–1757, 2002. [DOI: 10.1182/blood.v99.5.1745] [*PubMed* ID: 11861292]. [Citado en p. 37]

[303] D. Hanahan y R. A. Weinberg. Hallmarks of cancer: the next generation. *Cell*, 144(5): 646–674, 2011. [DOI: 10.1016/j.cell.2011.02.013] [*PubMed* ID: 21376230]. [Citado en p. 105]

[304] S. Z. Usmani, B. Nair, P. Qu, *et al.* Primary plasma cell leukemia: clinical and laboratory presentation, gene-expression profiling and clinical outcome with Total Therapy protocols. *Leukemia*, 26(11): 2398–2405, 2012. [*PubMed Central* ID: PMC3426639] [DOI: 10.1038/leu.2012.107] [*PubMed* ID: 22508408]. [Citado en p. 105]

[305] K. Todoerti, L. Agnelli, S. Fabris, *et al.* Transcriptional characterization of a prospective series of primary plasma cell leukemia reveals signatures associated with tumor progression and poorer outcome. *Clin. Cancer Res.*, 19(12): 3247–3258, 2013. [DOI: 10.1158/1078-0432.CCR-12-3461] [*PubMed* ID: 23599371]. [Citado en p. 105]

[306] S. Wieland, R. Thimme, R. H. Purcell, y F. V. Chisari. Genomic analysis of the host response to hepatitis B virus infection. *Proc. Natl. Acad. Sci. U.S.A.*, 101(17): 6669–6674, 2004. [*PubMed Central* ID: PMC404103] [DOI: 10.1073/pnas.0401771101] [*PubMed* ID: 15100412]. [Citado en p. 106]

[307] H. Zhu, J. P. Cong, G. Mamtora, *et al.* Cellular gene expression altered by human cytomegalovirus: global monitoring with oligonucleotide arrays. *Proc. Natl. Acad. Sci. U.S.A.*, 95(24): 14470–14475, 1998. [*PubMed Central* ID: PMC24397] [DOI: 10.1073/pnas.95.24.14470] [*PubMed* ID: 9826724]. [Citado en p. 106]

[308] C. N. Ellis, R. C. LaRocque, T. Uddin, *et al.* Comparative proteomic analysis reveals activation of mucosal innate immune signaling pathways during cholera. *Infect. Immun.*, 83(3): 1089–1103, 2015. [*PubMed Central* ID: PMC4333457] [DOI: 10.1128/IAI.02765-14] [*PubMed* ID: 25561705]. [Citado en p. 106]

[309] N. Lee, T. A. Yario, J. S. Gao, y J. A. Steitz. EBV noncoding RNA EBER2 interacts with host RNA-binding proteins to regulate viral gene expression. *Proc. Natl. Acad. Sci. U.S.A.*, 113(12): 3221–3226, 2016. [*PubMed Central* ID: PMC4812724] [DOI: 10.1073/pnas.1601773113] [*PubMed* ID: 26951683]. [Citado en p. 106]

[310] A. V. Nanni y N. Lee. Identification of host RNAs that interact with EBV noncoding RNA EBER2. *RNA Biol.*, 15(9): 1181–1191, 2018. [*PubMed Central* ID: PMC6284586] [DOI: 10.1080/15476286.2018.1518854] [*PubMed* ID: 30176159]. [Citado en p. 106]

[311] H. C. Lee, E. S. Lee, M. B. Uddin, *et al.* Released Tryptophanyl-tRNA Synthetase Stimulates Innate Immune Responses against Viral Infection. *J. Virol.*, 93(2), 2019. [*PubMed Central* ID: PMC6321899] [DOI: 10.1128/JVI.01291-18] [*PubMed* ID: 30355684]. [Citado en p. 106]

[312] J. L. Head y B. P. Lawrence. The aryl hydrocarbon receptor is a modulator of anti-viral immunity. *Biochem. Pharmacol.*, 77(4): 642–653, 2009. [*PubMed Central* ID: PMC2662440] [DOI: 10.1016/j.bcp.2008.10.031] [*PubMed* ID: 19027719]. [Citado en p. 106]

[313] M. F. Torti, F. Giovannoni, F. J. Quintana, y C. C. García. The Aryl Hydrocarbon Receptor as a Modulator of Anti-viral Immunity. *Front. Immunol.*, 12: 624293, 2021. [*PubMed Central* ID: PMC7973006] [DOI: 10.3389/fimmu.2021.624293] [*PubMed* ID: 33746961]. [Citado en p. 106]

[314] P. Xue, J. Fu, y Y. Zhou. The Aryl Hydrocarbon Receptor and Tumor Immunity. *Front. Immunol.*, 9: 286, 2018. [*PubMed Central* ID: PMC5816799] [DOI: 10.3389/fimmu.2018.00286] [*PubMed* ID: 29487603]. [Citado en p. 106]

[315] A. Bianchi-Smiraglia, A. Bagati, E. E. Fink, *et al.* Inhibition of the aryl hydrocarbon receptor/polyamine biosynthesis axis suppresses multiple myeloma. *J. Clin. Invest.*, 128(10): 4682–4696, 2018. [*PubMed Central* ID: PMC6159960] [DOI: 10.1172/JCI70712] [*PubMed* ID: 30198908]. [Citado en p. 106]

[316] L. Castagnoli, M. Iezzi, G. C. Ghedini, *et al.* Activated d16HER2 homodimers and SRC kinase mediate optimal efficacy for trastuzumab. *Cancer Res.*, 74(21): 6248–6259, 2014. [DOI: 10.1158/0008-5472.CAN-14-0983] [*PubMed* ID: 25164009]. [Citado en p. 107]

[317] D. M. Cittelly, P. M. Das, V. A. Salvo, *et al.* Oncogenic HER2Delta16 suppresses miR-15a/16 and deregulates BCL-2 to promote endocrine resistance of breast tumors. *Carcinogenesis*, 31(12): 2049–2057, 2010. [*PubMed Central* ID: PMC2994280] [DOI: 10.1093/carcin/bgq192] [*PubMed* ID: 16778220]. [Citado en p. 107]

[318] K. A. Avery-Kiejda, B. Morten, M. W. Wong-Brown, *et al.* The relative mRNA expression of p53 isoforms in breast cancer is associated with clinical features and outcome. *Carcinogenesis*, 35(3): 586–596, 2014. [DOI: 10.1093/carcin/bgt411] [*PubMed* ID: 24336193]. [Citado en pp. 107 y 108]

[319] G. Gadea, N. Arsic, K. Fernandes, *et al.* drives invasion through expression of its Δ133p53β variant. *Elife*, 5, 2016. [*PubMed Central* ID: PMC5067115] [DOI: 10.7554/eLife.14734] [*PubMed* ID: 27630122]. [Citado en pp. 107 y 108]

[320] K. Fujita, A. M. Mondal, I. Horikawa, *et al.* p53 isoforms Delta133p53 and p53beta are endogenous regulators of replicative cellular senescence. *Nat. Cell. Biol.*, 11(9): 1135–1142, 2009. [*PubMed Central* ID: PMC2802853] [DOI: 10.1038/ncb1928] [*PubMed* ID: 19701195]. [Citado en p. 108]

[321] K. Bischof, S. Knappskog, S. M. Hjelle, *et al.* Influence of p53 Isoform Expression on Survival in High-Grade Serous Ovarian Cancers. *Sci. Rep.*, 9(1): 5244, 2019. [*PubMed Central* ID: PMC6437169] [DOI: 10.1038/s41598-019-41706-z] [*PubMed* ID: 30918304]. [Citado en p. 108]

[322] P. Ozretić, N. Hanžić, B. Proust, *et al.* Expression profiles of p53/p73, NME and GLI families in metastatic melanoma tissue and cell lines. *Sci. Rep.*, 9(1): 12470, 2019. [*PubMed Central* ID: PMC6713730] [DOI: 10.1038/s41598-019-48882-y] [*PubMed* ID: 31462745]. [Citado en p. 108]

[323] I. Haaland, S. M. Hjelle, H. Reikvam, *et al.* p53 Protein Isoform Profiles in AML: Correlation with Distinct Differentiation Stages and Response to Epigenetic Differentiation Therapy. *Cells*, 10(4), 2021. [*PubMed Central* ID: PMC8068061] [DOI: 10.3390/cells10040833] [*PubMed* ID: 33917201]. [Citado en p. 108]

[324] K. Bischof, S. Knappskog, I. Stefansson, *et al.* High expression of the p53 isoform γ is associated with reduced progression-free survival in uterine serous carcinoma. *BMC Cancer*, 18(1): 684, 2018. [*PubMed Central* ID: PMC6019524] [DOI: 10.1186/s12885-018-4591-3] [*PubMed* ID: 29940909]. [Citado en p. 108]

[325] Y. T. Zheng, H. Y. Yang, T. Li, *et al.* Amiloride sensitizes human pancreatic cancer cells to erlotinib in vitro through inhibition of the PI3K/AKT signaling pathway. *Acta Pharmacol. Sin.*, 36(5): 614–626, 2015. [*PubMed Central* ID: PMC4422948] [DOI: 10.1038/aps.2015.4] [*PubMed* ID: 25864651]. [Citado en p. 109]

[326] L. J. Leon, N. Pasupuleti, F. Gorin, y K. L. Carraway. A cell-permeant amiloride derivative induces caspase-independent, AIF-mediated programmed necrotic death of breast cancer cells. *PLoS One*, 8(4): e63038, 2013. [*PubMed Central* ID: PMC3639988] [DOI: 10.1371/journal.pone.0063038] [*PubMed* ID: 23646172]. [Citado en p. 109]

[327] M. Hegde, J. Roscoe, P. Cala, y F. Gorin. Amiloride kills malignant glioma cells independent of its inhibition of the sodium-hydrogen exchanger. *J. Pharmacol. Exp. Ther.*, 310(1): 67–74, 2004. [DOI: 10.1124/jpet.103.065029] [*PubMed* ID: 15010500]. [Citado en p. 109]

[328] W. Harley, C. Floyd, T. Dunn, *et al.* Dual inhibition of sodium-mediated proton and calcium efflux triggers non-apoptotic cell death in malignant gliomas. *Brain Res.*, 1363: 159–169, 2010. [*PubMed Central* ID: PMC2996276] [DOI: 10.1016/j.brainres.2010.09.059] [*PubMed* ID: 20869350]. [Citado en p. 109]

[329] L. L. Hall, K. P. Smith, M. Byron, y J. B. Lawrence. Molecular anatomy of a speckle. *Anat. Rec. A Discov. Mol. Cell Evol. Biol.*, 288(7): 664–675, 2006. [*PubMed Central* ID: PMC2563428] [DOI: 10.1002/ar.a.20336] [*PubMed* ID: 16761280]. [Citado en p. 109]

[330] N. Allende-Vega, S. Dayal, U. Agarwala, *et al.* p53 is activated in response to disruption of the pre-mRNA splicing machinery. *Oncogene*, 32(1): 1–14, 2013. [DOI: 10.1038/onc.2012.38] [*PubMed* ID: 22349816]. [Citado en p. 109]

[331] G. Ghosh y J. A. Adams. Phosphorylation mechanism and structure of serine-arginine protein kinases. *FEBS J.*, 278(4): 587–597, 2011. [*PubMed Central* ID: PMC3079193] [DOI: 10.1111/j.1742-4658.2010.07992.x] [*PubMed* ID: 21205204]. [Citado en p. 109]

[332] D. Kaida, H. Motoyoshi, E. Tashiro, *et al.* Spliceostatin A targets SF3b and inhibits both splicing and nuclear retention of pre-mRNA. *Nat. Chem. Biol.*, 3(9): 576–583, 2007. [DOI: 10.1038/nchembio.2007.18] [*PubMed* ID: 17643111]. [Citado en p. 109]

[333] D. L. Spector y A. I. Lamond. Nuclear speckles. *Cold Spring Harb. Perspect. Biol.*, 3(2), 2011. [*PubMed Central* ID: PMC3039535] [DOI: 10.1101/cshperspect.a000646] [*PubMed* ID: 20926517]. [Citado en p. 109]

Anexos

Material suplementario correspondiente al Capítulo 1

"Transcriptome analysis reveals significant differences between primary plasma cell leukemia and multiple myeloma even when sharing a similar genetic background"

Blood Cancer Journal
(2019), 9(12):90
DOI: 10.1038/s41408-019-0253-1

Supplemental Figures captions

Supplemental Figure 1. (A) Unsupervised analysis using multidimensional scaling (MDS) based on gene expression data from the CoMMpas study. 73 MM samples with del17p were selected for the analysis. Only the 35,345 genes interrogated by the HTA were considered for the analysis. **(B)** Sample classification in subgroups in the MDS from the CoMMpass dataset was performed using model-based methods from the mclust R package (v.5.4.1). The best model was chosen from a list of 14 methods according to their Bayesian Information Criterion (BIC). The best fitted model according to the BIC was a spherical multivariate normal model with one component. This model was selected as the best approximation because it is a one component generalization of the top two models, EII (spherical, equal volume) and VII (spherical, unequal volume), that fitted CoMMpass data similarly well with a BIC = -1435.9.

Supplemental Figure 2. Heatmap of the 65 differentially expressed genes identified by KEGG enrichment analysis based on gene expression. The heatmap was constructed using the freely available web tool Heatmapper.

Supplemental Figure 3. KEGG enrichment analysis based on genes with deregulated exons detected in pPCL and MM samples. Statistical significance of the enrichment is expressed as -log10 FDR using the Benjamini-Hochberg method.

Supplemental Figure 4. Validation of differential expression of exons by qRT-PCR. The results are represented as ΔCt between pPCL and MM samples, using *PGK1* as endogenous control gene. Statistically significant differences between pPCL and MM samples are represented as ***$p < 0.001$, **$p < 0.01$, *$p < 0.05$ and n.s no significant (two-sided Student's t-test for unpaired samples).

Supplemental Figure 5. (A) Gene expression analysis of *SRSF1* and *SRSF3 genes* by qRT-PCR. The results are represented as ΔCt between pPCL and MM samples, using *18S* as endogenous control gene. Statistically significant differences between pPCL and MM samples are represented as ***$p < 0.001$, **$p < 0.01$ (two-sided Student's t-test for unpaired samples). Pearson correlation of gene expression measured by qRT-PCR in pPCL and MM samples. **(B)** Pearson correlation analysis between gene expression of SR protein family based on HTAS data and the 13 validated exons. Statistical significances are represented as ***$p < 0.001$, **$p < 0.01$, *$p < 0.05$. **(C)** Pearson correlation analysis between *SRSF1* gene expression and the expression of *CD27* exon 2, *NEDD4L* exon 3 and *RNF11* exon 3. **(D)** Pearson correlation analysis between *SRSF3* gene expression and the expression of *CD27* exon 2 and *MERTK* exon 3

Supplemental Figure 6. Unsupervised analysis based on the expression of the expression of 158,625 isoforms in MM and pPCL samples using multidimensional scaling (MDS) of 19 samples (9 pPCL and 10 MM). Samples tend to be clustered according isoform expression in two groups.

Supplemental Figure 7. (A) Coding isoforms overexpressed (upper-red) and underexpressed (below-blue) from genes without total expression changes. The data is represented as the magnitude of isoform change (log2 FC) between pPCL and MM samples. The selected isoforms for experimental validation, based on higher, lower and medium FC are highlight in yellow. **(B)** Structure of the analysed isoforms (*IKZF1, SF1, KLC1, ASS1, RPTOR, IRF5, RPL10, RPL12* and *DLGAP4* genes) is highlighted in yellow. The two *IKZF1* non-coding isoforms are highlighted in blue. The protein domains are also indicates. The selected isoform for The yellow boxes Pictures were taken from the genome browser Ensembl and modified. **(C)** Differential expression of *IKZF1* isoforms detected in HTA analysis. Coding isoforms are represented by blue columns and non-coding isoforms by dark grey. The light blue column represents the coding isoform that does not have specific sequence for their identification among the all isoforms.

Supplemental Figure 8. Gene expression of SR proteins in pPCL compared to MM patients from HTA results. Columns in red, represents *p*-value < 0.05 and columns in pink, *p*-value > 0.05, for SR gene expression.

Supplemental table 1. *TP53* status

Patient	Group	*TP53* deletion (%) by FISH	*TP53* status	AA change	Mutation cDNA	Mutation allelic fraction	Mutant p53 transactivation activity
46061	MM	71	WT				
46541	MM	83	WT				
46363	MM	83	WT				
45814	MM	75	WT				
45627	MM	83	WT				
44335	MM	95	WT				
44522	MM	96	Mut	p.Y126C	c.377A>G	100%	This codon is close to the end of an exon: splicing can be altered
47803	MM	98	Mut	p.R213X	c.637C>t	100%	The activity of truncated p53 is assumed to be nil
44728	MM	93	Mut	p.C275R	c.823T>C	80%	This mutant is inactive
47405	MM	94	WT				
17012	pPCL	88	no gDNA				
22335	pPCL	93	Mut	p.H179R	c.536A>G	100%	This mutant is inactive
28262	pPCL	72	WT				
30655	pPCL	87	Mut	p.Y205D	c.613T>G	80%	This mutant is inactive
32186	pPCL	97	Mut	p.R280T	c.839G>C	100%	This mutant is inactive
47555	pPCL	97	WT				
45785	pPCL	84	WT				
48401	pPCL	20	Mut	p.L257Q	c.770T>A	50%	This mutant is inactive
20230	pPCL	89	WT				

AA: aminoacid; WT: wild type *TP53*; Mut: mutated *TP53*; no gDNA: genomic DNA no available.

Suplemental Figure 1

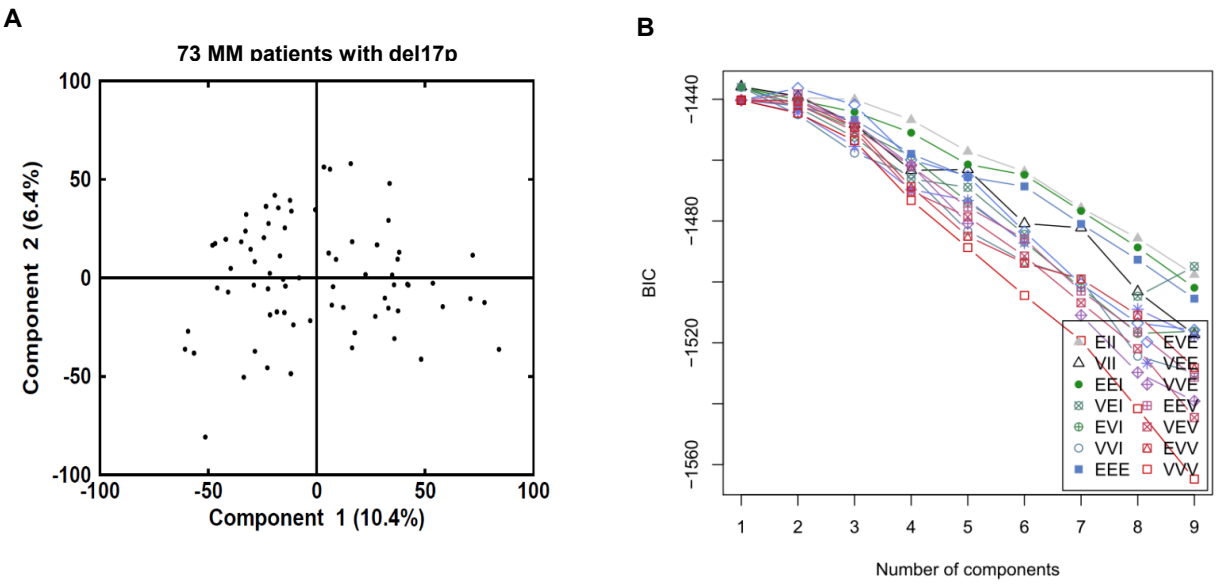

Suplemental Figure 2

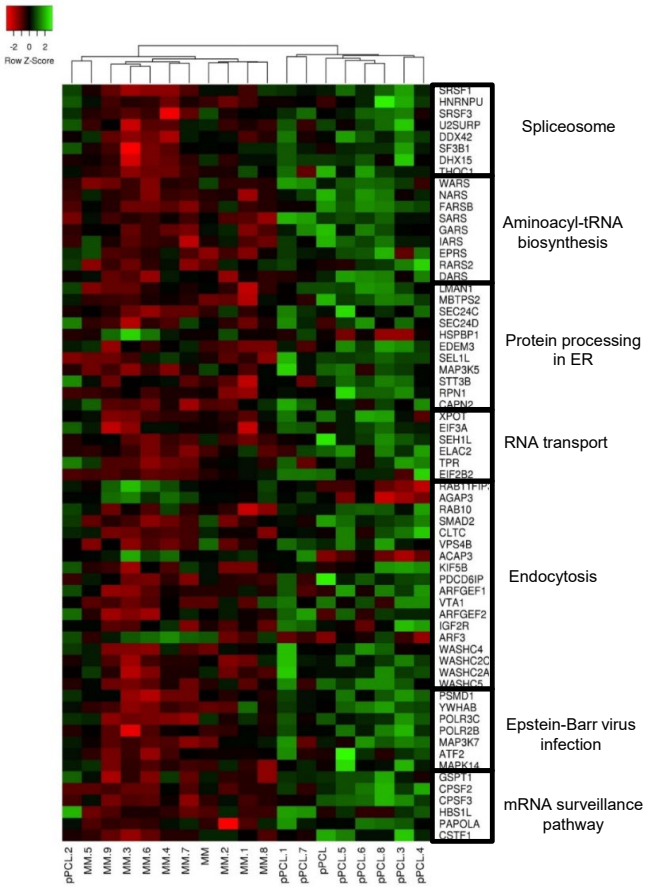

Supplemental table 2. Primers used in qRT-PCR

Gene	Assay ID	Catalog number
SRSF1	Hs00199471_m1	4448892
SRSF3	Hs00751507_s1	4448892
SF3B1	Hs00961640_g1	4448892
DDX42	Hs00201296_m1	4448892
DHX15	Hs00154713_m1	4448892
HNRNPU	Hs00244919_m1	4448892
THOC1	Hs01018285_m1	4448892
U2SURP	Hs01030366_m1	4448892
TP53	Hs01034249_m1	4331182
18S (endogenous control gene)	Hs99999901_s1	4331182
WARS	Hs00188259_m1	4448892
AHR	Hs00169233_m1	4453320
DUSP5	Hs00244839_m1	4453320
CD79A	Hs00998119_m1	4448892
GADD45A	Hs00169255_m1	4453320
GADD45B	Hs00169587_m1	4453320
PDE4B	Hs00277080_m1	4448892

Suplemental Figure 3

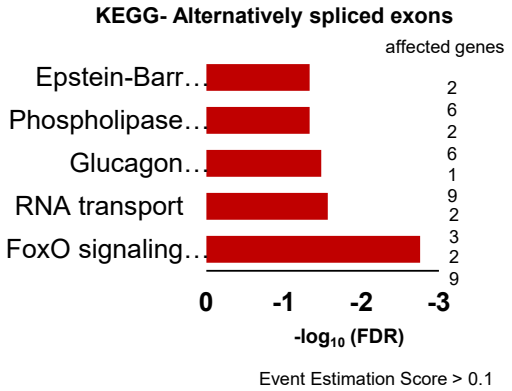

Supplemental table 3. Validation of cassette exon (CE) events

Gene	FC HTAs	FC qRT-PCR	Splicing Event Estimate
TRA2B	2.7	1.5	More exon inclusion in pPCL (CE)
TUBG1	3.1	1.6	More exon inclusion in pPCL (CE)
BCL2	2.5	3.0	More exon inclusion in pPCL (CE)
COA3	4.9	2.8	More exon inclusion in pPCL (CE)
COG8	2.7	1.7	More exon inclusion in pPCL (CE)
PI4KB	3.1	1.4	More exon inclusion in pPCL (CE)
PPM1B	3.4	2.6	More exon inclusion in pPCL (CE)
RNF11	-3.6	-2.1	More exon exclusion in pPCL (CE)
MERTK	-32.7	-2.4	More exon exclusion in pPCL (CE)
SULF2	-145.8	-9.1	More exon exclusion in pPCL (CE)
CD27	-27.6	-9.4	More exon exclusion in pPCL (CE)
NEDD4L	-27.7	-4.5	More exon exclusion in pPCL (CE)
KRAS	-2.4	-1.1	More exon exclusion in pPCL (CE)

Supplemental table 4. Primers used in qRT-PCR (SYBR Green-based detection)

Gene	Oligo Name	Sequence 5' to 3'
TRA2B	TRA2B_Fw	GATGAAGCGTGAGTTTCCTGC
	TRA2B_Rv	GTGACATTGGAGTCAATCGGC
TUBG1	TUBG1_Fw	CTGTCGCCAGTATGACAAGC
	TUBG1_Rv	AGAAAGAGATGCGTGAGGTCC
BCL2	BCL2_Fw	TGCAGTTGGGCAACAGAGAA
	BCL2_Rv	ACATGTGTTGGGATTGCCCT
COA3	COA3_Fw	GCGTCAGGGTCCTAATCTGG
	COA3_Rv	CACAGAGCTGCCACGTCTAA
COG8	COG8_Fw	GCTGATTTCCGGGGTCAGTT
	COG8_Rv	GGGGTGGGAAATCTAGGAGC
PI4KB	PI4KB_Fw	TGGACAGTGAGATCCGTTGC
	PI4KB_Rv	GGGGCAGATAGAAGTCCACG
PPM1B	PPM1B_Fw	CTTGCGGATTCCCAACGTTTT
	PPM1B_Rv	ACGAGTATGCCTGAGGTTGG
RNF11	RNF11_Fw	CAATTCGATTTCTGCCGTGC
	RNF11_Rv	CAGTGCTGCATCAACTGGCT
SULF2	SULF2_E5_Fw	ACCAATGACAGCGTGAGCTT
	SULF2_E5_Rv	GCGTGAATATTGTGGGGCTG
MERTK	MERTK_E3_Fw	CATAACCAGTGTGCAGCGTTC
	MERTK_E3_Rv	ATGGGATCAGACACGATCTCTTC
NEDD4L	NEDD4L_E3_Fw	CTTCTGCTCCATTGCTGTTGA
	NEDD4L_E3_Rv	TGCTATTATCAGACTCACACTTGGT
CD27	CD27_E2_Fw	AGCATAGAAAGGCTGCTCAGT
	CD27_E2_Rv	GTGCCGACAGCTCTCACAGT
KRAS	KRAS_oE4_Fw	ACATTGGTGAGAGAGATCCGA
	KRAS_oE4_Rv	ACACAGCCAGGAGTCTTTTCT

Supplemental Figure 4

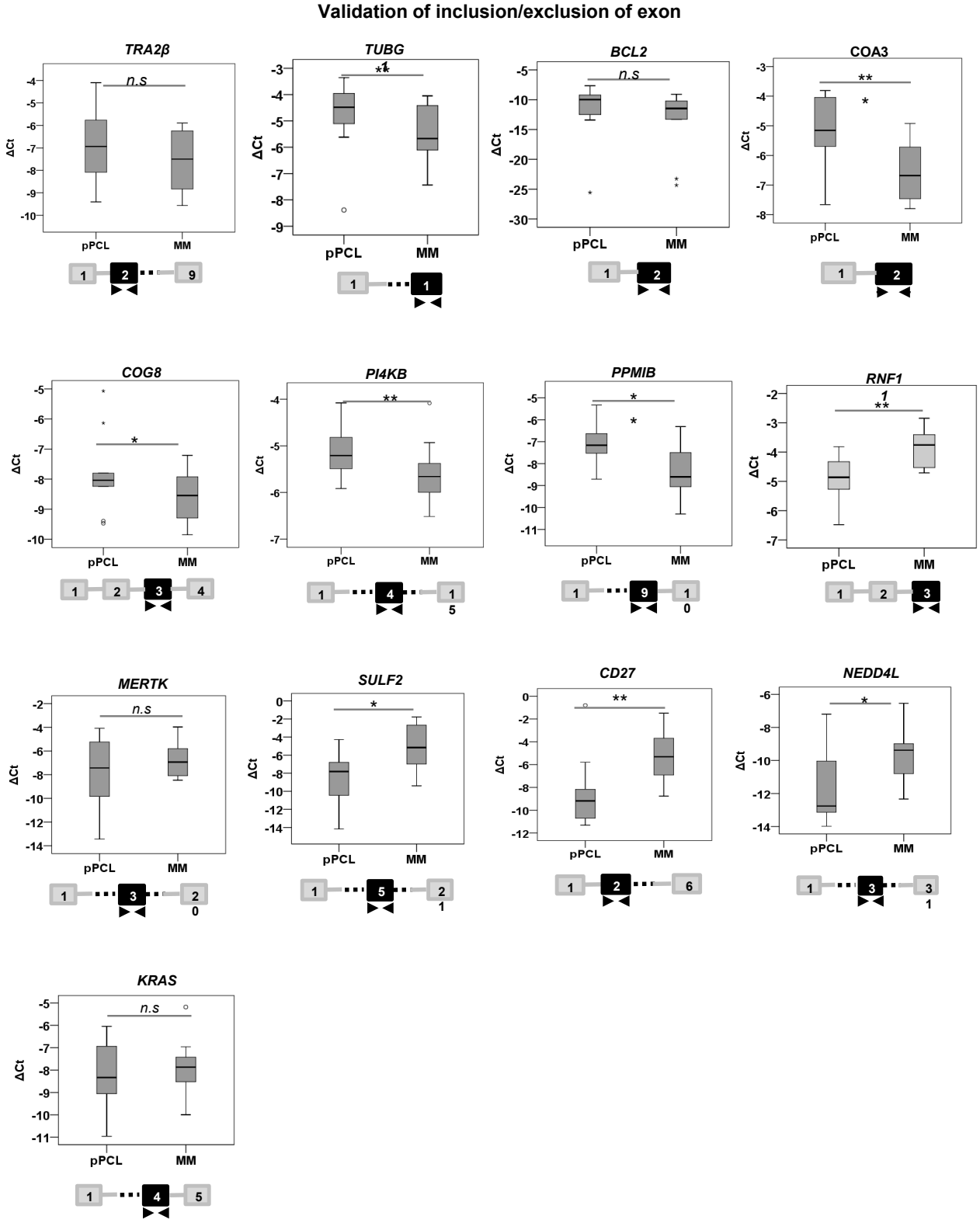

Supplemental Figure 5

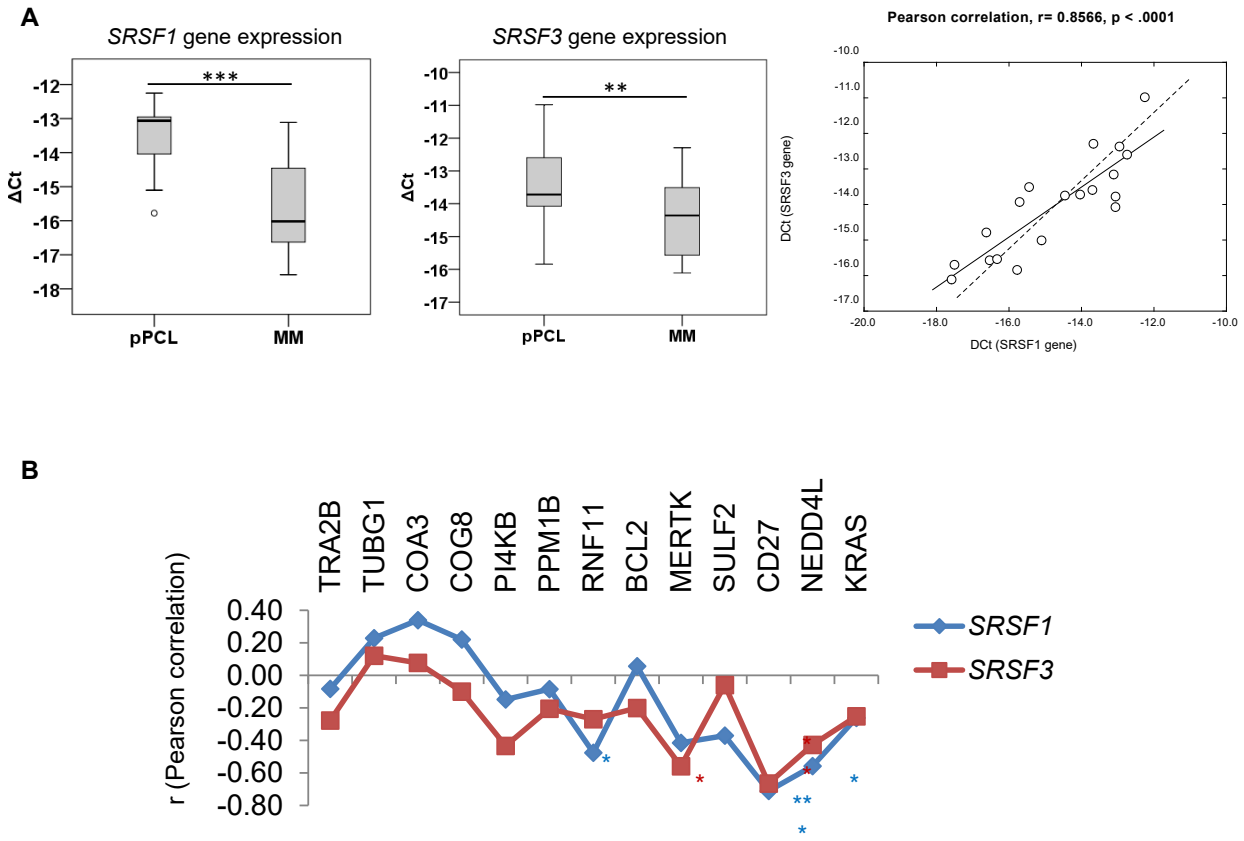

Supplemental Figure 5

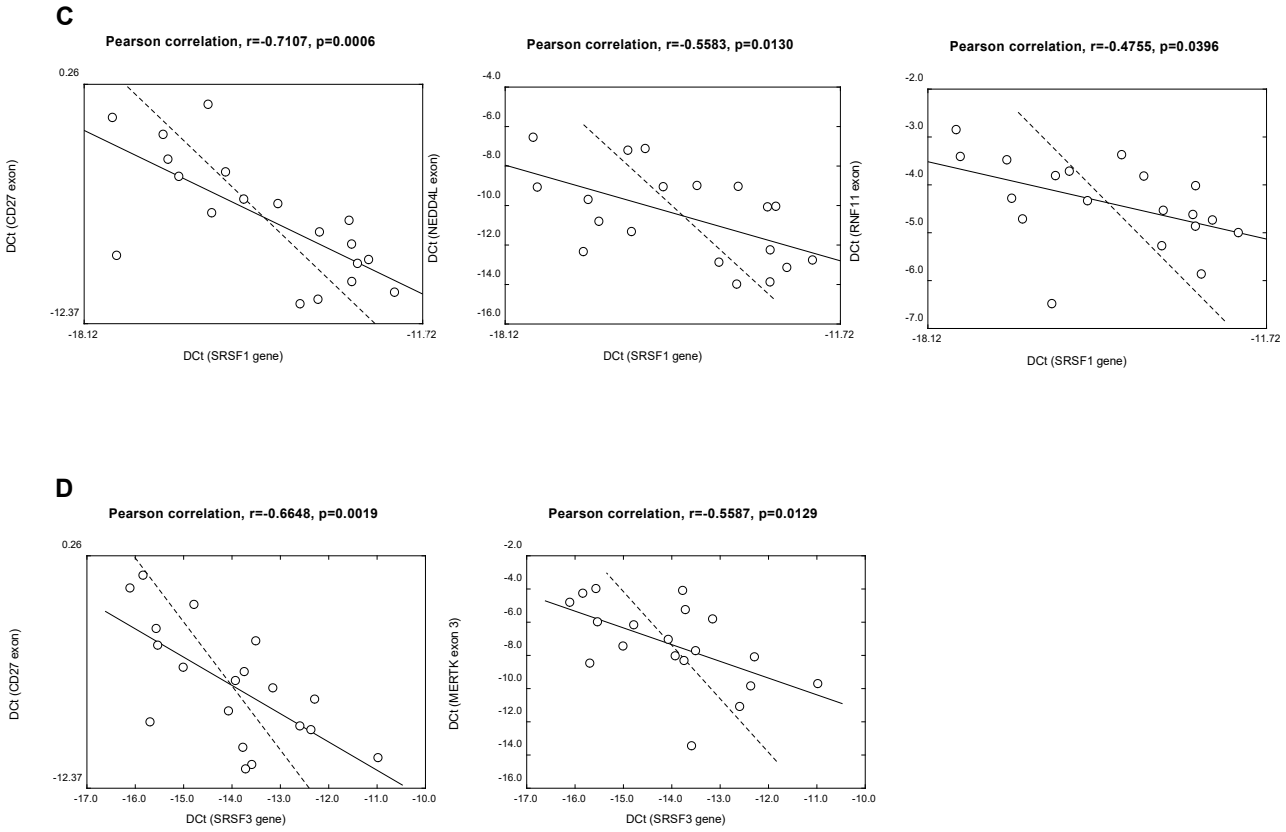

Suplemental Figure 6

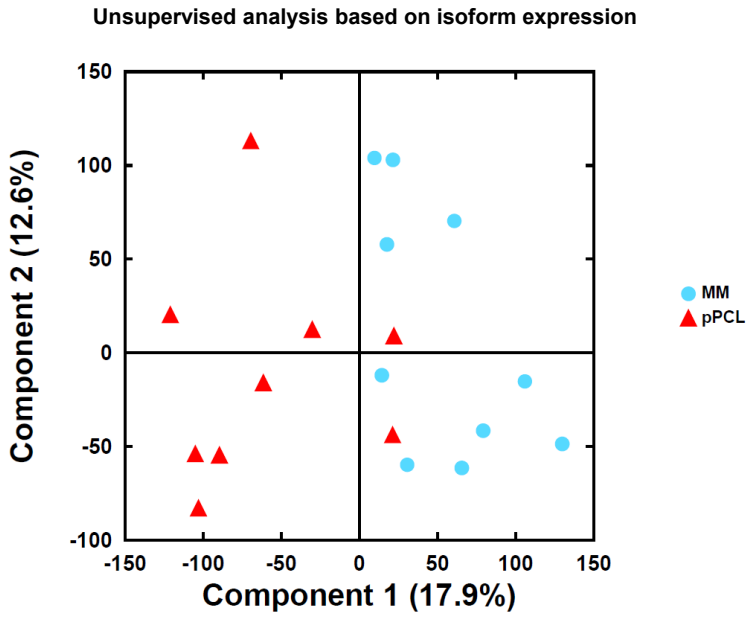

Suplemental Figure 7

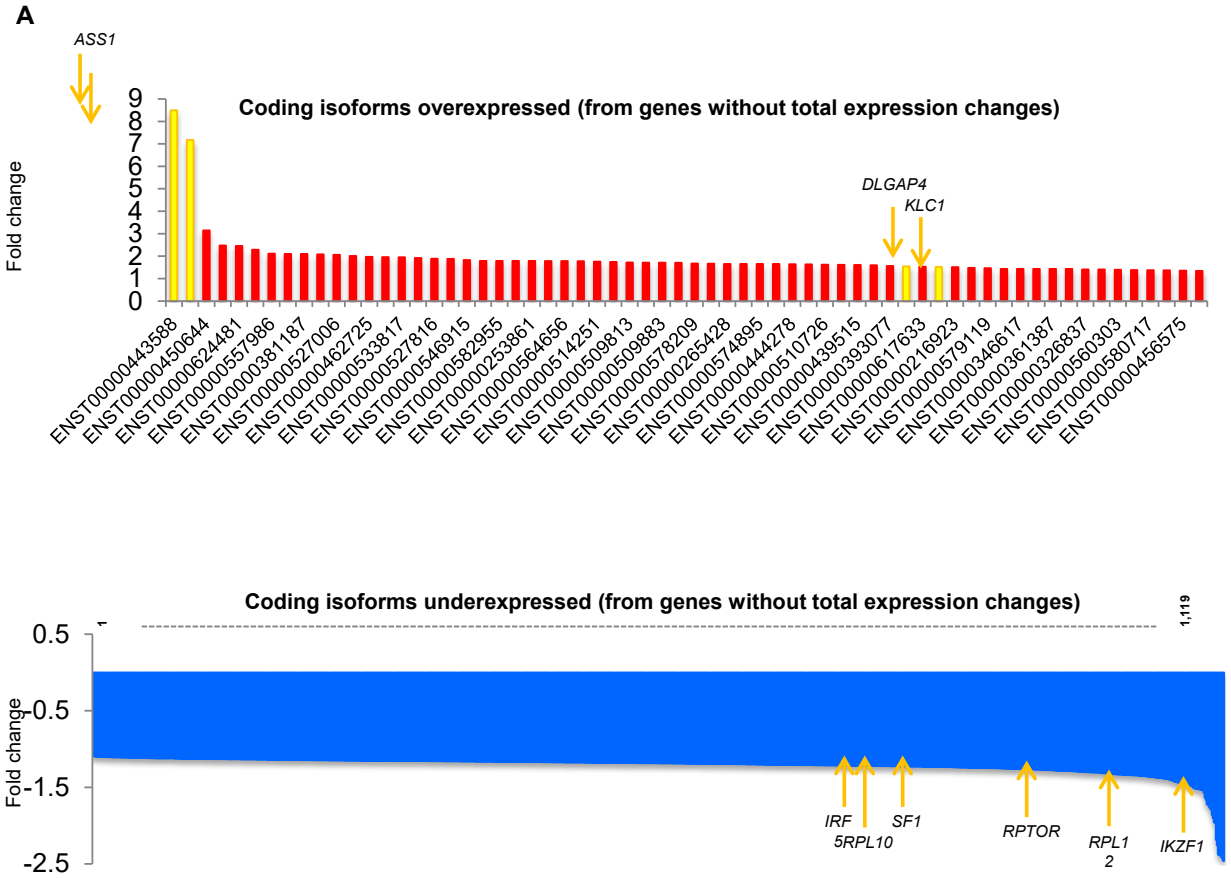

Supplemental table 5. Summary of tested deregulated coding isoforms (from genes without total expression changes)

HTA

GENE				ISOFORM		
HGNC	Ensembl ID	FC	*q*-value	Isoform	Fold Change	*q*-value
RPTOR	ENSG00000141564	1.0903	0.204	ENST00000576366	0.787	0.005
RPL10	ENSG00000147403	0.9421	0.204	ENST00000449494	0.817	0.005
IRF5	ENSG00000128604	0.9122	0.062	ENST00000464557	0.820	0.005
IKZF1	ENSG00000185811	0.8126	0.075	ENST00000413698	0.676	0.016
IKZF1	ENSG00000185811	0.8126	0.075	ENST00000646110	0.669	0.021
IKZF1	ENSG00000185811	0.8126	0.075	ENST00000612658	0.692	0.046
RPL12	ENSG00000197958	0.9923	0.374	ENST00000536368	0.745	0.028
DLGAP4	ENSG00000080845	1.0600	0.204	ENST00000340491	1.541	0.036
SF1	ENSG00000168066	1.0045	0.425	ENST00000413725	0.815	0.046
KLC1	ENSG00000126214	1.0131	0.420	ENST00000553436	1.518	0.046
ASS1	ENSG00000130707	1.0251	0.414	ENST00000372393	7.174	0.046
ASS1	ENSG00000130707	1.0251	0.414	ENST00000443588	8.497	0.046

Supplemental table 6. Primers used in qRT-PCR (SYBR Green-based detection) ISOFORM VALIDATION

Gene	Isoform (ensembl anotation)	Oligo Name	Sequence 5' to 3'
IKZF1	ENST00000413698	IKZF1_698_Fw	CGTACGTGCATGTTCCTTCATC
		IKZF1_698_Rv	TGTTACTCCACTGCCATGCT
	ENST00000646110	IKZF1_110_Fw	AGCAGGACACTCTAACAAGTGAC
		IKZF1_110_Rv	GCATCAAGACCAAGTAGCCG
	ENST00000612658	IKZF1_658_Fw	ACCCGAGGATCAGTCTTGG
		IKZF1_658_Rv	GTTGCCCTTCTGGGTGAAT
SF1	ENST00000413725	SF1_Fw	GCCCTCCTCCAATGGGTAAA
		SF1_Rv	CTAGTTCTGTGGTGGAGGCG
RPL10	ENST00000449494	RPL10_ENS682_Fw	TATCATGTCCATCCGCACCA
		RPL10_ENS682_Rv	GAACGCCCTCTACGATGTGTT
RPL12	ENST00000536368	RPL12_Fw	CTGAGGTGCACCGGAGGT
		RPL12_Rv	TGTTTTTCTGTTTCTTTCTGTCTCTT
KLC1	ENST00000553436	KLC1_Fw	TGAGAACATGGAGAAGCGCA
		KLC1_Rv	TCTAGCACATGAGACAGGAGGA
IRF5	ENST00000464557	IRF5_Fw	TCCTAAGTGCTACCCGAATGC
		IRF5_Rv	ACCTCTCTAGGGCCATTCATCT
DLGAP4	ENST00000340491	DLGAP4_Fw	TGTCTCTTTGTCTCTGCCCTC
		DLGAP4_Rv	AGAACCCCCAAAGGATGTGC
RPTOR	ENST00000576366	RPTOR_Fw	GACACGGAAGATGTTCGACAAG
		RPTOR_Rv	GAAGCAACGCTCTCAGTGT
ASS1	ENST00000372393	ASS1_393_Fw	CAGCGCACTGTATGAGGACC
		ASS1_393_Rv	CAGCTGAGCTCAAACCGGA
	ENST00000443588	ASS1_588_Fw	CAGTCCAGCGCACTGTATGA
		ASS1_588_Rv	GGGAGCAATGACCTTTCCTGT

Supplemental Figure 7

B

IKZF1: ENST00000413698 and ENST00000646110

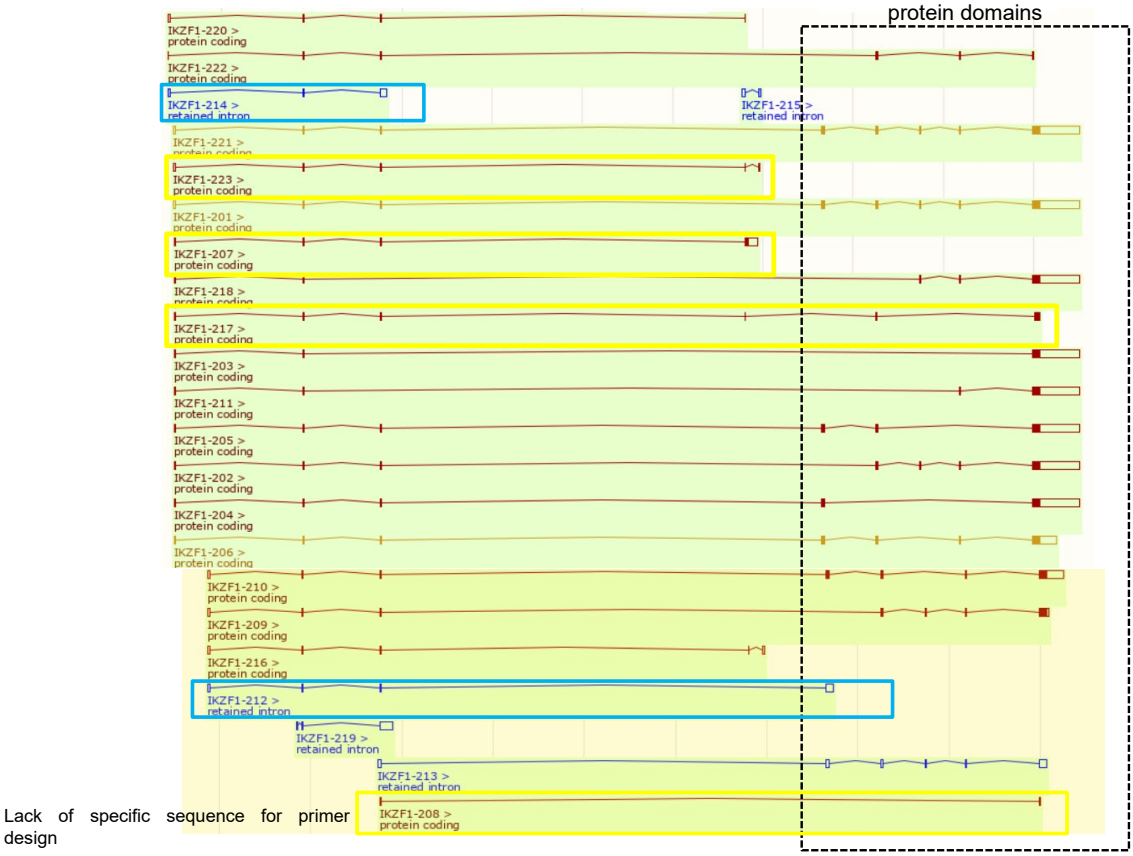

Lack of specific sequence for primer design

SF1: ENST00000413725

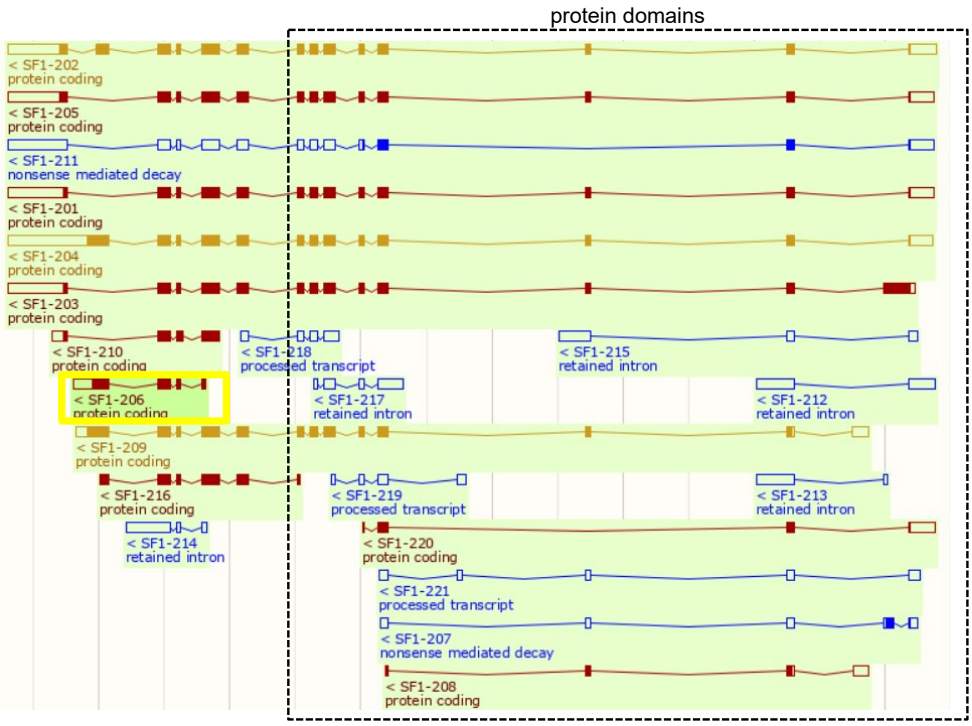

KLC1:ENST00000553436

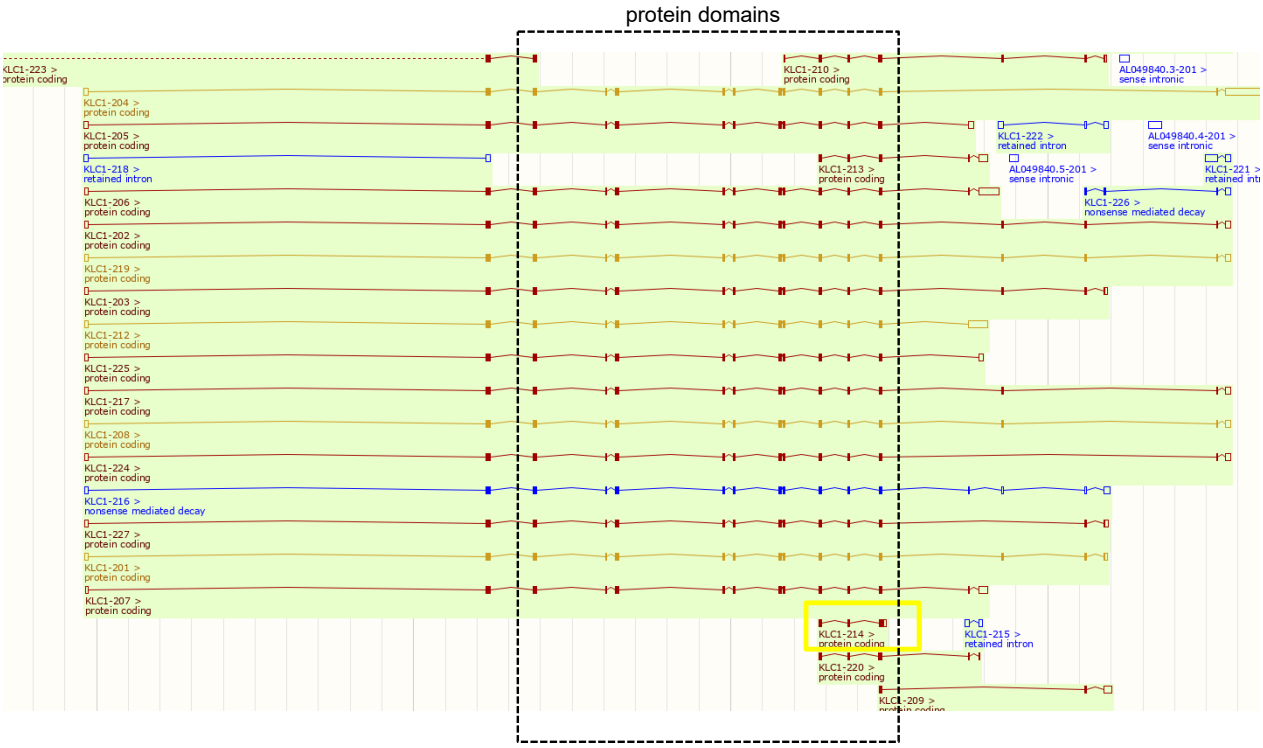

ASS1: ENST00000443588 and ENST00000372393

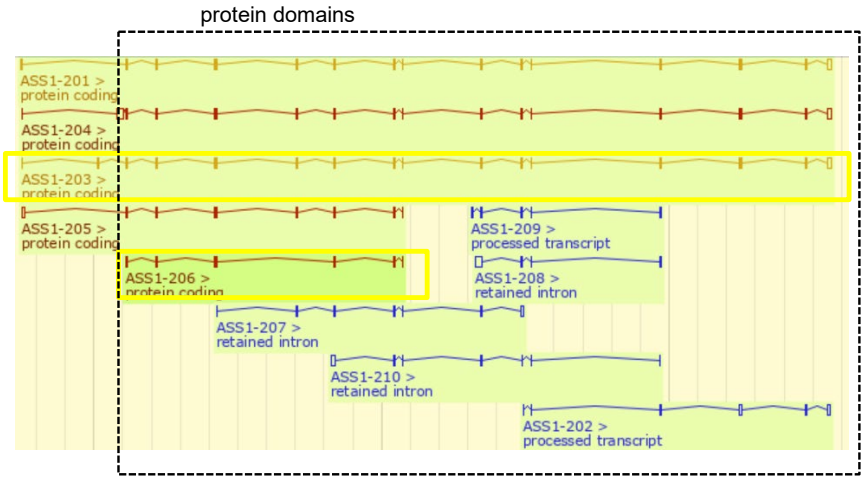

RPTOR: ENST00000576366

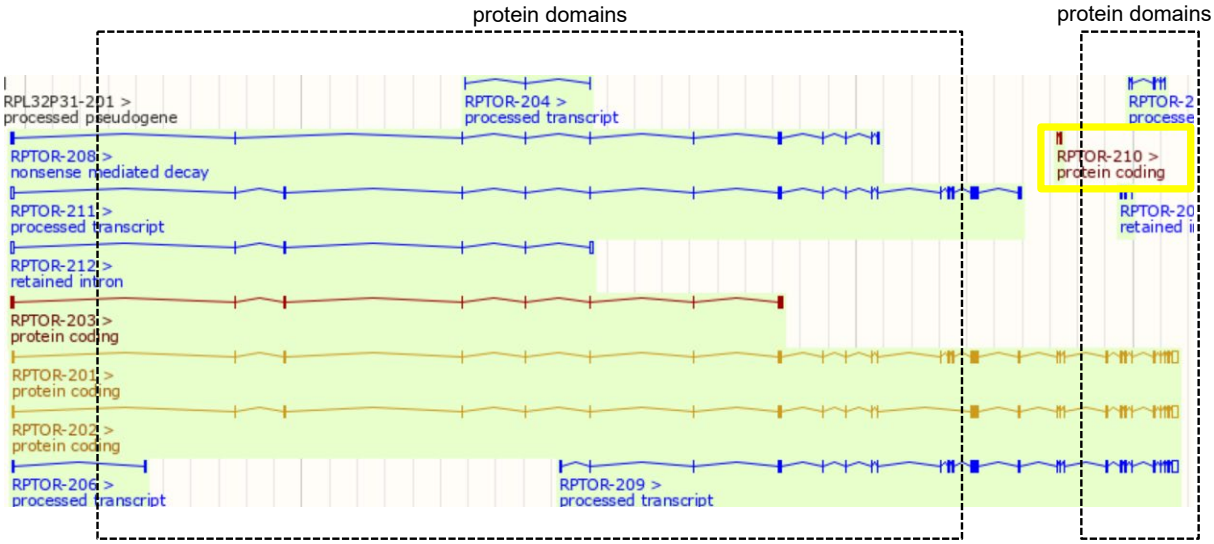

IRF5: ENST00000464557

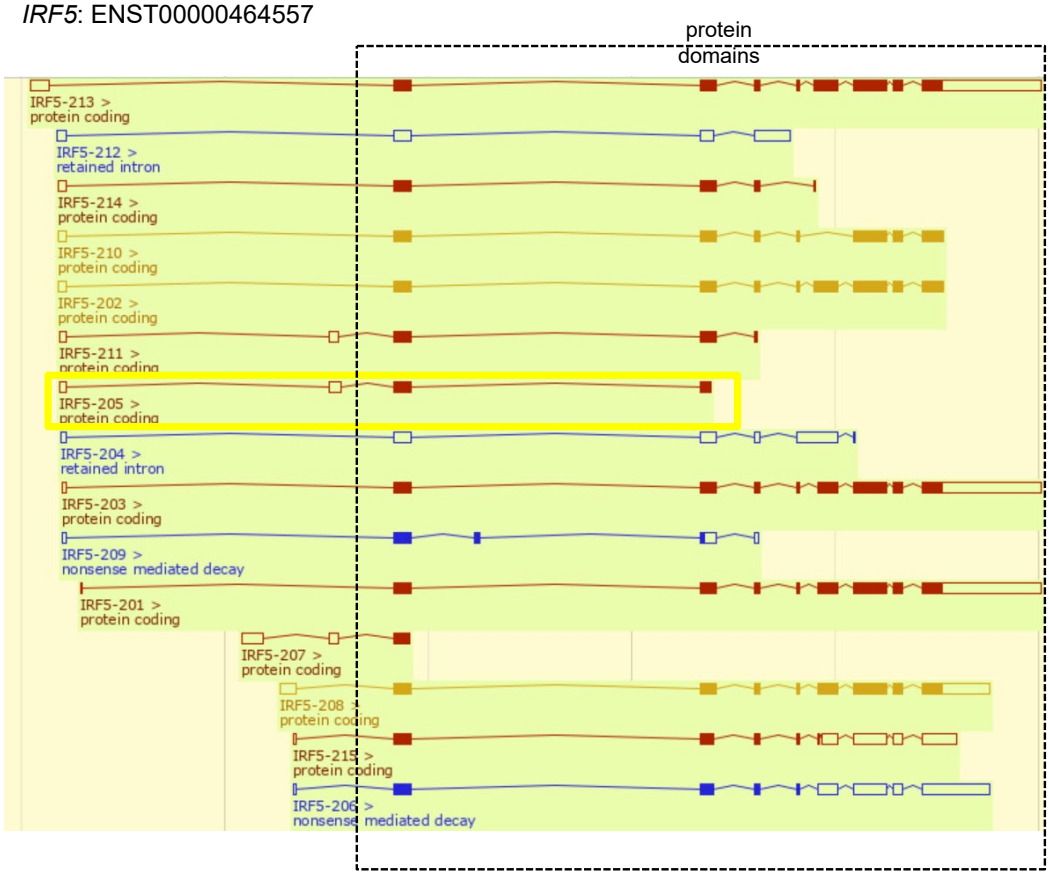

RPL10: ENST00000449494

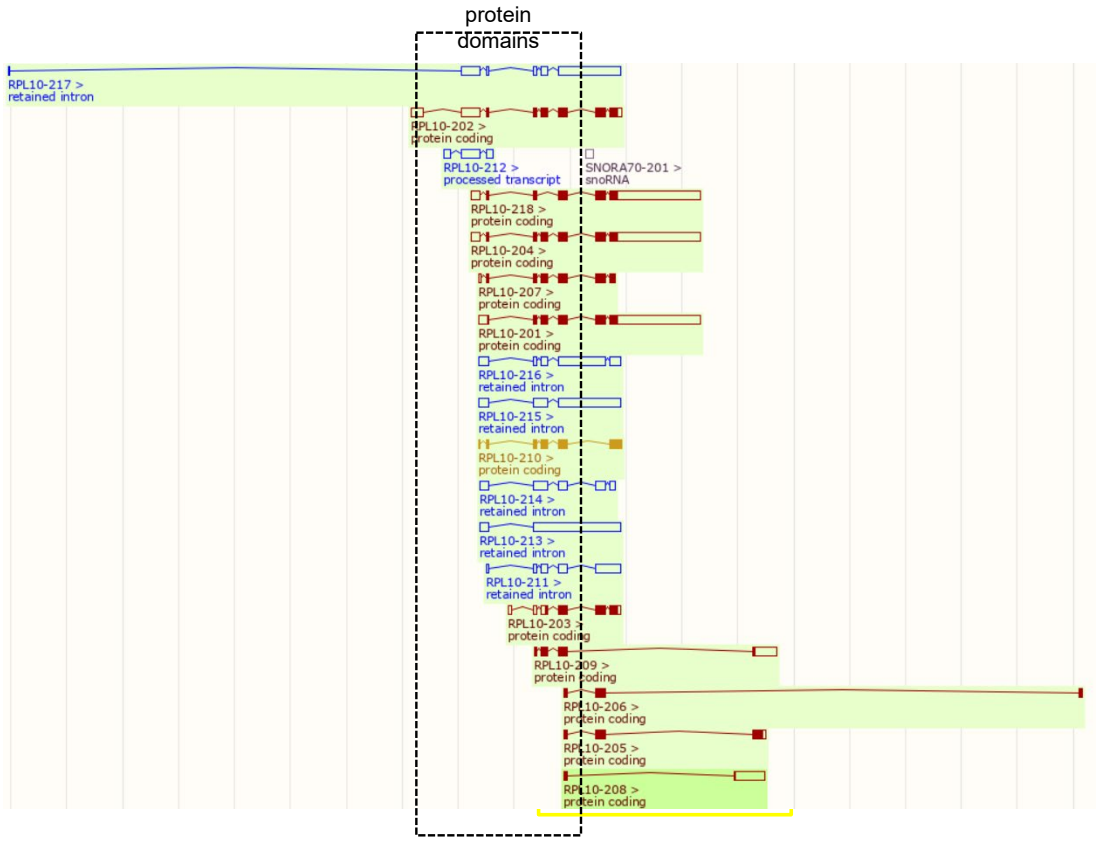

RPL12: ENST00000536368

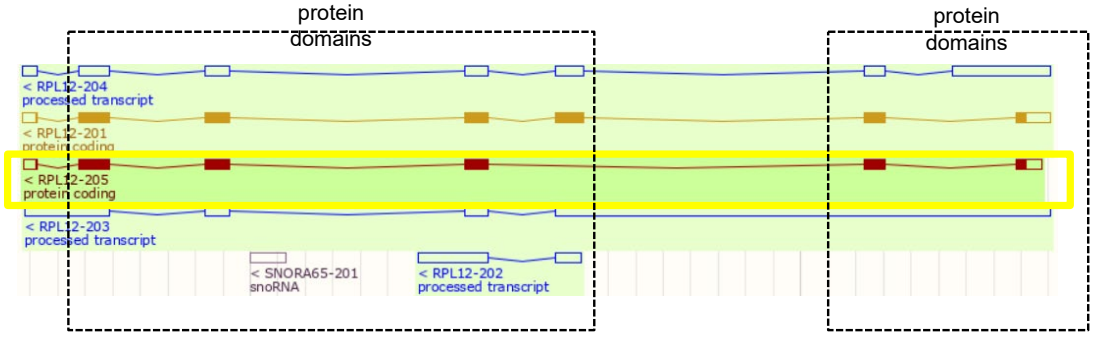

DLGAP4: ENST00000340491

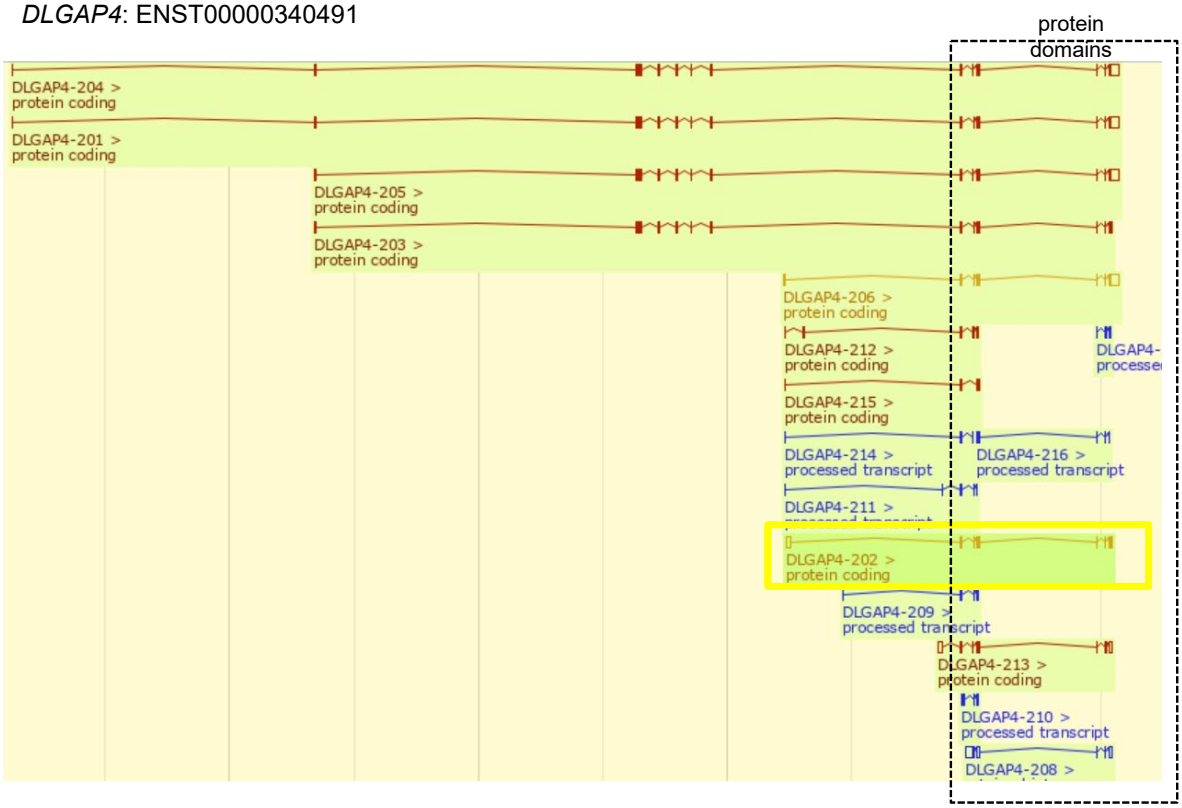

Supplemental Figure 7

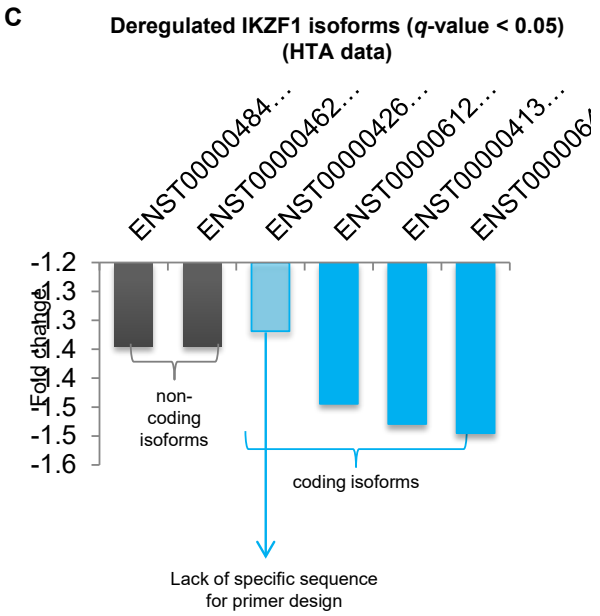

Supplemental Figure 8

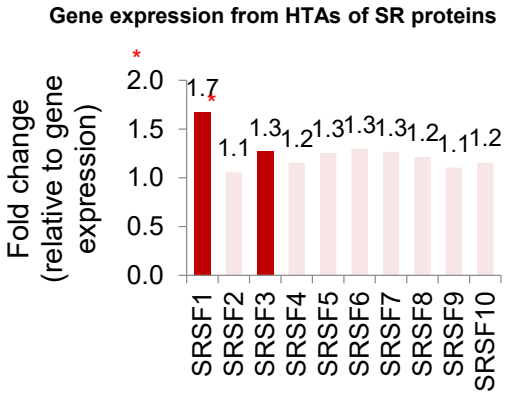

Supplemental table 7. Pathways affected by inclusion or exclusion of exons

Pathway	No. of affected genes	FDR	Genes
FoxO signaling pathway	26	0.00175	*PLK2, PLK3, MAPK14, AKT1, GABARAPL1, FBXO25, IKBKB, ARAF, KRAS, SMAD2, SMAD3, ATM, PCK2, PIK3CB, PIK3R1, PRKAB2, PRKAG1, BCL6, SGK1, SOS2, BRAF, TGFB2, TGFBR1, SETD7, HOMER2, HOMER1*
RNA transport	26	0.02720	*SNUPN, SRRM1, RPP40, STRAP, DDX20, XPOT, NUP35, NUP188, GEMIN5, UPF2, RGPD4, NUP98, ELAC1, NUP133, NUP107, XPO5, RANBP2, RGPD3, DDX39B, RAE1, THOC5, EIF3J, EIF2B4, EIF2B5, RBM8A, THOC1*
Glucagon signaling pathway	19	0.03300	*ATF2, AKT1, PLCB1, ACACA, ITPR1, PCK2, PDHB, PFKL, PHKA2, PHKB, PHKG2, PLCB2, PLCB3, PPP3CB, PRKAB2, PRKAG1, PPP4R3B, CREB3L2, CAMK2D*
Phospholipase D signaling pathway	23	0.04650	*ADCY3, RAPGEF4, DGKQ, DNM2, AKT1, PTK2B, PLCB1, PLA2G4D, GRM5, KRAS, PIK3CB, PIK3R1, PLCB2, PLCB3, PLCG2, AGPAT5, RALGDS, SHC1, SOS2, TSC1, PIP5K1A, PLPP1, CYTH1*
Epstein-Barr virus infection	29	0.04650	*HDAC5, POLR3A, RBPJL, ATF2, MAPK14, AKT1, DDX58 GTF2E2, HDAC1, HLA-F, HLA-G, HSPA2, IKBKB, IRF3, ITGAL, PIK3CB, PIK3R1, PLCG2, POLR3B, PSMD4, PSMD13, MAP2K4, POLR3D, TBP, TNFAIP3, POLR1C, CD44, NCOR2, HDAC4*

Material suplementario correspondiente al Capítulo 2

"Expression of p53 protein isoforms predicts survival in patients with multiple myeloma"

American Journal of Hematology
(2022), Feb 21
DOI: 10.1002/ajh.26507

Supplementary Figure 1

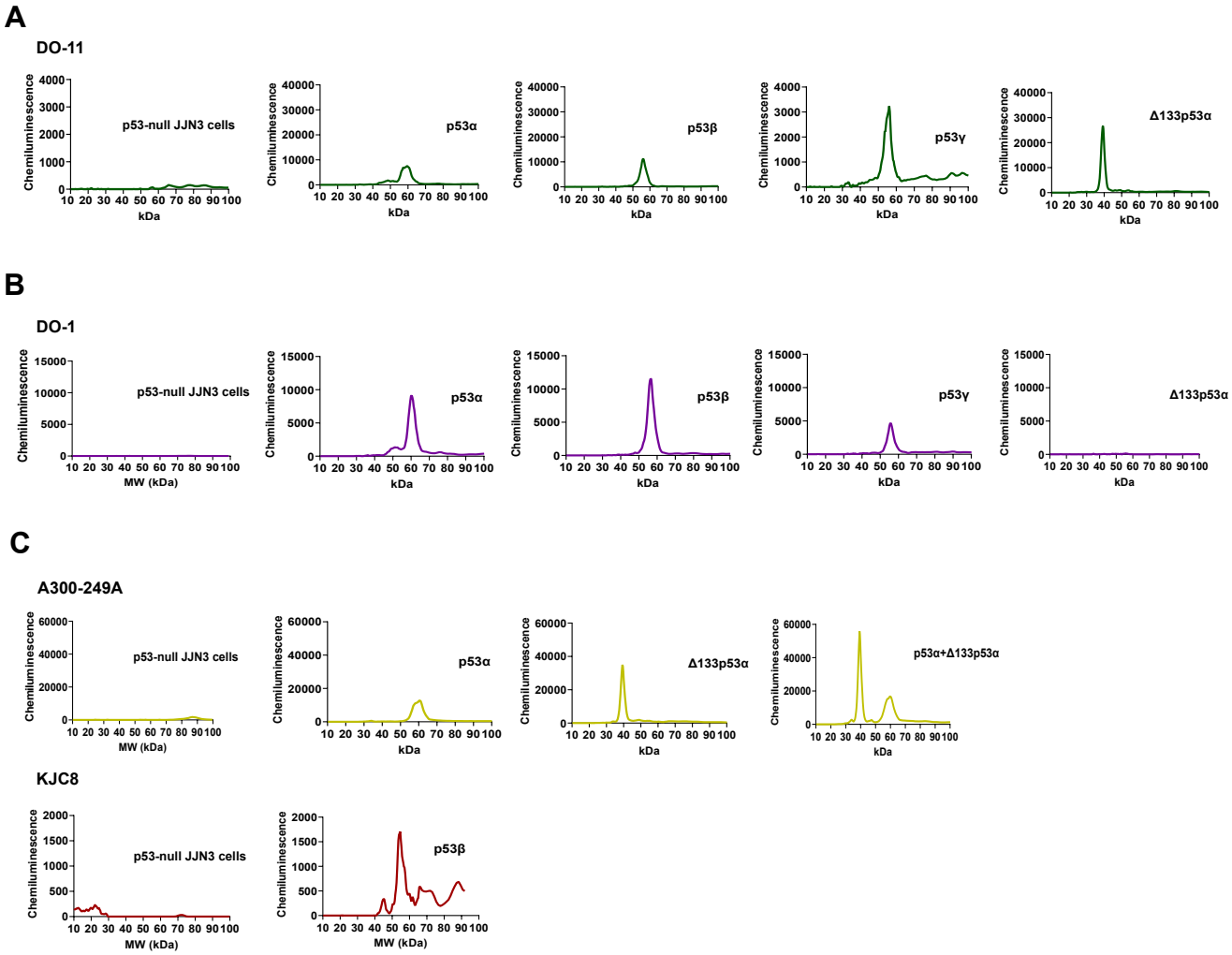

Supplementary Figure 1

D

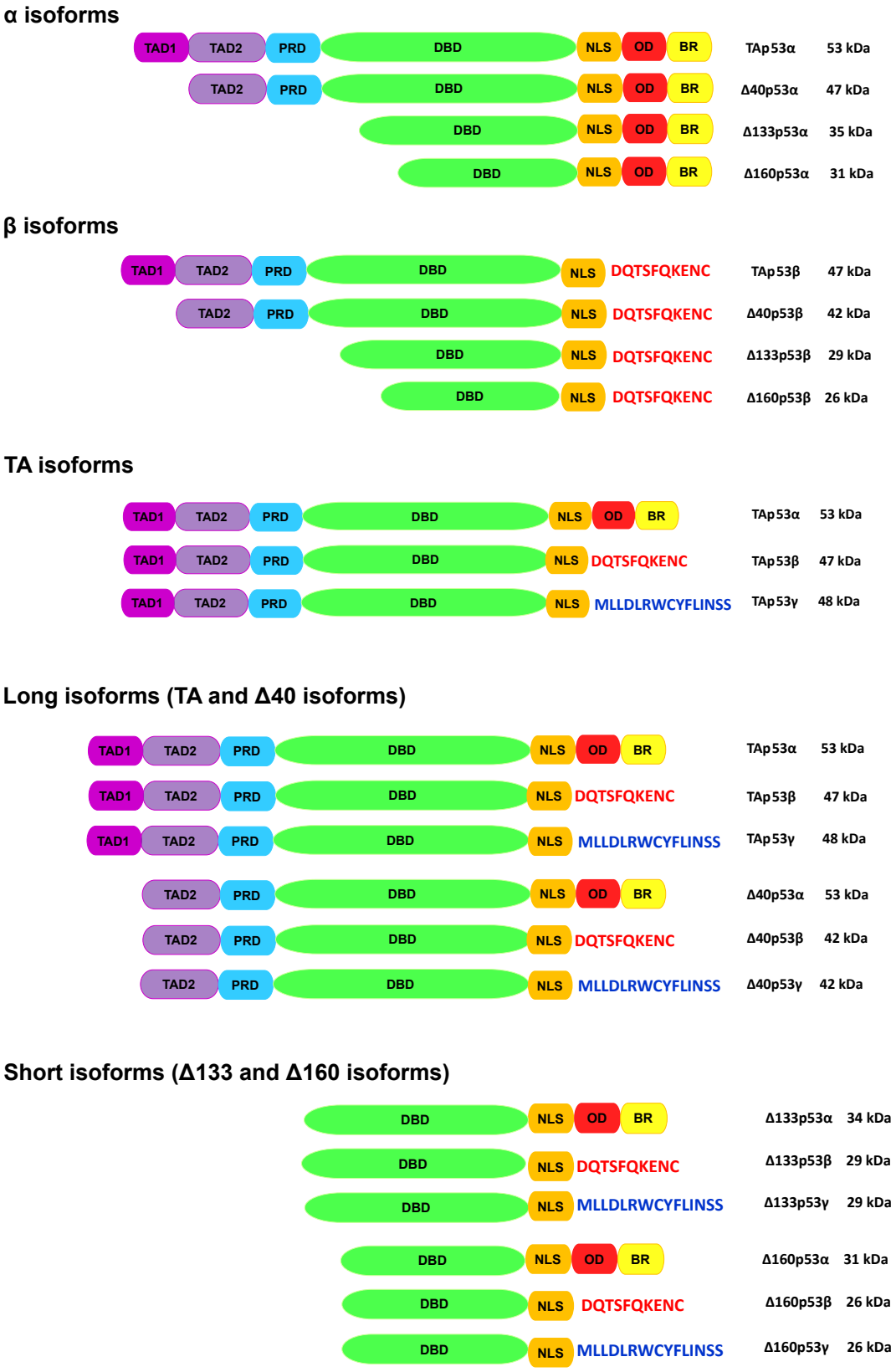

Supplementary Figure 1

E

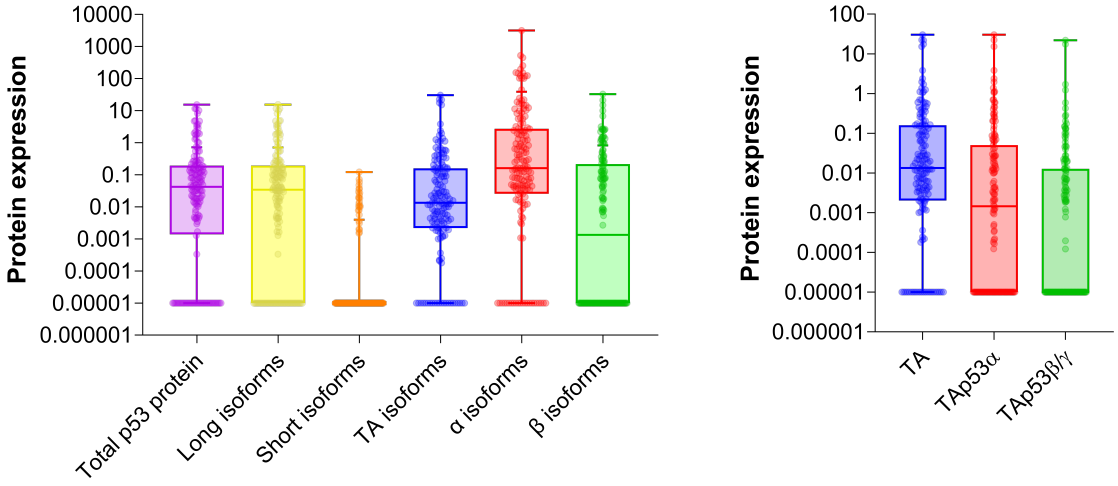

F

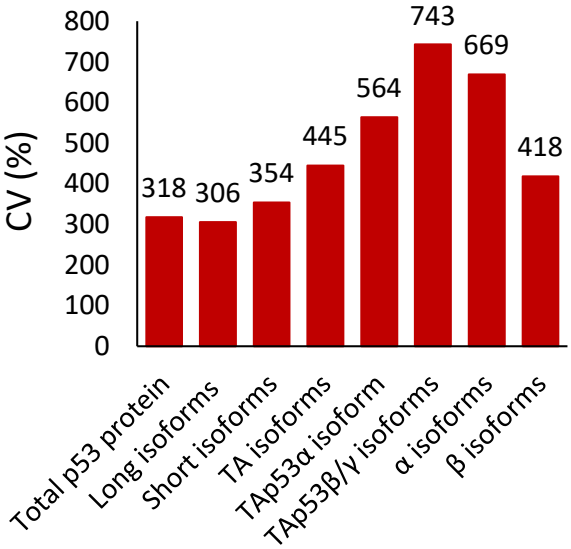

Supplementary Figure 2

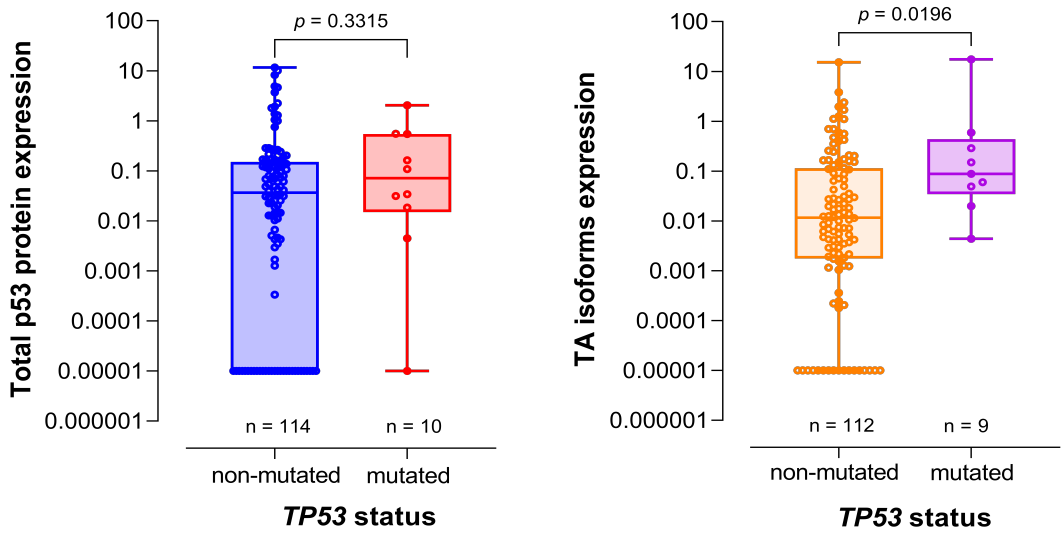

Supplementary Figure 3

A

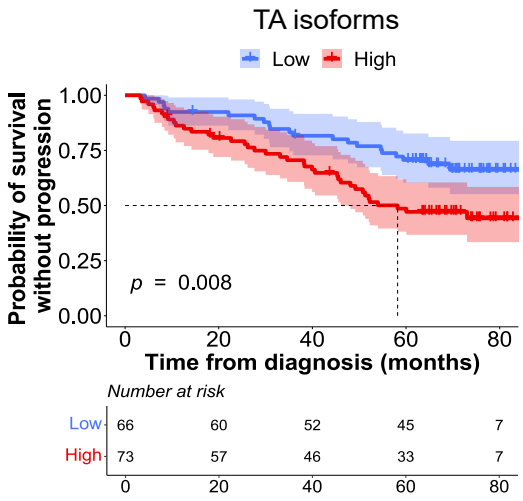

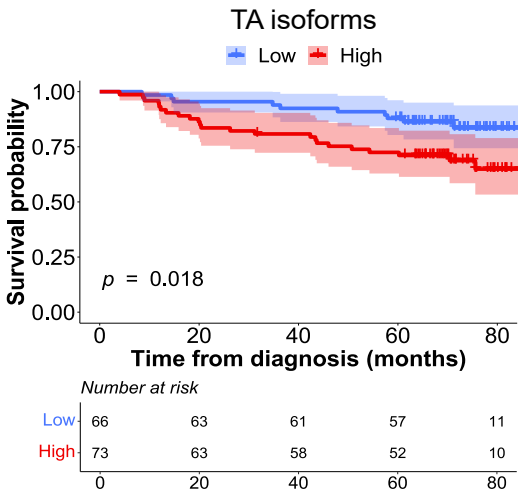

B

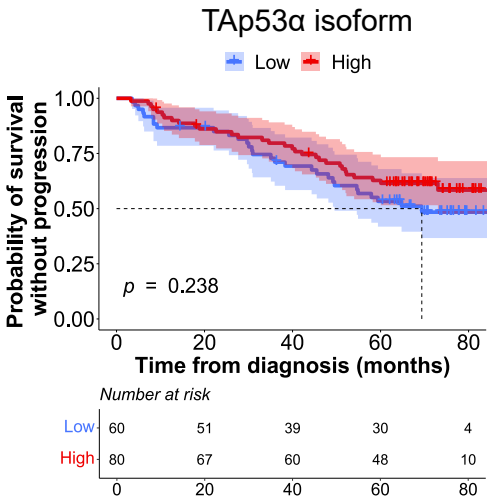

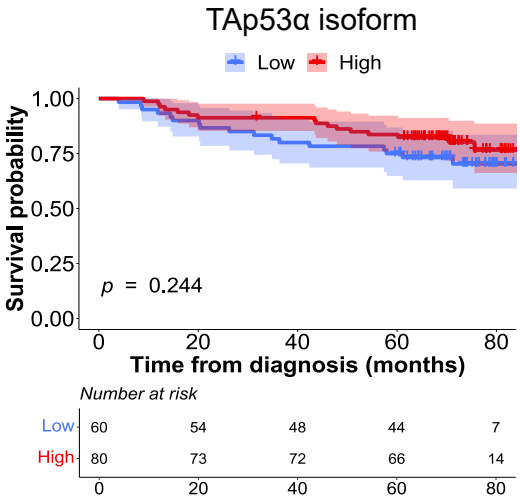

Supplementary Figure 3

C

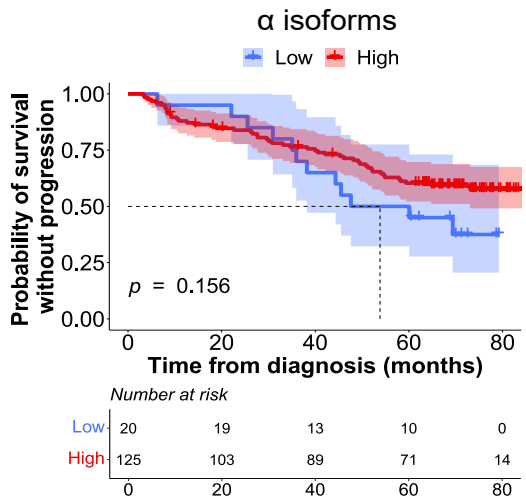

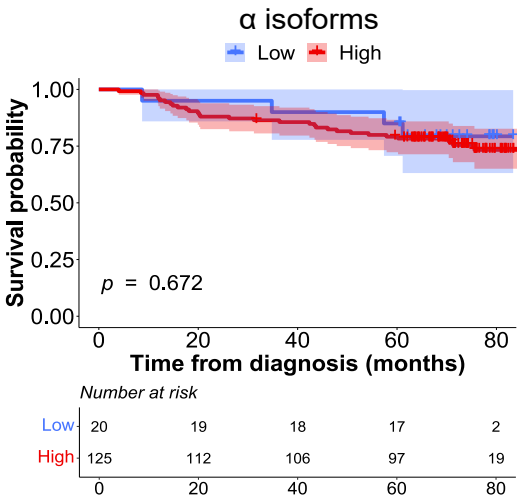

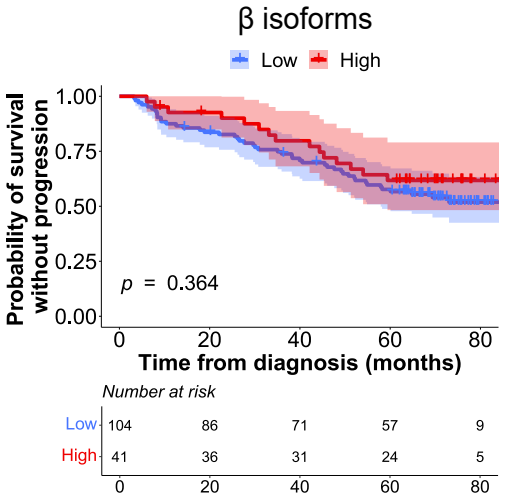

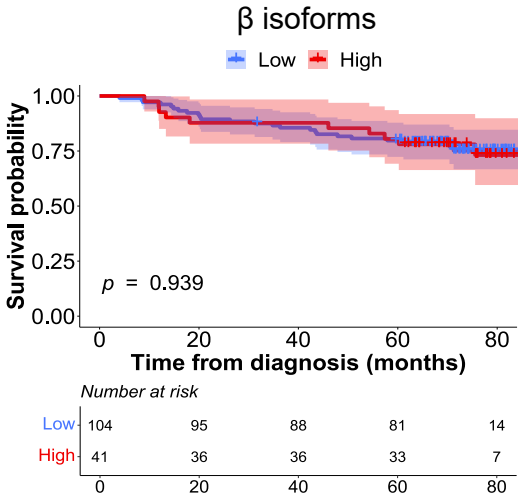

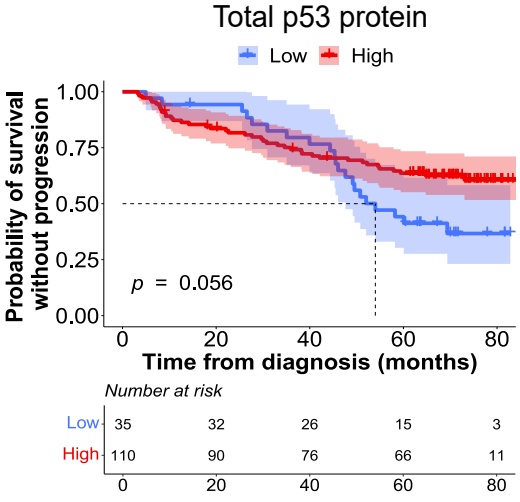

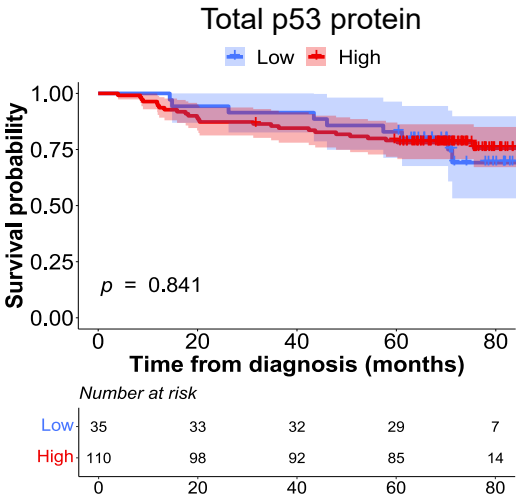

Supplementary Figure 4

A

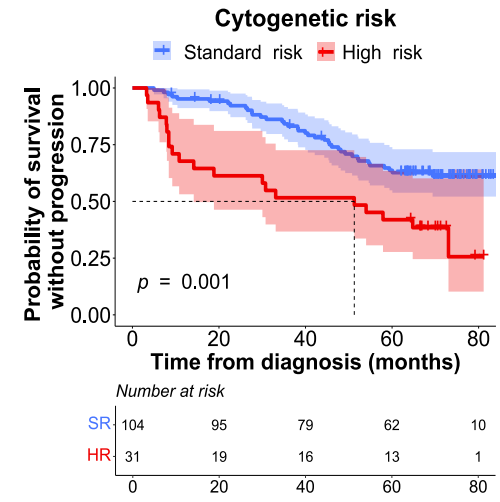

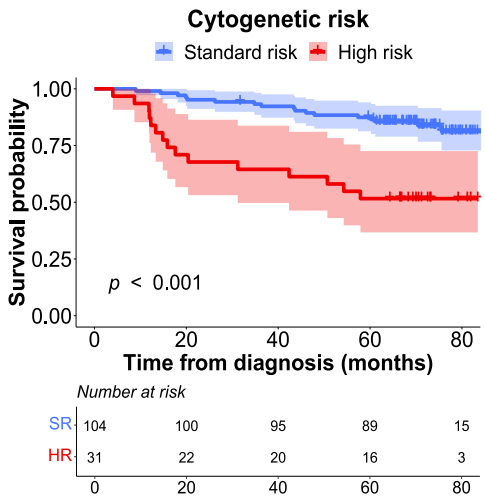

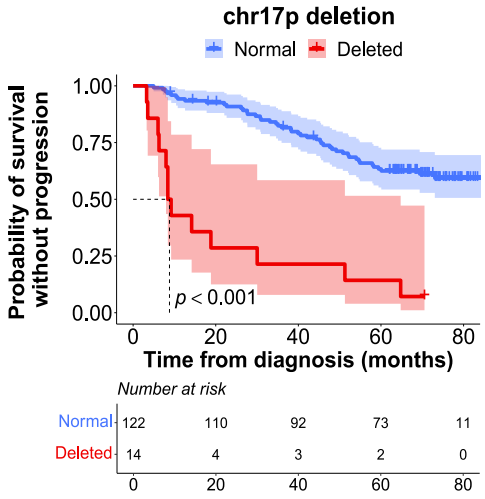

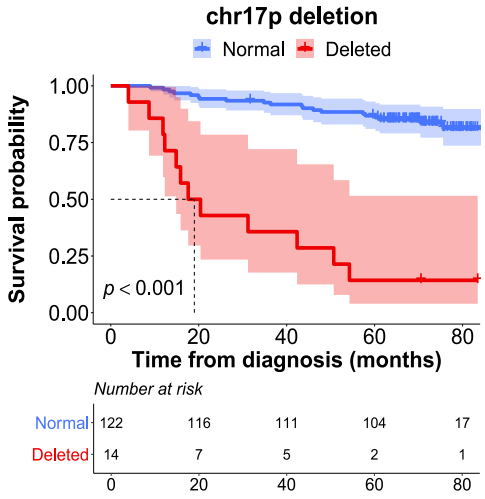

B

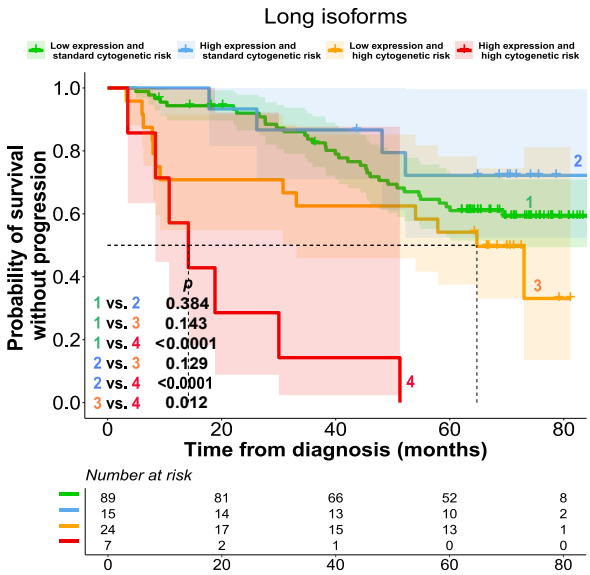

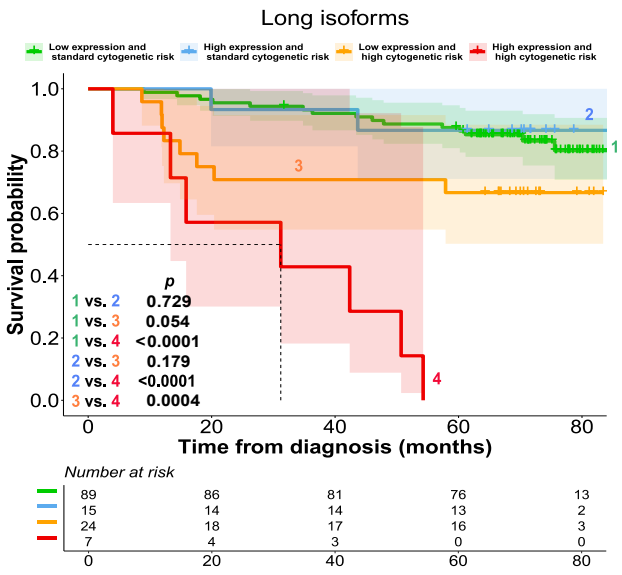

Supplementary Figure 5

A

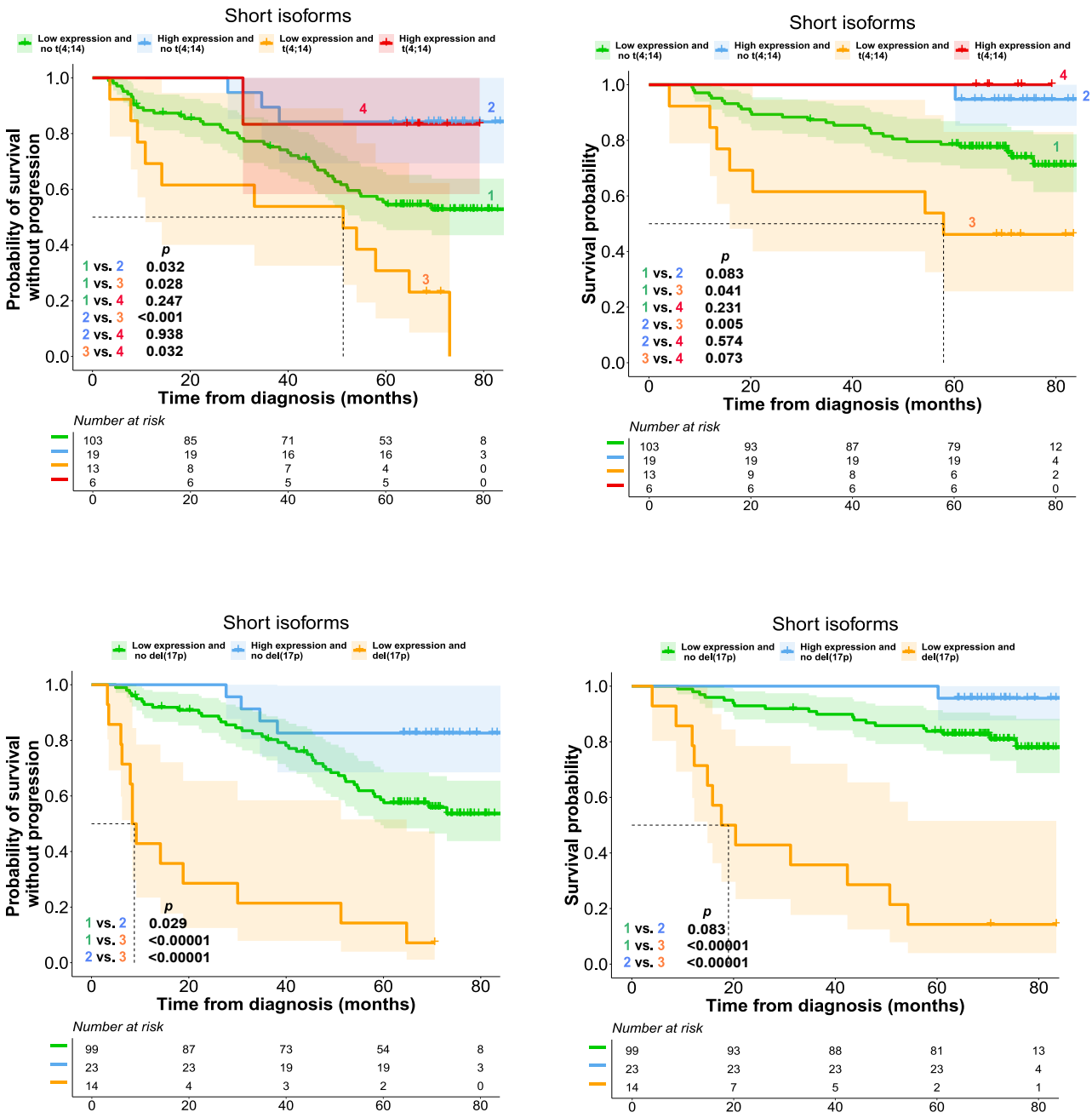

Supplementary Figure 5

B

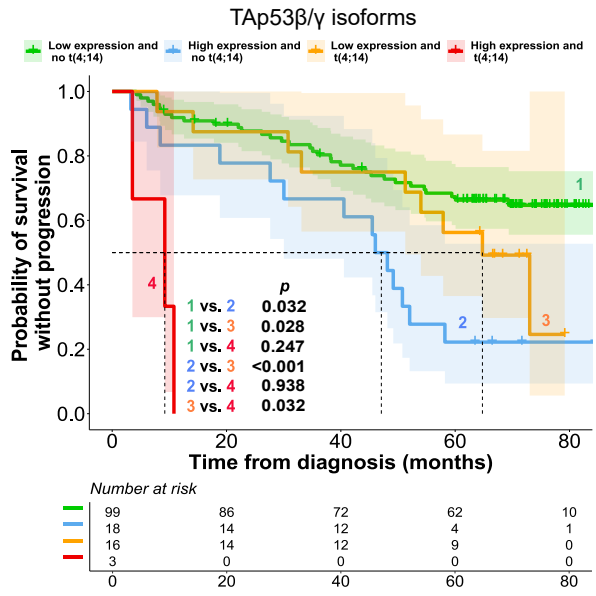

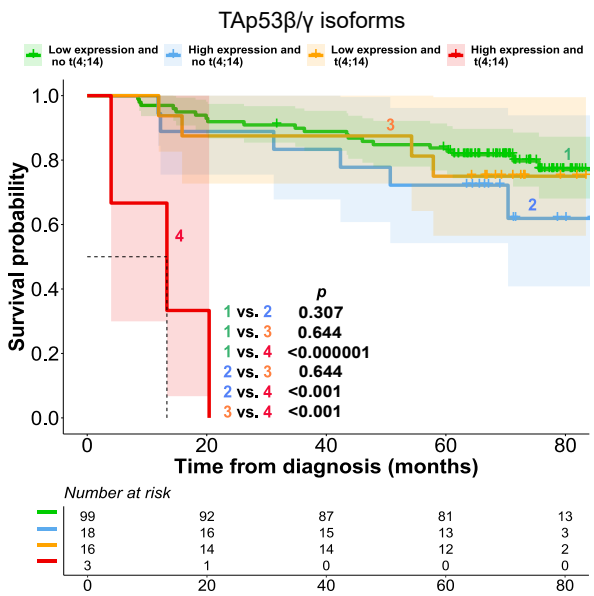

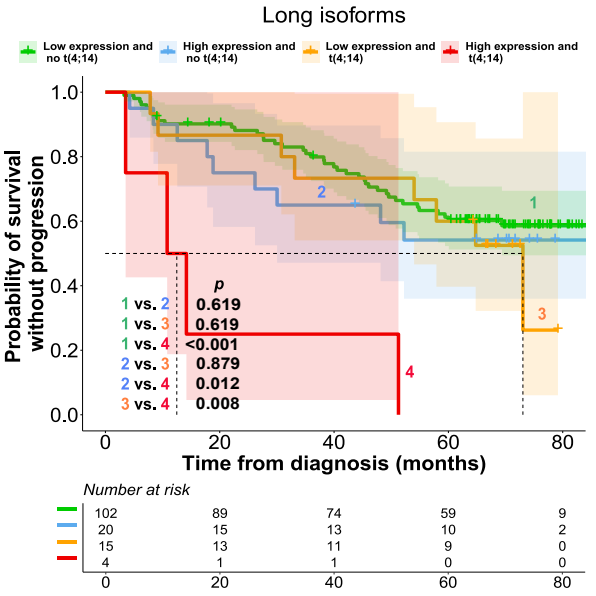

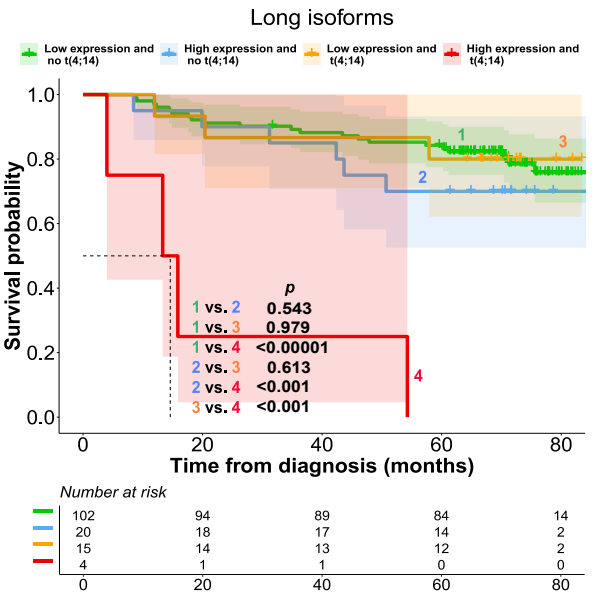

Supplementary Figure 5

C

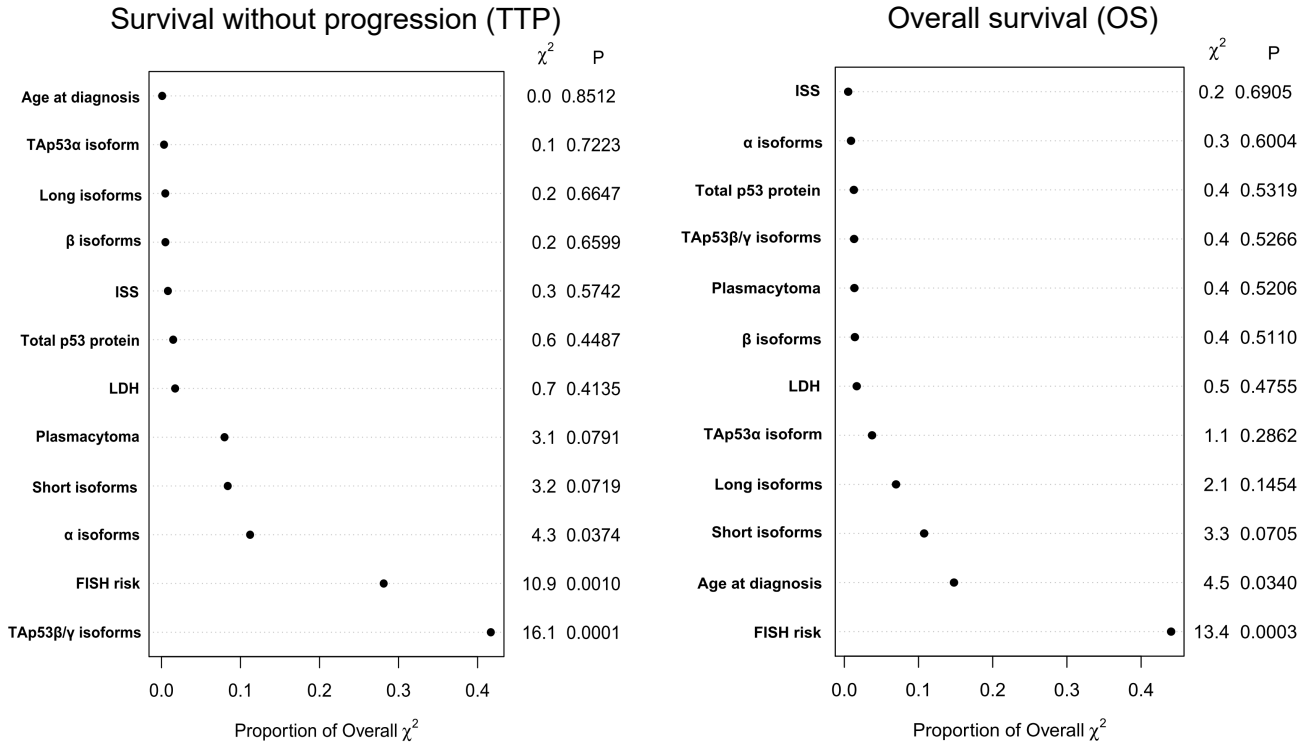

Supplementary Figure 6

A

p53 mRNA isoforms

B

p53 mRNA subclasses of isoforms

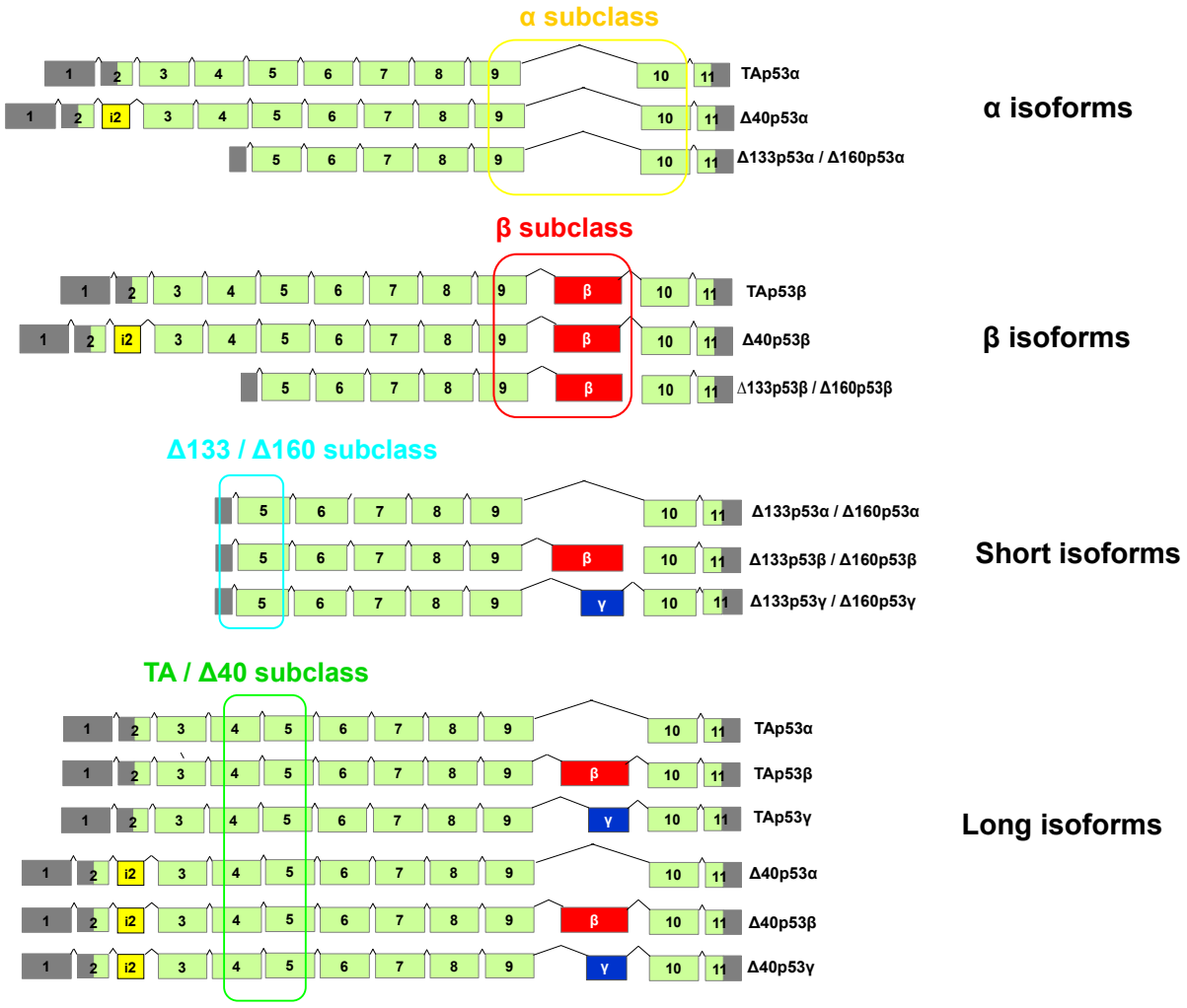

Supplementary Figure 6

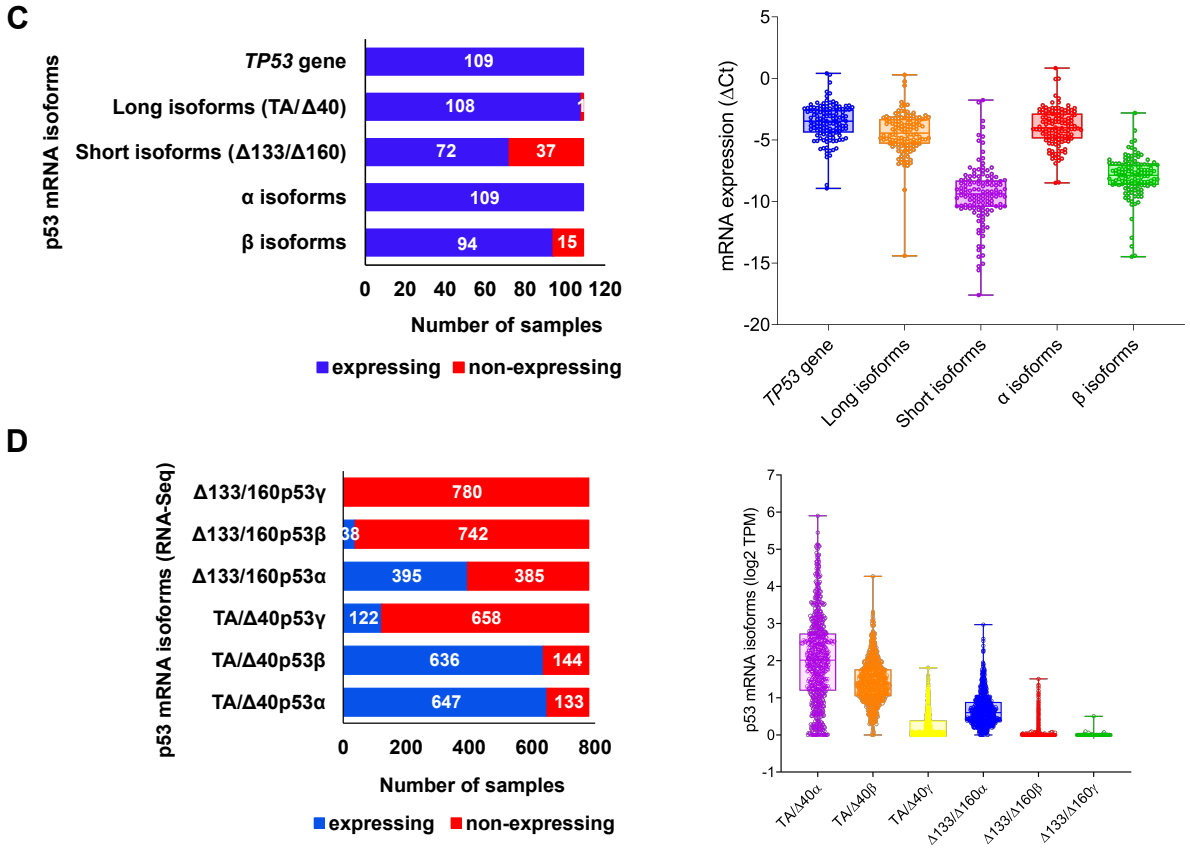

PATIENT CHARACTERISTICS	ALL PATIENTS (N=458)	PROTEIN COHORT (N=156)	*p*
Age years	58 (31-65)	59 (31-65)	0.362
Gender			
Male	240 (52%)	81 (51.9%)	0.918
Female	218 (48%)	75 (48.1%)	
Myeloma subtype			
IgG	273 (60%)	99 (63.5%)	0.957
IgA	107 (23%)	36 (23.1%)	
Light chain	69 (15.1%)	19 (12.2%)	
Non secretor	6 (1%)	2 (1.3%)	
ISS Stage			
I	179 (39%)	46 (30.1%)	0.094
II	166 (37%)	62 (40.5%)	
III	107 (24%)	45 (29.4%)	
ISS-R Stage			
I	182 (49%)	69 (47.6%)	0.609
II	151 (40%)	64 (44.1%)	
III	40 (11%)	12 (8.3%)	
ECOG			
0	195 (43%)	62 (40.5%)	0.8
1	182 (40%)	62 (40.5%)	
2	62 (14%)	21 (13.7%)	
3	16 (3%)	8 (5.2%)	
Hemoglobin (g/dL)	10.9 (4.8-16.8)	10.6 (6.7-15.5)	0.101
Creatinine (mg/dL)	0.9 (0.3-2)	0.9 (0.4-1.9)	0.815
B2-microglobuline (mg/L)	3.6 (0-62)	4 (1.5-17.4)	0.022
LDH			
High	65 (15%)	17 (11.2%)	0.274
Normal	376 (85%)	135 (88.8%)	
Plasmacytoma			
Yes	101 (22%)	29 (18.6%)	0.361
No	357 (78%)	127 (81.4%)	
Cytogenetics			
t(4;14)	58/402 (14%)	20/152 (13.2%)	0.701
t(14;16)	17/394 (4%)	5/151 (3.3%)	0.594
del(17p)	35/388 (9%)	14/147 (9.5%)	0.857
gain(1q)	168/385 (44%)	77/152 (50.7%)	0.141
del(1p)	27/382 (7%)	15/152 (9.9%)	0.278
Cytogenetic risk			
High	92/379 (24%)	32/146 (21.9%)	0.569
Standard	287/379 (76%)	114/146 (78.1%)	

p53 protein isoforms	Detected by antibody	Group
TAp53α	DO-1, DO-11 and A300-249A	TA and long isoforms, and total p53
TAp53β	DO-1, DO-11 and KJC8	
TAp53γ	DO-1 and DO-11	
Δ40p53α	DO-11 and A300-249A	Long isoforms and total p53
Δ40p53β	DO-11 and KJC8	
Δ40p53γ	DO-11	
Δ133p53α	DO-11	Short isoforms and total p53
Δ133p53β	DO-11 and KJC8	
Δ133p53γ	DO-11	
Δ160p53α	DO-11	Short isoforms and total p53
Δ160p53β	DO-11 and KJC8	
Δ160p53γ	DO-11	

Supplementary Material

Supplementary Figure 1. Detection of the ectopic expression of p53α, p53β, p53γ, and Δ133p53α protein isoforms in null-p53 JJN3 myeloma cells by the DO-11 **(A)**, DO-1 **(B)**, A300-249A and KJC8 **(C)** antibodies. **(D)** Schematic representation of human p53 protein isoforms, included in this study, grouped based on the molecular mechanisms that lead to their formation as: α, β, TA, long and short isoforms. The main domains of p53 protein isoforms are represented by colors and amino acid (aa) numbering. TAD1: transactivation domain 1, aa 1-42 [purple]; TAD2: transactivation domain 2, aa 43-63 [violet]); PRD: proline-rich domain, aa 64-92 [blue]), DBD: DNA-binding domain, aa 101-292 [green]; NLS: nuclear localization signal, aa 305-322 [orange]; OD: oligomerization domain, aa 326-356 [red]; BR: basic region, aa 364-393 [yellow]. The molecular weight of each p53 isoform protein is indicated. **(E)** Protein isoform expression was assessed for α, β, TA, long and short protein isoforms (left) and TAp53α and TAp53β/γ isoforms (right), by CNIA and normalized to GAPDH abundance in each case. The Y axis are expressed on log scale. **(F)** Variability of each isoform protein measurement across all the MM samples was measured and represented by percentage coefficient of variation (CV%).

Supplementary Figure 2. Association of total p53 protein and TA isoforms with mutations of *TP53* gene. Distribution of the expression of total p53 protein and TA isoforms based on the presence or absence of *TP53* mutations assessed by next-generation sequencing (NGS).

Supplementary Figure 3. Probability of survival without progression (TTP) and of overall survival (OS) of MM patients by level of TA **(A)**, TAp53α **(B)** and levels of α and β isoforms, and total p53 protein **(C)**.

Supplementary Figure 4. (A) TTP and OS of MM patients by cytogenetic risk and del(17p)**. (B)** TTP and OS of MM patients by cytogenetic risk and level of long p53 protein isoforms, simultaneously. The log-rank (Mantel–Cox) test *p* values are shown.

Supplementary Figure 5. (A) TTP and OS of MM patients by t(4;14) or del(17p) and expression of short protein isoforms. **(B)** TTP and OS of MM patients by t(4;14) and expression of TAp53β/γ or long isoforms. **(C)** Contribution of variables to explaining the model adjustment calculated by the relative proportion of χ2.

Supplementary Figure 6. Schematic representation of the twelve p53 mRNA isoforms structures. **(A)** The protypical *TP53* gene is composed of 11 exons. Translated and numbered exons for the full-length TAp53α protein are represented by light green boxes. The β and γ exons codifying the β and γ isoforms are shown in red and blue. The 3' and 5' UTR regions are represented by bright green ovals. The P1 and P2 promoters in combination to the alternative splicing and start codons led to the TA, ∆40 and short isoforms, respectively. **(B)** The p53 isoforms can be grouped into subclasses depending on the molecular mechanisms that lead to their formation. The figure shows the groups of isoforms included in this study at mRNA level: α, β, long (TA/Δ40) and short (Δ133/Δ160) isoforms, as well as the primers' location by arrows. **(C)** Number of MM patients with and without expression of each p53 mRNA isoform (left), and the distribution of the expression for each p53 mRNA isoforms in MM samples by qRT-PCR (right). **(D)** Number of MM patients with and without expression of each p53 mRNA isoform based on RNA-Seq data from 780 MM patients included in the MMRF CoMMpass trial (NCT01454297). p53 mRNA expressions were dichotomized using the 95th percentile of the median expression of all genes within chromosome Y in women samples. In the right panel is shown the distribution of the expression for each mRNA isoform. TTP and OS of MM patients according to levels of short mRNA isoforms **(E)** and the *TP53* gene **(F)**.

Material suplementario correspondiente al Capítulo 3

"Amiloride, an old diuretic drug, is a potential therapeutic agent for multiple myeloma"

Clinical Cancer Research
(2017), 23(21): 6602-6615
DOI: 10.1158/1078-0432.CCR-17-0678

Supplemental Figure 1

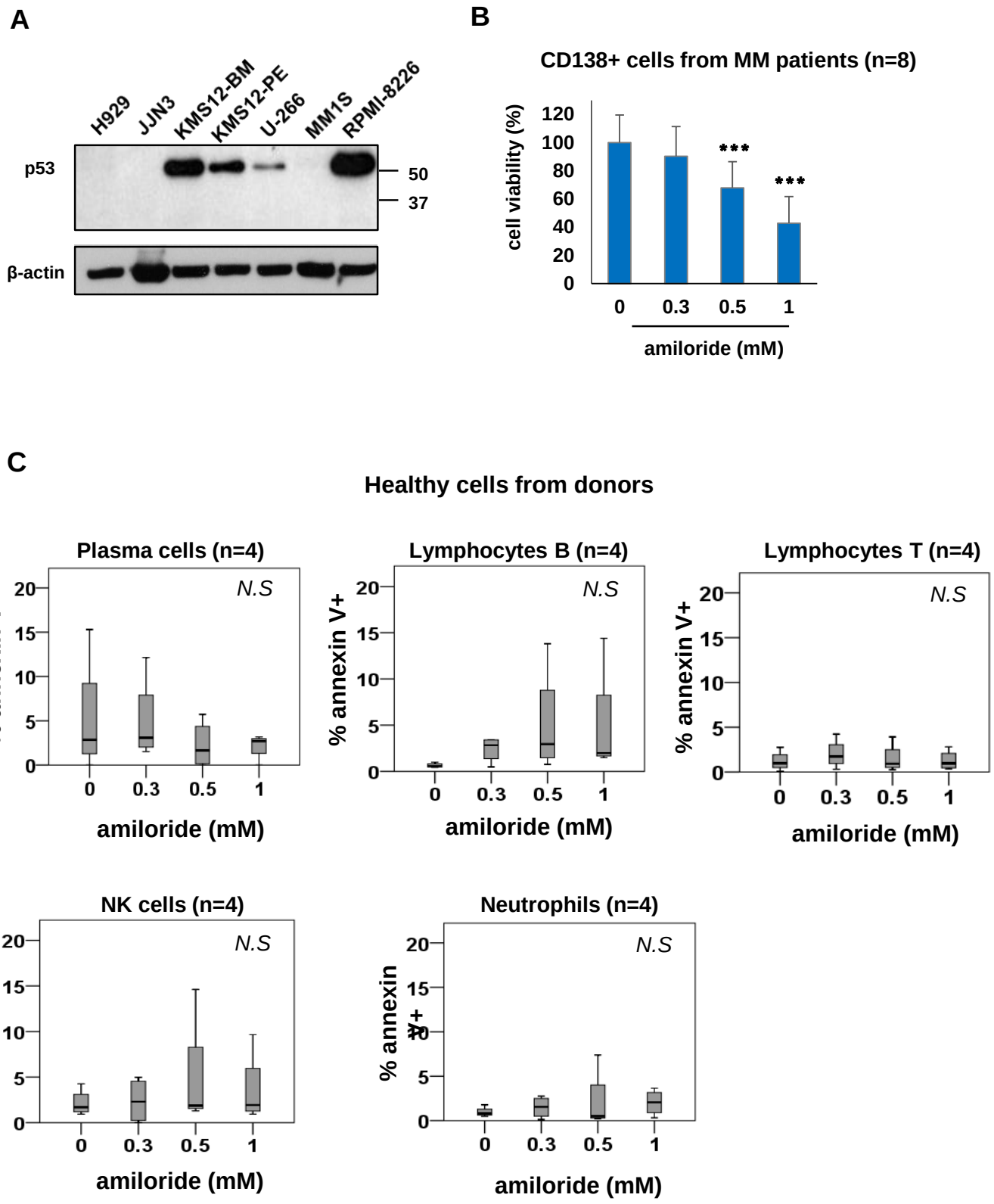

Supplemental Figure 2

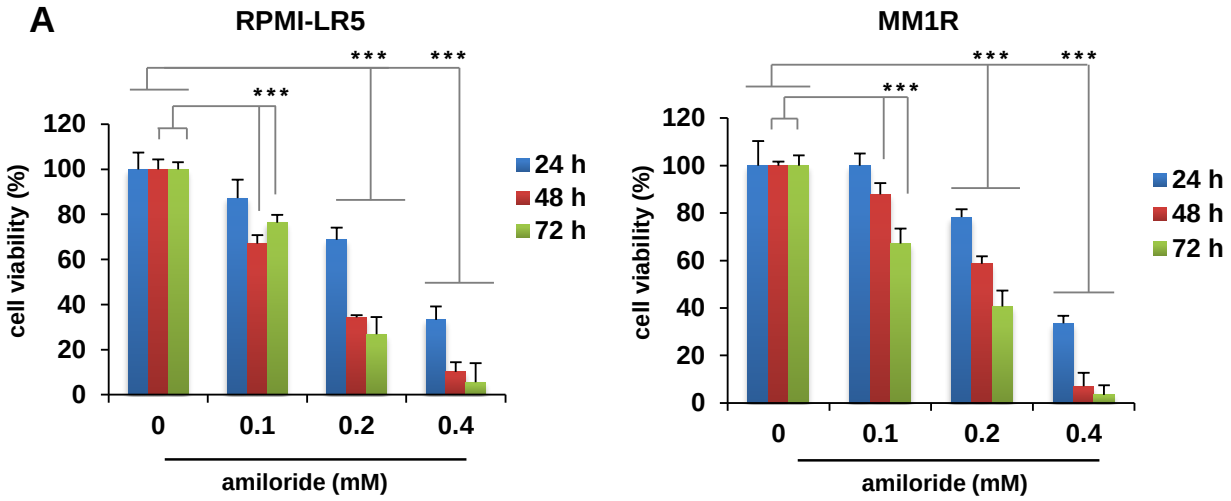

B

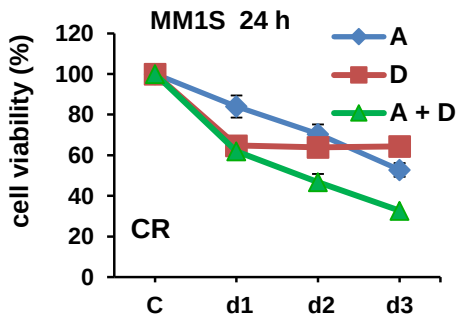

	Drugs concentration (μM)		CI
Drug	A	D	A + D
d1	133	6.7	0.421
d2	200	10	0.529
d3	300	15	0.518

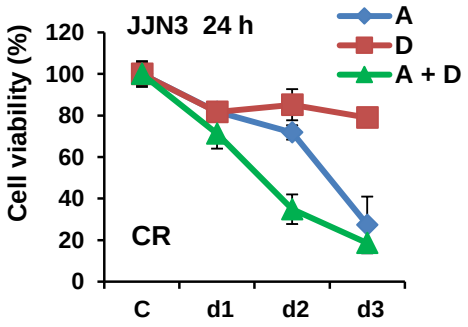

	Drugs concentration (μM)		CI
Drug	A	D	A + D
d1	200	6.7	0.789
d2	300	10	0.645
d3	500	15	0.790

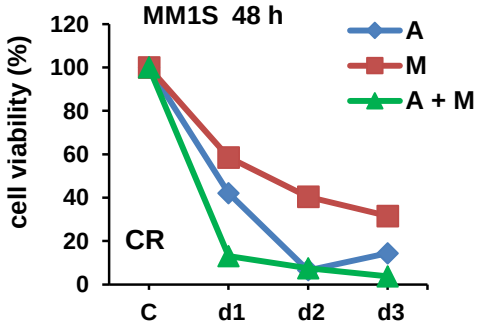

	Drugs concentration (μM)		CI
Drug	A	M	A + M
d1	200	2.3	0.734
d2	300	3.4	0.709
d3	500	5.1	0.696

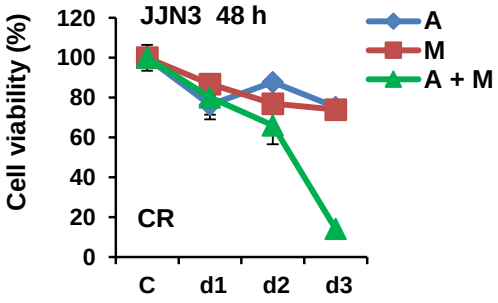

	Drugs concentration (μM)		CI
Drug	A	M	A + M
d1	100	4	0.786
d2	200	8	0.234
d3	400	16	0.003

Supplemental Figure 2

C

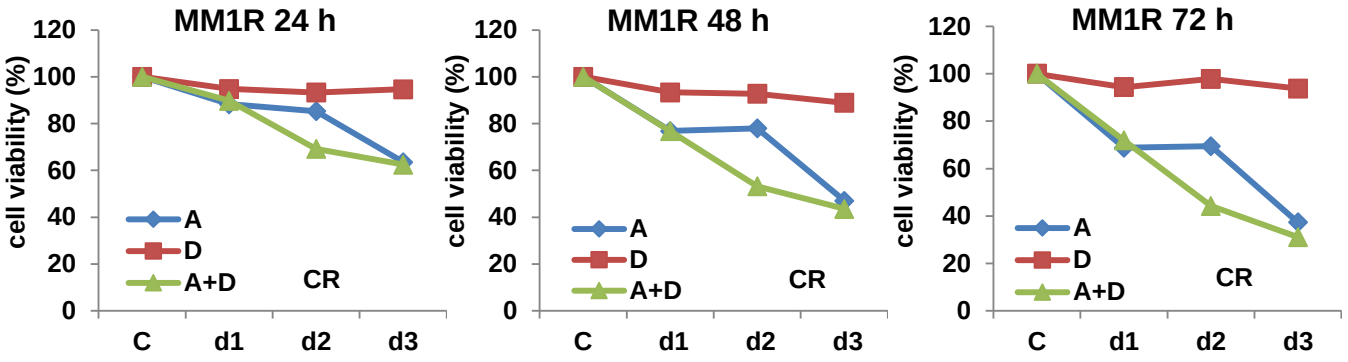

	Drugs concentration (μM)		CI
Drug	A	D	A + D
d1	50	5	0.987
d2	100	10	0.549
d3	200	20	0.828

	Drugs concentration (μM)		CI
Drug	A	D	A + D
d1	50	5	0.800
d2	100	10	0.507
d3	200	20	0.673

	Drugs concentration (μM)		CI
Drug	A	D	A + D
d1	50	5	0.920
d2	100	10	0.532
d3	200	20	0.587

D

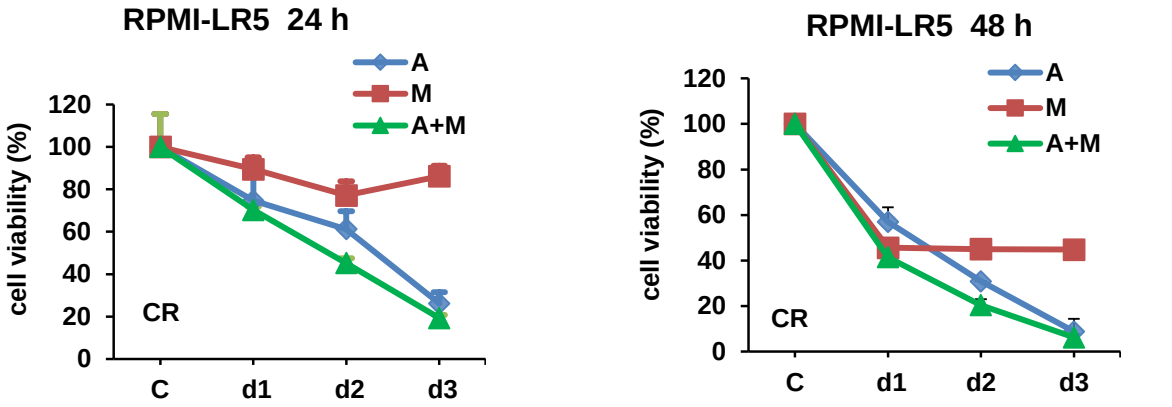

	Drugs concentration (μM)		CI
Drug	A	M	A + M
d1	100	4	0.798
d2	200	8	0.790
d3	400	16	0.701

	Drugs concentration (μM)		CI
Drug	A	M	A + M
d1	100	4	0.710
d2	200	8	0.829
d3	400	16	0.807

Supplemental Figure 2

E

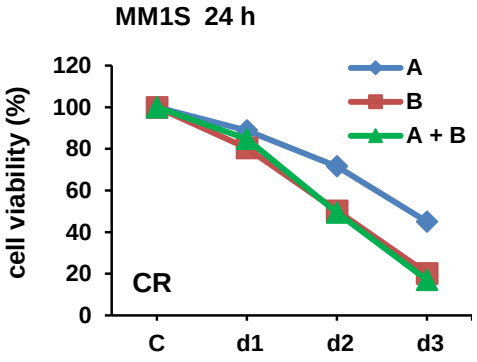

	Drugs concentration (μM)		CI
Drug	A	B	A + B
d1	200	0.0033	1.6
d2	300	0.005	1.3
d3	500	0.0075	1.6

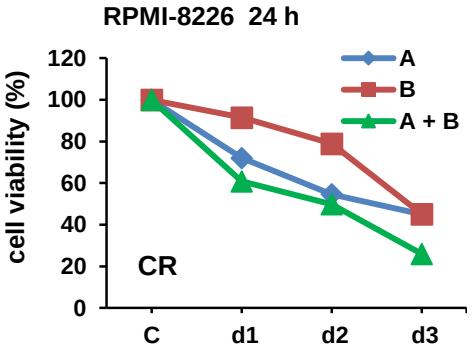

	Drugs concentration (μM)		CI
Drug	A	B	A + B
d1	100	0.0022	1.5
d2	200	0.0033	1.7
d3	300	0.0050	2.1

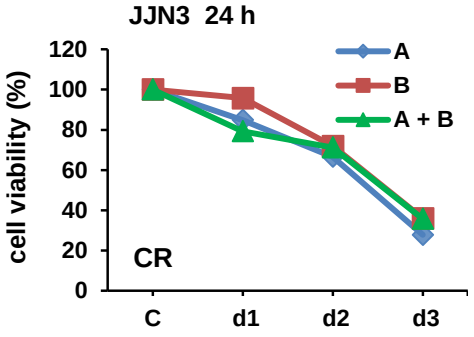

	Drugs concentration (μM)		CI
Drug	A	B	A + B
d1	200	0.0033	2.1
d2	300	0.0050	2.0
d3	500	0.0075	2.4

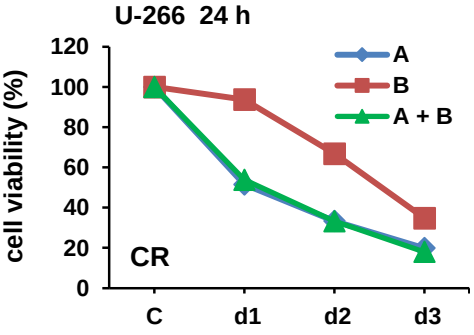

	Drugs concentration (μM)		CI
Drug	A	B	A + B
d1	200	0.0033	2.1
d2	300	0.0050	1.4
d3	500	0.0075	2.1

Supplemental Figure 3

A

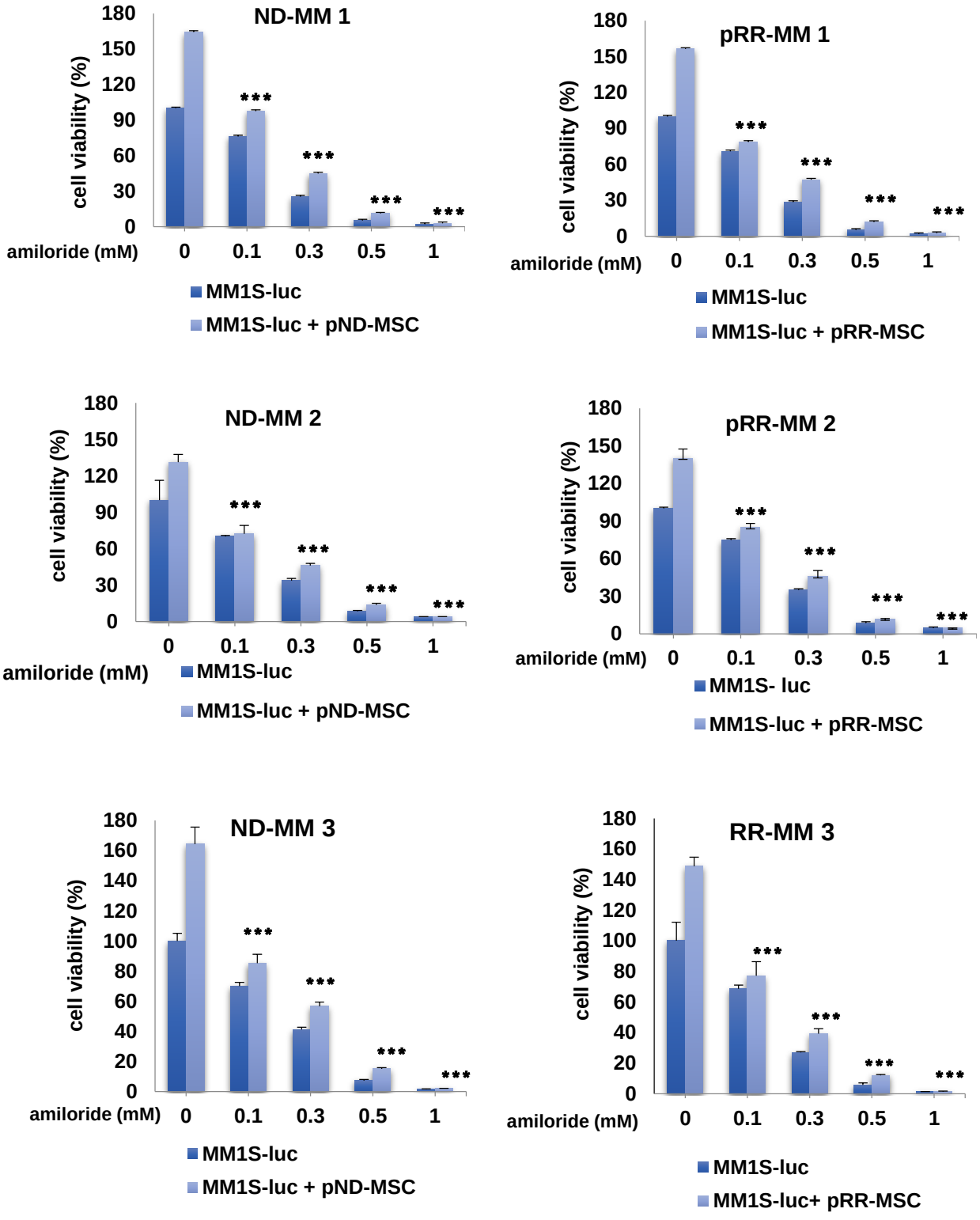

Supplemental Figure 3

B

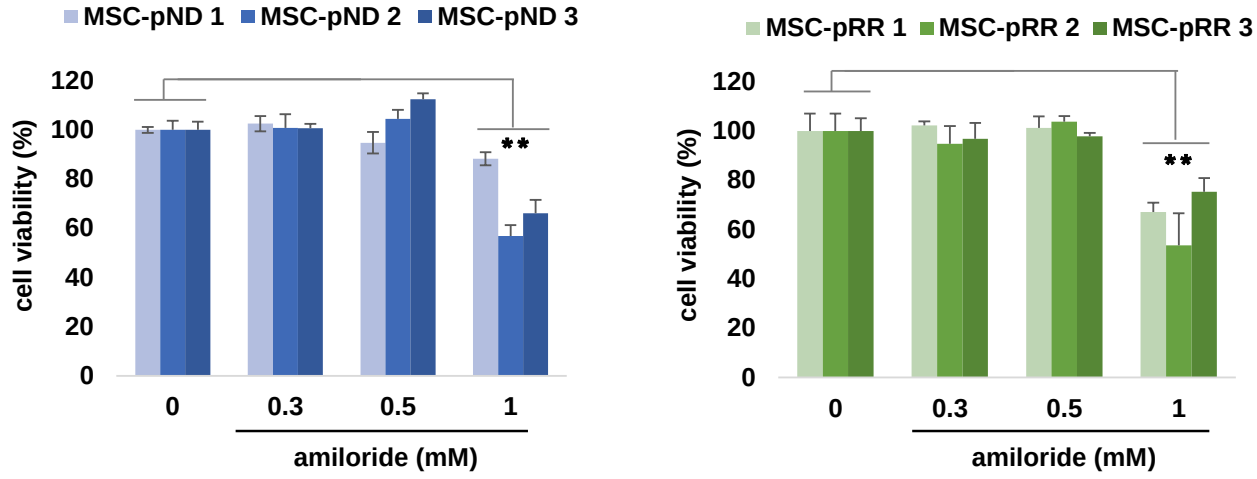

Supplemental Figure 4

A

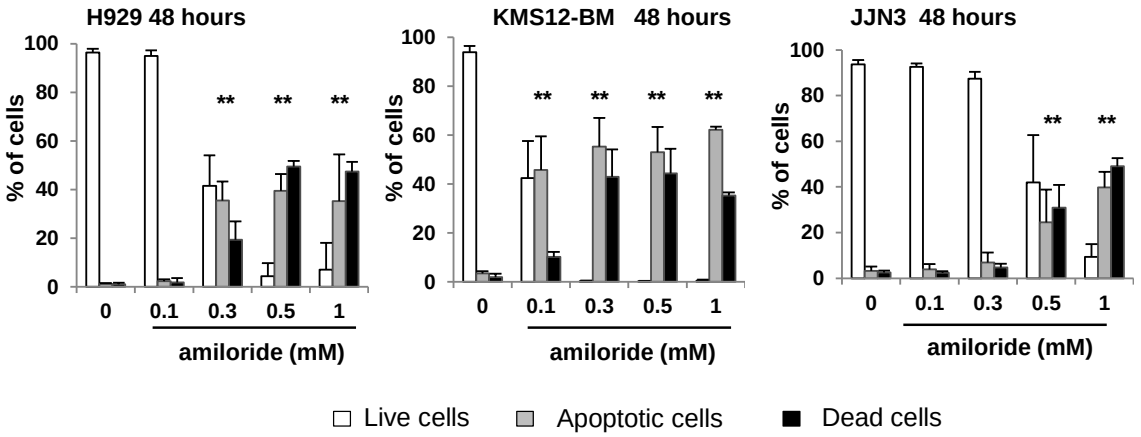

B

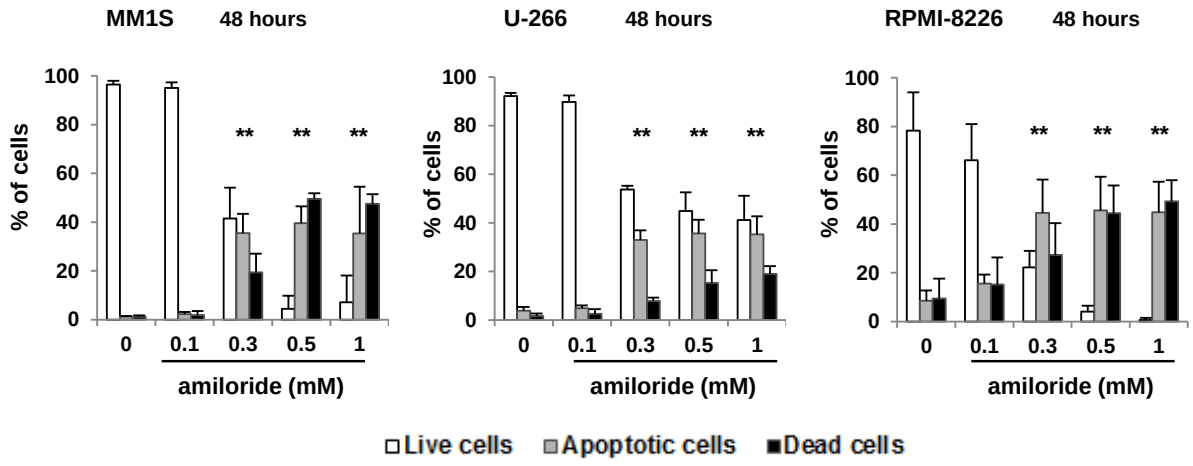

Supplemental Figure 5

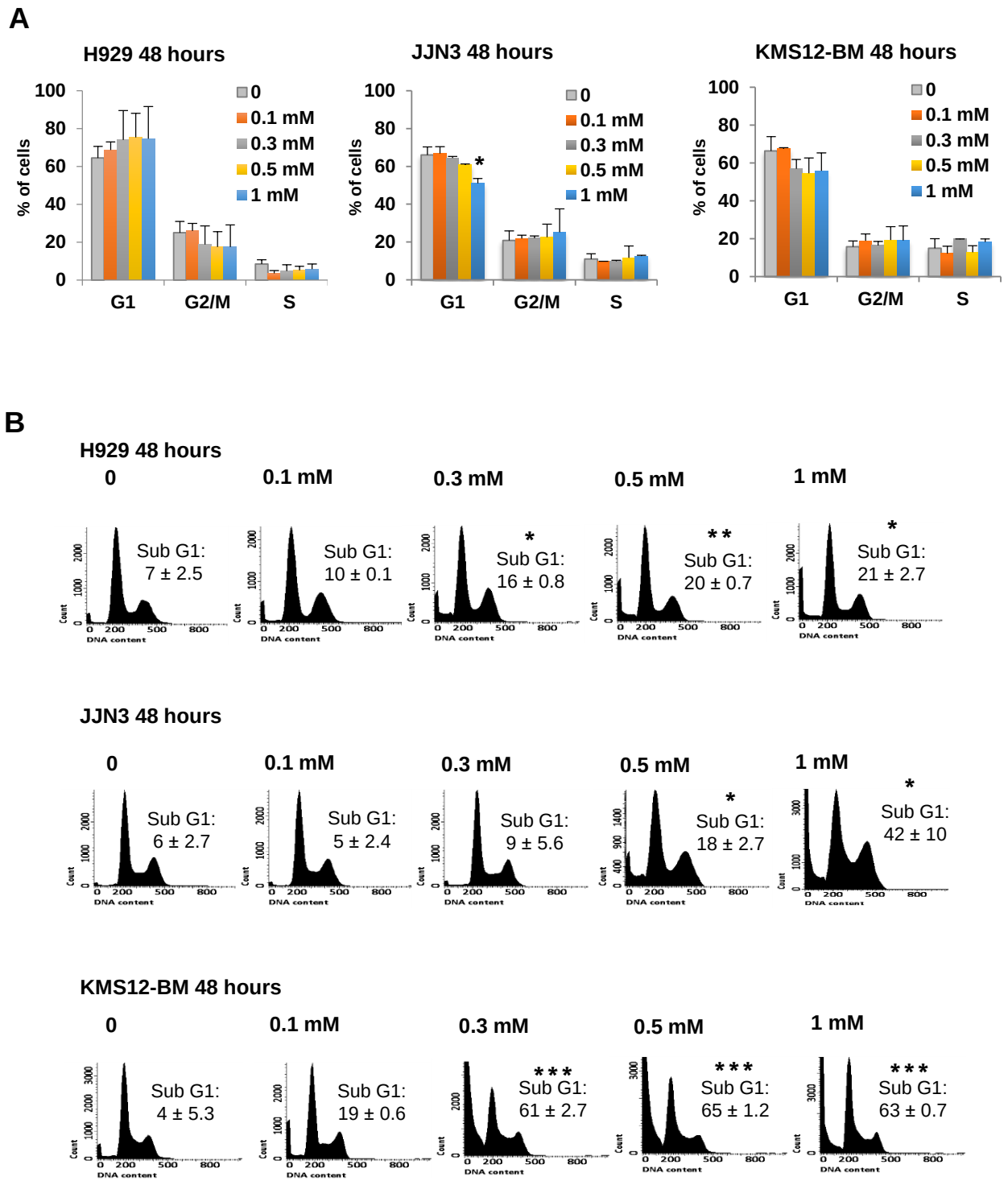

Supplemental Figure 6

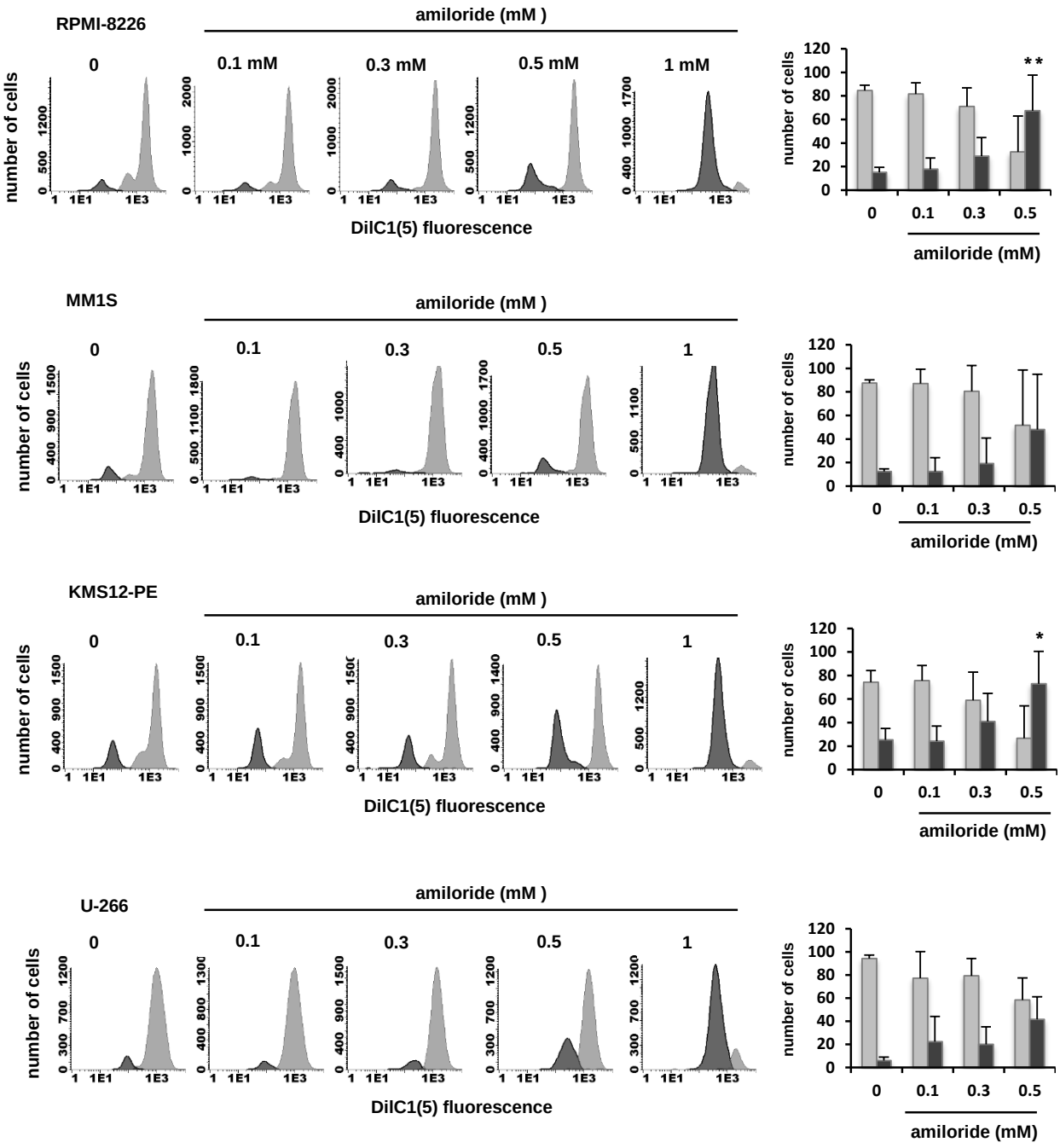

Supplemental Figure 7

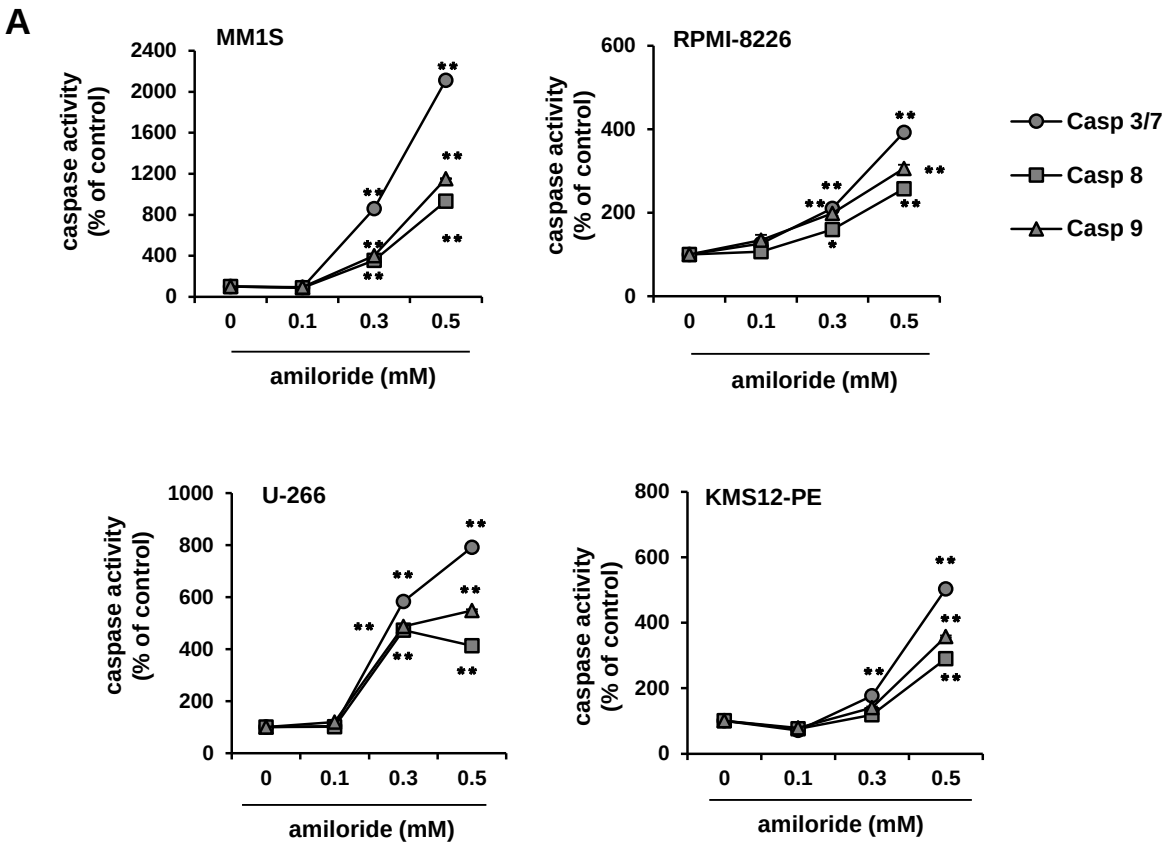

Supplemental Figure 8

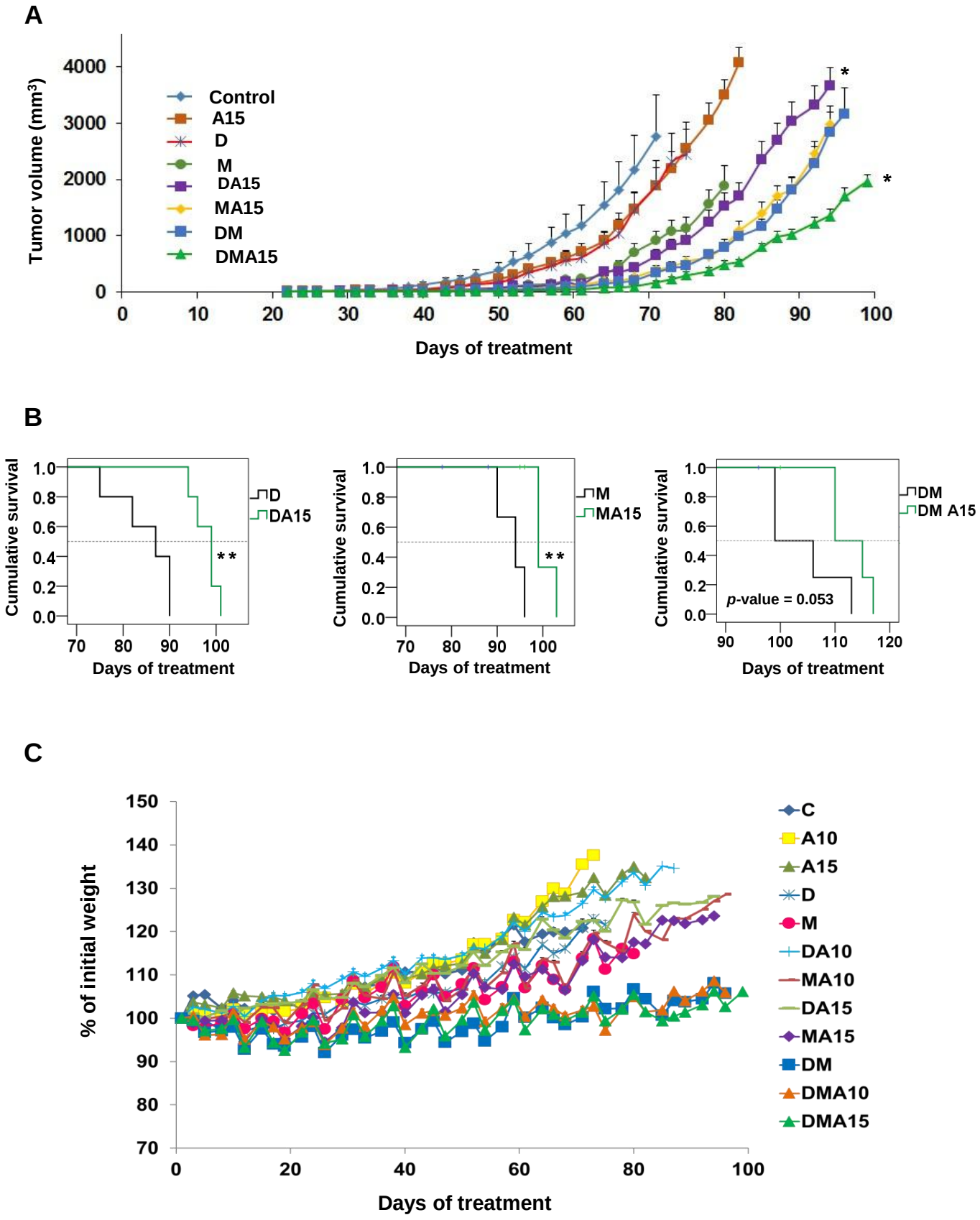

Supplemental Figure 9

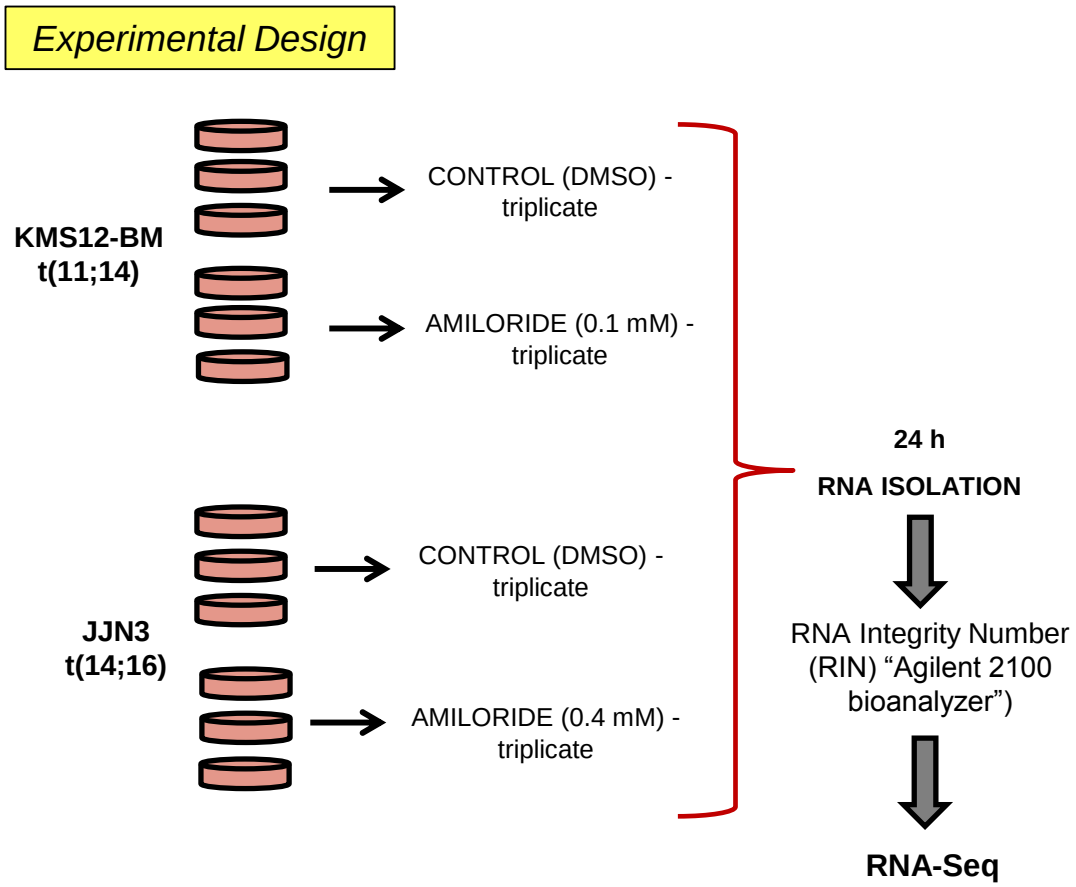

Supplemental Figure 10

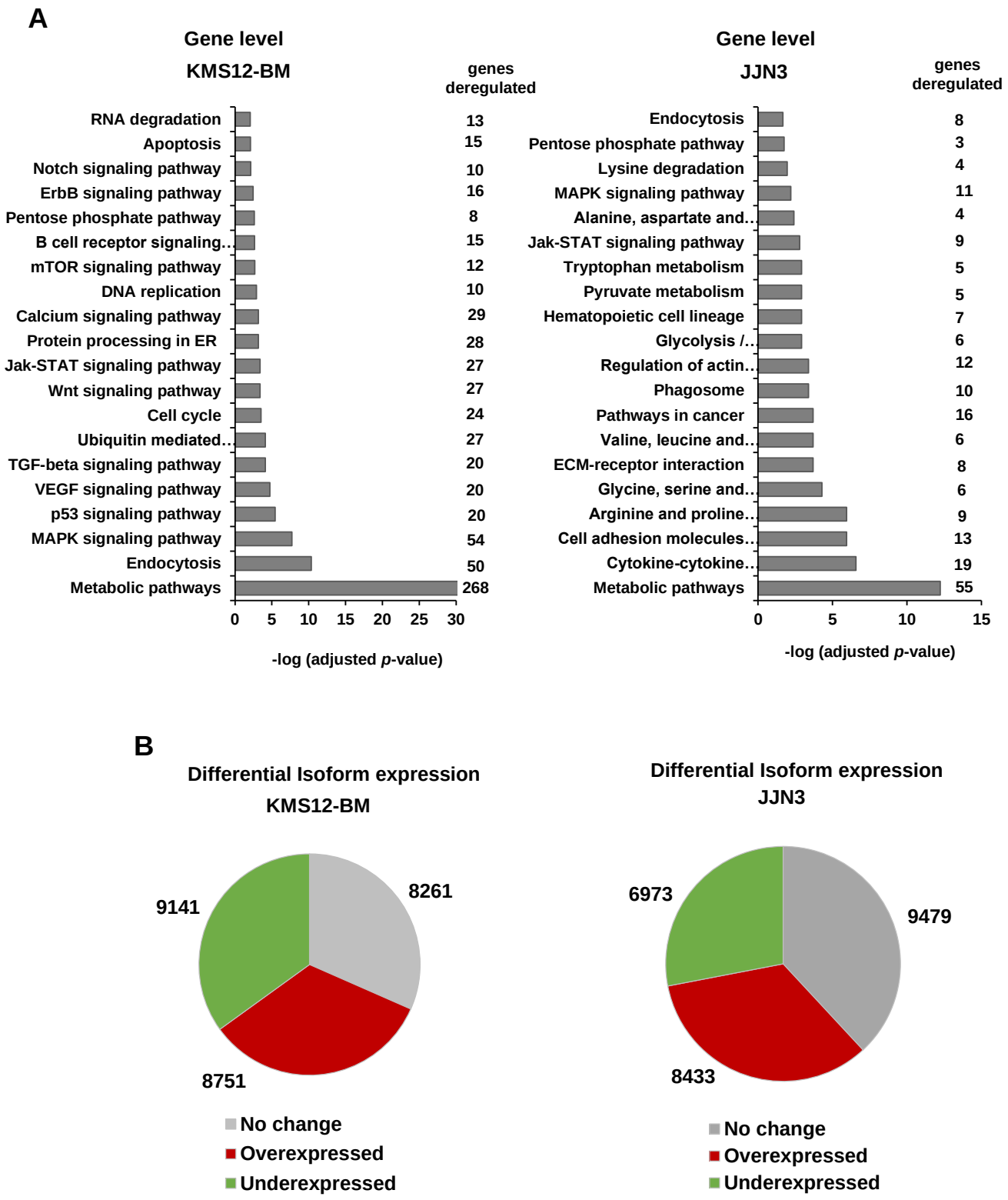

Supplemental Figure 11

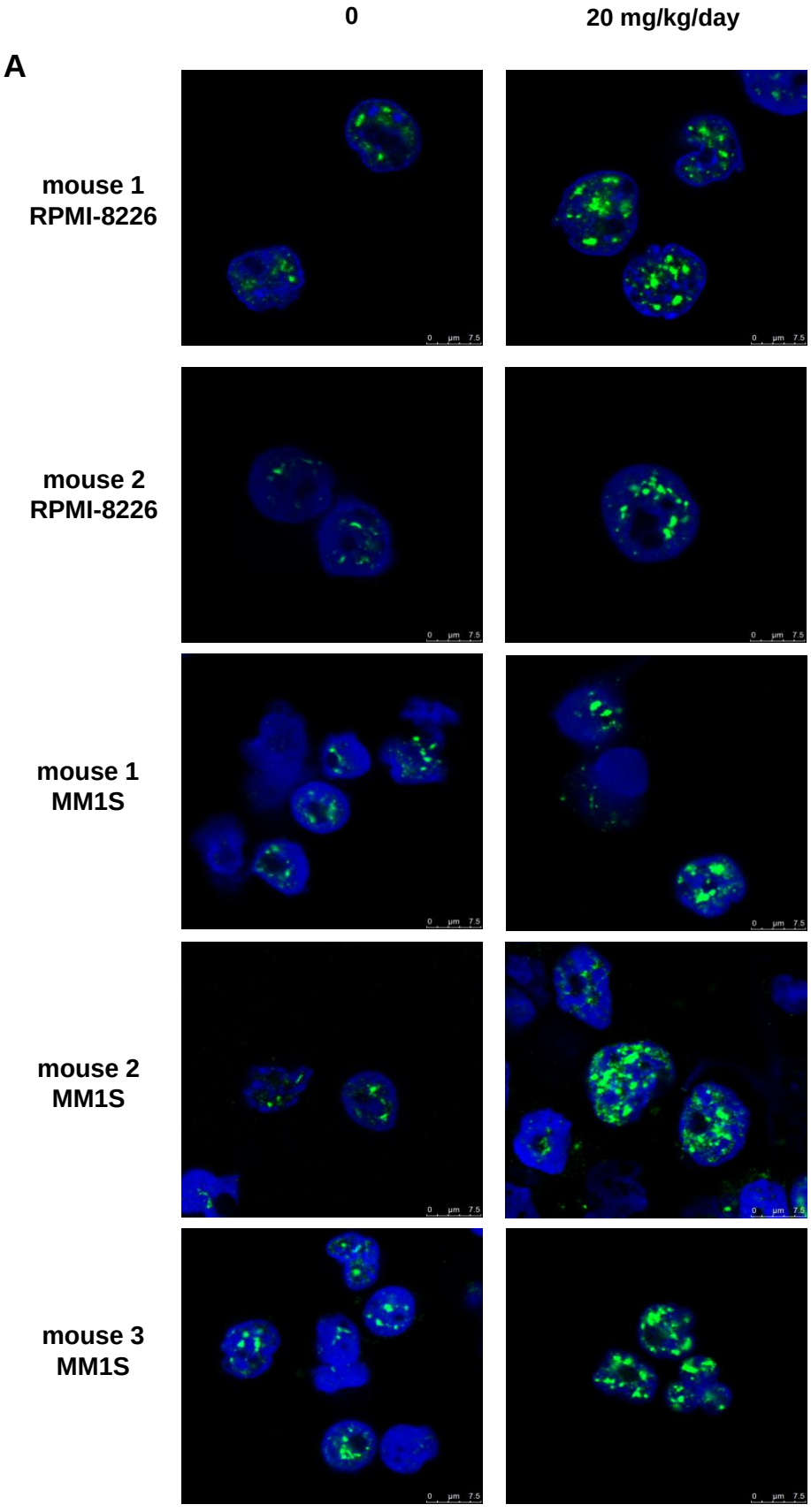

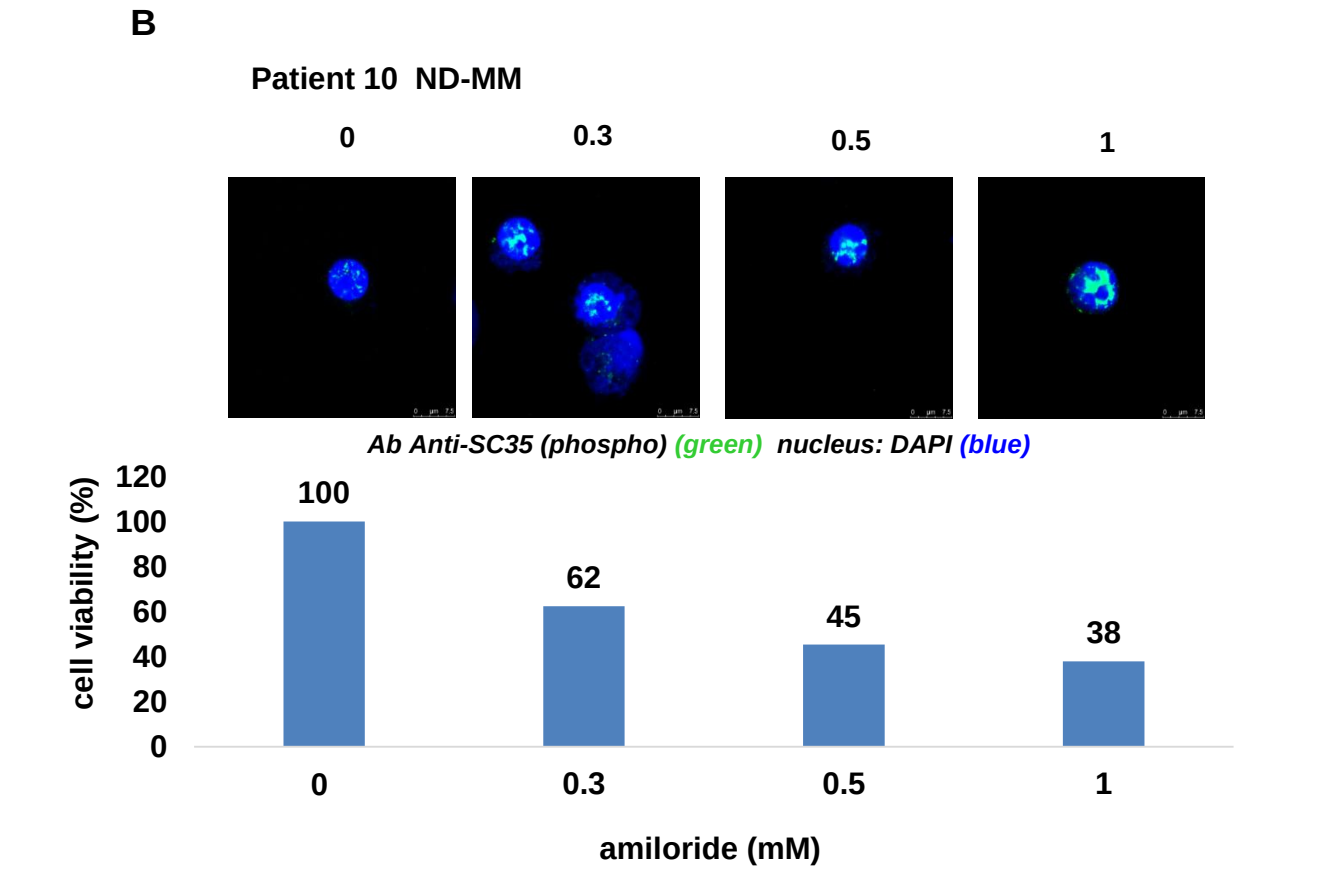
B
Patient 10 ND-MM
0
0.3
0.5
1
Ab Anti-SC35 (phospho) (green) nucleus: DAPI (blue)
cell viability (%)
120
100
80
60
40
20
0
100
62
45
38
0
0.3
0.5
1
amiloride (mM)

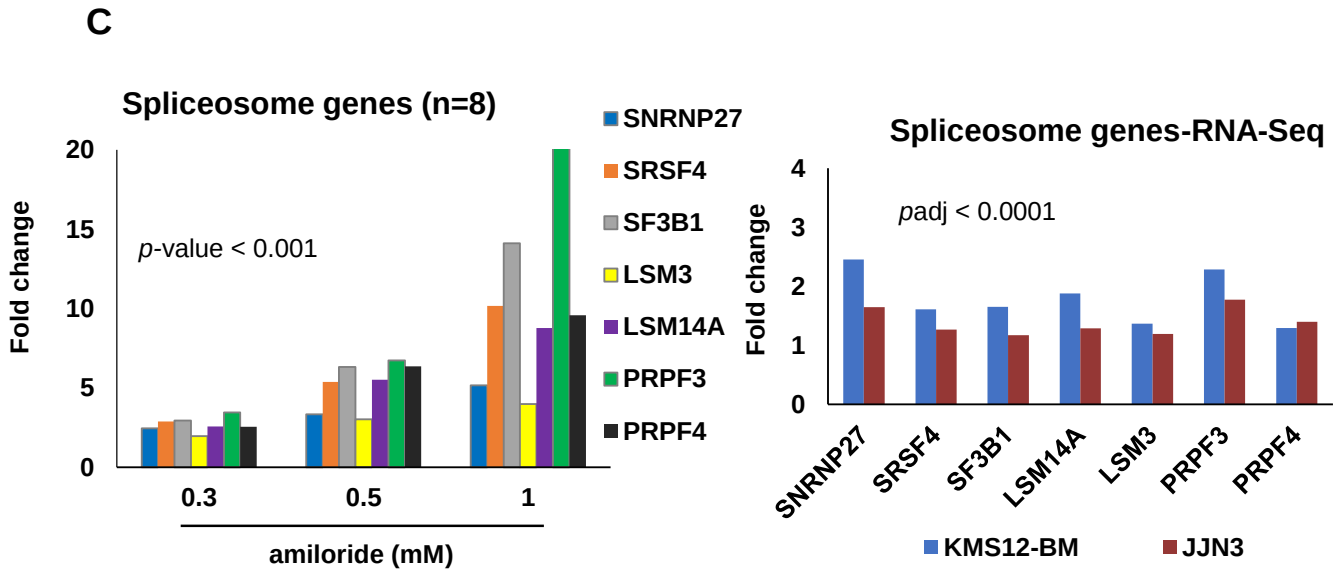
C
Spliceosome genes (n=8)
Fold change
20
15
10
5
0
p-value < 0.001
0.3
0.5
1
amiloride (mM)
SNRNP27
SRSF4
SF3B1
LSM3
LSM14A
PRPF3
PRPF4
Spliceosome genes-RNA-Seq
Fold change
4
3
2
1
0
padj < 0.0001
SNRNP27
SRSF4
SF3B1
LSM14A
LSM3
PRPF3
PRPF4
KMS12-BM
JJN3

Supplemental Figure 12

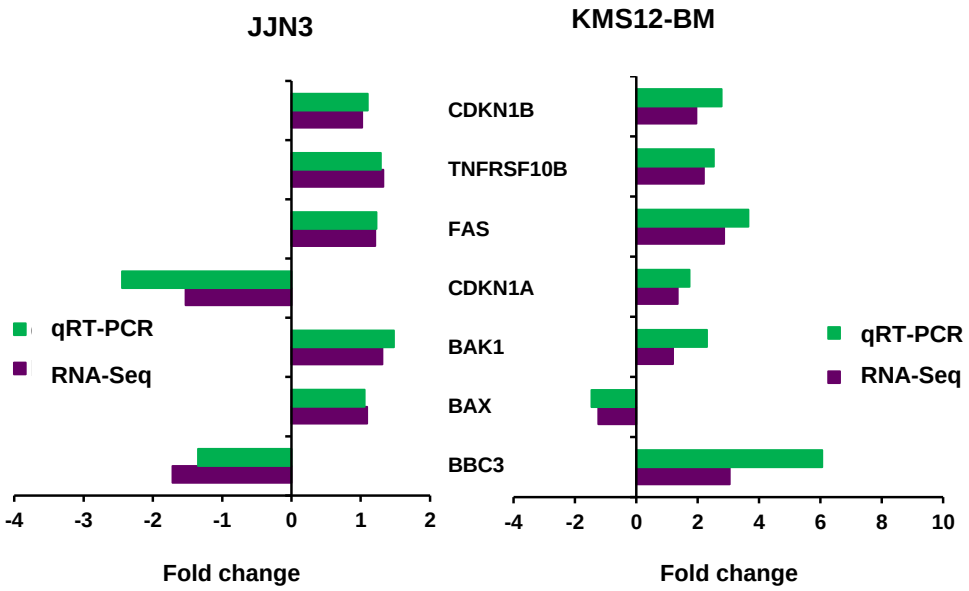

Supplemental Figure 13

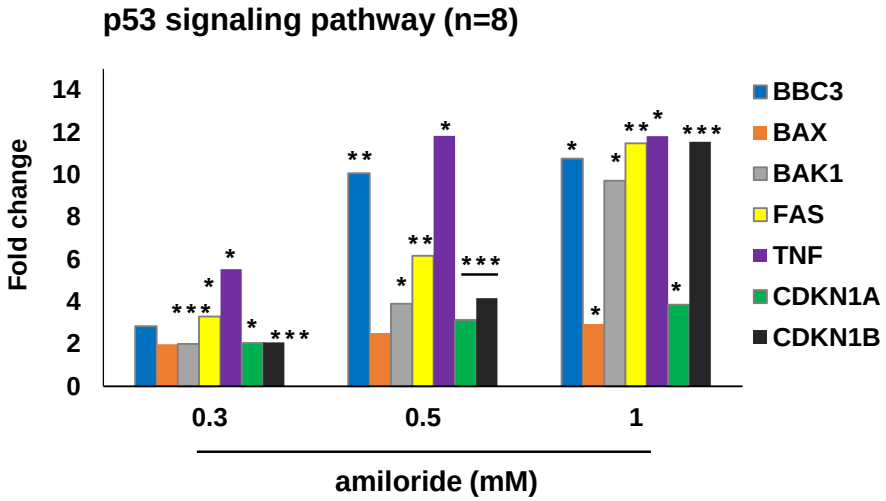

Supplemental Material

Supplemental Experimental Procedures

1. Evaluation of the combinations of amiloride with other anti-myeloma agents

Cells were treated for 24, 48 and 72 hours with double combinations at different doses of amiloride and other antimyeloma agents. Cell viability was analyzed by MTT assay and a constant ratio experimental design was used. The potency of each combination in different cell lines was quantified with the Calcusyn software (Biosoft, Ferguson, MO, USA), which is based in the Chou Talalay method and calculates a combination index (CI) with the following interpretation:

Combination index	Interpretation
<0.3,	strong synergism
0.3-0.7	synergism
0.7-0.85	moderate synergism
0.85-0.90	slight synergism
0.90-1.10	additive effect
>1.10	antagonism

2. Effect of MSCs on amiloride-induced growth inhibition

The methods for isolation and expansion of MSCs have been described by Garayoa *et al.* (1). Next, the MSCs were plated in 96-well culture dishes (8000/well) (3 biological replicates) and allowed to reach confluence during 48 hours. Then, medium was removed and 20,000 luciferase-expressing myeloma cells (MM1S-luc) in RPMI 1640 containing 10% fetal bovine serum were plated on top of the MSCs and treated for 48 hours with different concentrations of amiloride. After the incubation period, luciferin substrate (Caliper Life Sciences, Hopkinton, MA) at a final concentration of 150 g/mL was added for 10 minutes and bioluminescence (photons/sec) was analyzed in a Xenogen IVIS Imaging System 50 Series (Caliper Life Sciences).

3. MM xenograft murine model

To fit the tumor growth curves, we used the exponential model y = A*ekx resorting to the EXFIT option of the SIMFIT package (www.simfit.org.uk). The k parameter corresponds to the tumor growth rate and the A parameter to the initial tumor size. The k parameter together with its standard error (Sk) were extracted for each condition to compare the different drug experiments. The regression parameters comparison was carried out using a t-test for unequal variances. The area under the curve (AUC) for each growth curve was calculated by cubic splines fitting using the COMPARE option of SIMFIT. Differences between each pair of AUCs were tested, inside the x-overlap window of both curves, using COMPARE under the formula 200(A0)/(B1+B2), with A0 being the integral of the absolute difference between curves 1 and 2, B1 and B2 being the AUC of both curves considering a zero-base line for the y values. Differences between curves were expressed as percentages"

4. Immunoblotting

Whole cell lysates were collected using RIPA buffer (Santa Cruz Biotechnology) containing protease and phosphatase inhibitors (Roche). Protein samples were subjected to SDS-PAGE electrophoresis and transferred to 0.45 µm polyvinylidene fluoride (PVDF) membrane using iBlot® Dry Blotting System (Invitrogen). The antibodies used for immunoblotting were: anti-p53 protein (Cell Signaling) and anti-β-actin-HRP (Sigma-Aldrich) as control for protein loading. The chemiluminescence was detected using Clarity Western ECL Substrate (BioRad).

5. RNA sequencing

Twelve total RNAs were measured for quantity and quality using Agilent 2100 Bioanalyzer (Agilent Technologies). All samples reached the minimum standards, concentrations higher than 200 ng/µl and RIN values over 8.0. Libraries were constructed following a TruSeq Stranded mRNA Sample Preparation Guide (Illumina). Briefly, mRNA was purified from 4 µg of total RNA using oligo (dT) magnetic beads. The purified mRNA was fragmented into small pieces using fragmentation buffer in

combination of heat treatment (94ºC, 8 min). Taking these short fragments as templates, first-strand cDNA was synthesized using reverse transcriptase and random hexamer primers. The addition of Actinomycin D prevents spurious DNA-dependent synthesis, while allowing RNA-dependent synthesis, improving strand specificity detection. Second-strand cDNA synthesis was followed using RNase H, which removes the RNA template, and a DNA polymerase I which synthesizes a replacement strand, incorporating dUTP in place of dTTP to generate ds cDNA. The incorporation of dUTP quenches the second strand during amplification, because the next polymerase does not incorporate past this nucleotide in further amplification. At the end of this process a blunt-ended cDNA is obtained. Indexes and sequencing adapters were ligated to short cDNA fragments after purification with Ampure XP beads (Beckman Coulter), and which were used to distinguish different sequencing samples.

The final cDNA library was generated with an amplification step and purification process, then libraries were first quantified and validated with Agilent 2100 Bioanalyzer (Agilent Technologies). Next, libraries were normalized and pooled for clustering generation and sequencing using Illumina HiSeq™ 2500 with a configuration of 100 cycles Paired-end Reads, following manufacturer's instructions (Illumina), at Life sequencing S.L. (Valencia, Spain).

6. RNA sequencing analysis

All sequencing software tools were run with the default or recommended settings. RNA-Seq analysis was carried out in eight cores and 32 GB of RAM computer. The operating system was Ubuntu 14.04.2 LTS using version of X_86 64 bits. Paired-end FASTQ files for 12 samples were used in the RNA-Seq analyses. Adapter and quality trimming was done by the cutadapt tool version v1.4 (http://dx.doi.org/10.14806/ej.17.1.200) removing all bases with a Phred quality average threshold < 20 (Q < 20). FASTQ files quality was assessed using FASTQC (http://www.bioinformatics.bbsrc.ac.uk/projects/fastqc/) before and after the trimming process. The trimmed reads were mapped against the Homo sapiens genome

GRCh37 assembly obtained from Ensembl (http://www.ensembl.org/data/ftp/index.html) using in a first step the Bowtie2 aligner version 2.2.6 (2), in order to find the mean insert size to calculate the mean mate inner distance for each sample. The reads were then re-aligned using the TopHat v2.0.11 aligner (3). TopHat writes read data in the BAM format which is the binary version of the Sequence Alignment/Map (SAM) files, these files were used for downstream analyses at gene and isoform levels.

Regarding the gene level analyses, HTSeq version 0.6.0 was used to count the number of reads per gene from BAM files (4) considering the intersection-strict model whereby the whole read must fall entirely inside the feature to be counted. Reads that align multiple features are deleted to avoid double counting, and using GRCh37.82.gtf file from Ensembl as gene model. Low expression genes (those whose sums of reads were ≤ 1 in all samples) were removed. After the filtering process, the remaining genes were normalized dividing the counts by the sample-specific size factors, estimated using the median ratio method (5). Based on normalized count data, DESeq2 R package version 1.12.3 (6) (http://doi.org/10.1186/s13059-014-0550-8) modelled gene expression according a negative binomial distribution and generated a list of genes ranked based on the false discovery rate (FDR) using the Benjamini-Hochberg procedure.

The alternative splicing isoforms were detected using cufflinks version 2.2.1 following the Tuxedo pipeline (7). The isoforms were analyzed following 2 sequential approaches. First, a global analysis of isoforms was carried out considering all the isoforms with an absolute value of fold change (|FC|) ≥ 2 as differentially expressed between the contrasted conditions and using them for further analysis. Second, only the isoforms with a |FC| ≥ 2 between contrasted conditions corresponding to genes without expression modifications were considered. These genes were those not identified as a significant (FDR > 0.05 and |FC| < 2) by the DESeq2 package. The resulting isoforms were also used for downstream analysis.

4

Differential alternative splicing events were detected using rMATS version 3.0.9 (8), which identifies the number of observed reads that unambiguously support the presence or absence of each splicing event. Most of the significant AS events (FDR < 0.05) were classifying into five main types of pattern: patterns: skipped exon (SE), alternative 5' splice site (A5SS), alternative 3' splice site (A3SS), mutually exclusive exons (MXE) and retained introns (RIs). rMATS also calculates the difference in the ratio of these events between two conditions, calculating a false discovery rate.

The enrichment analysis was conducted through the Webgestalt web tool (9) in all analysis levels, using as data sources the Gene Ontology and the KEGG databases.

Supplemental tables

Supplemental Table 1. Molecular classification of human myeloma cell lines (HMCLs) as previously described (10–12). OD: oligomerization domain; DBD: DNA-binding domain.

	HMCLs Name	IGH translocations	*TP53* status	Mutation	Type of mutation	Domain of p53
1	NCI-H929	t(4;14)	wild type (WT)	-	-	-
2	JJN3	t(14;16)	deletion (DEL)	-	-	-
3	KMS12-BM	t(11;14)	mutated (MUT)	R337L	missense	OD
4	KMS12-PE	t(11;14)	mutated (MUT)	R337L	missense	OD
5	U-266	CCND1 insertion	mutated (MUT)	A161T	missense	DBD
6	MM1S	t(14;16)	wild type (WT)	-	-	-
7	RPMI-8226	t(14;16)	mutated (MUT)	E285K	missense	DBD

Supplemental Table 2. Patients' characteristics

Code	Patient No.	Age	Gender	Disease status	Treatment	FISH 17p	Experiments
P1	42394	55	M	Newly-diagnosed		normal	Citotoxicity of amiloride on PC from total BM sample
P2	42532	87	M	Newly-diagnosed		normal	Citotoxicity of amiloride on PC from total BM sample
P3	42598	87	F	Newly-diagnosed		normal	Citotoxicity of amiloride on PC from total BM sample
P4	42869	83	M	Newly-diagnosed		deletion	Citotoxicity of amiloride on PC from total BM sample
P5	50393	83	F	Newly-diagnosed		normal	Citotoxicity of amiloride on PC from total BM sample
P6	43449	63	M	Refractory/Progression	VTD/VDL-PACE/pembrolizumab-LD	deletion	Citotoxicity of amiloride on PC from total BM sample
P7	43226	63	M	Refractory	VTD-ASCT/ixazomib maintenance/KRD	deletion	Citotoxicity of amiloride on PC from total BM sample
P8	32585	72	M	Relapse	VMP	normal	Citotoxicity of amiloride on PC from total BM sample
P9	50616	76	M	Newly-diagnosed		normal	Citotoxicity of amiloride on PC from total BM sample
P10	47687	73	M	Refractory	VMP	normal	Citotoxicity of amiloride on PC from total BM sample
P11	50150	84	F	Newly-diagnosed		normal	Cell viability and RNA isolation of CD138+ fraction treated with amiloride
P12	50161	61	F	Newly-diagnosed		normal	Cell viability and RNA isolation of CD138+ fraction treated with amiloride
P13	50160	46	M	Newly-diagnosed		normal	Cell viability and RNA isolation of CD138+ fraction treated with amiloride
P14	40420	81	M	Relapse	VMP/LD	normal	Cell viability and RNA isolation of CD138+ fraction treated with amiloride
P15	50204	83	F	Newly-diagnosed		normal	Cell viability and RNA isolation of CD138+ fraction treated with amiloride
P16	50207	69	F	Relapse	VMP	normal	Cell viability and RNA isolation of CD138+ fraction treated with amiloride
P17	48886	58	F	Refractory	VTD	normal	Cell viability and RNA isolation of CD138+ fraction treated with amiloride
P18	50007	84	F	Newly-diagnosed		normal	Cell viability and RNA isolation of CD138+ fraction treated with amiloride

Supplemental Table 3. Amiloride-induced transcript isoforms expression changes of genes which encode proteins involved in spliceosome complex and its regulation. Only common transcript isoforms in both cell lines are shown. The direction of the change upon amiloride treatment is indicated (FC ≥ 2: upregulation or FC ≤ -2: downregulation), and the proteins are classified according to the spliceosome complexes to which they belong. The transcript isoforms with a log2 (FC) = 99 were those transcripts only expressed in amiloride treated-cells; and the transcript isoforms with log2 (FC) = -99 were those transcripts only expressed in control cells.

		KMS12-BM	JJN3		
Gene Symbol	**Transcript**	**log2 (FC)**	**log2 (FC)**	**Protein**	**Spliceosome complex**
SNRPC	ENST00000244520	7.14	1.22	159 aa	U1 snRNP
SF3A2	ENST00000586396	-1.21	-1.69	135 aa	U2 snRNP
U2AF1	ENST00000464750	6.22	99.00	75 aa	U2 snRNP-related
EIF4A3	ENST00000576547	-9.93	-8.82	125 aa	EJC/TREX complex
SRSF1	ENST00000258962	16.04	1.10	248 aa	common component (SR protein)
SRSF10	ENST00000259043	7.78	7.64	127 aa	common component (SR protein)
HNRNPC	ENST00000556513	4.44	7.33	231 aa	common component (hnRNP protein)
HNRNPC	ENST00000553753	1.01	1.49	288 aa	
HNRNPC	ENST00000420743	1.78	99.00	306 aa	
HNRNPC	ENST00000555215	99.00	4.14	187 aa	
HNRNPC	ENST00000557768	3.22	1.99	54 aa	
TXNL4A	ENST00000269601	99.00	99.00	142 aa	U5 snRNP and U4/U6-U5 tri-snRNP complexes
TXNL4A	ENST00000588162	-99.00	-99.00	57 aa	

Supplemental Table 4. Amiloride-induced transcript expression changes of genes involved in p53 pathway in KMS12-BM cell line. The direction of the change upon amiloride treatment is indicated (FC ≥ 2: upregulation or FC≤ -2: downregulation). The transcript isoforms with a log2 (FC) = 99 were those transcripts only expressed in amiloride treated-cells; and the transcript isoforms with log2 (FC) = -99 were those transcripts only expressed in control cells.

Gene Symbol	Transcript	log2 (FC)	Biotype	Protein
CDK4	ENST00000547853	99.00	Protein coding	2 aa
CDK4	ENST00000550419	1.06	Nonsense mediated decay	201 aa
CDK4	ENST00000546489	-99.00	Protein coding	208 aa
CDK4	ENST00000552254	1.70	Protein coding	203 aa
CDK4	ENST00000549606	3.88	Protein coding	40 aa
CDK4	ENST00000547281	-1.21	Protein coding	186 aa
CDK4	ENST00000552862	3.26	Protein coding	115 aa
CDK4	ENST00000551800	-99.00	Protein coding	132 aa
CDK4	ENST00000312990	1.01	Protein coding	111 aa
CDK4	ENST00000257904	-4.83	Protein coding	303 aa
CDK4	ENST00000551888	6.00	Processed transcript	no protein
CDK4	ENST00000552388	-1.48	Protein coding	170 aa
CDK4	ENST00000551706	3.52	Retained intron	no protein
TP53	ENST00000514944	99.00	Protein coding	155 aa
TP53	ENST00000505014	99.00	Retained intron	no protein
TP53	ENST00000269305	4.17	Protein coding	393 aa
CHEK1	ENST00000532669	1.08	Protein coding	192 aa
CHEK1	ENST00000438015	-2.05	Protein coding	476 aa
CHEK1	ENST00000544373	-7.36	Protein coding	382 aa
CHEK1	ENST00000532449	-99.00	Protein coding	442 aa
CHEK1	ENST00000278916	99.00	Protein coding	432 aa
CHEK1	ENST00000498122	-99.00	Nonsense mediated decay	89 aa
CHEK1	ENST00000427383	-99.00	Protein coding	492 aa
CHEK1	ENST00000528761	99.00	Processed transcript	no protein
CHEK1	ENST00000524737	-99.00	Protein coding	476 aa
SHISA5	ENST00000417841	99.00	Protein coding	112 aa
SHISA5	ENST00000466424	-99.00	Processed transcript	no protein
SHISA5	ENST00000426002	-4.64	Protein coding	137 aa
SHISA5	ENST00000460758	1.62	Retained intron	no protein
CCNB1	ENST00000506572	-2.40	Protein coding	401 aa
CCNB1	ENST00000508407	99.00	Protein coding	244 aa
CCNB1	ENST00000507798	1.87	Protein coding	185 aa
CCNB1	ENST00000505500	-10.47	Protein coding	396 aa
BID	ENST00000473439	-1.53	Processed transcript	no protein
BID	ENST00000399765	2.57	Protein coding	99 aa
SESN1	ENST00000520364	5.51	Retained intron	no protein

SESN1	ENST00000523632	-5.86	Retained intron	no protein
SESN1	ENST00000356644	1.30	Protein coding	492 aa
SESN1	ENST00000368971	-5.92	Retained intron	no protein
CDK1	ENST00000519078	1.04	Protein coding	189 aa
CDK1	ENST00000373809	2.74	Protein coding	240 aa
CDK1	ENST00000395284	-99.00	Protein coding	297 aa
CCND1	ENST00000535993	-99.00	Retained intron	no protein
CCND1	ENST00000542367	-99.00	Retained intron	no protein
RFWD2	ENST00000367667	11.86	Nonsense mediated decay	113 aa
RFWD2	ENST00000367666	-1.58	Protein coding	566 aa
RRM2B	ENST00000519125	-5.73	Retained intron	no protein
RRM2B	ENST00000519317	1.17	Protein coding	139 aa
BAX	ENST00000345358	-99.00	Protein coding	192 aa
BAX	ENST00000515540	-1.81	Nonsense mediated decay	41 aa
GTSE1	ENST00000491863	6.92	Retained intron	no protein
ATR	ENST00000383101	-1.74	Protein coding	2580 aa
PERP	ENST00000421351	3.78	Protein coding	193 aa
CDKN2A	ENST00000361570	99.00	Protein coding	170 aa
CDKN2A	ENST00000498628	-1.15	Protein coding	105 aa

References

1. Garayoa M, Garcia JL, Santamaria C, Garcia-Gomez A, Blanco JF, Pandiella A, et al. Mesenchymal stem cells from multiple myeloma patients display distinct genomic profile as compared with those from normal donors. Leukemia. 2009;23:1515–27.
2. Langmead B, Salzberg SL. Fast gapped-read alignment with Bowtie 2. Nat Methods. 2012;9:357–9.
3. Kim D, Pertea G, Trapnell C, Pimentel H, Kelley R, Salzberg SL. TopHat2: accurate alignment of transcriptomes in the presence of insertions, deletions and gene fusions. Genome Biol. 2013;14:R36.
4. Anders S, Pyl PT, Huber W. HTSeq--a Python framework to work with high-throughput sequencing data. Bioinforma Oxf Engl. 2015;31:166–9.
5. Anders S, Huber W. Differential expression analysis for sequence count data. Genome Biol. 2010;11:R106.
6. Love MI, Huber W, Anders S. Moderated estimation of fold change and dispersion for RNA-seq data with DESeq2. Genome Biol. 2014;15:550.
7. Trapnell C, Roberts A, Goff L, Pertea G, Kim D, Kelley DR, et al. Differential gene and transcript expression analysis of RNA-seq experiments with TopHat and Cufflinks. Nat Protoc. 2012;7:562–78.
8. Shen S, Park JW, Lu Z, Lin L, Henry MD, Wu YN, et al. rMATS: robust and flexible detection of differential alternative splicing from replicate RNA-Seq data. Proc Natl Acad Sci U S A. 2014;111:E5593-5601.
9. Wang J, Duncan D, Shi Z, Zhang B. WEB-based GEne SeT AnaLysis Toolkit (WebGestalt): update 2013. Nucleic Acids Res. 2013;41:W77-83.
10. Surget S, Descamps G, Brosseau C, Normant V, Maïga S, Gomez-Bougie P, et al. RITA (Reactivating p53 and Inducing Tumor Apoptosis) is efficient against TP53abnormal myeloma cells independently of the p53 pathway. BMC Cancer. 2014;14:437.
11. Moreaux J, Klein B, Bataille R, Descamps G, Maïga S, Hose D, et al. A high-risk signature for patients with multiple myeloma established from the molecular classification of human myeloma cell lines. Haematologica. 2011;96:574–82.
12. Teoh PJ, Chung TH, Sebastian S, Choo SN, Yan J, Ng SB, et al. p53 haploinsufficiency and functional abnormalities in multiple myeloma. Leukemia. 2014;28:2066–74.

Supplemental Figure Legends

Figure S1. (A) Protein expression of p53 in MM cell lines. Basal protein level of p53 was analyzed by Western blot in 7 MM cell lines. β-actin was used as loading control. **(B) Cell viability of isolated CD138+ cells from MM patients.** Cells were treated with the indicated doses of amiloride for 24 h and cell viability was analyzed by CellTiter-Glo luminescent assays. The average of luminescent values of control untreated samples was taken as 100%. The statistically significant differences between untreated and treated cells were determined with Student's t-test and represented as ***$p < 0.001$ (C) BM cells obtained from four donors were treated *ex vivo* with increasing concentrations of amiloride for 48 h. After the incubation period, cells were stained with the combination of annexin-V-FITC and five monoclonal antibodies (CD38-APC-H7, CD45-OC515, CD56-PE, CD19-PECy7 and CD3-APC) for the analysis of apoptosis in plasma cells and T lymphocytes (CD3+), B lymphocytes (CD19+), NK cells (CD56+/CD3-) and granulocytes (SSChigh/CD45+dim). Results are presented as the percentage of Annexin V-positive cells (Mann–Whitney U test).

Figure S2. (A) Melphalan resistant MM cell line RPMI-LR5 (panel left) and dexamethasone resistant MM cell line MM1R (panel right) were treated with the indicated doses of amiloride for 24, 48 and 72 h, and cell viability was analyzed by CellTiter-Glo luminescent assays. The average of luminescent values of control untreated samples was taken as 100%. Results are the means of three independent experiments. The statistically significant differences between untreated and treated cell lines were determined with Student's t-test. **(B,C,D)** MM cell lines were treated with the indicated double combinations of amiloride with dexamethasone or melphalan or **(E)** bortezomib. Cell viability was analyzed by MTT assay as represented in the graphs and the combination indexes (CI) were calculated with the Calcusyn software. CIs of < 0.3, 0.3-0.7, 0.7-0.85, 0.85-0.90, 0.9-1.10, and > 1.10 indicate strong synergism, synergism, moderate synergism, slight synergism, additive effect, and antagonism,

respectively. C: control; A: amiloride; D: dexamethasone; M: melphalan; B: bortezomib; d1, d2 and d3: drug concentrations used in the study; CR: constant ratio.

Figure S3. (A) MM1S-luc cells were treated for 48 hours with the indicated concentrations of amiloride in the presence or absence of MSCs derived from newly-diagnosed (ND) and relapsed/refractory (RR) MM patients, and proliferation was analyzed by bioluminescence (photons/sec). The statistically significant differences between untreated and treated cocultured cells were determined with Student's t-test and represented as $**p < 0.01$ **(B)** MSCs were cultured with different doses of amiloride for 48 hours, and cell viability was analyzed by CellTiter-Glo luminescent assays. The statistically significant differences between untreated and treated cells were determined with Student's t-test and represented as $**p < 0.01$

Figure S4. Amiloride induced apoptosis in MM cells. H929, KMS12-BM, JJN3 cells **(A)** and MM1S, U-266 and RPMI **(B)** were treated with increasing concentrations of amiloride for 48 h, and the induction of apoptosis was analyzed by flow cytometry after annexin-V/PI staining. Data are the means ± SD of three independent experiments. Statistically significant differences between untreated and treated cell lines are represented as $**p < 0.01$ (Student's t-test).

Figure S5. Amiloride did not induce changes in the cell cycle profile of MM cells. The indicated MM cell lines were incubated with increasing concentrations of amiloride for 48 h and the cell cycle was analyzed by flow cytometry. (A) Data are the means ± SD of three independent experiments. (B) The histograms show the phases of the cell cycle, including the subG1 peak. Statistically significant differences between untreated and treated cell lines are represented as $***p < 0.001$, $**p < 0.01$ and $*p < 0.05$ (Student's t-test).

Figure S6. Amiloride deregulated mitochondrial potential in MM cells. The indicated MM cell lines were incubated with increasing concentrations of amiloride for 24 h and the mitochondrial membrane depolarization was examined by flow cytometry after DilC1(5) staining (MitoStep). Dark grey color represented the depolarized cells

and grey color the cells without mitochondrial membrane depolarization. Data are the means ± SD of three independent experiments. Statistically significant differences between untreated and treated cell lines are represented as **$p < 0.01$ and *$p < 0.05$ (Student's t-test).

Figure S7. **Activity of amiloride through caspase-dependent and independent mechanisms. (A)** The activity of caspase 8, caspase 9 and caspase 3/7 was analyzed by luminescent caspase assays in different MM cell lines. **(B)** Pharmacologic inhibition of the activity of caspases with the pan-caspase inhibitor Z-VAD-FMK. MM1S and KMS12-BM cells were preincubated with the pan-caspase inhibitor (50 nM) for one hour and then were treated with amiloride (MM1S at 0.2 mM, and KMS12-BM at 0.1 mM) for 24 additional hours. The abrogated activity of caspase 3/7 was corroborated by luminescent caspase assay. Bortezomib (MM1S at 5 nM, and KMS12-BM at 10 nM) was used as positive control of caspase-dependent mechanism. Data are the means ± SD of three independent experiments. Statistically significant differences between untreated and treated cell lines are represented as **$p < 0.01$ and *$p < 0.05$ (Student's t-test).

Figure S8. The triple and double combination of dexamethasone and melphalan with amiloride displayed superior anti-MM activity and improved median survival compared with single agents and double combinations in a subcutaneous plasmacytoma model. CB17-SCID mice subcutaneously inoculated with 3 x 10^6 MM1S cells in the right flank were randomized to receive vehicle, amiloride (15 mg/kg, oral, daily), dexamethasone (0.5 mg/kg, i.p., 2 days weekly), melphalan (2.5 mg/kg, i.p., 2 days weekly) in monotherapy and the respective double and triple combinations (n = 5/group). **(A)** Evolution of tumor volumes of the plasmacytomas. Statistical differences between groups were evaluated fitting an exponential regression model and the regression parameters were compared using a *t*-test for unequal variances. and represented as *$p < 0.05$. Bars indicate standard errors of the mean. **(B)** Kaplan-Meier curves representing the survival of each treatment group. Mice were sacrificed

when their tumor diameters reached 2 cm or when they became moribund. Statistically significant differences were analyzed by the log-rank test, and represented as $**p < 0.01$ and $*p < 0.05$. **(C)** The toxicity profile of drugs *in vivo*, showed a lower body weight loss in all treated mice. It is represented as percentage of mouse body weight variation during the study in the xenograft plasmacytoma.

Figure S9. **Experimental design for RNA-Seq assay.** KMS12-BM and JJN3 cell lines, untreated or treated with amiloride (0.1 mM and 0.4 mM, respectively) for 24 h. The RNA was isolated and prepared for next-generation sequencing analysis.

Figure S10. Pathway enrichment analysis at gene level and differential transcript isoforms expression. (A) Summary of the biologically relevant pathways significantly enriched in KEGG analysis for amiloride-deregulated genes detected in KMS12-BM and JJN3 cell lines. Statistical significance of the enrichment was expressed as -log10 (Benjamini-Hochberg adjusted *p* - value). **(B)** Differential expression of transcript isoforms. Deregulates transcript isoforms were identified using Cufflinks following the Tuxedo pipeline when untreated and treated cell lines where compared. Only the isoforms that have a $|FC| \geq 2$ were considered as differentially expressed.

Figure S11. Validation of spliceosomal machinery alterations (A) CB17-SCID mice were subcutaneously inoculated into the right flank with $3x10^6$ MM1S (*TP53* WT; n = 6) cells or RPMI (*TP53* MUT; n = 4) cells in 100 µL of RPMI-1640 medium and 100 µL of Matrigel. After 11 weeks, when tumors had a large size, all mice were randomized into 2 groups, the control groups receiving the vehicle alone-PBS and the amiloride treatment groups receiving 20 mg/kg/day for two consecutive days, orally. Mice were sacrificed at third day and SC35-staining nuclear speckles detected by immunofluorescence assays. The figure shows the results corresponding to all mice. **(B)** CD138+ cells from one newly-diagnosed MM patient were treated with amiloride for 24 hours and SC35-staining nuclear speckles detected by immunofluorescence assay. **(C)** CD138+ cells from MM patients were treated with amiloride for 24 hours and the mRNA levels of spliceosome components were tested. The results are shown as the

magnitude of change between treated and untreated cells, using 18S rRNA as endogenous control. Results are combined to those from RNA-Seq results.

Figure S12. Validation of gene expression. The mRNA levels of *BBC3 (PUMA), BAX, BAK1, CDKN1A (p21), CDKN1B, TNFRSF10B* and *FAS (CD95)* were assessed by qRT-PCR. Results are the mean of three independent experiments. The direction of the fold change detected in the mRNA levels evaluated by both RNA-Seq data and qRT-PCR, concur.

Figure S13. Validation of p53 pathway activation in patient cells. CD138+ cells from MM patients were treated with amiloride for 24 hours and the mRNA levels of p53 signaling pathway were tested. The results are shown as the magnitude of change between treated and untreated cells, using 18S rRNA as endogenous control. Statistically significant differences between untreated and treated cell lines are represented as ***$p < 0.001$, **$p < 0.01$ and *$p < 0.05$ (Student's t-test).